

**Effects of Complementary
and Alternative Medicines (CAM)
on the Metabolism and Transport
of Anticancer Drugs**

KIM MOOIMAN

Cover design: Kim Mooiman

Lay-out & printing: Optima Grafische Communicatie, Rotterdam, The Netherlands

Mooiman, K.D.

Effects of Complementary and Alternative Medicines (CAM) on the Metabolism and
Transport of Anticancer Drugs

ISBN/EAN: 978-94-6169-457-7

© 2013 Kim Mooiman

Effects of Complementary and Alternative Medicines (CAM) on the Metabolism and Transport of Anticancer Drugs

Effecten van complementaire en alternatieve geneesmiddelen op
het metabolisme en transport van oncolytica
(met een samenvatting in het Nederlands)

PROEFSCHRIFT

ter verkrijging van de graad van doctor aan de Universiteit Utrecht
op gezag van de rector magnificus, prof. dr. G.J. van der Zwaan,
ingevolge het besluit van het college voor promoties in het
openbaar te verdedigen op woensdag 18 december 2013
des middags te 2.30 uur

door

Kim Delia Mooiman

geboren op 22 mei 1986
te Woerden

Promotoren:

Prof. dr. J.H.M. Schellens

Prof. dr. J.H. Beijnen

Co-promotor:

Dr. ir. I. Meijerman

The research described in this thesis was performed at the Department of Pharmaceutical Sciences, Division of Pharmacoepidemiology & Clinical Pharmacology of the Utrecht University in Utrecht, The Netherlands. Furthermore, part of the research was performed at the Department of Clinical Pharmacology of the Netherlands Cancer Institute in Amsterdam, and at the Department of Pharmacy and Pharmacology of the Slotervaart Hospital in Amsterdam, The Netherlands.

Financial support by the Utrecht Institute for Pharmaceutical Sciences (UIPS), The Netherlands Laboratory for Anticancer Drug Formulation (NLADF), Shimadzu Benelux B.V. and the Dutch Cancer Society for the publication of this thesis is gratefully acknowledged.

The Dutch Cancer Society funded the research published in this thesis under grant agreement UU 2007-3795.

CONTENTS

Chapter 1 Introduction

- 1.1 General introduction 11
- 1.2 Relevance of *in vitro* and clinical data for predicting CYP3A4-mediated herb-drug interactions in cancer patients 21

Chapter 2 Effects of CAM on CYP3A4- and CYP2C9-mediated metabolism of anticancer drugs

- 2.1 The effect of complementary and alternative medicines (CAM) on CYP3A4-mediated metabolism of three different substrates: 7-benzyloxy-4-trifluoromethylcoumarin (BFC), midazolam and docetaxel 51
- 2.2 Development and validation of a LC-MS/MS method for the *in vitro* analysis of 1-hydroxymidazolam in human liver microsomes: application for determining CYP3A4 inhibition in complex matrix mixtures 71
- 2.3 The effect of complementary and alternative medicines (CAM) on CYP2C9 activity 91

Chapter 3 Nuclear receptor-mediated inhibition of CYP3A4 induction

- 3.1 Evaluation of a reporter gene assay as suitable *in vitro* system to screen for novel PXR antagonists 111
- 3.2 Milk thistle's active components silybin and iso-silybin: Novel inhibitors of PXR-mediated CYP3A4 induction 131

Chapter 4 Effects of CAM on P-gp and BCRP mediated transport of anticancer drugs

- 4.1 The effect of complementary and alternative medicines (CAM) on P-gp and BCRP mediated transport of topotecan and imatinib 161

Chapter 5	Effects of Chinese herbal medicines (CHM) on CYP3A4-mediated metabolism of anticancer drugs	
5.1	Effect of Chinese herbs on CYP3A4 activity and expression <i>in vitro</i>	185
5.2	Letter to the editor regarding 'A prospective, controlled study of botanical compound mixture LCS101 for chemotherapy-induced hematological complications in breast cancer' by Yaal-Hahoshen et al. (The Oncologist 2011; 16; 1197-1202)	201
Chapter 6	Conclusions and perspectives	207
Chapter 7	In short	
	Summary	216
	Nederlandse samenvatting	220
Chapter 8	Appendix	
	Dankwoord	226
	List of co-authors	232
	List of publications	236
	About the author	238



CHAPTER 1

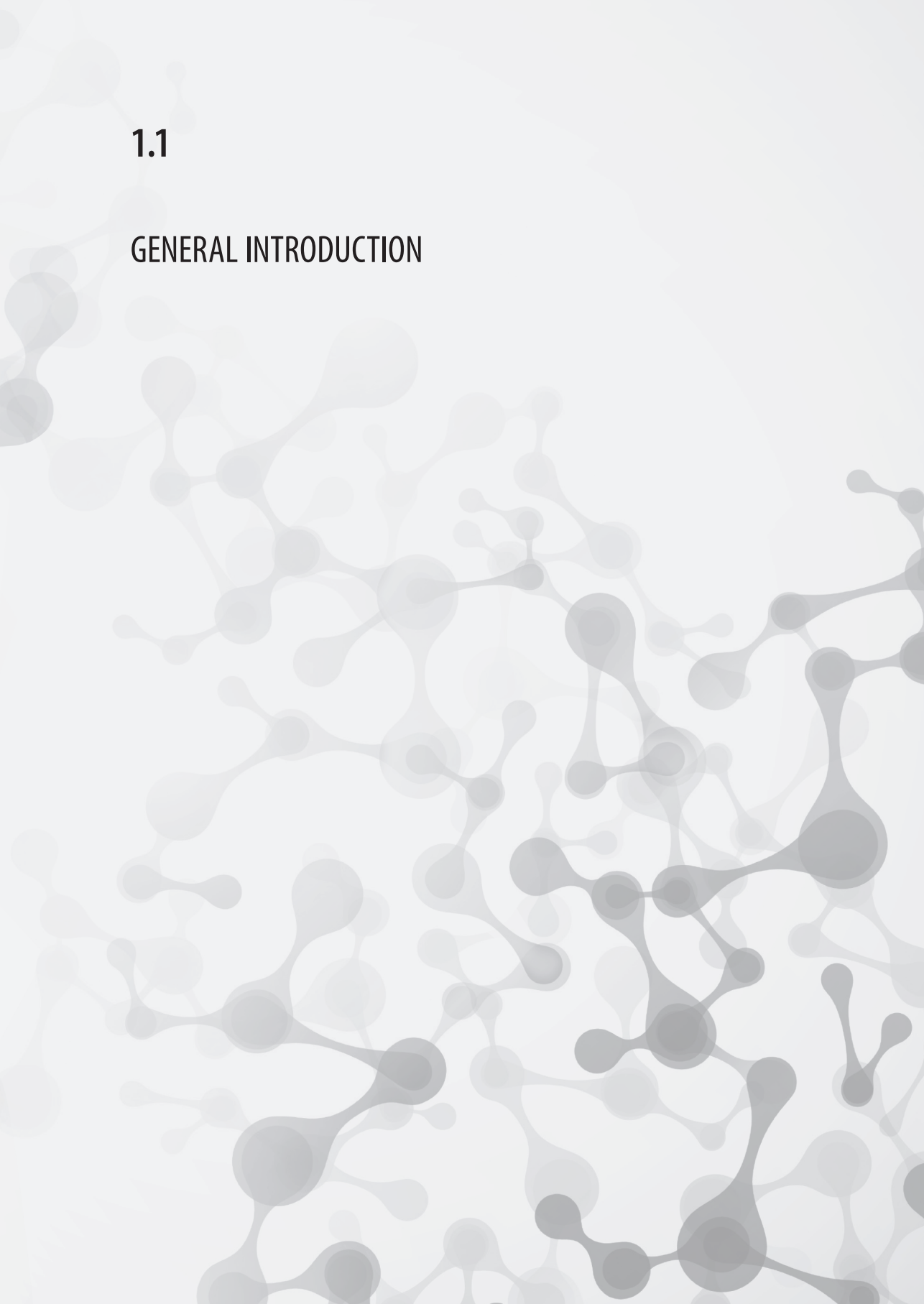
INTRODUCTION





1.1

GENERAL INTRODUCTION



Cancer is often treated with multiple anticancer drugs or hormonal agents in combination with supplemental therapies to prevent or treat side effects¹. In addition, cancer patients often use complementary and alternative medicines (CAM) for various reasons such as reducing side effects of chemotherapy, improving their quality of life and slowing the progression of cancer^{2,3}. The most popular CAM among cancer patients are herbal supplements such as milk thistle, St. John's wort and Echinacea; and dietary supplements such as β -carotene and vitamins^{2,4,5}. In general, the use of CAM is considered safe for patients. However, the concomitant use of anticancer drugs and CAM could result in serious safety problems: undertreatment or increased toxicities. These safety problems are mainly caused by pharmacokinetic interactions.

Almost all pharmacokinetic interactions between CAM and anticancer drugs involve cytochrome P450 (CYP) metabolizing enzymes and drug efflux transporters. Major players in the metabolism and elimination of anticancer drugs are the metabolizing enzymes CYP3A4, CYP2C9 and the drug efflux transporters P-glycoprotein (P-gp; ABCB1) and Breast Cancer Resistance Protein (BCRP; ABCG2)⁶⁻⁹. Both inhibition and induction of these enzymes and transporters by CAM could easily result in altered plasma levels of anticancer drugs and subsequently serious safety problems due to their narrow therapeutic windows.

Clinically relevant pharmacokinetic interactions between St. John's wort and the anticancer drugs irinotecan¹⁰ and imatinib^{11,12} have already been reported. However, clinical pharmacokinetic interactions between other CAM and anticancer drugs are less well documented. Consequently, for the majority of CAM it is unknown whether concomitant use with anticancer drugs is safe. To address this issue it is crucial to expand our knowledge of the effects of CAM on the metabolism and transport of anticancer drugs. In literature, several *in vitro* studies have been performed to determine the effects of CAM on the expression and activity of CYP enzymes and drug efflux transporters. However, the effect of each CAM was often separately determined in different *in vitro* studies. Due to differences in the phytochemical content of CAM products, equipment and personnel, it is not possible to compare the potency of multiple CAM to affect the metabolism and transport of anticancer drugs from the different *in vitro* studies. Furthermore, the majority of the *in vitro* studies assessed the effects of CAM by using one substrate while it has been recommended to use multiple substrates^{13,14}. In these published studies predominantly model substrates have been used and relevant oncolytic substrates were not or scarcely included. However, depending on the substrate used, a compound can significantly differ in its potency to influence the activity of CYP enzymes and drug efflux transporters.

Therefore, this thesis focuses on the *in vitro* potency of the following CAM to affect the metabolism and transport of multiple substrates, in particular anticancer drugs: β -carotene, Echinacea (*Echinacea purpurea*), garlic (*Allium sativum*), green tea (*Camellia sinensis*), *Ginkgo biloba*, ginseng (*Eleutherococcus senticosus*), grape seed (*Vitis vinifera*), milk thistle (*Silybum marianum*), saw palmetto (*Serenoa serrulata*), St. John's wort (*Hypericum perforatum*), valerian (*Valeriana officinalis*), vitamin B₆, B₁₂ and C. This selection is based on the frequency of use by cancer patients and the potential to interact with anticancer drugs^{2-5, 15}. Ultimately, the obtained *in vitro* results are useful as first indication for clinical trials to establish the clinical relevance of potential CAM-anticancer drug interactions.

Since there are large interspecies differences between animals with regard to the regulation of CYP enzymes and drug transporter expression and activity, *in vitro* studies are currently one of the best tools to predict clinical pharmacokinetic interactions between CAM and anticancer drugs. It is therefore important to determine the extrapolatability of *in vitro* data to the clinic. To address this issue in **Chapter 1.2** the *in vitro* and clinical effects of St. John's wort, milk thistle, garlic and ginseng on CYP3A4 have been compared. The selection of these CAM was based on the availability of clinical studies that used the model CYP3A4 substrate midazolam and anticancer drugs, which are scarcely used as CYP3A4 substrates.

Chapter 2 focuses on the pharmacokinetic interactions between CAM and anticancer drugs on the level of drug metabolism. The two major enzymes that are involved in the metabolism of anticancer drugs are CYP3A4 and CYP2C9. The inhibiting effects of CAM on CYP3A4-mediated metabolism of 7-benzyloxy-4-trifluoromethyl-coumarin (BFC) (fluorescent CYP3A4 substrate), midazolam (CYP3A4 model substrate) and docetaxel (CYP3A4 metabolized anticancer drug) are described in **Chapter 2.1**. To support this *in vitro* study, an analytical assay based on liquid-chromatography coupled to tandem mass spectrometry (LC-MS/MS) has been developed and validated to quantify 1-hydroxymidazolam, the major metabolite of midazolam (**Chapter 2.2**). In **Chapter 2.3** the inhibiting effects of CAM on CYP2C9-mediated metabolism of 7-methoxy-4-trifluoromethylcoumarine (MFC) (fluorescent CYP2C9 substrate) and tolbutamide (CYP2C9 model substrate) are discussed.

Besides inhibition of CYP enzymes, the induction of these enzymes can also have serious consequences for cancer patients. Plasma levels of anticancer drugs might decrease, subsequently resulting in a reduced therapeutic efficacy of chemotherapy. **Chapter 3** focuses on the induction of CYP3A4, because this enzyme metabolizes the majority of the anticancer drugs and is highly inducible by various drugs such as rifampicin. More

importantly, multiple anticancer drugs such as paclitaxel and erlotinib are also known to induce CYP3A4. The obtained *in vitro* results from this thesis identified St. John's wort and β -carotene as strong CYP3A4 inducers and Ginkgo biloba as moderate CYP3A4 inducer (**Chapter 3.2**). These findings are in accordance with published results from other *in vitro* studies which also demonstrated St. John's wort, β -carotene and Ginkgo biloba as CYP3A4 inducers¹⁶⁻²³. CYP3A4 induction may result in a reduced efficacy of anticancer drugs and it is therefore important to prevent this process. Since the induction of CYP3A4 is mainly regulated by the Pregnane X Receptor (PXR)^{24,25}, PXR antagonists could inhibit CYP3A4 induction and possibly increase the efficacy of anticancer drugs. In **Chapter 3.1** the known PXR antagonists A-792611²⁶, ketoconazole²⁷, trabectedin²⁸, sulforaphane²⁹, leflunomide³⁰, thymolphtalein³¹ and coumestrol³² were tested in multiple *in vitro* assays in order to rank their inhibitory potencies. Thereafter, the frequently used CAM were evaluated for their ability to inhibit PXR-mediated CYP3A4 induction in order to discover novel potent PXR antagonists in **Chapter 3.2**.

Drug efflux transporters are also frequently involved in pharmacokinetic interactions between CAM and anticancer drugs. Both P-gp and BCRP are expressed in multiple human tumors and play an important role in the transport of a broad spectrum of clinically relevant anticancer drugs. The effects of CAM on P-gp and BCRP mediated transport of the anticancer drugs topotecan and imatinib are presented in **Chapter 4**.

In recent years, not only Western CAM but also Chinese herbs have become more popular among cancer patients³³. Possible pharmacokinetic interactions between Chinese herbs and anticancer drugs, however, have not been well documented. Therefore **Chapter 5** focuses on the effects of Chinese herbs on CYP3A4. In **Chapter 5.1** the *in vitro* inhibition and induction of CYP3A4 by four popular Chinese herbs *Oldenlandia diffusa*, *Codonopsis tangshen*, *Rehmannia glutinosa* and *Astragalus propinquus* is described. Part of these Chinese herbs, *Oldenlandia diffusa* and *Astragalus propinquus*, has been included in a formulation called LCS101 that consists of fourteen different Chinese herbs. The clinical effect of this botanical mixture on conventional chemotherapy complications in breast cancer patients is commented in **Chapter 5.2**.

In summary, the *in vitro* effects of frequently used CAM on CYP3A4/CYP2C9-mediated metabolism and P-gp/BCRP mediated transport of specific model and oncolytic substrates are described in this thesis. In addition, the *in vitro* effects of popular Chinese herbs on the expression and activity of CYP3A4 are presented. The presented results contribute to the knowledge of the potency of CAM to affect the metabolism and transport of anticancer drugs. More importantly, the *in vitro* results are useful for clinical researchers as a first indication for potential pharmacokinetic interactions between CAM and anticancer drugs in cancer patients. Based on the presented data, clinical trials can be conducted to establish the clinical effects of CAM and the clinical relevance of CAM-anticancer drug interactions obtained *in vitro*.

REFERENCES

1. Harmsen S, Meijerman I, Beijnen JH, Schellens JH. Nuclear receptor mediated induction of cytochrome P450 3A4 by anticancer drugs: A key role for the pregnane X receptor. *Cancer Chemother Pharmacol* 2009; 64(1): 35-43.
2. Tascilar M, de Jong FA, Verweij J, Mathijssen RH. Complementary and alternative medicine during cancer treatment: Beyond innocence. *Oncologist* 2006; 11(7): 732-41.
3. Werneke U, Earl J, Seydel C, Horn O, Crichton P, Fannon D. Potential health risks of complementary alternative medicines in cancer patients. *Br J Cancer* 2004; 90(2): 408-13.
4. Gupta D, Lis CG, Birdsall TC, Grutsch JF. The use of dietary supplements in a community hospital comprehensive cancer center: Implications for conventional cancer care. *Support Care Cancer* 2005; 13(11): 912-9.
5. McCune JS, Hatfield AJ, Blackburn AA, Leith PO, Livingston RB, Ellis GK. Potential of chemotherapy-herb interactions in adult cancer patients. *Support Care Cancer* 2004; 12(6): 454-62.
6. Anzenbacher P, Anzenbacherova E. Cytochromes P450 and metabolism of xenobiotics. *Cell Mol Life Sci* 2001; 58(5-6): 737-4.
7. He SM, Yang AK, Li XT, Du YM, Zhou SF. Effects of herbal products on the metabolism and transport of anticancer agents. *Expert Opin Drug Metab Toxicol* 2010; 6(10): 1195-213.
8. Breedveld P, Beijnen JH, Schellens JH. Use of P-glycoprotein and BCRP inhibitors to improve oral bioavailability and CNS penetration of anticancer drugs. *Trends Pharmacol Sci* 2006; 27(1): 17-24.
9. Sharom FJ. ABC multidrug transporters: Structure, function and role in chemoresistance. *Pharmaco-genomics* 2008; 9(1): 105-27.
10. Mathijssen RH, Verweij J, de Bruijn P, Loos WJ, Sparreboom A. Effects of St. John's wort on irinotecan metabolism. *J Natl Cancer Inst* 2002; 94(16): 1247-9.
11. Frye RF, Fitzgerald SM, Lagattuta TF, Hruska MW, Egorin MJ. Effect of St. John's wort on imatinib mesylate pharmacokinetics. *Clin Pharmacol Ther* 2004; 76(4): 323-9.
12. Smith P, Bullock JM, Booker BM, Haas CE, Berenson CS, Jusko WJ. The influence of St. John's wort on the pharmacokinetics and protein binding of imatinib mesylate. *Pharmacotherapy* 2004; 24(11): 1508-14.
13. Miller VP, Stresser DM, Blanchard AP, Turner S, Crespi CL. Fluorometric high-throughput screening for inhibitors of cytochrome P450. *Ann N Y Acad Sci* 2000; 919: 26-32.
14. Wang EJ, Casciano CN, Clement RP, Johnson WW. Active transport of fluorescent P-glycoprotein substrates: Evaluation as markers and interaction with inhibitors. *Biochem Biophys Res Commun* 2001; 289(2): 580-5.
15. Sparreboom A, Cox MC, Acharya MR, Figg WD. Herbal remedies in the United States: Potential adverse interactions with anticancer agents. *J Clin Oncol* 2004; 22(12): 2489-503.
16. Gutmann H, Poller B, Buter KB, Pfrunder A, Schaffner W, Drewe J. *Hypericum perforatum*: Which constituents may induce intestinal MDR1 and CYP3A4 mRNA expression? *Planta Med* 2006; 72(8): 685-90.
17. Moore LB, Goodwin B, Jones SA, Wisely GB, Serabjit-Singh CJ, Willson TM, Collins JL, Kliever SA. St. John's wort induces hepatic drug metabolism through activation of the pregnane X receptor. *Proc Natl Acad Sci USA* 2000; 97(13): 7500-2.
18. Godtel-Armbrust U, Metzger A, Kroll U, Kelber O, Wojnowski L. Variability in PXR-mediated induction of CYP3A4 by commercial preparations and dry extracts of St. John's wort. *Naunyn Schmiedebergs Arch Pharmacol* 2007; 375(6): 377-82.

19. Wang K, Mendy AJ, Dai G, Luo HR, He L, Wan YJ. Retinoids activate the RXR/SXR-mediated pathway and induce the endogenous CYP3A4 activity in Huh7 human hepatoma cells. *Toxicol Sci* 2006; 92(1): 51-60.
20. Ruhl R, Sczech R, Landes N, Pfluger P, Kluth D, Schweigert FJ. Carotenoids and their metabolites are naturally occurring activators of gene expression via the pregnane X receptor. *Eur J Nutr* 2004; 43(6): 336-43.
21. Li L, Stanton JD, Tolson AH, Luo Y, Wang H. Bioactive terpenoids and flavonoids from *Ginkgo biloba* extract induce the expression of hepatic drug-metabolizing enzymes through pregnane X receptor, constitutive androstane receptor, and aryl hydrocarbon receptor-mediated pathways. *Pharm Res* 2009; 26(4): 872-8.
22. Satsu H, Hiura Y, Mochizuki K, Hamada M, Shimizu M. Activation of pregnane X receptor and induction of MDR1 by dietary phytochemicals. *J Agric Food Chem* 2008; 56(13): 5366-73.
23. Yeung EY, Sueyoshi T, Negishi M, Chang TK. Identification of *Ginkgo biloba* as a novel activator of pregnane X receptor. *Drug Metab Dispos* 2008; 36(11): 2270-6.
24. Harmsen S, Koster AS, Beijnen JH, Schellens JH, Meijerman I. Comparison of two immortalized human cell lines to study nuclear receptor-mediated CYP3A4 induction. *Drug Metab Dispos* 2008; 36(6): 1166-71.
25. Pascussi JM, Gerbal-Chaloin S, Drocourt L, Maurel P, Vilarem MJ. The expression of CYP2B6, CYP2C9 and CYP3A4 genes: A tangle of networks of nuclear and steroid receptors. *Biochim Biophys Acta* 2003; 1619(3): 243-5.
26. Healan-Greenberg C, Waring JF, Kempf DJ, Blomme EA, Tirona RG, Kim RB. A human immunodeficiency virus protease inhibitor is a novel functional inhibitor of human pregnane X receptor. *Drug Metab Dispos* 2008; 36(3): 500-7.
27. Huang H, Wang H, Sinz M, Zoeckler M, Staudinger J, Redinbo MR, Teotico DG, Locker J, Kalpana GV, Mani S. Inhibition of drug metabolism by blocking the activation of nuclear receptors by ketoconazole. *Oncogene* 2007; 26(2): 258-6.
28. Synold TW, Dussault I, Forman BM. The orphan nuclear receptor SXR coordinately regulates drug metabolism and efflux. *Nat Med* 2001; 7(5): 584-90.
29. Zhou C, Poulton EJ, Grun F, Bammler TK, Blumberg B, Thummel KE, Eaton DL. The dietary isothiocyanate sulforaphane is an antagonist of the human steroid and xenobiotic nuclear receptor. *Mol Pharmacol* 2007; 71(1): 220-9.
30. Ekins S, Kholodovych V, Ai N, Sinz M, Gal J, Gera L, Welsh WJ, Bachmann K, Mani S. Computational discovery of novel low micromolar human pregnane X receptor antagonists. *Mol Pharmacol* 2008; 74(3): 662-7.
31. Dring AM, Anderson LE, Qamar S, Stoner MA. Rational quantitative structure-activity relationship (RQSAR) screen for PXR and CAR isoform-specific nuclear receptor ligands. *Chem Biol Interact* 2010; 188(3): 512-25.
32. Wang H, Li H, Moore LB, Johnson MD, Maglich JM, Goodwin B, Itoop OR, Wisely B, Creech K, Parks DJ, et al. The phytoestrogen coumestrol is a naturally occurring antagonist of the human pregnane X receptor. *Mol Endocrinol* 2008; 22(4): 838-57.
33. Youns M, Hoheisel JD, Efferth T. Toxicogenomics for the prediction of toxicity related to herbs from traditional Chinese medicine. *Planta Med* 2010; 76(17): 2019-25.



1.2

RELEVANCE OF *IN VITRO* AND CLINICAL DATA FOR PREDICTING CYP3A4-MEDIATED HERB-DRUG INTERACTIONS IN CANCER PATIENTS

K.D. Mooiman *

A.K.L. Goey *

J.H. Beijnen

J.H.M. Schellens

I. Meijerman

* These authors contributes equally

Published in Cancer Treatment Reviews 2013; 39(7): 773-783

ABSTRACT

The use of complementary and alternative medicines (CAM) by cancer patients is increasing. Concomitant use of CAM and anticancer drugs could lead to serious safety issues in patients. CAM have the potential to cause pharmacokinetic interactions with anticancer drugs, leading to either increased or decreased plasma levels of anticancer drugs. This could result in unexpected toxicities or a reduced efficacy. Significant pharmacokinetic interactions have already been shown between St. John's wort (SJW) and the anticancer drugs imatinib and irinotecan.

Most pharmacokinetic CAM-drug interactions involve drug metabolizing cytochrome P450 (CYP) enzymes, in particular CYP3A4. The effect of CAM on CYP3A4 activity and expression can be assessed *in vitro*. However, no data have been reported yet regarding the relevance of these *in vitro* data for the prediction of CAM-anticancer drug interactions in clinical practice. To address this issue, a literature research was performed to evaluate the relevance of *in vitro* data to predict clinical effects of CAM frequently used by cancer patients: SJW, milk thistle, garlic and *Panax ginseng* (*P. ginseng*). Furthermore, in clinical studies the sensitive CYP3A4 substrate probe midazolam is often used to determine pharmacokinetic interactions. Results of these clinical studies with midazolam are used to predict pharmacokinetic interactions with other drugs metabolized by CYP3A4. Therefore, this review also explored whether clinical trials with midazolam are useful to predict clinical pharmacokinetic CAM-anticancer drug interactions.

In vitro data of SJW have shown CYP3A4 inhibition after short-term exposure and induction after long-term exposure. In clinical studies using midazolam or anticancer drugs (irinotecan and imatinib) as known CYP3A4 substrates in combination with SJW, decreased plasma levels of these drugs were observed, which was expected as a consequence of CYP3A4 induction. For garlic, no effect on CYP3A4 has been shown *in vitro* and also in clinical studies garlic did not affect the pharmacokinetics of both midazolam and docetaxel.

Milk thistle and *P. ginseng* predominantly showed CYP3A4 inhibition *in vitro*. However, in clinical studies these CAM did not cause significant pharmacokinetic interactions with midazolam, irinotecan, docetaxel and imatinib. Most likely, factors as poor pharmaceutical availability, solubility and bioavailability contribute to the lack of significant clinical interactions.

In conclusion, *in vitro* data are useful as a first indication for potential pharmacokinetic drug interactions with CAM. However, the discrepancies between *in vitro* and clinical results for milk thistle and *P. ginseng* show that clinical studies are required for confirmation of potential interactions. At last, midazolam as a model substrate for CYP3A4, has convincingly shown to correctly predict clinical interactions between CAM and anticancer drugs.

INTRODUCTION

The use of complementary and alternative medicines (CAM) is popular among cancer patients. For example, 75% of colorectal cancer patients¹, 90% of prostate cancer patients² and 91% of pediatric cancer patients³ have been reported to use CAM. The most popular CAM among cancer patients are herbal supplements and vitamins⁴. Cancer patients use these CAM in combination with their conventional therapies for different reasons, such as reducing side effects of chemotherapy, slowing progression of cancer, and improving quality of life^{5,6}.

The concomitant use of anticancer drugs and CAM, however, could lead to serious safety issues in cancer patients, as CAM have the potential to cause pharmacokinetic and -dynamic interactions with anticancer drugs^{4,7-9}. Especially for anticancer drugs, which have narrow therapeutic windows, pharmacokinetic interactions could easily lead to clinically relevant effects. Decreased or increased plasma levels of these drugs could result in a lower therapeutic efficacy or a higher risk of toxicity^{4,5}. Clinically relevant pharmacokinetic interactions between anticancer drugs and CAM have already been reported between the frequently used CAM St. John's wort (SJW) and the anticancer drugs irinotecan¹⁰ and imatinib^{11,12}.

Almost all pharmacokinetic CAM-anticancer drug interactions involve cytochrome P450 (CYP) metabolizing enzymes, drug transporters (e.g. P-glycoprotein), and other metabolic pathways⁶. The majority of currently prescribed anticancer drugs is metabolized by CYP3A4¹³. For anticancer drugs such as docetaxel, erlotinib, imatinib, irinotecan, paclitaxel and vincristine, CYP3A4 is the main CYP enzyme involved in their metabolism.

Several *in vitro* and clinical studies have been performed to determine the effects of CAM on CYP3A4. However, no data have been reported regarding the predictive value of these *in vitro* data for clinical CAM-anticancer drug interactions. Therefore, the main focus of this review is to determine the relevance of *in vitro* data to predict clinical pharmacokinetic CAM-anticancer drug interactions. To address this issue, a literature research was performed to evaluate *in vitro* and clinical effects on CYP3A4 by frequently used CAM: SJW, milk thistle, garlic and *Panax ginseng* (*P. ginseng*). This selection is based on the high frequency of use by cancer patients and the availability of both *in vitro* and clinical data regarding pharmacokinetic CAM-drug interactions. As there are large inter-species differences in the regulation of CYP3A expression and activity¹⁴, animal data are not included in this review.

In clinical studies, the sensitive CYP3A4 substrate probe midazolam is often used to determine pharmacokinetic interactions¹⁵. The second focus of this review was therefore to assess the relevance of clinical trials with midazolam to predict clinical pharmacokinetic interactions between CAM and anticancer drugs.

METHODS TO INVESTIGATE PHARMACOKINETIC CAM-DRUG INTERACTIONS

The following chapters will provide an overview of *in vitro* and clinical effects of CAM on CYP3A4 activity and expression. To facilitate the interpretation of these *in vitro* and clinical results, the methods to determine *in vitro* and clinical pharmacokinetic interactions will be described briefly.

***In vitro* inhibition assays of CYP3A4**

To determine the inhibiting effect of CAM on CYP3A4 activity, different *in vitro* test systems can be used: cultured cell lines, human liver microsomes (subcellular fractions of a human liver consisting of smooth endoplasmic reticulum vesicles containing the main CYP enzymes)^{16, 17}, Supersomes™ (human lymphoblast cells containing an overexpression of CYP enzymes)¹⁸ and primary human hepatocytes¹⁹. The use of microsomes and Supersomes™ is preferred and recommended by the Food and Drug Administration (FDA)²⁰⁻²². Compared to cell lines and hepatocytes, microsomes and Supersomes™ are commercially available and the results obtained by these test systems are not confounded by cellular uptake or other intracellular metabolic processes.²⁰ A drawback of microsomes and Supersomes™ is that they do not completely mimic the physiological hepatic environment²⁰.

The ability of CAM to inhibit CYP3A4 activity is determined by treating cells, microsomes, Supersomes™ or hepatocytes with a CYP3A4 substrate in the absence or presence of CAM or potent CYP3A4 model inhibitors (preferably ketoconazole²⁰). The amount of CYP3A4 inhibition is established by determining changes in the metabolism of model substrates of CYP3A4 by monitoring the decrease of metabolite formation. For quantification of the metabolites, two standard assays are frequently used: liquid chromatography coupled with tandem mass spectrometry (LC-MS/MS) or a fluorescence assay. Although a fluorescence assay is fast, cost-effective and sensitive, LC-MS/MS is preferred²³, because of the higher sensitivity and specificity²⁴. Other disadvantages of the fluorescence assay are the possible interference of fluorescence (quenching) by CAM and inadequate selectivity of many CYP substrate probes. These substrate probes are often also metabolized by other CYP enzymes, besides CYP3A4. Recombinantly expressed single CYP enzymes (Supersomes™) can be used to overcome this selectivity problem²³. For LC-MS/MS, preferred CYP3A4 substrates are midazolam and testosterone²⁰. For the fluorescence assay, four fluorescence substrates have been reported useful in screening CYP3A4 inhibition: 7-benzyloxyquinoline (BQ), 7-benzyloxy-4-trifluoromethylcoumarin (BFC), dibenzyl-fluorescein (DBF) and 7-benzyloxyresorufin (BzRes). BFC and DBF are preferred substrates, as the incubation time and total amount of CYP3A4 required are lower compared to BQ and BzRes²⁵. The amount of CYP3A4 inhibition is usually expressed as IC_{50} , the concentration required to achieve 50% of the maximum inhibition.

It is important to realize that CYP3A4 inhibition is system-dependent²¹. Different test systems deviate in their interaction with CAM, which can result in under- or overprediction of CYP3A4 inhibition. Therefore, it is recommended to combine multiple test systems and methods of quantification to confirm CYP3A4 inhibition by CAM. However, in the majority of the reported *in vitro* studies in literature only one test system was used.

***In vitro* induction assays of CYP3A4**

Besides inhibition of CYP3A4 by CAM, CAM can also induce this CYP enzyme by affecting the gene expression of CYP3A4. CYP3A4 gene expression is mainly regulated by the nuclear pregnane X receptor (PXR)²⁶. Activation of PXR results in transcription of the CYP3A4 gene and CYP3A4 induction. Primary human hepatocytes are the most accepted and reliable *in vitro* test system to evaluate CYP3A4 induction by CAM. However, major drawbacks are high costs, poor availability and rapid decrease in CYP expression^{22,27}. Alternatively, cultured cell lines are commonly used, such as the human hepatocarcinoma derived cell line HepG2, the human colon carcinoma derived cell line LS180²⁷, and a novel primary human hepatocyte clone, the Fa2N-4 cell line. Disadvantages of the use of cell lines compared to primary hepatocytes are: lower expression of CYP enzymes, lower basal enzyme activities and absence of all phenotypic characteristics of human hepatocytes, such as receptor function and expression²³.

To determine CYP3A4 induction by CAM, hepatocytes or cell lines are treated with CAM or a model inducer (preferably rifampicin²⁰). The amount of CYP3A4 induction can be quantified by two frequently used standard assays: detecting mRNA levels using real-time polymerase chain reaction (RT-PCR) and the protein expression assay using Western blotting. However, it is complicated to demonstrate CYP3A4 induction at the level of gene and protein expression, due to low levels of CYP3A4 in cell lines and the rapid decrease in CYP3A4 levels in hepatocytes²⁷. An assay without these limitations is the reporter gene assay. In this assay, transfected cell lines are used in which a luminescent signal can be measured proportional to PXR-mediated CYP3A4 gene induction^{20, 22, 27}. Despite the fact that PXR is artificially increased in this assay, CYP3A4 induction measured by the reporter gene assay has been shown to correlate with CYP3A4 gene and protein expression in human hepatocytes²⁷.

Changes in CYP3A4 gene or protein expression do not necessarily lead to changes in the activity of this enzyme. Therefore, it is also important to determine the effect of CAM on CYP3A4 activity, which is mostly done with LC-MS/MS or a fluorescence assay as described above²⁰.

Overall, similar to the determination of CYP3A4 inhibition it is also important to confirm CYP3A4 induction by CAM with multiple test systems and methods of quantification.

Clinical pharmacokinetic interaction studies

If *in vitro* data reveal significant inhibition or induction of CYP enzymes by CAM, clinical studies are often conducted to determine the presence of pharmacokinetic interactions in humans. Several factors are involved in the execution of clinical interaction studies, such as study design, chosen probe drugs, and pharmacokinetic endpoints.

To compare plasma concentrations of a CYP3A4 substrate (S, midazolam) with and without interacting drug (I, CAM) the following study designs can be applied: randomized crossover (S followed by S + I, S + I followed by S), one-sequence crossover (S followed by S + I (or reversed)) and a parallel design (S in group 1, S + I in group 2)²². In each of these study designs midazolam plasma concentrations with and without CAM are compared²². Of these study designs, a randomized crossover design should be preferred over a one-sequence design to correct for sequence, period and carry-over effects²⁸. The majority of the clinical studies described in this review have applied a one-sequence crossover design.

The most sensitive CYP substrates should be selected for clinical interaction studies. A CYP substrate is considered "sensitive" when its area under the plasma concentration-time curve (AUC) increases ≥ 5 -fold when co-administered with a potent CYP inhibitor²². For CYP3A4, oral midazolam is a recommended sensitive substrate²², as CYP3A4 plays a major role in the biotransformation of midazolam to its metabolites 1-hydroxy- and 4-hydroxymidazolam²⁹.

After selection of the study design and a sensitive CYP3A4 substrate, an appropriate pharmacokinetic endpoint should be chosen. Frequently, pharmacokinetic exposure parameters such as the AUC and the maximum plasma concentration (C_{max}) are main endpoints. Occasionally, the pre- and postsupplementation phenotypic ratio of 1-hydroxymidazolam to midazolam is determined^{30,31}, which provides a useful estimate of midazolam clearance³². The AUC, however, more accurately reflects systemic drug exposure and is therefore a recommended pharmacokinetic parameter for drug interaction studies^{17,22}. Strong inhibitors of CYP3A4 will cause ≥ 5 -fold increase of midazolam AUC, while moderate (≥ 2 - and < 5 -fold increase) or weak (1.25- and < 2 -fold increase) CYP3A4 inhibitors will cause less significant elevations of the AUC of midazolam.

As anticancer drugs and midazolam may differ in their affinity for CYP3A4, interaction studies with CAM and anticancer drugs have to confirm the results obtained by midazolam. By comparing the results of CAM with midazolam and anticancer drugs, it is possible to determine the predictive value of midazolam as model substrate for pharmacokinetic interactions.

COMPARISON BETWEEN *IN VITRO* AND CLINICAL DATA ABOUT CAM-DRUG INTERACTIONS

The following paragraphs provide an overview of the *in vitro* and clinical effects of popular CAM (St. John's wort, milk thistle, garlic and *P. ginseng*) on CYP3A4. For each CAM the predictive value of *in vitro* data for the clinic will be discussed. Additionally, the clinical use of the CYP3A4 probe midazolam to predict CYP3A4-mediated interactions between CAM and anticancer drugs in humans will be assessed.

St. John's wort

St. John's wort (*Hypericum perforatum*, SJW), used for treatment of mild to moderate depression³³, is a popular herbal medicine among cancer patients¹⁰. According to a survey among cancer patients, SJW belongs to the top 10 of used CAM⁶.

In vitro effects of SJW on CYP3A4 and drug metabolism

Several *in vitro* studies have been performed to determine the effects of SJW and its main components hyperforin, hypericin and quercitrin on CYP3A4 (**Table 1A**)³³. CYP3A4 mediated metabolism of midazolam and testosterone was inhibited by hyperforin, hypericin and I3-II8-biapigenin in microsomes^{34, 35}. SJW extract inhibited CYP3A4 activity in SupersomesTM³⁶. Hypericin also inhibited CYP3A4 activity in baculosomes (insect cells containing an overexpression of CYP enzymes¹⁸) and CYP3A4-mediated metabolism of cortisol in microsomes³⁷.

Reviewing these *in vitro* studies, CYP3A4 inhibition by SJW has been shown in the preferred test systems (microsomes or SupersomesTM) and should be considered as relevant. The IC₅₀ values (0.038 – 17.2 μM) of SJW main components are comparable to an average IC₅₀ value (0.03 μM) of the potent CYP3A4 inhibitor ketoconazole³⁸.

Besides CYP3A4 inhibition by SJW also CYP3A4 induction was shown in multiple *in vitro* studies. In LS180 cells hypericin, hyperforin and quercitrin induced CYP3A4 mRNA expression³³. Accordingly, the inducing effect of SJW extract and hyperforin on CYP3A4 mRNA expression has been demonstrated in hepatocytes^{26, 39}. Hyperforin also induced CYP3A4 protein expression and activity and increased the metabolism of docetaxel in hepatocytes^{39, 40}. Induction of PXR-mediated CYP3A4 expression by the standardized SJW extract has been demonstrated in LS180 cells using a CYP3A4 reporter gene assay by our research group²⁷. The extent of CYP3A4 induction by SJW and its main component hyperforin is comparable to the induction by the potent inducer rifampicin^{26, 33, 39} and should therefore be considered as relevant.

Overall, both CYP3A4 inhibition and induction by SJW and its main components has been demonstrated. Whether inhibition or induction occurs, may depend on the duration of incubation with SJW. Inhibition of CYP3A4 by SJW was observed with incubation

Table 1A. Effect of SJW on the activity of CYP3A4 *in vitro*.

Models	CAM/component	SJW product	Assay	Results	Ref.
LS180 cells	10 μ M hyperforin	Phytoflan, Heidelberg Germany		7 times \uparrow mRNA	
	10 μ M hypericin	Sigma, Buchs Switzerland	RT-PCR	11 times \uparrow mRNA	33
	10 μ M quercitrin	Extrasynthèse, Genay, France		7 times \uparrow mRNA	
Human hepatocytes	1 μ M hyperforin and 7-75 μ g/mL SJW extract	Apin Chemicals Limited, Abingdon, UK 1. Nature's Way Products, Springville, USA 2. Nature's Plus, Melville, USA 3. Nutraceutical, Park City, USA	Reporter gene assay	6-7 times \uparrow mRNA	26
	1-2.5 μ M hyperforin	(Purified from SJW leaf/flower mixtures and identified)	RT-PCR, Western blotting and HPLC- UV (testosterone)	\uparrow mRNA, protein, CYP3A4 activity (by hyperforin)	39
	0.2-1 μ M hypericin	Sigma-Aldrich, St. Louis, USA	RT-PCR, Western blotting and HPLC- UV (testosterone)	\leftrightarrow mRNA, protein, CYP3A4 activity (by hypericin)	39
	0.1-1.5 μ M hyperforin	(Purified from SJW leaf/flower mixtures and identified)	LC-MS (docetaxel)	2.6-7 times \uparrow CYP3A4 activity	40
	0.1-100 μ M hyperforin	Phytolab GmbH, Vestenbergsgreuth, Germany	LC-MS (midazolam and testosterone)	\downarrow CYP3A4 activity IC_{50} = resp. 9.6 μ M and 8.4 μ M	34
HLM	hypericin	BIOMOL, Plymouth Meeting, USA			
	hyperforin, 13-118-biapiogenin	Isolated and purified from commercial SJW products: Centrum Herbals, Madison or Quanterra, Morris Plains, USA	HPLC-MS (testosterone)	\downarrow CYP3A4 activity K_i = resp. 4.2; 0.49 and 0.038 μ M	35
Rat liver microsomes	50 μ M hypericin	Sigma Chemical Co., St. Louis, USA	HPLC-UV (cortisol)	35% \downarrow CYP3A4 activity	37
Baculosomes	50 μ M hypericin	Sigma Chemical Co., St. Louis, USA	Fluorescence assay (Vivid red)	\downarrow CYP3A4 activity IC_{50} = 868 nM	37
Supersomes™	0.39-850 μ g/mL SJW extract	Hypericum Stada®, Bad Vilbel, Germany	Fluorescence assay (BQ and BFC)	\downarrow CYP3A4 activity IC_{50} = resp. 10.3 and 11.8 μ M	36
	8-400 μ g/mL SJW extract	Hypericum Stada®, Bad Vilbel, Germany	HPLC-UV (testosterone)	\downarrow CYP3A4 activity IC_{50} = 17.2 μ M	36

Abbreviations: HLM, human liver microsomes; RT-PCR, real-time polymerase chain reaction; HPLC-UV, high-performance liquid chromatography with ultraviolet detection; LC-MS, liquid chromatography mass spectrometry; BQ, 7-benzyloxyquinoline; BFC, 7-benzyloxy-4-trifluoromethylcoumarin; IC_{50} , half maximal inhibitory concentration; K_i , *in vitro* inhibition constant; \leftrightarrow , unchanged; \downarrow , decrease and \uparrow , increase.

times of 10-60 min³⁴⁻³⁷, whereas induction was found after incubation with SJW for at least 30-96 h^{26, 27, 33, 39, 40}. Inhibition after short-term incubation could be explained by competitive inhibition⁷, as hyperforin has been reported as a competitive inhibitor of CYP3A4³⁵. Induction is expected after prolonged exposure, as the SJW constituent hyperforin activates PXR-mediated CYP3A4 gene transcription and causes CYP3A4 induction²⁶. In clinical practice, SJW is generally administered for a prolonged period of time and therefore CYP3A4 induction is more likely to occur than inhibition.

Clinical pharmacokinetic interactions between SJW and midazolam

Several studies have been reported about clinical pharmacokinetic interactions between SJW and midazolam in healthy volunteers (**Table 1B**). In these studies a one-sequence crossover design was applied: midazolam administration was followed by SJW supplementation after which subjects received the second administration of midazolam. In accordance with the *in vitro* data, induction of CYP3A4 after supplementation with SJW (300-500 mg extract two or three times daily) has been observed in all of these studies, regardless of the pharmacokinetic endpoint (AUC, clearance, phenotypic ratio), brand of SJW extract, duration of SJW supplementation (10 days - 8 weeks), subjects' age or ethnicity.

Interestingly, SJW has a more potent inductive effect on intestinal CYP3A4 than on CYP3A4 located in the liver. This has been shown by studies administering both oral and intravenous (IV) midazolam: the increase of clearance of midazolam was greater after oral administration⁴¹⁻⁴⁴. This finding suggests that oral CYP3A4 substrates (both intestinal and hepatic CYP3A4 involved) are more susceptible to CYP3A4 induction by SJW than IV substrates (predominantly hepatic CYP3A4 involved).

Furthermore, the magnitude of CYP3A4 induction by a SJW product depends on its hyperforin content⁴⁵, which has shown to be the main SJW constituent responsible for induction in *in vitro* studies^{26, 33, 39}. This has been demonstrated by a study in which a SJW product with low hyperforin content did not significantly decrease the AUC of midazolam⁴⁶.

Overall, clinical interaction studies with SJW and midazolam showed that SJW significantly induced CYP3A4 (primarily intestinal CYP3A4), resulting in a decreased bioavailability of the orally taken model substrate midazolam. Thus, *in vitro* results demonstrating CYP3A4 induction by SJW^{26, 33, 39} were extrapolatable to the clinical setting with midazolam.

Clinical pharmacokinetic interactions between SJW and anticancer drugs

For cancer patients it is important to be aware of potential pharmacokinetic interactions between SJW and anticancer drugs. Based on the interaction between SJW and midazolam, pharmacokinetic interactions with anticancer drugs metabolized by CYP3A4

Table 1B. Effect of SJW on the pharmacokinetics of selected substrate drugs in healthy volunteers and patients.

Subjects	Dose SJW	SJW Product	Substrate	Results	Ref.
	300 mg (0.3% hypericin), thrice daily, 14 days	Sundown Herbals, Boca Raton, USA	MDZ (P.O., IV)	52% ↓ AUC _{0-∞} oral MDZ, 21% ↓ AUC _{0-∞} IV MDZ	41
	300 mg (0.3% hypericin), thrice daily, 8 weeks	Rexall-Sundown Pharmaceuticals, Boca Raton, USA	MDZ (P.O., IV)	53% ↑ CL oral MDZ, 3% ↑ CL IV	42
Healthy volunteers (n=12)	300 mg, thrice daily, 14 days	TruNature, Leiner Health Products, Carson, USA	MDZ (P.O.)	33% ↑ CL oral MDZ, baseline CL MDZ restored 7 days after completion	86
	300 mg (0.3% hypericin), thrice daily, 28 days	Vitamer, Lake Forest, USA	MDZ (P.O.)	141% ↑ 1-OH MDZ / MDZ serum ratio	30
	300 mg (0.3% hypericin), thrice daily, 28 days	Wild Oats Markets, Inc, Boulder, USA	MDZ (P.O.)	98% ↑ 1-OH MDZ / MDZ serum ratio	31
Healthy volunteers (n=20)	500 mg, twice daily, 14 days	Kneipp Werke, Würzburg, Germany	MDZ (P.O.)	15% ↓ AUC _{0-∞} oral MDZ	46
Healthy volunteers (n=21)	300 mg (0.3% hypericin), thrice daily, 12 days	Jarsin 300 dragée, LI 160, Lichtwer Pharma AG, Berlin, Germany	MDZ (P.O., IV)	168% ↑ CL oral MDZ 44% ↑ CL IV MDZ	43
Healthy volunteers (n=30)	300 mg, thrice daily, 10 days	Unknown	MDZ (P.O., IV)	190% ↑ CL oral MDZ 56% ↑ CL IV MDZ	44
Healthy volunteers (n=42)	300-900 mg, twice/ thrice daily, 14 days	1: Jarsin 300 dragée, LI 160, Lichtwer Pharma AG, Berlin, Germany 2A: Type A, Kneipp Werke, Würzburg, Germany 2B: Kneipp Johanniskraut Dragees H, Kneipp Werke, Würzburg, Germany	MDZ (P.O.)	↓ AUC oral MDZ (sign. correlation with hyperforin content)	45
Cancer patients (n=5)	300 mg, thrice daily, 18 days	Bio Nutrition Health Products, Den Bosch, The Netherlands	Irinotecan (IV)	42% ↓ AUC SN-38, ↓ myelosuppression	10
Healthy volunteers (n=12)	300 mg, thrice daily, 14 days	Kira, LI 160, Lichtwer Pharma AG, Berlin, Germany	Imatinib (P.O.)	30% ↓ AUC _{0-∞}	12
Healthy volunteers (n=10)	300 mg, thrice daily, 14 days	HBC Inc., Los Angeles, USA	Imatinib (P.O.)	32% ↓ AUC _{0-∞}	11

Abbreviations: P.O., oral administration; IV, intravenous administration; 1-OH MDZ, 1-hydroxymidazolam; MDZ, midazolam; CL, total plasma clearance; AUC_{0-∞}, area under the plasma concentration-time curve from time zero to infinity; ↓, decrease and ↑, increase.

could be expected. Thus far, the effect of SJW on the pharmacokinetics of anticancer drugs has been investigated for irinotecan¹⁰ and imatinib^{11,12} (**Table 1B**).

In a randomized crossover study five cancer patients were treated with irinotecan (350 mg/m², IV) and SJW¹⁰. In irinotecan's metabolism CYP3A4 mediates the formation of the parent drug to the metabolites APC and NPC. NPC is then converted by human carboxylesterase 2 to the active metabolite SN-38, which is subsequently glucuronidized to SN-38G by UDP glucuronosyl transferases. Drug transporters such as P-gp and Breast Cancer Resistance Protein are involved in the elimination of irinotecan⁴⁷. In accordance to the CYP3A4 induction in midazolam studies, SJW significantly decreased the AUC of irinotecan's active metabolite SN-38 by 42%. Consequently, there was also a substantial difference in the degree of myelosuppression: the decrease of leukocyte and neutrophil counts was greater after irinotecan alone compared to the course with irinotecan and SJW combined.

In a one-sequence crossover study including twelve healthy subjects, fourteen days of SJW intake also decreased systemic exposure to imatinib¹², which is mainly metabolized by CYP3A4 to the active N-desmethylated piperazine derivative (CGP74588). In the presence of SJW the AUC_{0-∞} of imatinib (400 mg/day) was significantly decreased by 30%. Similar results were observed in another one-sequence crossover trial with SJW and imatinib¹¹. In this trial two weeks of SJW supplementation resulted in a significant 32% reduction of the AUC of imatinib. In addition, according to bioequivalence criteria the interactions in both imatinib trials were shown to be clinically relevant^{11,12}.

The results with the anticancer drugs were in accordance with the clinical interaction studies with midazolam. Hence, midazolam has been shown to be a good predictor for CYP3A4-based interactions between SJW and anticancer drugs.

Milk thistle

Milk thistle (*Silybum marianum*) is the fourth most popular herbal medicine among cancer patients⁶. Milk thistle is supposed to have anti-oxidative, anti-inflammatory, anti-fibrotic, liver regenerating and anti-lipid-peroxidative effects. It is commonly used for gastrointestinal disturbances or diseases of the liver or biliary tract^{48,49}. Milk thistle contains silymarin, which is a mixture of at least seven flavonolignans and one flavonoid. The main constituent of silymarin is the flavonolignan silibinin⁵⁰.

***In vitro* effects of milk thistle on CYP3A4 and drug metabolism**

To determine the effect of milk thistle on CYP3A4, several *in vitro* studies have been performed (**Table 2A**). The inhibitory effect of the milk thistle extract, silymarin and silibinin on CYP3A4 activity has been demonstrated in microsomes⁵¹⁻⁵⁵. In hepatocytes silymarin also inhibited CYP3A4 activity⁵⁶. Furthermore, inhibition of CYP3A4 activity by silibinin was demonstrated in *Escherichia Coli* MV1304 cells⁵⁷. The extent of CYP3A4 inhibition by

milk thistle, silymarin and silibinin (IC_{50} 's of 27-60 μM ⁵³⁻⁵⁵) is moderate to weak compared to ketoconazole (IC_{50} of 0.03 μM ³⁸).

Furthermore, silibinin had no effect on CYP3A4 activity in baculosomes³⁷ and on CYP3A4 mRNA and protein expression in hepatocytes⁵⁸, although sufficient concentrations (0-100 μM) of silibinin were examined. In Caco-2 cells (human adenocarcinoma colon cells), both milk thistle extract and silibinin inhibited CYP3A4 mRNA expression, but their effects on CYP3A4 protein expression were conflicting: milk thistle caused a decreased expression, while silibinin caused an increased expression of CYP3A4⁵⁹.

Overall, the majority of *in vitro* studies showed inhibition of CYP3A4 by milk thistle. Based on these findings, it is interesting to investigate whether milk thistle also inhibits CYP3A4 in the clinic.

Clinical pharmacokinetic interactions between milk thistle and midazolam

Two one-sequence crossover studies have been performed with milk thistle and oral midazolam (**Table 2B**). In the first study with twelve healthy volunteers, a 28-day supplementation of 175 mg milk thistle twice daily (standardized to 80% silymarin) did not significantly affect the pre- and postsupplementation metabolic ratio of 1-hydroxymidazolam/midazolam⁶⁰. Accordingly, in a later interaction study fourteen days of milk thistle intake (300 mg, three times daily, standardized to 80% silymarin) did not influence the AUC of midazolam or the metabolic ratio of 1-hydroxymidazolam/midazolam⁶¹. A lack of clinical CYP3A4 inhibition could be related to the low bioavailability of silymarin (including silibinin), which is the component responsible for CYP3A4 inhibition *in vitro*⁶⁰⁻⁶². Silymarin has been shown to be practically insoluble in water, and in *in vitro* studies it was dissolved in the organic solvents dimethyl sulfoxide (DMSO) or methanol. Unfortunately, the bioavailability of silymarin was not measured in the two reported milk thistle-midazolam studies.

The reported data indicate that commercially available milk thistle products, dosed as 175 – 300 mg two-three times daily, do not significantly alter clinical CYP3A4 activity. Thus, the observed inhibition of CYP3A4 by milk thistle *in vitro* could not be reproduced in clinical studies with midazolam.

Clinical pharmacokinetic interactions between milk thistle and anticancer drugs

One single-sequence crossover trial explored the pharmacokinetic interaction between milk thistle and irinotecan⁴⁷.

Short-term (four days) and long-term (twelve days) intake of 200 mg milk thistle extract (three times daily) did not significantly alter the pharmacokinetics of irinotecan (125 mg/m², IV) or its metabolites SN-38, SN-38G and APC (**Table 2B**). These results are in concordance with the results obtained with midazolam.

Table 2A. Effect of milk thistle on the activity of CYP3A4 *in vitro*.

Models	CAM/component	Milk thistle product	Assay	Results	Ref.
HLM	MT extract (normalized to 10 μM silibinin)	Indena USA Inc., Seattle, USA	HPLC-UV (midazolam and testosterone)	43% ↓ CYP3A4 activity	51
	100 μM silymarin	Madaus GmbH, Cologne, Germany	LC-MS (testosterone)	> 90% ↓ CYP3A4 activity	52
	0-100 μM silibinin	Ivax-CR, Opava, Czech Republic	HPLC-UV (nifedipine)	↓ CYP3A4 activity IC ₅₀ = 27 & 60 μM	53
	0-300 μM silibinin	Purified and provided by Dept. of Chemistry, Madaus, Germany	HPLC-UV (nifedipine)	↓ CYP3A4 activity IC ₅₀ = 29 & 46 μM	55
	0-400 μM silibinin	Ivax-CR, Opava, Czech Republic	HPLC-UV (testosterone)	↓ CYP3A4 activity IC ₅₀ = 49.8 μM	54
Human hepatocytes	100 μM silymarin	Sigma, St. Louis, USA	HPLC-UV (testosterone)	50% ↓ CYP3A4 activity	56
	0-100 μM silibinin	Purified and provided by Galena Opava a.s., Czech Republic	Northern blotting	↔ mRNA, protein	58
<i>E. coli</i> MV1304 cells	0-250 μM silibinin	Sigma-Aldrich, St. Louis, USA	HPLC-UV (testosterone)	↓ CYP3A4 activity K _i = 132 μM	57
Baculosomes	0-50 μM silibinin	Sigma Chemical Co., St. Louis, USA	Fluorescence assay (Vivid red)	↔ CYP3A4 activity	37
	0-50 μM silibinin	Sigma Chemical Co., St. Louis, USA	HPLC-UV (cortisol)	↔ CYP3A4 activity	37
Caco-2 cells	0-75 μg/mL MT extracts	Local retail outlets, Ottawa, USA	RT-PCR and Western blotting	↓ mRNA, protein	59
	0-10 μM silibinin	Sigma-Aldrich, St. Louis, USA	RT-PCR and Western blotting	↓ mRNA ↑ protein	59

Abbreviations: HLM, human liver microsomes; HPLC-UV, high-performance liquid chromatography with ultraviolet detection; LC-MS, liquid chromatography mass spectrometry; MT, milk thistle; RT-PCR, real-time polymerase chain reaction; IC₅₀, half maximal inhibitory concentration; K_i, *in vitro* inhibition constant; ↔, unchanged and ↓, decrease.

Table 2B. Effect of milk thistle on the pharmacokinetics of selected substrate drugs in healthy volunteers and patients.

Subjects	Dose milk thistle	Milk thistle product	Substrate	Results	Ref.
Healthy volunteers (n=12)	175 mg (80% silymarin), twice daily, 28 days	Wild Oats Markets, Inc, Boulder, USA	MDZ (P.O.)	No sign. effect on 1-OH MDZ / MDZ serum ratio	60
Healthy volunteers (n=19)	300 mg (80% silymarin), thrice daily, 14 days	Enzymatic Therapy, Inc, Green Bay, USA	MDZ (P.O.)	No sign. effect on AUC _{0-∞} MDZ, and 1-OH MDZ / MDZ serum ratio	61
Cancer patients (n=6)	200 mg (80% silymarin), thrice daily, 4 and 12 days	GNC, Pittsburgh, USA	Irinotecan (IV)	No sign. effect on AUC irinotecan, SN-38, SN-38G, APC.	47

Abbreviations: AUC_{0-∞}, area under the serum concentration-time curve from time zero extrapolated to infinity; no sign., not statistically significant; 1-OH MDZ, 1-hydroxymidazolam; MDZ, midazolam; P.O., oral administration; IV, intravenous administration.

The two studies with midazolam and the one with irinotecan used different brands of milk thistle products, but all were standardized to 80% silymarin. The milk thistle dose varied between 175 – 300 mg, administered two or three times daily. Despite the reported wide variation in bioavailability and silymarin-release properties in different milk thistle products⁶¹, the clinical outcome was the same. Presumably, the water solubility in the gastrointestinal tract and bioavailability of silymarin was too low to achieve inhibition of intestinal and hepatic CYP3A4. This is supported by the study with irinotecan⁴⁷, in which analysis of silibinin plasma levels (C_{max} silibinin: range 0.0249-0.257 μM) revealed that these levels were too low to achieve CYP3A4 inhibition considering reported IC_{50} values of silibinin ranging from 27 to 60 μM ⁵³⁻⁵⁵.

The lack of an interaction between milk thistle and irinotecan could thus be predicted based on the results obtained with midazolam. As milk thistle is poorly bioavailable⁶³, it will mainly affect intestinal CYP3A4. Therefore, milk thistle is expected to have a greater effect on systemic exposure of oral midazolam than on exposure to IV drugs such as irinotecan.

Garlic

Garlic (*Allium sativum*) is listed in the top 10 of CAM used by cancer patients⁶. This herb is assumed to have anticancer, immune-enhancing, antiplatelet, chemopreventive, antihypertensive, procirculatory, hypolipidemic and hepatoprotective effects^{64, 65}. One of the major garlic components responsible for these effects is allicin⁶⁴. After crushing garlic or wetting garlic powder, allicin is formed from the garlic constituent alliin by the enzyme alliinase⁶⁶.

In vitro effects of garlic on CYP3A4 and drug metabolism

Several *in vitro* studies have been performed to determine whether garlic and its major component allicin are able to affect CYP3A4.

In two *in vitro* studies, garlic extracts did not inhibit CYP3A4 activity in SupersomesTM⁶⁷ and in Fa2N-4 cells⁶⁸. Furthermore, the garlic extract had no effect on CYP3A4 transcription in HepG2 cells (**Table 3A**)⁶⁹. However, in the same study the garlic extract increased mRNA expression, which was not likely to be PXR-mediated. In contrast, allicin⁶⁵ and the extracts of commercial garlic products⁶⁴ were also shown to inhibit CYP3A4 activity in SupersomesTM^{64, 65}. However, the decreased fluorescent signal is not likely to be caused by inhibition of CYP3A4 by garlic, since very high concentrations of garlic (25 mg/mL) were used compared to the used concentrations of garlic (0-200 $\mu\text{g/mL}$) in the studies demonstrating no effect. More likely, the great amount of garlic extract interfered with the fluorescent signal (i.e. quenching).

Since the majority of the *in vitro* studies demonstrated no effect, it is possible that garlic has also no inhibitory effect on CYP3A4 in the clinic.

Table 3A. Effect of garlic on the activity of CYP3A4 *in vitro*.

Models	CAM/component	Garlic product	Assay	Results	Ref.
Supersomes™	0-98 µM allicin	LKT Laboratories, St. Paul, USA	Fluorescence assay (BFC)	↓ CYP3A4 activity IC ₅₀ = 43.73 µM	65
	0-98 µM allicin	LKT Laboratories, St. Paul, USA	Fluorescence assay (BzRes)	↓ CYP3A4 activity IC ₅₀ = 60.10 µM	65
	25 mg/mL garlic extracts	Local commercial outlets, Ottawa, USA	Fluorescence assay (BzRes)	17.4 – 95.8% ↓ CYP3A4 activity	64
	0-5 ng/mL garlic	Local pharmacy, Bremen, Germany	HPCL-UV (testosterone)	↔ CYP3A4 activity	67
Fa2N-4 cells	0-200 µg/mL garlic extract	Nature's Way, Springville, USA	RT-PCR LC-MS (midazolam)	↔ mRNA and CYP3A4 activity	68
Human hepatocytes	0.1 µg/mL garlic	Local commercial outlets, Ottawa, USA	Northern blotting	2 times ↑ mRNA	69
HepG2 cells	0.1 µg/mL garlic	Local commercial outlets, Ottawa, USA	Reporter gene assay	No fold induction of CYP3A4	69

Abbreviations: BFC, 7-benzyloxy-4-trifluoromethylcoumarin; BzRes, 7-benzyloxyresorufin; HPCL-UV, high-performance liquid chromatography with ultraviolet detection; LC-MS, liquid chromatography mass spectrometry; RT-PCR, real-time polymerase chain reaction; IC₅₀, half maximal inhibitory concentration; ↔, unchanged and ↓, decrease.

Clinical pharmacokinetic interactions between garlic and midazolam

Indeed, the absence of CYP3A4 inhibition by garlic *in vitro* has also been observed in two crossover trials with a fixed sequence for garlic and midazolam administration. In twelve healthy volunteers, intake of 500 mg garlic oil for 28 days (three times daily) did not significantly affect serum ratios of 1-hydroxymidazolam/midazolam³¹. An additional study with elderly volunteers also showed no significant alterations of the 1-hydroxymidazolam/midazolam ratio after supplementation of 500 mg garlic oil for 28 days (three times daily) (**Table 3B**)³⁰. A lack of a pharmacokinetic interaction between garlic and midazolam may be due to the use of garlic oil in both studies. After administration of garlic oil the enzyme alliinase will get inactivated by the acid gastric environment, which decreases the formation and bioavailability of allicin⁷⁰. Furthermore, vegetable oil present in the formulations is also known to cause a loss of alliin, which also negatively affects the formation of allicin⁷⁰. Unfortunately, the amount of allicin formation and bioavailability in both clinical studies were not determined.

Clinical pharmacokinetic interactions between garlic and anticancer drugs

Based on the absence of a clinical pharmacokinetic interaction between garlic and midazolam, interactions with anticancer drugs predominantly metabolized by CYP3A4 are not expected. Indeed, in a one-sequence crossover study with breast cancer patients supplementation of 600 mg enteric coated garlic tablets (3,600 µg allicin per tablet) twice daily for twelve days did not significantly alter the pharmacokinetics of docetaxel

Table 3B. Effect of garlic on the pharmacokinetics of selected substrate drugs in healthy volunteers and patients.

Subjects	Dose garlic	Garlic product	Substrate	Results	Ref.
Healthy volunteers (n=12)	500 mg garlic oil, thrice daily, 28 days	Wild Oats Markets, Inc, Boulder, USA	MDZ (P.O.)	No sign. effect on 1-OH MDZ/ MDZ serum ratio	31
Healthy volunteers (n=12)	500 mg garlic oil, thrice daily, 28 days	Vitamer, Lake Forest, USA	MDZ (P.O.)	No sign. effect on 1-OH MDZ/ MDZ serum ratio	30
Breast cancer patients (n=10)	600 mg (3,600 µg allicin), twice daily, 12 days	GarliPure, Maximum Allicin Formula, Natrol, Chatsworth, USA	Docetaxel (IV)	No sign. effect on AUC ₀₋₈ docetaxel	71

Abbreviations: AUC₀₋₈, area under the plasma concentration-time curve from 0-8 h; no sign., not statistically significant; 1-OH MDZ, 1-hydroxymidazolam; MDZ, midazolam; P.O., oral administration; IV, intravenous administration.

(Table 3B)⁷¹, which is mainly metabolized by CYP3A4 into four major metabolites⁷². Despite minimizing gastric inactivation of alliinase by using enteric coated tablets, no interaction occurred. This result was in concordance with the midazolam studies. Thus, the clinical use of midazolam has proven to be a good predictor of pharmacokinetic interactions with other CYP3A4 substrates, such as docetaxel.

P. ginseng

P. ginseng belongs to the twenty most frequently used CAM among cancer patients⁶. *P. ginseng* has been supposed to have anti-neoplastic, anti-aging, anti-oxidative and immunomodulatory effects^{73, 74}. This herb is used for cancer prevention, erectile dysfunction, improved cognitive functions and enhanced physical functions⁷⁵. *P. ginseng* consists of ginsenosides and sapogenins, of which ginsenosides are the main components⁷³.

***In vitro* effects of *P. ginseng* on CYP3A4 and drug metabolism**

The effect of *P. ginseng* on CYP3A4 has been determined in several *in vitro* studies (Table 4A). The flavonoid kaempferol was shown to inhibit CYP3A4 activity in baculosomes and microsomes³⁷. Ginsenosides Rh₂, C-K and all sapogenins exhibited moderate CYP3A4 inhibition in baculosomes and Rg₃ showed relatively weak CYP3A4 inhibition⁷³. In microsomes, ginsenosides Rh₁ and F₁ inhibited CYP3A4 activity respectively by 54% and 60%^{51, 74}. Ginsenoside Rd^{76, 77} and sapogenins PPD and PPT⁷⁶ were shown to be relatively moderate and strong inhibitors of CYP3A4 activity in microsomes with corresponding IC₅₀ values of respectively 81.7, 14.1 and 7.1 µM. Ginsenosides Rb₂ and Rc, however, had limited inhibitory effects in these microsomes. Also the inhibitory effect of ginsenosides Rb₁, Rb₂, Rc, Rd, Re, Rf, Rg was weak compared to ketoconazole³⁸.

Long-term (48 hours) exposure of *P. ginseng* had no effect on CYP3A4 mRNA expression in hepatocytes and CYP3A4 transcription in HepG2 cells⁶⁹. Thus, *P. ginseng* is apparently no inducer of CYP3A4.

Table 4A. Effect of *P. ginseng* on the activity of CYP3A4 *in vitro*.

Models	CAM/component	<i>P. ginseng</i> product	Assay	Results	Ref.
Human hepatocytes	500 µg/mL ginseng	Local commercial outlets, Ottawa, USA	Northern blotting	↔ mRNA	69
HepG2 cells	500 µg/mL ginseng	Local commercial outlets, Ottawa, USA	Reporter gene assay	no fold induction of CYP3A4	69
Baculosomes	0-50 µM kaempferol	Sigma Chemical Co., St. Louis, USA	fluorescence assay (Vivid red)	↓ CYP3A4 activity IC ₅₀ = 260.7 nM	37
	0-50 µM Rh ₂ , C-K ^e and Rg ₃	Obtained and purified from <i>P. ginseng</i> fruits, Liaoning Xinbin Pharmaceutical, Fushun, China	fluorescence assay (Vivid red)	↓ CYP3A4 activity IC ₅₀ = resp. 9.8; 9.1; 25.2 µM	73
Rat liver microsomes	50 µM kaempferol	Sigma Chemical Co., St. Louis, USA	HPLC-UV (cortisol)	89.7% ↓ CYP3A4 activity	37
HLM	0-100 µM Rh ₁ , F ₁	Fermenta Herb Institute Inc., Tokyo, Japan	HPLC-UV (testosterone)	↓ CYP3A4 activity IC ₅₀ = resp. 76.9; >100 µM	74
	10 µM Rh ₁ , F ₁	Flachsmann Canada Ltd., Brampton, Canada	HPLC-UV (midazolam)	resp. 54% and 60% ↓ CYP3A4 activity	51
	0-100 µM PPD, PPT, Rd	Fermenta Herb Institute Inc., Tokyo, Japan	HPLC-UV (testosterone)	↓ CYP3A4 activity IC ₅₀ = resp. 14.1; 7.1; 81.7 µM	76
	0-200 µM Rd, Rb ₂ , Rc	Indofine Chemical Co., Somerville, USA	HPLC-UV (testosterone)	↓ CYP3A4 activity IC ₅₀ = resp. 62; 133; 197 µM	77
	0-200 µM Rb ₁ , Rb ₂ , Rc, Rd, Re, Rf, Rg	Indofine Chemical Co., Somerville, USA	Fluorescence assay (BzRes and BFC)	All IC ₅₀ > 200 µM IC ₅₀ 's of Rd resp. 74; 58 µM and of Rb ₂ resp. 178; 165 µM	38

Abbreviations: HLM, human liver microsomes; HPLC-UV, high-performance liquid chromatography with ultraviolet detection; IC₅₀, half maximal inhibitory concentration; ↔, unchanged, ↓, decrease.

Overall, the majority of *in vitro* studies showed that *P. ginseng* is a competitive inhibitor of CYP3A4. Therefore, an effect of *P. ginseng* on CYP3A4 could be expected in the clinic.

Clinical pharmacokinetic interactions between *P. ginseng* and midazolam

In contrast to the results obtained *in vitro*, inhibition of CYP3A4 by *P. ginseng* has not been reported in clinical studies with midazolam (Table 4B). The sequence of *P. ginseng* and midazolam administration was fixed in these studies. In twelve healthy volunteers a 28-day supplementation period of 500 mg *P. ginseng* (three times daily, standardized to 5% ginsenosides) did not significantly affect the 1-hydroxymidazolam/midazolam serum ratio³¹. Also in elderly volunteers, no significant effect of *P. ginseng* (500 mg, three times daily, standardized to 5% ginsenosides) on the 1-hydroxymidazolam/midazolam serum ratio was observed³⁰. Presumably, the inhibiting potency of ginsenosides is too

Table 4B. Effect of *P. ginseng* on the pharmacokinetics of selected substrate drugs in healthy volunteers and patients.

Subjects	Dose <i>P. ginseng</i>	<i>P. ginseng</i> product	Substrate	Results	Ref.
Healthy volunteers (n=12)	500 mg (5% ginsenosides), thrice daily, 28 days	Wild Oats Markets, Inc, Boulder, USA Vitamer	MDZ (P.O.)	No sign. effect on 1-OH MDZ/MDZ serum ratio	31
Healthy volunteers (n=12)	500 mg (5% ginsenosides), thrice daily, 28 days	Vitamer, Lake Forest, USA	MDZ (P.O.)	No sign. effect on 1-OH MDZ/MDZ serum ratio	30
Healthy volunteers (n=12)	500 mg (5% ginsenosides, twice daily, 28 days	Vitamer, Lake Forest, USA	MDZ (P.O.)	Significant 34% ↓ of AUC _{0-∞} MDZ	78
CML patient (n=1)	Energy drink, daily intake, 3 months	Full Throttle energy drink	Imatinib (P.O.)	Imatinib-induced hepatotoxicity	80

Abbreviations: AUC_{0-∞}, area under the serum concentration-time curve from time zero extrapolated to infinity; CML, chronic myelogenous leukemia; 1-OH MDZ, 1-hydroxymidazolam; MDZ, midazolam; No sign., not statistically significant; P.O., oral administration; ↓, decrease.

low to cause significant clinical CYP3A4 inhibition. Rather high plasma concentrations of ginsenosides are required for inhibition of CYP3A4, as the IC₅₀ values of several ginsenosides have shown to be more than 1,000 times higher than the IC₅₀ value of the potent CYP3A4 inhibitor ketoconazole³⁸.

One clinical study, however, found significant induction of CYP3A4 by *P. ginseng*. Intake of 500 mg *P. ginseng* (twice daily for 28 days, standardized to 5% ginsenosides) by healthy volunteers significantly decreased the AUC of oral midazolam by 34%, which suggested induction of CYP3A4⁷⁸. Interestingly, this significant result differed from the observations in the two other trials with midazolam, despite a similar composition of the *P. ginseng* product (500 mg extract, standardized to 5% ginsenosides) and a lower dosing frequency. Possibly, differences in assessments of CYP3A4 activity were responsible for these conflicting results. A one-hour postdose serum concentration ratio of 1-hydroxymidazolam/midazolam was the primary outcome in studies showing no apparent interaction between *P. ginseng* and midazolam^{30, 31}, while midazolam AUC_{0-∞} was calculated in the clinical study which suggested CYP3A4 induction by *P. ginseng*⁷⁸. It has been reported that determination of the AUC of midazolam is more accurate to assess CYP3A4 activity than a single sample collection of midazolam⁷⁹. Therefore it is possible that a CYP3A4 induction by *P. ginseng* may have been missed in the studies with a one-sampling strategy.

The discussed clinical studies with *P. ginseng* and midazolam show inconsistent results: two studies reported no pharmacokinetic interaction, while in one study the AUC of midazolam was significantly decreased after *P. ginseng* administration. The latter result indicates that *P. ginseng* could also reduce the systemic exposure of oncolytic substrates for CYP3A4.

Clinical pharmacokinetic interactions between *P. ginseng* and anticancer drugs

Thus far, no clinical interaction studies with *P. ginseng* and anticancer drugs have been reported. Only one case report described the onset of imatinib-induced hepatotoxicity in a patient with chronic myelogenous leukemia (CML) who had been receiving imatinib for nine years. After concomitant use of imatinib and an energy drink containing *P. ginseng* for three months hepatotoxicity became apparent by abnormal liver function test results (alanine aminotransferase 1069 U/L, aspartate aminotransferase 481 U/L, alkaline phosphatase 124 IU/L, total bilirubin 1.4 mg/dL, albumin 4.0 g/dL) and liver biopsy⁸⁰. Liver enzyme levels returned to normal after discontinuation of imatinib and *P. ginseng* intake and treatment with prednisone. Restart with imatinib did not result in recurrent elevations in liver enzyme levels. Imatinib itself may cause hepatotoxicity, but this usually occurs within the first 1-2 years of therapy. It is more likely that the described hepatotoxicity was caused by concomitant administration of *P. ginseng*, as the Horn drug interaction probability scale suggested a probable interaction between imatinib and *P. ginseng*. According to the authors the underlying mechanism of this interaction might be inhibition of CYP3A4 and possibly also the drug transporter P-gp by *P. ginseng* (**Table 4B**). However, the proposed pharmacokinetic interaction between *P. ginseng* and imatinib in the case report⁸⁰ should be questioned, as no pharmacokinetic parameters of imatinib or its metabolites have been determined in the affected patient. Furthermore, the ingested energy drink also contained other components besides *P. ginseng* (e.g. guarana extract, caffeine, taurine and B-vitamins)⁸¹ which might have affected the metabolism of imatinib. Thus, to draw more definitive conclusions about a pharmacokinetic interaction between *P. ginseng* and imatinib, a (pre) clinical interaction study with an appropriate sample size and pharmacokinetic endpoints should be executed.

DISCUSSION

The review of available literature indicates that the value of *in vitro* research to predict clinical effects on CYP3A4 is different for each reported herb. The *in vitro* inductive effect of SJW was extrapolatable to the clinic, using midazolam and the anticancer drugs irinotecan and imatinib as CYP3A4 substrates (**Table 1B**). Also for garlic *in vitro* results were extrapolatable: no effect on CYP3A4 has been observed both in *in vitro* and in clinical studies (**Table 3A, 3B**). However, for milk thistle and *P. ginseng* CYP3A4 inhibition was observed *in vitro*, but these results were not reproducible in clinical studies (**Table 2B, 4B**).

The poor correlation between *in vitro* and clinical results observed for milk thistle and *P. ginseng* reveal limitations that are commonly observed for CAM-drug interaction studies. For example, the phytochemical content (and the interacting potential) of herbal medicines is usually highly variable among different brands, but also within

batches⁸². This has been demonstrated for 25 different ginseng preparations for which phytochemical analysis showed a high interproduct variability in ginsenosides content (15- to 36 fold variation)⁸³. Furthermore, measured concentrations of ginsenosides were lower than the labeled amount of ginsenosides in the majority of *P. ginseng* preparations. In the described clinical *P. ginseng* studies, however, phytochemical analyses of the *P. ginseng* products were in agreement with the amount of ginsenosides stated on the label. Possibly, ginsenosides are too weak CYP3A4 inhibitors (as shown in *in vitro* studies) to achieve clinically significant interactions.

Besides variations in phytochemical content, also variability in drug-releasing properties and bioavailability are observed in commercial CAM products. Analysis of nine milk thistle products showed that the amount of released silibinin in an aqueous buffered solution varies considerably, ranging from 0 to 85%⁸⁴. Furthermore, bioavailability of milk thistle has shown to be poor and highly variable. It is likely that these factors all contribute to a lack of clinically significant effects of milk thistle on CYP3A4.

To improve extrapolatability of *in vitro* interaction studies it is recommended to confirm effects of CAM in multiple test systems and assays for quantification within a single *in vitro* study. By this, more robust results can be obtained and it is also possible to prevent interlaboratory differences and the use of different product brands. The extrapolatability can also be improved by assays that closely mimic physiological conditions in terms of pH and the composition of gastric fluid. Early detection of poor soluble components will then reveal the low likelihood of CYP3A4-mediated CAM-drug interactions in humans.

In contrast to the occasionally poor *in vitro* – clinical extrapolation of CYP3A4-based interactions, the clinical use of midazolam has shown to be a good predictor of pharmacokinetic interactions between CAM and anticancer drugs metabolized by CYP3A4. Specifically, the occurrence of clinical CYP3A4-mediated interactions between anticancer drugs and SJW, milk thistle and garlic, correlated well with clinical results obtained with these CAM and midazolam.

RECOMMENDATIONS

Based on the available pharmacokinetic data of SJW, milk thistle, garlic and *P. ginseng*, it is possible to provide recommendations towards concomitant use of these CAM by cancer patients.

For SJW it is recommended not to combine hyperforin-rich SJW extracts with imatinib or irinotecan in order to prevent undertreatment of cancer patients. Additionally, caution is warranted when combining SJW with other anticancer drugs metabolized by CYP3A4 (e.g. docetaxel, paclitaxel, vinorelbine, gefitinib), as the systemic exposure and possibly also the efficacy of these therapies could be diminished. However, it is presumably safe to combine hyperforin-poor (≤ 0.13 mg hyperforin per day) SJW extracts with imatinib or irinotecan as this hyperforin dose did not significantly affect the systemic exposure to midazolam⁴⁵.

For milk thistle and garlic it is presumably safe to combine these CAM with respectively irinotecan and docetaxel and other anticancer drugs metabolized by CYP3A4.

For *P. ginseng* it is not possible to provide recommendations about the concomitant use with anticancer drugs, because clinical interaction studies should be executed with *P. ginseng* and anticancer drugs metabolized by CYP3A4. However, it should be noted that the determined absence or presence of pharmacokinetic interactions between CAM and anticancer drugs are only applicable for the tested brands of CAM products. Due to substantial interproduct variabilities, the interacting potential of other brands may differ.

CONCLUSION

This review summarizes that *in vitro* data are used to discover effects of CAM on CYP3A4 and for certain CAM, such as SJW, these effects can be extrapolated to clinical studies. Occasionally, significant effects on CYP3A4 *in vitro* do not predict significant interactions in clinical trials. These discrepancies can be largely attributed to differences between *in vitro* test systems and the physiological environment. To improve extrapolation from *in vitro* to the clinic, *in vitro* conditions should closely mimic physiological conditions, as accurate prediction of clinical pharmacokinetic interactions is complicated by several factors (e.g. poor pharmaceutical availability, solubility and bioavailability of CAM). Therefore, clinical studies are required for confirmation and assessment of the clinical relevance of CAM-drug interactions obtained *in vitro*. In clinical trials midazolam has been shown to be a useful probe drug to correctly predict the presence or absence of clinical CYP3A4-based interactions between CAM and anticancer drugs.

REFERENCES

1. Sewitch MJ, Rajput Y. A literature review of complementary and alternative medicine use by colorectal cancer patients. *Complement Ther Clin Pract* 2010; 16: 52-6.
2. Bishop FL, Rea A, Lewith H, Chan YK, Saville J, Prescott P, et al. Complementary medicine use by men with prostate cancer: a systematic review of prevalence studies. *Prostate Cancer Prostatic Dis* 2011; 14: 1-13.
3. Bishop FL, Prescott P, Chan YK, Saville J, von Elm E, Lewith GT. Prevalence of complementary medicine use in pediatric cancer: a systematic review. *Pediatrics* 2010; 125: 768-76.
4. Sparreboom A, Cox MC, Acharya MR, Figg WD. Herbal remedies in the United States: potential adverse interactions with anticancer agents. *J Clin Oncol* 2004; 22: 2489-503.
5. Tascilar M, de Jong FA, Verweij J, Mathijssen RH. Complementary and alternative medicine during cancer treatment: beyond innocence. *Oncologist* 2006; 11: 732-41.
6. Werneke U, Earl J, Seydel C, Horn O, Crichton P, Fannon D. Potential health risks of complementary alternative medicines in cancer patients. *Br J Cancer* 2004; 90: 408-13.
7. Pal D, Mitra AK. MDR- and CYP3A4-mediated drug-herbal interactions. *Life Sci* 2006; 78: 2131-45.
8. Gouws C, Steyn D, Du Plessis L, Steenekamp J, Hamman JH. Combination therapy of Western drugs and herbal medicines: recent advances in understanding interactions involving metabolism and efflux. *Expert Opin Drug Metab Toxicol* 2012; 8: 973-84.
9. Unger M. Pharmacokinetic drug interactions between anticancer therapeutics and drugs of complementary medicine: mechanisms and clinical relevance. *Forsch Komplementmed* 2011; 18: 213-8.
10. Mathijssen RH, Verweij J, de Bruijn P, Loos WJ, Sparreboom A. Effects of St. John's wort on irinotecan metabolism. *J Natl Cancer Inst* 2002; 94: 1247-9.
11. Smith P, Bullock JM, Booker BM, Haas CE, Berenson CS, Jusko WJ. The influence of St. John's wort on the pharmacokinetics and protein binding of imatinib mesylate. *Pharmacotherapy* 2004; 24: 1508-14.
12. Frye RF, Fitzgerald SM, Lagattuta TF, Hruska MW, Egorin MJ. Effect of St. John's wort on imatinib mesylate pharmacokinetics. *Clin Pharmacol Ther* 2004; 76: 323-9.
13. He SM, Yang AK, Li XT, Du YM, Zhou SF. Effects of herbal products on the metabolism and transport of anticancer agents. *Expert Opin Drug Metab Toxicol* 2010; 6: 1195-213.
14. Martignoni M, Groothuis GM, de Kanter R. Species differences between mouse, rat, dog, monkey and human CYP-mediated drug metabolism, inhibition and induction. *Expert Opin Drug Metab Toxicol* 2006; 2: 875-94.
15. Foti RS, Rock DA, Wienkers LC, Wahlstrom JL. Selection of alternative CYP3A4 probe substrates for clinical drug interaction studies using *in vitro* data and *in vivo* simulation. *Drug Metab Dispos* 2010; 38: 981-7.
16. NoAb BioDiscoveries. Metabolic Stability - Microsomes http://www.noabbiobdiscoveries.com/assays/invitro/metabolic_stability_subcellular.pdf; date of last access: June 26, 2012.
17. European Medicines Agency. Guideline on the Investigation of Drug Interactions 2010; http://www.emea.europa.eu/docs/en_GB/document_library/Scientific_guideline/2010/05/WC500090112.pdf; date of last access: June 25, 2012.
18. Vogel HG, Hock FJ, Maas J, Mayer D. *Drug Discovery and Evaluation: Safety and Pharmacokinetic Assays*: p. 553. New York: Springer; 2006.

19. Bhogal RH, Hodson J, Bartlett DC, Weston CJ, Curbishley SM, Haughton E, et al. Isolation of primary human hepatocytes from normal and diseased liver tissue: a one hundred liver experience. *PLoS One* 2011; 6: e18222.
20. Bjornsson TD, Callaghan JT, Einolf HJ, Fischer V, Gan L, Grimm S, et al. The conduct of *in vitro* and *in vivo* drug-drug interaction studies: a PhRMA perspective. *J Clin Pharmacol* 2003; 43: 443-69.
21. Parkinson A, Kazmi F, Buckley DB, Yerino P, Ogilvie BW, Paris BL. System-dependent outcomes during the evaluation of drug candidates as inhibitors of cytochrome P450 (CYP) and uridine diphosphate glucuronosyltransferase (UGT) enzymes: human hepatocytes versus liver microsomes versus recombinant enzymes. *Drug Metab Pharmacokinet* 2010; 25: 16-27.
22. U.S. Department of Health and Human Services, Food and Drug Administration, Center for Drug Evaluation (CDER), Center for Biologics Evaluation and Research (CBER). Guidance for Industry: Drug Interaction Studies - Study Design, Data Analysis, and Implications for Dosing and Labeling. 2012; <http://www.fda.gov/downloads/Drugs/GuidanceComplianceRegulatoryInformation/Guidances/UCM292362.pdf>; date of last access: June 25, 2012.
23. Na DH, Ji HY, Park EJ, Kim MS, Liu KH, Lee HS. Evaluation of metabolism-mediated herb-drug interactions. *Arch Pharm Res* 2011; 34: 1829-42.
24. Particle Sciences. Mass Spectrometry in Bioanalysis. 2009; http://www.particlesciences.com/docs/technical_briefs/TB_4.pdf; date of last access: June 25, 2012.
25. Stresser DM, Blanchard AP, Turner SD, Erve JC, Dandeneau AA, Miller VP, et al. Substrate-dependent modulation of CYP3A4 catalytic activity: analysis of 27 test compounds with four fluorometric substrates. *Drug Metab Dispos* 2000; 28: 1440-8.
26. Moore LB, Goodwin B, Jones SA, Wisely GB, Serabjit-Singh CJ, Willson TM, et al. St. John's wort induces hepatic drug metabolism through activation of the pregnane X receptor. *Proc Natl Acad Sci USA* 2000; 97: 7500-2.
27. Harmsen S, Koster AS, Beijnen JH, Schellens JH, Meijerman I. Comparison of two immortalized human cell lines to study nuclear receptor-mediated CYP3A4 induction. *Drug Metab Dispos* 2008; 36: 1166-71.
28. Health Canada. Therapeutic Products Programme: Guidance Document: Drug-Drug Interactions: Studies *In Vitro* and *In Vivo* 2000; http://www.hc-sc.gc.ca/dhp-mps/alt_formats/hpfb-dgpsa/pdf/prodpharma/drug_medi_int-eng.pdf; date of last access: June 25, 2012.
29. Kronbach T, Mathys D, Umeno M, Gonzalez FJ, Meyer UA. Oxidation of midazolam and triazolam by human liver cytochrome P450III_{A4}. *Mol Pharmacol* 1989; 36: 89-96.
30. Gurley BJ, Gardner SF, Hubbard MA, Williams DK, Gentry WB, Cui Y, et al. Clinical assessment of effects of botanical supplementation on cytochrome P450 phenotypes in the elderly: St John's wort, garlic oil, Panax ginseng and Ginkgo biloba. *Drugs Aging* 2005; 22: 525-39.
31. Gurley BJ, Gardner SF, Hubbard MA, Williams DK, Gentry WB, Cui Y, et al. Cytochrome P450 phenotypic ratios for predicting herb-drug interactions in humans. *Clin Pharmacol Ther* 2002; 72: 276-87.
32. Zhu B, Ou-Yang DS, Cheng ZN, Huang SL, Zhou HH. Single plasma sampling to predict oral clearance of CYP3A probe midazolam. *Acta Pharmacol Sin* 2001; 22: 634-8.
33. Gutmann H, Poller B, Buter KB, Pfrunder A, Schaffner W, Drewe J. Hypericum perforatum: which constituents may induce intestinal MDR1 and CYP3A4 mRNA expression? *Planta Med* 2006; 72: 685-90.
34. Hokkanen J, Tolonen A, Mattila S, Turpeinen M. Metabolism of hyperforin, the active constituent of St. John's wort, in human liver microsomes. *Eur J Pharm Sci* 2011; 42: 273-84.

35. Obach RS. Inhibition of human cytochrome P450 enzymes by constituents of St. John's wort, an herbal preparation used in the treatment of depression. *J Pharmacol Exp Ther* 2000; 294: 88-95.
36. Hansen TS, Nilsen OG. *In vitro* CYP3A4 metabolism: inhibition by Echinacea purpurea and choice of substrate for the evaluation of herbal inhibition. *Basic Clin Pharmacol Toxicol* 2008; 103: 445-9.
37. Patel J, Buddha B, Dey S, Pal D, Mitra AK. *In vitro* interaction of the HIV protease inhibitor ritonavir with herbal constituents: changes in P-gp and CYP3A4 activity. *Am J Ther* 2004; 11: 262-77.
38. Henderson GL, Harkey MR, Gershwin ME, Hackman RM, Stern JS, Stresser DM. Effects of ginseng components on c-DNA-expressed cytochrome P450 enzyme catalytic activity. *Life Sci* 1999; 65: 209-14.
39. Komoroski BJ, Zhang S, Cai H, Hutzler JM, Frye R, Tracy TS, et al. Induction and inhibition of cytochromes P450 by the St. John's wort constituent hyperforin in human hepatocyte cultures. *Drug Metab Dispos* 2004; 32: 512-8.
40. Komoroski BJ, Parise RA, Egorin MJ, Strom SC, Venkataramanan R. Effect of the St. John's wort constituent hyperforin on docetaxel metabolism by human hepatocyte cultures. *Clin Cancer Res* 2005; 11: 6972-9.
41. Wang Z, Gorski JC, Hamman MA, Huang SM, Lesko LJ, Hall SD. The effects of St. John's wort (*Hypericum perforatum*) on human cytochrome P450 activity. *Clin Pharmacol Ther* 2001; 70: 317-26.
42. Hall SD, Wang Z, Huang SM, Hamman MA, Vasavada N, Adigun AQ, et al. The interaction between St. John's wort and an oral contraceptive. *Clin Pharmacol Ther* 2003; 74: 525-35.
43. Dresser GK, Schwarz UI, Wilkinson GR, Kim RB. Coordinate induction of both cytochrome P4503A and MDR1 by St John's wort in healthy subjects. *Clin Pharmacol Ther* 2003; 73: 41-50.
44. Xie R, Tan LH, Polasek EC, Hong C, Teillol-Foo M, Gordi T, et al. CYP3A and P-glycoprotein activity induction with St. John's Wort in healthy volunteers from 6 ethnic populations. *J Clin Pharmacol* 2005; 45: 352-6.
45. Mueller SC, Majcher-Peszynska J, Uehleke B, Klammt S, Mundkowski RG, Miekisch W, et al. The extent of induction of CYP3A by St. John's wort varies among products and is linked to hyperforin dose. *Eur J Clin Pharmacol* 2006; 62: 29-36.
46. Mueller SC, Majcher-Peszynska J, Mundkowski RG, Uehleke B, Klammt S, Sievers H, et al. No clinically relevant CYP3A induction after St. John's wort with low hyperforin content in healthy volunteers. *Eur J Clin Pharmacol* 2009; 65: 81-7.
47. van Erp NP, Baker SD, Zhao M, Rudek MA, Guchelaar HJ, Nortier JW, et al. Effect of milk thistle (*Silybum marianum*) on the pharmacokinetics of irinotecan. *Clin Cancer Res* 2005; 11: 7800-6.
48. Lee LS, Andrade AS, Flexner C. Interactions between natural health products and antiretroviral drugs: pharmacokinetic and pharmacodynamic effects. *Clinical Infect Dis* 2006; 43: 1052-9.
49. Saller R, Meier R, Brignoli R. The use of silymarin in the treatment of liver diseases. *Drugs* 2001; 61: 2035-63.
50. Kroll DJ, Shaw HS, Oberlies NH. Milk thistle nomenclature: why it matters in cancer research and pharmacokinetic studies. *Integr Cancer Ther* 2007; 6: 110-9.
51. Etheridge AS, Black SR, Patel PR, So J, Mathews JM. An *in vitro* evaluation of cytochrome P450 inhibition and P-glycoprotein interaction with goldenseal, Ginkgo biloba, grape seed, milk thistle, and ginseng extracts and their constituents. *Planta Med* 2007; 73: 731-41.
52. Doehmer J, Tewes B, Klein KU, Gritzko K, Muschick H, Mengs U. Assessment of drug-drug interaction for silymarin. *Toxicol In Vitro* 2008; 22: 610-7.
53. Zuber R, Modriansky M, Dvorak Z, Rohovsky P, Ulrichova J, Simanek V, et al. Effect of silybin and its congeners on human liver microsomal cytochrome P450 activities. *Phytother Res* 2002; 16: 632-8.

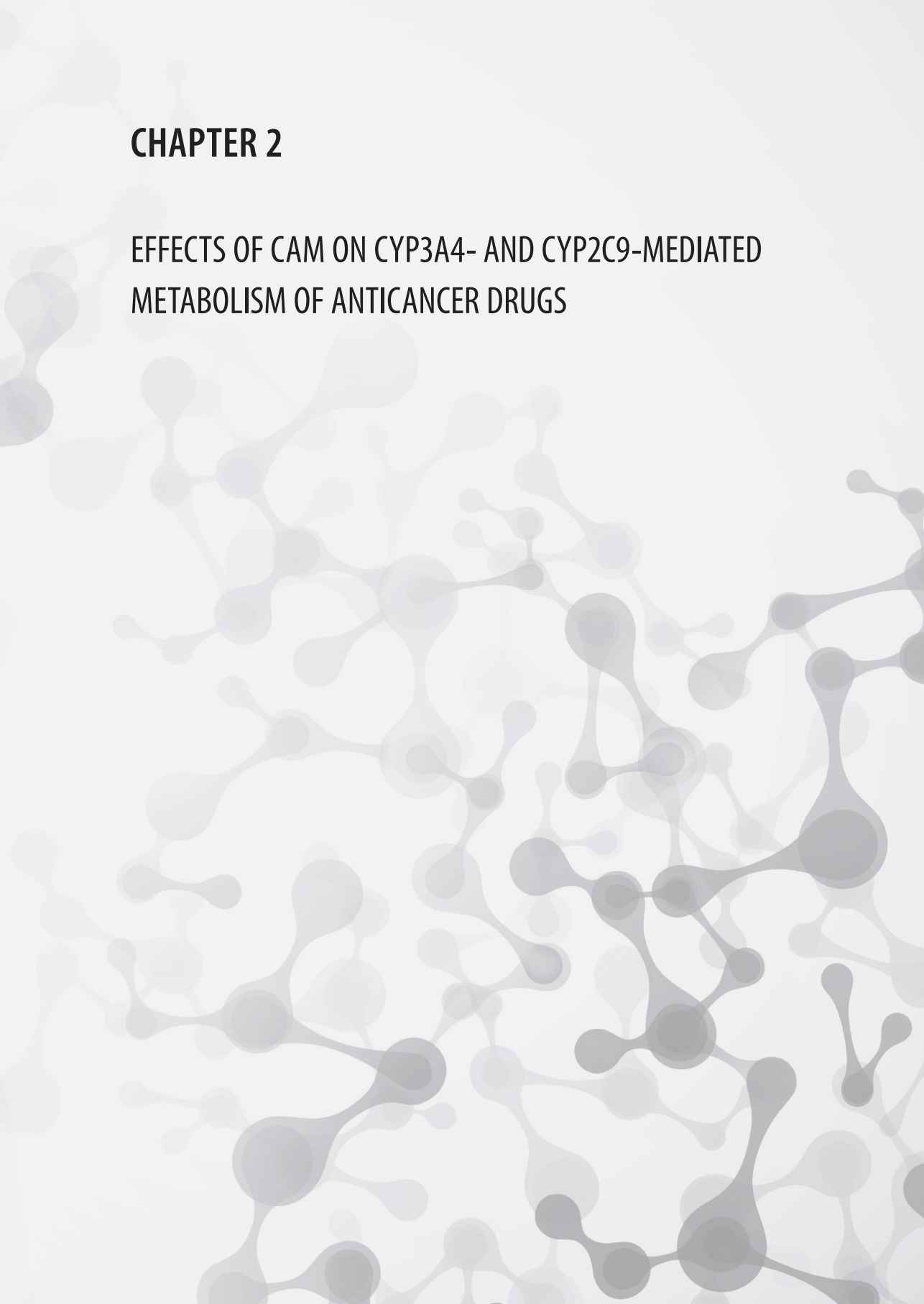
54. Jancova P, Anzenbacherova E, Papouskova B, Lemr K, Luzna P, Veinlichova A, et al. Silybin is metabolized by cytochrome P450 2C8 *in vitro*. *Drug Metab Dispos* 2007; 35: 2035-9.
55. Beckmann-Knopp S, Rietbrock S, Weyhenmeyer R, Bocker RH, Beckurts KT, Lang W, et al. Inhibitory effects of silibinin on cytochrome P-450 enzymes in human liver microsomes. *Pharmacol Toxicol* 2000; 86: 250-6.
56. Venkataramanan R, Ramachandran V, Komoroski BJ, Zhang S, Schiff PL, Strom SC. Milk thistle, a herbal supplement, decreases the activity of CYP3A4 and uridine diphosphoglucuronosyl transferase in human hepatocyte cultures. *Drug Metab Dispos* 2000; 28: 1270-3.
57. Sridar C, Goosen TC, Kent UM, Williams JA, Hollenberg PF. Silybin inactivates cytochromes P450 3A4 and 2C9 and inhibits major hepatic glucuronosyltransferases. *Drug Metab Dispos* 2004; 32: 587-94.
58. Kosina P, Maurel P, Ulrichova J, Dvorak Z. Effect of silybin and its glycosides on the expression of cytochromes P450 1A2 and 3A4 in primary cultures of human hepatocytes. *J Biochem Mol Toxicol* 2005; 19: 149-53.
59. Budzinski JW, Trudeau VL, Drouin CE, Panahi M, Arnason JT, Foster BC. Modulation of human cytochrome P450 3A4 (CYP3A4) and P-glycoprotein (P-gp) in Caco-2 cell monolayers by selected commercial-source milk thistle and goldenseal products. *Can J Physiol Pharm* 2007; 85: 966-78.
60. Gurley BJ, Gardner SF, Hubbard MA, Williams DK, Gentry WB, Carrier J, et al. *In vivo* assessment of botanical supplementation on human cytochrome P450 phenotypes: *Citrus aurantium*, *Echinacea purpurea*, milk thistle, and saw palmetto. *Clin Pharmacol Ther* 2004; 76: 428-40.
61. Gurley B, Hubbard MA, Williams DK, Thaden J, Tong Y, Gentry WB, et al. Assessing the clinical significance of botanical supplementation on human cytochrome P450 3A activity: comparison of a milk thistle and black cohosh product to rifampin and clarithromycin. *J Clin Pharmacol* 2006; 46: 201-13.
62. Ghosh A, Biswas S, Ghosh T. Preparation and Evaluation of Silymarin beta-cyclodextrin Molecular Inclusion Complexes. *J Young Pharm* 2011; 3: 205-10.
63. Javed S, Kohli K, Ali M. Reassessing bioavailability of silymarin. *Altern Med Rev*. 2011; 16: 239-49.
64. Foster BC, Foster MS, Vandenhoeck S, Krantis A, Budzinski JW, Arnason JT, et al. An *in vitro* evaluation of human cytochrome P450 3A4 and P-glycoprotein inhibition by garlic. *J Pharm Pharm Sci* 2001; 4: 176-84.
65. Zou L, Harkey MR, Henderson GL. Effects of herbal components on cDNA-expressed cytochrome P450 enzyme catalytic activity. *Life Sci* 2002; 71: 1579-89.
66. Lawson LD, Gardner CD. Composition, stability, and bioavailability of garlic products used in a clinical trial. *J Agric Food Chem* 2005; 53: 6254-61.
67. Engdal S, Nilsen OG. *In vitro* inhibition of CYP3A4 by herbal remedies frequently used by cancer patients. *Phytother Res* 2009; 23: 906-12.
68. Ho BE, Shen DD, McCune JS, Bui T, Rislis L, Yang Z, et al. Effects of garlic on cytochromes P450 2C9- and 3A4-mediated drug metabolism in human hepatocytes. *Sci Pharm* 2010; 78: 473-81.
69. Raucy JL. Regulation of CYP3A4 expression in human hepatocytes by pharmaceuticals and natural products. *Drug Metab Dispos* 2003; 31: 533-9.
70. Lawson LD, Wang ZJ. Low alliinase release from garlic supplements: a major problem due to the sensitivities of alliinase activity. *J Agric Food Chem* 2001; 49: 2592-9.
71. Cox MC, Low J, Lee J, Walshe J, Denduluri N, Berman A, et al. Influence of garlic (*Allium sativum*) on the pharmacokinetics of docetaxel. *Clin Cancer Res* 2006; 12: 4636-40.

72. Marre F, Sanderink GJ, de Sousa G, Gaillard C, Martinet M, Rahmani R. Hepatic biotransformation of docetaxel (Taxotere) *in vitro*: involvement of the CYP3A subfamily in humans. *Cancer Res* 1996; 56: 1296-302.
73. Hao M, Zhao Y, Chen P, Huang H, Liu H, Jiang H, et al. Structure-activity relationship and substrate-dependent phenomena in effects of ginsenosides on activities of drug-metabolizing P450 enzymes. *PLoS One* 2008; 3: e2697.
74. Liu Y, Ma H, Zhang JW, Deng MC, Yang L. Influence of ginsenoside Rh1 and F1 on human cytochrome p450 enzymes. *Planta Med* 2006; 72: 126-31.
75. Izzo AA, Ernst E. Interactions between herbal medicines and prescribed drugs: an updated systematic review. *Drugs* 2009; 69: 1777-98.
76. Liu Y, Zhang JW, Li W, Ma H, Sun J, Deng MC, et al. Ginsenoside metabolites, rather than naturally occurring ginsenosides, lead to inhibition of human cytochrome P450 enzymes. *Toxicol Sci* 2006; 91: 356-64.
77. He N, Edeki T. The inhibitory effects of herbal components on CYP2C9 and CYP3A4 catalytic activities in human liver microsomes. *Am J of Th* 2004; 11: 206-12.
78. Malati CY, Robertson SM, Hunt JD, Chairez C, Alfaro RM, Kovacs JA, et al. Influence of Panax ginseng on cytochrome P450 (CYP)3A and P-glycoprotein (P-gp) activity in healthy participants. *J Clin Pharmacol* 2011; 52(6): 932-39.
79. Penzak SR, Busse KH, Robertson SM, Formentini E, Alfaro RM, Davey RT, Jr. Limitations of using a single postdose midazolam concentration to predict CYP3A-mediated drug interactions. *J Clin Pharmacol* 2008; 48: 671-80.
80. Bilgi N, Bell K, Ananthakrishnan AN, Atallah E. Imatinib and Panax ginseng: a potential interaction resulting in liver toxicity. *Ann Pharmacother* 2010; 44: 926-8.
81. The Coca-Cola Company. Product Descriptions: Full Throttle. http://www.virtualvender.coca-cola.com/ft/index.jsp?brand_id=700; date of last access: June 25, 2012.
82. Winslow LC, Kroll DJ. Herbs as medicines. *Arch Intern Med* 1998; 158: 2192-9.
83. Harkey MR, Henderson GL, Gershwin ME, Stern JS, Hackman RM. Variability in commercial ginseng products: an analysis of 25 preparations. *Am J Clin Nutr* 2001; 73: 1101-6.
84. Schulz HU, Schurer M, Krumbiegel G, Wachter W, Weyhenmeyer R, Seidel G. The solubility and bioequivalence of silymarin preparations. *Arzneimittelforschung* 1995; 45: 61-4.
85. Imai H, Kotegawa T, Tsutsumi K, Morimoto T, Eshima N, Nakano S, et al. The recovery time-course of CYP3A after induction by St John's wort administration. *Br J Clin Pharmacol* 2008; 65: 701-7.



CHAPTER 2

EFFECTS OF CAM ON CYP3A4- AND CYP2C9-MEDIATED METABOLISM OF ANTICANCER DRUGS





2.1

THE EFFECT OF COMPLEMENTARY AND ALTERNATIVE MEDICINES (CAM) ON CYP3A4-MEDIATED METABOLISM OF THREE DIFFERENT SUBSTRATES: 7-BENZYLOXY-4-TRIFLUOROMETHYLCOUMARIN (BFC), MIDAZOLAM AND DOCETAXEL

K.D. Mooiman
R.F. Maas-Bakker
J.J.M.A. Hendriks
P.C.D. Bank
H. Rosing
J.H. Beijnen
J.H.M. Schellens
I. Meijerman

Submitted for publication

ABSTRACT

Concomitant use of complementary and alternative medicine (CAM) and anticancer drugs can affect the pharmacokinetics of anticancer drugs by inhibiting the metabolizing enzyme Cytochrome P450 3A4 (EC 1.14.13.157). Several *in vitro* studies determined whether CAM can inhibit CYP3A4, but these studies revealed contradictory results. A plausible explanation for these conflicting results is the use only of a single model CYP3A4 substrate in each study.

Therefore, the aim was to determine the potential of selected CAM (β -carotene, Echinacea, garlic, Ginkgo biloba, ginseng, grape seed extract, green tea extract, milk thistle, saw palmetto, valerian, vitamin B₆, B₁₂ and C) to inhibit CYP3A4-mediated metabolism of different substrates: 7-benzyloxy-4-trifluoromethyl-coumarin (BFC), midazolam and docetaxel. The effect of CAM on CYP3A4-mediated metabolism of an anticancer drug has never been determined before *in vitro*, which makes the present study unique. The oncolytic CYP3A4 substrate docetaxel was used to establish the predictive value of the model substrates for pharmacokinetic interactions between CAM and anticancer drugs *in vitro* and to more closely predict these interactions *in vivo*.

The results confirmed grape seed and green tea as potent inhibitors and milk thistle as moderate inhibitor of CYP3A4-mediated metabolism of BFC, midazolam and docetaxel.

Clinical studies are required to determine the clinical relevance of the determined CYP3A4 inhibition by grape seed, green tea and milk thistle.

INTRODUCTION

In the past thirty years, the use of Complementary and Alternative Medicines (CAM) by cancer patients has increased rapidly. The estimated worldwide prevalence of CAM use by cancer patients increased from 31% in the late 1990s till 83% nowadays ¹. Cancer patients use CAM more frequently compared to the general population. Most popular CAM among cancer patients are herbal supplements such as Echinacea, garlic, Ginkgo biloba, ginseng, milk thistle, saw palmetto, St. John's Wort and valerian, and dietary supplements such as β -carotene and vitamins B₆, B₁₂ and C ²⁻⁴.

Reasons for cancer patients to combine CAM and conventional therapies include: improvement of the quality of life, improvement of the immune system, retardation of the progression of cancer and reduction of chemotherapy side effects ^{3,5}. However, the concomitant use of anticancer drugs and CAM could lead to serious safety issues, especially because of the narrow therapeutic window of most anticancer drugs ¹. The main cause of these safety issues is an increased risk for pharmacokinetic (PK) interactions, which arise when one drug affects the absorption, distribution, metabolism or elimination of another drug ⁶.

Most PK interactions are caused by changes in the functionality or expression of cytochrome P450 (CYP) enzymes. Of these enzymes, CYP3A4 (EC 1.14.13.157) is the most important CYP enzyme as it is most abundant in the liver and it metabolizes more than 50% of all drugs. Moreover, the majority of the currently prescribed anticancer drugs is metabolized by CYP3A4 (**Table 1**) ^{7,8}.

Table 1. Anticancer drugs metabolized by CYP3A4 ⁸.

Anticancer drug classes	Anticancer drugs
Alkylating agents	Busulfan, cyclophosphamide, ifosfamide, trabectedin
Antimetabolites	Cytarabine
Vinca alkaloids	Vinblastine, vincristine, vinorelbine
Taxanes	Docetaxel, paclitaxel
Topoisomerase inhibitors	Irinotecan, etoposide
Protein kinase inhibitors	Bortezomib, erlotinib, gefitinib, imatinib, sorafenib
Other anticancer drugs	Exemestane, letrozole, tamoxifen, tretinoin

Inhibition of CYP3A4 by CAM can result in increased plasma levels of most anticancer drugs and subsequently in toxicity ³. In literature, several *in vitro* studies have been performed to determine the inhibiting effect of frequently used CAM on CYP3A4. However, these studies revealed diverse effects for the majority of the CAM. Echinacea, garlic, ginseng and milk thistle were shown to both inhibit and not affect CYP3A4 ⁹⁻³³. Furthermore, several *in vitro* studies demonstrated a different degree in CYP3A4 inhibition by β -carotene,

Ginkgo biloba, grape seed, valerian, St. John's Wort, green tea, saw palmetto and vitamin C^{10-13, 16, 18, 20-22, 34-39, 39-50}. Moreover, no *in vitro* studies were reported with vitamin B₆ and B₁₂.

The majority of the performed *in vitro* studies determined the effects of CAM on CYP3A4 activity by using only one substrate. However, the use of multiple substrates is recommended to confirm CYP3A4 inhibition because of its complex inhibition kinetics and simultaneous metabolism of multiple compounds^{51,52}. Depending on the probe substrate used, it has been shown that an individual compound can differ significantly in its potency to inhibit CYP3A4. For example, it has been shown that 18 flavonoids inhibit CYP3A4 in a different rank order of potency, depending on the use of triazolam or testosterone as probe substrate⁵³. The inhibitory potency, frequently expressed in an IC₅₀ value, is also dependent on several factors such as the protein concentration of CYP3A4, incubation times, the type of substrate and the concentration of the substrate^{51,52}. Therefore, the present study determined and confirmed the effect of CAM on the CYP3A4 mediated metabolism of three different CYP3A4 substrates. First, in Supersomes™ the inhibition of CYP3A4-mediated metabolism of 7-benzyloxy-4-trifluoromethyl-coumarin (BFC) by CAM was assessed. Second, in human liver microsomes (HLM) the inhibition of CYP3A4-mediated metabolism of midazolam and docetaxel was determined. The effect of CAM on CYP3A4-mediated metabolism of an anticancer drug has never been determined before *in vitro*, which makes the present study unique. It is important to establish the predictive value of the model substrates for PK interactions between CAM and anticancer drugs *in vitro* and to more closely predict whether the observed CYP3A4 inhibition can cause these interactions in cancer patients too. Furthermore, the present study determined the effects of standardized extracts instead of extracting commercial products, since the phytochemical compounds of CAM are frequently unknown and variable among different brands and since commercial products can be adulterated. Also the potency of the compounds can vary because of differences in the processing methods and storage⁵⁴. By using standardized extracts the present study was able to overcome this limitation, since the identity and purity of these extracts is well known.

MATERIALS AND METHODS

Reagents and chemicals

Standardized extracts of milk thistle, Ginkgo biloba, Echinacea, ginseng, St. John's wort, saw palmetto, grape seed, valerian and vitamin C were obtained from Chromadex (Irvine, CA, USA). Standardized extracts of β -carotene, garlic, green tea, vitamin B₆ and B₁₂ were purchased from ABCR GmbH & Co KG (Karlsruhe, Germany), Organic Herb Inc., LTK laboratories Inc. (St. Paul, USA), UPS (Rockville, MD, USA) and Sigma-Aldrich (Zwij-

Table 2. Details of the standardized CAM extracts.

CAM	Product Information	Contents	
β -carotene	ABCR GmbH&Co KG [Lot # 1030612]	97% β -carotene	
Echinacea <i>Echinacea purpurea</i>	Chromadex [Lot # 00030217-012]	0.94% caftaric acid 0.03% chlorogenic acid 0.04% cynarin	0.05% echinacoside 1.80% cichoric acid
Garlic <i>Allium sativum</i>	Organic Herb Inc. [100-20100122]	Garlic extract (100:1)	Allicin scordinin alliin
<i>Ginkgo biloba</i>	Chromadex [Lot # 00030299-1917]	4.78% quercetin 3.73% kaempferol 2.13% isorhamnetin 12.0% quercetin glycoside 9.65% kaempferol glycoside 5.19% isorhamnetin glycoside	1.61% bilobalide 1.41% ginkgolide A 0.31% ginkgolide J 5.57% ginkgolide B 0.38% ginkgolide C
Ginseng <i>Eleutherococcus senticosus</i>	Chromadex [Lot # 00030302-019]	0.439% eleutheroside E	0.245% eleutheroside B
Grape seed <i>Vitis vinifera</i>	Chromadex [Lot # 00036130-11]	5.08% epigallocatechin 0.93% catechin 6.30% epicatechin	0.02% epigallocatechin gallate 0.03% epicatechin gallate
Green tea <i>Camellia sinensis</i>	LTK Laboratories Inc. [G6817]	99.61% tea polyphenols 65.38% EGCG 82.79% catechins	1.17% caffeine 3.98% water 0.18% sulfated ash
Milk Thistle <i>Silybum marianum</i>	Chromadex [Lot # 00030402-101]	29.6% silybin A+B 2.97% taxifolin	14.7% silychristin
Saw Palmetto <i>Serenoa serrulata</i>	Chromadex [Lot # 00030726-841]	0.13% campesterol 0.07% stigmasterol 0.43% β -sistosterol 0.21% methyl caproate 0.93% methyl octanoate 2.53% methyl decanoate 28.61% methyl dodecanoate 10.63% methyl myristate	8.55% methyl palmitate 1.81% methyl stearate 30.40% methyl oleate 5.28% methyl linolenate 0.75% methyl linoleate 0.17% methyl arachidate 0.02% methyl EPA 0.11% methyl DHA
St. John's wort <i>Hypericum perforatum</i>	Chromadex [Lot # 00030798-155]	1.87% rutin 0.24% pseudohypericin	0.01% hyperforin 0.06% hypericin
Valerian <i>Valeriana officinalis</i>	Chromadex [Lot # 34899-045]	0.16% valerenic acids	
Vitamin B ₆	Sigma-Aldrich [Lot # 120M13271V]	> 98% pyridoxine	
Vitamin B ₁₂	Sigma-Aldrich [Lot # 030M1567]	> 98% vitamin B ₁₂	
Vitamin C	Chromadex [Lot # 111021-641]	Vitamin C	

Abbreviations: DHA, docosahexaenoic acid; EPA, eicosapentaenoic acid.

drecht, The Netherlands), respectively. An overview of details of these standardized extracts is shown in **Table 2**. Acetonitrile was obtained from Biosolve (Valkenswaard, The Netherlands) and ketoconazole and nicotinamide adenine dinucleotide phosphate (NADPH) tetra sodium salt from Sigma-Aldrich (Zwijndrecht, The Netherlands). CYP3A4 substrate 7-benzyloxy-4-trifluoromethyl-coumarin (BFC) and human cDNA expressed CYP3A4 + reductase and b5 (CYP3A4+OR+b5+) Supersomes™ were purchased from BD-Bioscience (Breda, The Netherlands). Human pooled liver microsomes (HLM) originated from BD Gentest (Breda, The Netherlands). Midazolam, 1-hydroxymidazolam and labeled 1-hydroxymidazolam-¹³C₃ and docetaxel-D₉ were obtained from Toronto Research Canada (TRC, North York, Canada) and docetaxel from Sigma-Aldrich (Zwijndrecht, The Netherlands). LC-MS grade water, methanol of HPLC quality and acetonitrile of HPLC-S gradient were purchased from Biosolve (Valkenswaard, The Netherlands). Ammonium hydroxide solution 28-30%, acetic acid and ammonium acetate were obtained from Sigma-Aldrich. Tert-Butyl Methyl Ether (TBME) for liquid chromatography and sodium hydroxide were purchased from Merck (Darmstadt, Germany).

Supersomes™ and Human Liver Microsomes

Supersomes™ are recombinant cDNA-expressed cytochrome P450 enzymes prepared from a baculovirus-infected insect cell system. The CYP3A4 content of the human 3A4 Supersomes™ used in this study was reported to be 233 pmol/mg protein. The Supersomes™ also contained Cytochrome b5 (4.3 pmol/mg protein) and Cytochrome C reductase with an activity of 2.6 pmol/min.mg.

A pooled mixture of HLM from 25 different individual donors (mixed genders) was used in this study. The total P450 content was reported to be 330 pmol/mg. According to the product insert the HLM contained 420 pmol/mg Cytochrome b5 and Cytochrome C reductase with an activity of 200 pmol/min.mg.

CYP3A4-mediated metabolism of BFC in Supersomes™

The fluorometric CYP3A4 inhibition assay is based on the method as described by Stresser *et al.*⁵⁵. Incubations of the CYP3A4 expressing Supersomes™ were performed in black 96-well plates. For the CAM screen, all test compounds were diluted in 1 mg/mL NADPH solution to achieve an end concentration of 10 µg/mL for each CAM and 100 nM for ketoconazole. For the IC₅₀ curves, the concentrations ranged from 0 to 500 µg/mL for most CAM, except for: milk thistle (0-100 µg/mL), β-carotene (0-150 µg/mL) and Ginkgo biloba (0-250 µg/mL). The range of the concentrations was dependent on the quenching property, solubility and strength of CYP3A4 inhibition. After prewarming the dilutions of CAM and ketoconazole for 10 minutes at 37°C, 100 pmol of CYP3A4+OR+b5+ Supersomes™ and 50 mM of non-fluorescent BFC in 100 mM phosphate buffer was added. The final concentration of acetonitrile (the solvent of BFC, ketoconazole and all

CAM) did not exceed 2% during the incubations. The reaction mixtures were incubated for 30 minutes at 37°C. The reaction was stopped on ice by adding a solution of 80% acetonitrile and 20% 0.5 M Tris base. Formation of highly fluorescent metabolite of BFC 7-hydroxy-4-trifluoromethylcoumarin (HFC) was measured (at 405/530 nm) on a Mithras LB940 microplate reader (Berthold Technologies, Bad Wildbad, Germany).

CYP3A4-mediated metabolism of midazolam in human liver microsomes

The effects of CAM on CYP3A4-mediated metabolism of midazolam were determined by measuring the formation of the most important metabolite 1-hydroxymidazolam with a validated liquid-chromatography coupled to tandem mass spectrometry (LC-MS/MS) method⁵⁶ at the Utrecht University.

Incubations

Incubations were performed in triplicate in 2.0 mL polypropylene tubes (Sarstedt, Etten-Leur, The Netherlands). The cofactor solution consisted of 2.6 mM NADP⁺, 7.1 mM glucose-6-phosphate, 6.5 mM magnesium chloride and 0.8 U/mL glucose-6-phosphate dehydrogenase in 50 mM phosphate buffer, pH 7.4. For the CAM screen, the stock solutions of all fourteen CAM (3.125 mg/mL in 50% acetonitrile) were diluted in the cofactor solution to an end concentration of 25 µg/mL. For the IC₅₀ curves, the concentrations ranged from 0 to 100 µg/mL for the tested CAM, except for grape seed (0-50 µg/mL). Also the stock solution of positive control ketoconazole (500 µM in pure ACN) was diluted similarly to achieve an end concentration of 2 µM. The midazolam stock of 250 µM was diluted in 100 mM phosphate buffer and added to the CAM cofactor solution, resulting in an end concentration of 2.5 µM midazolam during the incubation. This end concentration is close to the Michaelis Menten constant K_m as determined in preliminary experiments (data not shown) and in accordance to Walsky *et al.*⁵⁷. The dilutions of CAM, ketoconazole and midazolam were pre-incubated at 37°C for 10 minutes and the reaction was started by adding a HLM solution in 50 mM phosphate buffer with an end concentration of 50 µg/mL HLM. In the 200 µL reaction volume, the concentration of acetonitrile was 2%. The reaction was stopped after 5 minutes with 100 µL ice cold 100 mM sodium hydroxide. At last, the labeled internal standard 1-hydroxymidazolam-¹³C₃ was added.

Bioanalytical analysis

Liquid-liquid extraction (LLE) was performed with Tert-Butyl Methyl Ether (TBME) and all samples were vortex-mixed for 30 seconds. After centrifugation for 5 minutes at 10,600 *g*, all samples were stored for one hour at -80°C. The organic phase was decanted in clean 1.5 mL polypropylene tubes and evaporated under a stream of nitrogen at 40°C. The residue was reconstituted in 250 µL methanol-water (50:50 v/v) and vortex-mixed for 30 seconds. After centrifugation for 5 minutes at 10,600 *g*, the clear supernatant was

transferred in a 250 μL glass insert placed in autosampler vials for liquid chromatography-quadrupole mass spectrometry (LC-MS/MS) analysis.

The samples were injected in Shimadzu LC10-AD liquid chromatography comprising of a DGU-14A degasser, a CTO-10Avp column oven (35°C), a Sil-HTc autosampler (4°C) and two LC10-AD μ -pumps (Shimadzu, Kyoto, Japan). The mobile phase consisted of methanol and 10 mM ammonium hydroxide in water (60:40 v/v), with a flow rate of 0.25 mL/min and total run time of 9 min. Midazolam and its metabolite 1-hydroxymidazolam were detected with a Finnigan TSQ Quantum Discovery Max triple quadrupole mass spectrometer (Thermo Fischer Scientific, Waltham, MA, USA) with electrospray ionization (ESI). To quantify the data reconstituted calibration standards of 1-hydroxymidazolam were applied in a range of 1-500 nM.

CYP3A4-mediated metabolism of docetaxel in human liver microsomes

To determine the effects of CAM on CYP3A4-mediated metabolism of docetaxel, the formation of the most important metabolite hydroxydocetaxel (M2)⁵⁸ was measured with a validated LC-MS/MS method⁵⁹ at the Slotervaart Hospital.

Incubations

The incubations of HLM with docetaxel were performed as described above with a few exceptions. For the CAM screen, stock solutions of 12.5 mg/mL in 50% acetonitrile were prepared for an end concentration of 100 $\mu\text{g/mL}$. For the IC_{50} curves, the concentrations ranged from 0 to 500 $\mu\text{g/mL}$ for the tested CAM. The stock solution of positive control ketoconazole was diluted similarly to achieve an end concentration of 500 nM. The docetaxel stock solution was diluted in 100 mM phosphate buffer to an end concentration of 2 μM , approximately the K_m as determined in preliminary experiments (data not shown) and by Royer *et al.*⁶⁰. The HLM solution consisted of 250 $\mu\text{g/mL}$ microsomes in 50 mM phosphate buffer. At last, the reaction was stopped after 30 minutes with 100 μL ice cold acetic acid [2% in water].

Bioanalytical analysis

The sample preparation of the docetaxel samples was the same as described above with minor modifications. D_9 -labelled docetaxel was used as internal standard and 0.1M ammonium acetate-acetonitrile (1:1 v/v) was used as reconstitution solvent. An aliquot was injected into a liquid chromatographic system consisting of a mobile phase degasser, a column oven (30°C), an autosampler (4°C) and a binary pump (Agilent Technologies, Palo Alto, CA, USA). A gradient eluent (consisting of methanol (A) and 10 mM ammonium hydroxide in water (B)) was used at a flow rate of 0.2 mL/min. Docetaxel and M2 were detected with an API-3000 triple quadrupole mass spectrometer coupled with a

turbo-ionspray interface (PE Sciex, Toronto, Canada). For quantification reconstituted calibration standards in a range of 0.5-500 ng/mL were used.

Statistical Analysis

The two-tailed Students *t*-test with 95% confidence ($p < 0.05$) was performed on data from the incubations with CAM, compared to data from the incubations with the negative controls, to determine the significance of CYP3A4 inhibition by CAM. All statistical determinations were performed with SPSS version 16.0 (SPSS Inc., Chicago, IL, USA). IC_{50} calculations of the inhibiting CAM were performed with GraphPad Prism 4.0 (GraphPad Software, San Diego, USA).

RESULTS

HLM were used to determine the effects of CAM on the CYP3A4-mediated metabolism of midazolam and docetaxel and Supersomes™ to determine the effect on the metabolism of BFC. Supersomes™ contain an overexpression of one single CYP enzyme (3A4)⁶¹ and HLM contain multiple CYP enzymes⁶². HLM are preferred as *in vitro* test system because HLM more closely mimic the clinical situation compared to Supersomes™. However, it is not possible to reliably determine the effect of CAM on the metabolism of BFC in HLM since this test system contains multiple CYP enzymes and the metabolism of BFC is not only primarily catalyzed by CYP3A4⁶³. Since the metabolism of midazolam and docetaxel are CYP3A specific, the preferred HLM could be used.

CAM screen

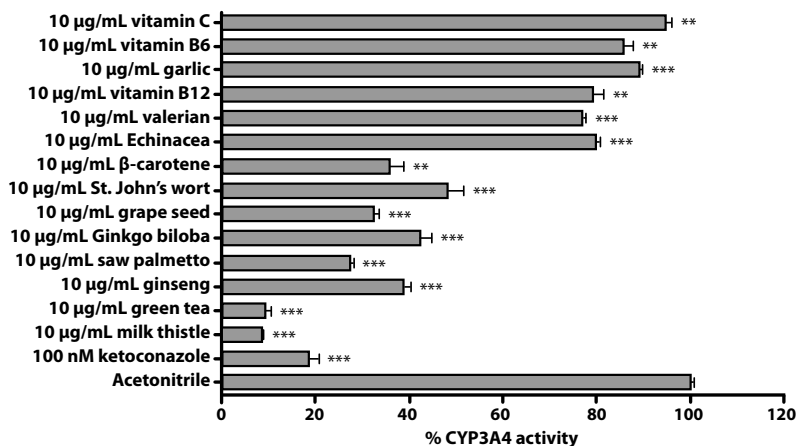
The inhibition of CYP3A4 activity by fourteen commonly used CAM was determined in three screens: a fluorescence assay, using BFC as the preferred CYP3A4 probe⁶⁴; a LC-MS/MS method, evaluating CYP3A4-mediated metabolism of the sensitive CYP3A4 substrate probe midazolam⁶⁵; and a LC-MS/MS method, using the anticancer drug docetaxel as a specific oncolytic CYP3A4 substrate⁸. The results of these CAM screens are shown in **Figure 1**.

Milk thistle is the most potent inhibitor of CYP3A4-mediated metabolism of BFC, followed by green tea, saw palmetto, grape seed, β -carotene, ginseng, Ginkgo biloba and St. John's wort. In contrast, the CAM screen with midazolam as CYP3A4 substrate revealed grape seed as the most potent inhibitor of CYP3A4 activity, followed by green tea, β -carotene, milk thistle, St. John's wort and Ginkgo biloba. The same order of inhibitory potency was confirmed in the screen with docetaxel as CYP3A4 substrate. None of the CAM caused significant autofluorescence or quenching of the fluorescent signal in

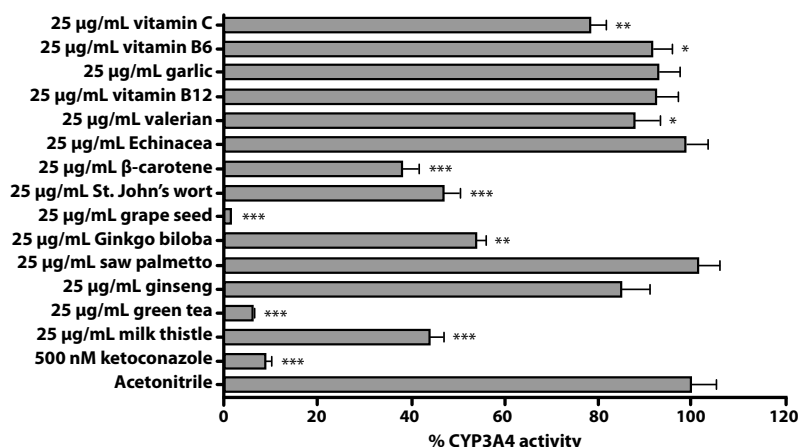
the fluorescence assay in the tested concentration ranges and no interference with the LC-MS/MS measurement of both midazolam and docetaxel was observed.

The majority of the CAM inhibited CYP3A4-mediated metabolism of BFC, midazolam and docetaxel, except for saw palmetto and ginseng. Saw palmetto and ginseng were categorized as potent inhibitors of CYP3A4-mediated metabolism of BFC, but these CAM showed practically no inhibition of the metabolism of both midazolam and docetaxel (Table 3).

A. CYP3A4-mediated metabolism of BFC



B. CYP3A4-mediated metabolism of midazolam



C. CYP3A4-mediated metabolism of docetaxel

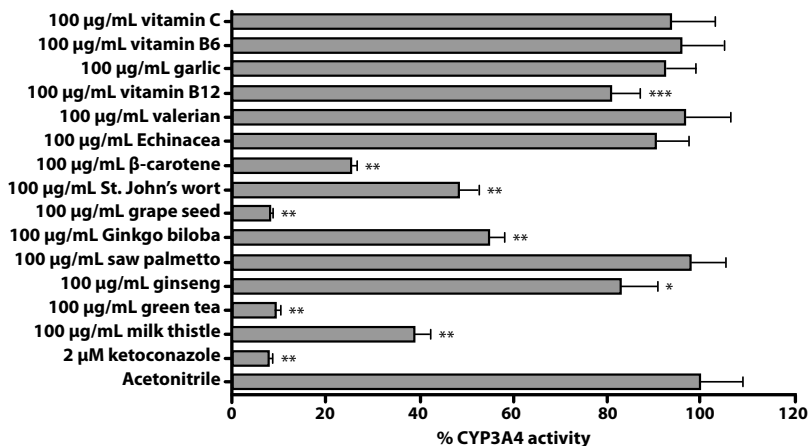


Figure 1. Effects of CAM on CYP3A4-mediated metabolism of BFC (A), midazolam (B) and docetaxel (C). For CYP3A4-mediated metabolism of BFC, CYP3A4+OR+b5 Supersomes™ were incubated with 2% negative control acetonitrile, 100 nM of the positive control ketoconazole and 10 µg/mL CAM for 30 minutes. After stopping the reaction, the formation of highly fluorescent HFC was measured. For CYP3A4-mediated metabolism of midazolam and docetaxel, human liver HLM were incubated with respectively 2% negative control acetonitrile, 500 nM of ketoconazole and 25 µg/mL CAM for 5 minutes and 2 µM ketoconazole and 10 µg/mL CAM for 30 minutes. After stopping the reaction, the formation of the metabolites 1-hydroxymidazolam and M2 was measured. The data are means ± SD of triplicate incubations from a representative experiment. The fold inductions compared to 2% acetonitrile are shown (* $P < 0.05$; ** $P < 0.01$; *** $P < 0.001$).

Table 3. Overview of the ranking order of CAM based on the degree of CYP3A4 inhibition.

Fluorescence assay with BFC			LC-MS/MS with midazolam			LC-MS/MS with docetaxel		
Rank	CAM	% Inhibition	Rank	CAM	% Inhibition	Rank	CAM	% Inhibition
1	Milk thistle	91.5	1	Grape seed	98.4	1	Grape seed	92.0
2	Green tea	90.7	2	Green tea	93.8	2	Green tea	90.9
3	Saw palmetto	72.6	3	β-carotene	61.9	3	β-carotene	74.6
4	Grape seed	67.7	4	Milk thistle	55.9	4	Milk thistle	61.0
5	β-carotene	64.2	5	St. John's wort	52.9	5	St. John's wort	51.6
6	Ginseng	61.3	6	Ginkgo Biloba	45.9	6	Ginkgo Biloba	45.1
7	Ginkgo Biloba	57.8	8	Ginseng	14.8	8	Ginseng	16.8
8	St. John's wort	51.7	14	Saw Palmetto	-1.64	14	Saw Palmetto	1.91

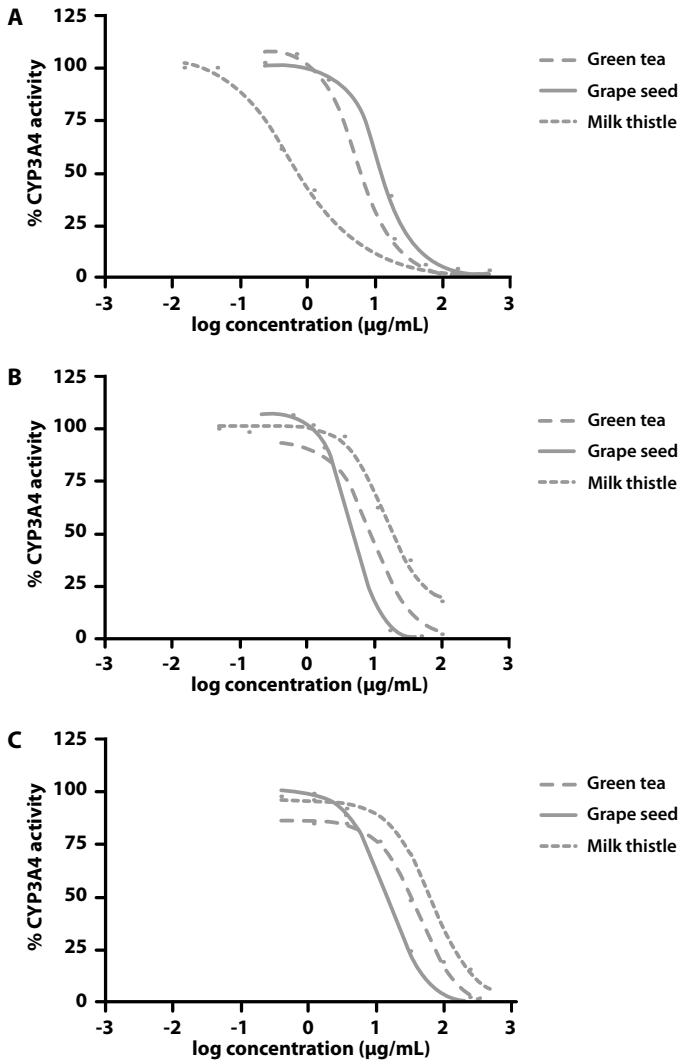


Figure 2. IC₅₀ curves of milk thistle, green tea and grape seed. The data of the IC₅₀ curves are means of duplicate incubations from a representative experiment. **A:** inhibition of CYP3A4-mediated metabolism of BFC; **B:** inhibition of CYP3A4-mediated metabolism of midazolam; **C:** inhibition of CYP3A4-mediated metabolism of docetaxel.

IC₅₀ curves

In order to predict the clinical relevance of the observed inhibition, the IC₅₀ values of the top 6 inhibiting CAM were determined, using the fluorescent substrate BFC, midazolam and docetaxel (**Table 4**). In addition, the IC₅₀ curves of milk thistle, green tea and grape seed are shown in **Figure 2**.

Table 4. Overview of the ranking order of CAM based on the degree of CYP3A4 inhibition.

Fluorescence assay with BFC			LC-MS/MS with midazolam			LC-MS/MS with docetaxel		
CAM	IC ₅₀ (µg/mL) [95% C.I.]	R ²	CAM	IC ₅₀ (µg/mL) [95% C.I.]	R ²	CAM	IC ₅₀ (µg/mL) [95% C.I.]	R ²
Ketoco- nazole	1.66x10 ⁻² [1.16-2.37 x10 ⁻²]	0.996	Ketoco- nazole	1.57x10 ⁻² [1.14-2.16 x10 ⁻²]	0.999	Ketoco- nazole	0.140 [0.0986- 0.196]	0.997
Milk thistle	0.639 [0.49-0.83]	0.997	Grape seed	4.58 [3.69-5.68]	0.999	Grape seed	15.3 [10.5-22.3]	0.999
Green tea	4.86 [2.79-8.46]	0.991	Green tea	9.96 [5.41-18.3]	0.991	Green tea	42.3 [36.2-49.4]	0.999
Ginseng	6.82 [3.58-13.0]	0.985	β-carotene	15.0 [12.6-17.8]	0.999	β-carotene	49.0 [37.3-64.4]	0.998
Saw Palmetto	8.45 [5.70-12.5]	0.995	Milk thistle	21.0 [9.56-46.2]	0.981	Milk thistle	66.2 [53.4-82.2]	0.999
Ginkgo biloba	8.83 [7.93-9.84]	0.999	St. John's wort	32.3 [10.9-95.7]	0.978	St. John's wort	115 [38.3-350]	0.997
Grape seed	12.7 [4.79-33.6]	0.991	Ginkgo Biloba	75.1 [53.0-106]	0.998	Ginkgo Biloba	155 [81.3-297]	0.997

Milk thistle and green tea are shown to be the most potent inhibitors of CYP3A4-mediated metabolism of BFC. In addition, grape seed and green tea most strongly inhibited the CYP3A4-mediated metabolism of midazolam and docetaxel: IC₅₀ < 10 µg/mL and IC₅₀ < 45 µg/mL, respectively (**Table 4**). Milk thistle moderately inhibited the metabolism of midazolam and docetaxel.

DISCUSSION AND CONCLUSION

In the present study fourteen standardized extracts of commonly used CAM²⁻⁴ were screened for their ability to inhibit CYP3A4 activity. These inhibitory effects were confirmed by determining the effects of CAM on CYP3A4-mediated metabolism of multiple CYP3A4 substrates: BFC, midazolam and docetaxel. Overall, grape seed and green tea were confirmed as potent inhibitors and milk thistle as a moderate inhibitor of CYP3A4-mediated metabolism of multiple substrates. In contrast, saw palmetto and ginseng did inhibit CYP3A4 mediated metabolism of BFC, but both CAM showed practically no inhibition of CYP3A4-mediated metabolism of midazolam and docetaxel. These results underline the complexity of CYP3A4 inhibition due to the variability with different substrates and inhibitor pairs⁵¹ and the propensity of CYP3A4 for time-dependent inhibition.

When comparing the CAM screens using the substrates BFC, midazolam and docetaxel, different concentrations of CAM were required to obtain the same level of CYP3A4 inhi-

bition. In addition, the IC_{50} values of each CAM varied for the different probe substrates. From literature it is known that there is a poor correlation in the IC_{50} values among traditional CYP3A4 substrates and fluorometric substrates due to several factors, such as the protein concentration of CYP3A4, incubation times and the type and concentration of the substrate^{51,52}. Since these factors differed between the docetaxel and midazolam assay, the IC_{50} values of the CAM were generally higher in the docetaxel assay compared to the midazolam assay. However, the potency to inhibit CYP3A4 showed the same rank order. Thus, the probe substrate midazolam has been shown to correctly predict PK interactions between CAM and docetaxel *in vitro*.

Although the *in vitro* results of these extracts can be extrapolated to the clinical situation by confirming CYP3A4 inhibition in multiple assays with different substrates (especially docetaxel) and methods for quantification, the application of these results for the clinical risk-assessment is still uncertain. Cancer patients use different commercial CAM products that vary in the phytochemical content, bioavailability and drug-releasing properties⁶⁶. Therefore, the effect of CAM extracts and not active components was evaluated, but still an accurate prediction of clinical PK interactions is complicated. An approach to predict the potential for CYP inhibition in human, is expressing the inhibitory potency in the volume in which the recommended human dose should be diluted to achieve the IC_{50} values in human⁶⁷. Based on the calculations suggested by Strandell *et al.*, the dosage and average content of CAM extracts in commercial products, CYP3A4 inhibiting CAM grape seed, green tea and milk thistle should be diluted in < 5.9 liters, which is in range of the human blood volume and therefore potent enough for further investigation. It should be mentioned that the bioavailability and distribution volumes are not taken into account in the described approach. Therefore, clinical studies should be conducted to determine the clinical relevance of the PK interaction between grape seed, green tea and milk thistle and anticancer drugs metabolized by CYP3A4.

In conclusion, grape seed and green tea were confirmed as potent inhibitors and milk thistle as moderate inhibitor of CYP3A4-mediated metabolism of multiple substrates. Since grape seed, green tea and milk thistle inhibited the CYP3A4-mediated metabolism of docetaxel, these CAM could cause PK interactions with anticancer drugs *in vivo*. Clinical studies are required to determine the clinical relevance of these interactions.

REFERENCES

1. Sparreboom A, Cox MC, Acharya MR, Figg WD. Herbal remedies in the United States: Potential adverse interactions with anticancer agents. *J Clin Oncol* 2004; 22(12): 2489-503.
2. McCune JS, Hatfield AJ, Blackburn AA, Leith PO, Livingston RB, Ellis GK. Potential of chemotherapy-herb interactions in adult cancer patients. *Support Care Cancer* 2004; 12(6): 454-62.
3. Tascilar M, de Jong FA, Verweij J, Mathijssen RH. Complementary and alternative medicine during cancer treatment: Beyond innocence. *Oncologist* 2006; 11(7): 732-41.
4. Gupta D, Lis CG, Birdsall TC, Grutsch JF. The use of dietary supplements in a community hospital comprehensive cancer center: Implications for conventional cancer care. *Support Care Cancer* 2005; 13(11): 912-9.
5. Werneke U, Earl J, Seydel C, Horn O, Crichton P, Fannon D. Potential health risks of complementary alternative medicines in cancer patients. *Br J Cancer* 2004; 90(2): 408-13.
6. Beijnen JH, Schellens JH. Drug interactions in oncology. *Lancet Oncol* 2004; 5(8): 489-96.
7. Anzenbacher P, Anzenbacherova E. Cytochromes P450 and metabolism of xenobiotics. *Cell Mol Life Sci* 2001; 58(5-6): 737-47.
8. He SM, Yang AK, Li XT, Du YM, Zhou SF. Effects of herbal products on the metabolism and transport of anticancer agents. *Expert Opin Drug Metab Toxicol* 2010; 6(10): 1195-213.
9. Modarai M, Silva E, Suter A, Heinrich M, Kortenkamp A. Safety of herbal medicinal products: Echinacea and selected alkylamides do not induce CYP3A4 mRNA expression. *Evid Based Complement Alternat Med* 2011; 2011: 1-7.
10. Hansen TS, Nilsen OG. *In vitro* CYP3A4 metabolism: Inhibition by Echinacea purpurea and choice of substrate for the evaluation of herbal inhibition. *Basic Clin Pharmacol Toxicol* 2008; 103(5): 445-9.
11. Hellum BH, Nilsen OG. *In vitro* inhibition of CYP3A4 metabolism and P-glycoprotein-mediated transport by trade herbal products. *Basic Clin Pharmacol Toxicol* 2008; 102(5): 466-75.
12. Hellum BH, Hu Z, Nilsen OG. The induction of CYP1A2, CYP2D6 and CYP3A4 by six trade herbal products in cultured primary human hepatocytes. *Basic Clin Pharmacol Toxicol* 2007; 100(1): 23-30.
13. Yale SH, Glurich I. Analysis of the inhibitory potential of Ginkgo biloba, Echinacea purpurea, and Serenoa repens on the metabolic activity of cytochrome P450 3A4, 2D6, and 2C9. *J Altern Complement Med* 2005; 11(3): 433-9.
14. Foster BC, Vandenhoek S, Hana J, Krantis A, Akhtar MH, Bryan M, Budzinski JW, Ramputh A, Arnanon JT. *In vitro* inhibition of human cytochrome P450-mediated metabolism of marker substrates by natural products. *Phytomedicine* 2003; 10(4): 334-42.
15. Modarai M, Gertsch J, Suter A, Heinrich M, Kortenkamp A. Cytochrome P450 inhibitory action of Echinacea preparations differs widely and co-varies with alkylamide content. *J Pharm Pharmacol* 2007; 59(4): 567-73.
16. Engdal S, Nilsen OG. *In vitro* inhibition of CYP3A4 by herbal remedies frequently used by cancer patients. *Phytother Res* 2009; 23(7): 906-12.
17. Ho BE, Shen DD, McCune JS, Bui T, Rislis L, Yang Z, Ho RJ. Effects of garlic on cytochromes P450 2C9- and 3A4-mediated drug metabolism in human hepatocytes. *Sci Pharm* 2010; 78(3): 473-81.
18. Zou L, Harkey MR, Henderson GL. Effects of herbal components on cDNA-expressed cytochrome P450 enzyme catalytic activity. *Life Sci* 2002; 71(13): 1579-89.

19. Foster BC, Foster MS, Vandenhoeck S, Krantis A, Budzinski JW, Arnason JT, Gallicano KD, Choudri S. An *in vitro* evaluation of human cytochrome P450 3A4 and P-glycoprotein inhibition by garlic. *J Pharm Pharm Sci* 2001; 4(2): 176-84.
20. Etheridge AS, Black SR, Patel PR, So J, Mathews JM. An *in vitro* evaluation of cytochrome P450 inhibition and P-glycoprotein interaction with goldenseal, Ginkgo biloba, grape seed, milk thistle, and ginseng extracts and their constituents. *Planta Med* 2007; 73(8): 731-41.
21. He N, Edeki T. The inhibitory effects of herbal components on CYP2C9 and CYP3A4 catalytic activities in human liver microsomes. *Am J Ther* 2004; 11(3): 206-12.
22. Patel J, Buddha B, Dey S, Pal D, Mitra AK. *In vitro* interaction of the HIV protease inhibitor ritonavir with herbal constituents: Changes in P-gp and CYP3A4 activity. *Am J Ther* 2004; 11(4): 262-77.
23. Hao M, Zhao Y, Chen P, Huang H, Liu H, Jiang H, Zhang R, Wang H. Structure-activity relationship and substrate-dependent phenomena in effects of ginsenosides on activities of drug-metabolizing P450 enzymes. *PLoS One* 2008; 3(7): e2697.
24. Liu Y, Ma H, Zhang JW, Deng MC, Yang L. Influence of ginsenoside Rh1 and F1 on human cytochrome p450 enzymes. *Planta Med* 2006; 72(2): 126-31.
25. Liu Y, Zhang JW, Li W, Ma H, Sun J, Deng MC, Yang L. Ginsenoside metabolites, rather than naturally occurring ginsenosides, lead to inhibition of human cytochrome P450 enzymes. *Toxicol Sci* 2006; 91(2): 356-64.
26. Budzinski JW, Trudeau VL, Drouin CE, Panahi M, Arnason JT, Foster BC. Modulation of human cytochrome P450 3A4 (CYP3A4) and P-glycoprotein (P-gp) in caco-2 cell monolayers by selected commercial-source milk thistle and goldenseal products. *Can J Physiol Pharmacol* 2007; 85(9): 966-78.
27. Beckmann-Knopp S, Rietbrock S, Weyhenmeyer R, Bocker RH, Beckurts KT, Lang W, Hunz M, Fuhr U. Inhibitory effects of silybinin on cytochrome P-450 enzymes in human liver microsomes. *Pharmacol Toxicol* 2000; 86(6): 250-6.
28. Doehmer J, Tewes B, Klein KU, Gritzko K, Muschick H, Mengs U. Assessment of drug-drug interaction for silymarin. *Toxicol in Vitro* 2008; 22(3): 610-7.
29. Jancova P, Anzenbacherova E, Papouskova B, Lemr K, Luzna P, Veinlichova A, Anzenbacher P, Simanek V. Silybin is metabolized by cytochrome P450 2C8 *in vitro*. *Drug Metab Dispos* 2007; 35(11): 2035-9.
30. Kosina P, Maurel P, Ulrichova J, Dvorak Z. Effect of silybin and its glycosides on the expression of cytochromes P450 1A2 and 3A4 in primary cultures of human hepatocytes. *J Biochem Mol Toxicol* 2005; 19(3): 149-53.
31. Sridar C, Goosen TC, Kent UM, Williams JA, Hollenberg PF. Silybin inactivates cytochromes P450 3A4 and 2C9 and inhibits major hepatic glucuronosyltransferases. *Drug Metab Dispos* 2004; 32(6): 587-94.
32. Venkataramanan R, Ramachandran V, Komoroski BJ, Zhang S, Schiff PL, Strom SC. Milk thistle, a herbal supplement, decreases the activity of CYP3A4 and uridine diphosphoglucuronosyl transferase in human hepatocyte cultures. *Drug Metab Dispos* 2000; 28(11): 1270-3.
33. Zuber R, Modriansky M, Dvorak Z, Rohovsky P, Ulrichova J, Simanek V, Anzenbacher P. Effect of silybin and its congeners on human liver microsomal cytochrome P450 activities. *Phytother Res* 2002; 16(7): 632-8.
34. Ruhl R, Sczech R, Landes N, Pfluger P, Kluth D, Schweigert FJ. Carotenoids and their metabolites are naturally occurring activators of gene expression via the pregnane X receptor. *Eur J Nutr* 2004; 43(6): 336-43.

35. Yasui H, Deo K, Ogura Y, Yoshida H, Shiraga T, Kagayama A, Sakurai H. Evidence for singlet oxygen involvement in rat and human cytochrome P450-dependent substrate oxidations. *Drug Metab Pharmacokinet* 2002; 17(5): 416-26.
36. Wang K, Chen S, Xie W, Wan YJ. Retinoids induce cytochrome P450 3A4 through RXR/VDR-mediated pathway. *Biochem Pharmacol* 2008; 75(11): 2204-13.
37. Wang K, Mendy AJ, Dai G, Luo HR, He L, Wan YJ. Retinoids activate the RXR/SXR-mediated pathway and induce the endogenous CYP3A4 activity in Huh7 human hepatoma cells. *Toxicol Sci* 2006; 92(1): 51-60.
38. Muto S, Fujita K, Yamazaki Y, Kamataki T. Inhibition by green tea catechins of metabolic activation of procarcinogens by human cytochrome P450. *Mutat Res* 2001; 479(1-2): 197-206.
39. Nishikawa M, Ariyoshi N, Kotani A, Ishii I, Nakamura H, Nakasa H, Ida M, Nakamura H, Kimura N, Kimura M, et al. Effects of continuous ingestion of green tea or grape seed extracts on the pharmacokinetics of midazolam. *Drug Metab Pharmacokinet* 2004; 19(4): 280-9.
40. Netsch MI, Gutmann H, Schmidlin CB, Aydogan C, Drewe J. Induction of CYP1A by green tea extract in human intestinal cell lines. *Planta Med* 2006; 72(6): 514-20.
41. Mirkov S, Komoroski BJ, Ramirez J, Graber AY, Ratain MJ, Strom SC, Innocenti F. Effects of green tea compounds on irinotecan metabolism. *Drug Metab Dispos* 2007; 35(2): 228-33.
42. Gaudineau C, Beckerman R, Welbourn S, Auclair K. Inhibition of human P450 enzymes by multiple constituents of the Ginkgo biloba extract. *Biochem Biophys Res Commun* 2004; 318(4): 1072-8.
43. Yeung EY, Sueyoshi T, Negishi M, Chang TK. Identification of Ginkgo biloba as a novel activator of pregnane X receptor. *Drug Metab Dispos* 2008; 36(11): 2270-6.
44. Li L, Stanton JD, Tolson AH, Luo Y, Wang H. Bioactive terpenoids and flavonoids from Ginkgo biloba extract induce the expression of hepatic drug-metabolizing enzymes through pregnane X receptor, constitutive androstane receptor, and aryl hydrocarbon receptor-mediated pathways. *Pharm Res* 2009; 26(4): 872-82.
45. He N, Cai HB, Xie HG, Collins X, Edeki TI, Strom SC. Induction of cyp3a in primary cultures of human hepatocytes by ginkgolides A and B. *Clin Exp Pharmacol Physiol* 2007; 34(7): 632-5.
46. Satsu H, Hiura Y, Mochizuki K, Hamada M, Shimizu M. Activation of pregnane X receptor and induction of MDR1 by dietary phytochemicals. *J Agric Food Chem* 2008; 56(13): 5366-73.
47. Raucy JL. Regulation of CYP3A4 expression in human hepatocytes by pharmaceuticals and natural products. *Drug Metab Dispos* 2003; 31(5): 533-9.
48. Gutmann H, Poller B, Buter KB, Pfrunder A, Schaffner W, Drewe J. Hypericum perforatum: Which constituents may induce intestinal MDR1 and CYP3A4 mRNA expression? *Planta Med* 2006; 72(8): 685-90.
49. Moore LB, Goodwin B, Jones SA, Wisely GB, Serabjit-Singh CJ, Willson TM, Collins JL, Kliewer SA. St. John's wort induces hepatic drug metabolism through activation of the pregnane X receptor. *Proc Natl Acad Sci USA* 2000; 97(13): 7500-2.
50. Komoroski BJ, Zhang S, Cai H, Hutzler JM, Frye R, Tracy TS, Strom SC, Lehmann T, Ang CY, Cui YY, et al. Induction and inhibition of cytochromes P450 by the St. John's wort constituent hyperforin in human hepatocyte cultures. *Drug Metab Dispos* 2004; 32(5): 512-8.
51. Miller VP, Stresser DM, Blanchard AP, Turner S, Crespi CL. Fluorometric high-throughput screening for inhibitors of cytochrome P450. *Ann N Y Acad Sci* 2000; 919: 26-32.

52. Parkinson A, Kazmi F, Buckley DB, Yerino P, Ogilvie BW, Paris BL. System-dependent outcomes during the evaluation of drug candidates as inhibitors of cytochrome P450 (CYP) and uridine diphosphate glucuronosyltransferase (UGT) enzymes: Human hepatocytes versus liver microsomes versus recombinant enzymes. *Drug Metab Pharmacokinet* 2010; 25(1): 16-27.
53. Ogilvie BW, Usuki E, Yerino P, Parkinson A. *In vitro* Approaches for studying the inhibition of drug-metabolizing enzymes and identifying the drug-metabolizing enzymes responsible for the metabolism of drugs (reaction phenotyping) with emphasis on cytochrome P450. In: *Drug-drug interactions*, Rodrigues AD, editor: 2008.
54. Winslow LC, Kroll DJ. Herbs as medicines. *Arch Intern Med* 1998; 158(20): 2192-9.
55. Stresser DM, Turner SD, Blanchard AP, Miller VP, Crespi CL. Cytochrome P450 fluorometric substrates: Identification of isoform-selective probes for rat CYP2D2 and human CYP3A4. *Drug Metab Dispos* 2002; 30(7): 845-52.
56. Mooiman KD, Maas-Bakker RF, Rosing H, Beijnen JH, Schellens JH, Meijerman I. Development and validation of a LC-MS/MS method for the *in vitro* analysis of 1-hydroxymidazolam in human liver microsomes: Application for determining CYP3A4 inhibition in complex matrix mixtures. *Biomed Chromatogr* 2013; 27(9): 1107-16.
57. Walsky RL, Obach RS. Validated assays for human cytochrome P450 activities. *Drug Metab Dispos* 2004; 32(6): 647-60.
58. Sparreboom A, Van Tellingen O, Scherrenburg EJ, Boesen JJ, Huizing MT, Nooijen WJ, Versluis C, Beijnen JH. Isolation, purification and biological activity of major docetaxel metabolites from human feces. *Drug Metab Dispos* 1996; 24(6): 655-8.
59. Hendriks JJ, Dubbelman AC, Rosing H, Schinkel AH, Schellens JH, Beijnen JH. Quantification of docetaxel and its metabolites in human plasma by liquid chromatography/tandem mass spectrometry. *Rapid Commun Mass Spectrom* 2013; 27(17): 1925-34.
60. Royer I, Monsarrat B, Sonnier M, Wright M, Cresteil T. Metabolism of docetaxel by human cytochromes P450: Interactions with paclitaxel and other antineoplastic drugs. *Cancer Res* 1996; 56(1): 58-65.
61. European Medicines Agency. Guideline on the investigation of drug interactions 2010. http://www.ema.europa.eu/docs/en_GB/document_library/Scientific_guideline/2012/07/WC500129-606.pdf.
62. Vogel HG, Hock FJ, Maas J, Mayer D, editors. *Drug discovery and evaluation: Safety and pharmacokinetic assays*. New York: Springer; 2006.
63. Renwick AB, Surry D, Price RJ, Lake BG, Evans DC. Metabolism of 7-benzyloxy-4-trifluoromethylcoumarin by human hepatic cytochrome P450 isoforms. *Xenobiotica* 2000; 30(10): 955-69.
64. Stresser DM, Blanchard AP, Turner SD, Erve JC, Dandeneau AA, Miller VP, Crespi CL. Substrate-dependent modulation of CYP3A4 catalytic activity: Analysis of 27 test compounds with four fluorometric substrates. *Drug Metab Dispos* 2000; 28(12): 1440-8.
65. Bjornsson TD, Callaghan JT, Einolf HJ, Fischer V, Gan L, Grimm S, Kao J, King SP, Miwa G, Ni L, et al. The conduct of *in vitro* and *in vivo* drug-drug interaction studies: A PhRMA perspective. *J Clin Pharmacol* 2003; 43(5): 443-69.
66. Goey AKL, Mooiman KD, Beijnen JH, Schellens JH, Meijerman I. Relevance of *in vitro* and clinical data for predicting CYP3A4-mediated herb-drug interactions in cancer patients. *Cancer Treatment Reviews* 2013; 39(7): 773-83.
67. Strandell J, Neil A, Carlin G. An approach to the *in vitro* evaluation of potential for cytochrome P450 enzyme inhibition from herbals and other natural remedies. *Phytomedicine* 2004; 11(2-3): 98-104.



2.2

DEVELOPMENT AND VALIDATION OF A LC-MS/MS METHOD FOR THE *IN VITRO* ANALYSIS OF 1-HYDROXYMIDAZOLAM IN HUMAN LIVER MICROSOMES: APPLICATION FOR DETERMINING CYP3A4 INHIBITION IN COMPLEX MATRIX MIXTURES

K.D. Mooiman
R.F. Maas-Bakker
H. Rosing
J.H. Beijnen
J.H.M. Schellens
I. Meijerman

Published in Biomedical Chromatography 2013; 27(9): 1107-1116

ABSTRACT

Complementary and alternative medicines (CAM) can affect the pharmacokinetics of anticancer drugs by interacting with the metabolizing enzyme cytochrome P450 (CYP) 3A4. To evaluate changes in the activity of CYP3A4 in patients, levels of 1-hydroxymidazolam in plasma are often determined with liquid chromatography-quadrupole mass spectrometry (LC-MS/MS). However, validated LC-MS/MS methods to determine *in vitro* CYP3A4 inhibition in human liver microsomes are scarce and not optimized for evaluating CYP3A4 inhibition by CAM. The latter is necessary because CAM are often complex mixtures of numerous compounds that can interfere with the selective measurement of 1-hydroxymidazolam.

Therefore, the aim was to validate and optimize a LC-MS/MS method for the adequate determination of CYP3A4 inhibition by CAM in human liver microsomes. After incubation of human liver microsomes with midazolam, liquid-liquid extraction with tert-butyl methyl ether was applied and dried samples were reconstituted in 50% methanol. These samples were injected onto a reversed-phase chromatography consisting of a Zorbax Extend-C₁₈ column (2.1 x 150 mm, 5.0 µm particle size), connected to a triple quadrupole mass spectrometer with electrospray ionization.

The described LC-MS/MS method was validated over linear range of 1.0 - 500 nM for 1-hydroxymidazolam. Results revealed good inter-assay accuracy ($\geq 85\%$ and $\leq 115\%$) and within-day and between-day precisions (coefficient variation $\leq 4.43\%$). Furthermore, the applicability of this assay for the determination of CYP3A4 inhibition in complex matrix mixtures was successfully demonstrated in an *in vitro* experiment in which CYP3A4 inhibition by known CAM (β -carotene, green tea, milk thistle and St. John's wort) was determined.

INTRODUCTION

The treatment of cancer patients comprises multiple anticancer drugs in combination with supplemental therapies to prevent or to reduce side effects¹. In addition, many cancer patients frequently use complementary and alternative medicines (CAM) such as herbal supplements and vitamins². Cancer patients use these CAM for different reasons, including the reduction of chemotherapy side effects, improvement of their quality of life and retardation of the cancer progression^{3,4}. However, concomitant use of CAM and chemotherapy could lead to serious problems. Pharmacokinetic and -dynamic interactions can occur between CAM and anticancer drugs by affecting drug transporters and cytochrome P450 (CYP) enzymes^{2,5}. CYP3A4 is the most important metabolizing enzyme because it metabolizes the majority of currently prescribed anticancer drugs. The pharmacokinetic (PK) interaction between grapefruit-containing products and CYP3A4 metabolized anticancer drugs is the best-known clinically relevant pharmacokinetic interaction⁶. However, for the majority of CAM it is not known whether these compounds can cause inhibition of CYP3A4. Therefore, it is important to evaluate the potential of other CAM to inhibit CYP3A4.

The conversion of the CYP3A4 probe substrate midazolam into its major metabolite 1-hydroxymidazolam is often applied to evaluate changes in CYP3A4 activity. For the simultaneous determination of midazolam and 1-hydroxymidazolam levels liquid chromatography-quadrupole mass spectrometry (LC-MS/MS) is a sensitive method⁷. Multiple validated LC-MS/MS methods have been reported for the determination of 1-hydroxymidazolam levels in plasma⁷⁻¹⁰. However, validated LC-MS/MS methods to determine 1-hydroxymidazolam levels after incubating human liver microsomes with midazolam are scarce¹¹⁻¹³. Moreover, these analyses have not been validated and optimized to determine the inhibiting effects of CAM on CYP3A4. Optimization of the LC-MS/MS method to evaluate CAM-mediated CYP3A4 inhibition is important because CAM are often complex mixtures of numerous compounds with a high potential to interfere with the selective measurement of 1-hydroxymidazolam.

Therefore the aim of the present study is to validate and optimize a LC-MS/MS method to adequately determine the inhibition of CYP3A4 mediated metabolism of midazolam by CAM in human liver microsomes. In the described LC-MS/MS method only the concentrations of 1-hydroxymidazolam were determined. It is not useful to establish the concentrations of midazolam since the human liver microsomes are incubated with an excess of midazolam and consequently the decrease in its concentrations is minor.

MATERIALS AND METHODS

Reagents and chemicals

Acetonitrile was obtained from Biosolve (Valkenswaard, The Netherlands) and ketoconazole and nicotinamide adenine dinucleotide phosphate (NADPH) tetra sodium salt were from Sigma-Aldrich (Zwijndrecht, The Netherlands). Human pooled liver microsomes originated from BD Gentest (Breda, The Netherlands). Midazolam, 1-hydroxy-midazolam and labeled 1-hydroxy-midazolam- $^{13}\text{C}_3$ were obtained from Toronto Research Canada (purity < 98%, TRC, North York, Canada). LC-MS grade water, methanol of HPLC quality and acetonitrile of HPLC-S gradient were purchased from Biosolve (Valkenswaard, The Netherlands). Ammonium hydroxide solution 28-30%, acetic acid and ammonium acetate were obtained from Sigma-Aldrich. Tert-butyl methyl ether (TBME) for liquid-liquid extraction (LLE) and sodium hydroxide were purchased from Merck (Darmstadt, Germany).

Standardized extracts of milk thistle and St. John's wort were obtained from Chromadex (Irvine, CA, USA). Standardized extracts of β -carotene and green tea were purchased from ABCR GmbH & Co KG (Karlsruhe, Germany) and LTK laboratories Inc. (St Paul, USA), respectively. Details of all standardized extracts are shown in **Table 1**.

Table 1. Details of the standardized CAM extracts.

CAM	Producer	Contents	
β -carotene	ABCR GmbH & Co KG	97.0% β -carotene	
Green tea	LTK Laboratories Inc.	99.6% tea polyphenols 65.4% EGCG 82.8% catechins	1.2% caffeine 4.0% water 0.2% sulfated ash
Milk Thistle	Chromadex	5.2% silybin A	10.6% silybin B
St. John's wort	Chromadex	1.9% rutin 0.2% pseudohypericin	0.01% hyperforin 0.06% hypericin

In vitro inhibition study with human liver microsomes

Incubations were performed in triplicate in 2.0 mL polypropylene tubes (Sarstedt, Etten-Leur, The Netherlands), using a NADPH regenerating system. The cofactor solution consisted of 2.6 mM NADP⁺, 7.1 mM glucose-6-phosphate, 6.5 mM magnesium chloride and 0.8 U/mL glucose-6-phosphate dehydrogenase in 50 mM phosphate buffer, pH 7.4. For the CAM screen, the dilutions of green tea, milk thistle, St. John's wort and β -carotene or the positive control ketoconazole in the cofactor solution were mixed with a solution of midazolam in 100 mM phosphate buffer and pre-incubated at 37°C for 10 min. The end concentrations of the CAM, ketoconazole and midazolam were 50 $\mu\text{g}/\text{mL}$, 1.0 μM and 2.5 μM , respectively. The end concentration of midazolam is close to the Michaelis Menten constant K_m as determined in previous experiments (data not shown) and in accordance

to Walsky and Obach¹⁴. Then, human liver microsomes (50 µg/mL) were incubated in a 200 µL reaction volume for 5 min at 37°C, with a concentration of 2% acetonitrile. At last, the reaction was stopped with 100 µL of ice-cold 100 mM sodium hydroxide and by preserving the samples on ice.

Chromatography and mass spectrometry

The LC-MS/MS analysis was performed on a Zorbax Extend-C₁₈ column (2.1 x 150 mm, particle size 5 µm, Agilent Technologies, Santa Clara, CA, USA) protected with a Zorbax Reliance Cartridge Guard Column (2.1 x 12.5 mm, 5 µm, Agilent Technologies). The HPLC system comprised of a DGU-14A degasser, a CTO-10Avp column oven (35°C), a Sil-HTc autosampler (4°C) and two LC10-ADµ-pumps (Shimadzu, Kyoto, Japan). The mobile phase consisted of methanol and water containing 10 mM ammonium hydroxide (60:40 v/v), with a flow rate of 0.25 mL/min. Midazolam and its metabolite 1-hydroxymidazolam were detected with a Finnigan TSQ Quantum Discovery Max triple quadrupole mass spectrometer (Thermo Fischer Scientific, Waltham, MA, USA) with electrospray ionization (ESI). The total run time was 9 min. Mass transitions of each compound are optimized in positive ion mode. An overview of mass transitions and MS/MS settings is shown in **Table 2**. Xcalibur software (version 1.4, Thermo Fisher Scientific) was used to quantify the data.

Table 2. Mass transitions and MS/MS settings

Parameters	MDZ	1-OH MDZ	4-OH MDZ	1-OH MDZ- ¹³ C ₃
Parent ion	326	342	342	347
Product ion	291	324	325	329
Collision Energy (V)	26	20	20	23
Scan time (sec)	0.1	0.1	0.2	0.1
Retention time (min)	7.2	5.2	4.3	5.2

Abbreviations: MDZ, midazolam; 1/4-OH MDZ, 1/4-hydroxymidazolam; 1-OH MDZ-¹³C₃, 1-hydroxymidazolam-¹³C₃. Parameters: Spray voltage, 4200 V; sheath gas pressure, 53 psi; ion sweep gas pressure, 2.0 psi; auxiliary gas pressure, 14 psi; capillary temperature, 304°C; tube lens offset, 95 V; collision gas pressure, 1.6 mTorr.

Preparation of stock and working solutions

Two stock solutions of 1-hydroxymidazolam from independent weightings were prepared in pure acetonitrile at a concentration of 500 µM. One of the stocks was used for the calibration standards and one for the quality control (QC) samples. For the calibration standards the stock solution was first diluted with acetonitrile in a range from 0.1 to 50 µM to obtain working solutions. The stock solution for the QC samples was diluted with acetonitrile to obtain the working solutions of 100 nM, 300 nM, 4 µM and 40 µM. For the internal standard, a stock solution of 5 µM 1-hydroxymidazolam-¹³C₃ was prepared. All working solutions were stored at -20°C.

Preparation of calibration standards and QC samples

Calibration standards were freshly prepared by diluting the working solutions 100 times with E/C buffer to obtain concentrations of 1.0, 2.5, 10, 50, 100 and 500 nM. This E/C buffer comprised of inactivated human liver microsomes to prevent possible further metabolism, cofactors, 100 mM phosphate buffer and acetonitrile in the same quantities as described above. In a similar way, the QC samples were diluted to three concentrations: 1 nM (lower limit of quantification, LLQ), 3 nM (low), 40 nM (medium) and 400 nM (high). The concentration of acetonitrile was 2%.

Sample preparation

As well as for the incubation samples, 100 μ L of 100 mM sodium hydroxide was added to the calibration standards and QC samples. After this, 50 μ L of the internal standard 1-hydroxymidazolam- $^{13}\text{C}_3$ stock of 5 μ M was added and all samples were vortex-mixed. Liquid-liquid extraction was performed with 1 mL of TBME and all samples were vortex-mixed for 30 seconds. After centrifugation for 5 min at 10,600 g , all samples were stored for 1 h at -80°C . The organic phase was decanted in clean 1.5 mL polypropylene tubes and evaporated under a stream of nitrogen at 40°C . The residue was reconstituted in 250 μ L methanol-water (50:50 v/v) and vortex-mixed for 30 s. After centrifugation for 5 min at 10,600 g , the clear supernatant was transferred in a 250 μ L glass insert placed in an autosampler vial for LC-MS/MS analysis.

OPTIMIZATION PROCEDURES

In literature, limited validated LC-MS/MS methods have been described to determine 1-hydroxymidazolam levels after incubating human liver microsomes with midazolam (Table 3)¹¹⁻¹³. Furthermore, these LC-MS/MS methods have not been optimized to

Table 3. Applied chromatography conditions and processing methods of validated LC-MS/MS methods for measuring 1-hydroxymidazolam in human liver microsomes.

Stationary phase	Mobile phase	Processing	RT	Reference
Zorbax SB-Phenyl Rapid Resolution column (Agilent) 2.1 x 100 mm 3.5 μ m column	Gradient elution A: 10 mM NH_4OAc + 10% MeOH B: HPLC grade ACN 0.25 mL/min	Protein precipitation with ACN	3.10 min	Dostalek <i>et al.</i> ¹¹
Agilent Zorbax SB-C18 4.6 x 150mm 5 μ m column	Gradient elution A: ACN:H ₂ O:FA, 5/95/0.1 (v/v/v) B: ACN:H ₂ O:FA, 95/5/0.1 (v/v/v) 0.3 and 0.5 mL/min	Filtration	2.71 min	Yao <i>et al.</i> ¹²
Phenomenex Synergi Fusion High pressure HPLC column 2.0 x 20.0 mm, 2.5 μ m	Gradient elution A: 95% H ₂ O, 5% ACN + 0.1% FA B: ACN + 0.1% FA (B) 1 mL/min	None	0.48 min	Youdim <i>et al.</i> ¹³

Abbreviations: ACN, acetonitrile; MeOH, methanol; NH_4OAc , ammonium acetate; FA, formic acid.

adequately determine the inhibiting effects of CAM on CYP3A4. Co-eluting matrix components such as CAM can cause ion enhancement or suppression of the analytes. To reduce the interference by CAM, the following actions were taken into account: a small injection volume; the application of a stable isotopically labeled internal standard; and the use of a low flow rate. However, to further overcome matrix effects of CAM, the mass spectrometry, chromatography and sample pre-treatment were optimized as described below¹⁵.

VALIDATION PROCEDURES

A full validation of the assay in human liver microsomes was performed according to the US Food and Drug Administration (2001) guidelines on bioanalytical method validation including linearity, accuracy and precision, recovery and ion suppression, carry-over, specificity and selectivity, and stability¹⁶.

Linearity

A total of six nonzero calibration standards at concentrations of 1.0, 2.5, 10, 50, 100 and 500 nM were freshly prepared in duplicate for each run and were analyzed in three independent runs. The linear regression of the peak area ratios of the analyte over the internal standard vs the concentration was applied for the calibration curve, using the reciprocal of the squared concentration ($1/\chi^2$) as weighting factor. The correlation coefficient (r^2) should be > 0.90 .

Accuracy and precision

The accuracy and precision of the assay were established by analyzing five replicates of QC samples of 1-hydroxymidazolam at the LLQ, low, medium and high concentration levels simultaneously with duplicate calibration standards in three separate runs. For the inter-assay accuracy the relative difference was determined between the mean concentration after three runs and the nominal concentration. This accuracy should be within 80-120% for the LLQ and 85-115% for the other concentrations. The intra- and inter-assay precisions were calculated with the coefficient of variation (CV, %). These precisions should be $< 20\%$ for the LLQ and $< 15\%$ for the other concentrations.

Recovery and ion suppression

The ion suppression (matrix effect) was determined by comparing the analyte peak area ratios of processed double blanks spiked with 1-hydroxymidazolam and the analyte peak ratios of unprocessed samples in reconstitution solvent. For the processed samples 200 μ L of E/C buffer was extracted and evaporated as described above. Subsequently,

a medium sample of 1-hydroxymidazolam (40 nM) in 250 μ L of reconstitution solvent was added in triplicate. The unprocessed samples comprised a medium sample of 1-hydroxymidazolam in the same volume of reconstitution solvent.

To assess the extraction recovery, the analyte peak area ratios of processed medium samples were compared with processed blanks spiked with the working solution of these medium samples in triplicate. The QC samples were processed as described above. The overall recovery was established by comparing the analyte peak area ratios of processed QC samples (3, 40 and 400 nM) with the analyte peak area ratios of unprocessed QC samples in reconstitution solvent.

Carry-over

Possible carry-over was checked by injecting two processed blank samples directly after injecting an ULQ sample (500 nM). The response of the first blank sample should be < 20% of the response of a processed LLQ sample.

Specificity and selectivity

The potential interference between the endogenous matrix, analyte and internal standard was determined in human pooled liver microsomes, derived from 25 freshly frozen human tissues. Double blanks and LLQ samples were prepared and processed in duplicate according to previously described procedures. To establish the potential interference between the analyte and internal standard, double blank samples were spiked separately with an ULQ sample and internal standard.

It was important to determine the interference of the complex CAM mixtures as these CAM consist of various (unknown) constituents that might interfere. The following CAM were selected: milk thistle, green tea, St. John's wort and β -carotene. Double blanks and LLQ samples were prepared and processed with or without addition of each CAM according to the described procedures.

The peak areas co-eluting with the analyte should be < 20% of the peak areas at LLQ level and peak areas co-eluting with the internal standard < 5%. Furthermore, the difference between the calculated concentrations and nominal concentrations of the LLQ samples should be < 20%.

Stability

The short-term stock stability of both 1-hydroxymidazolam and the internal standard was determined by analyzing aliquots of the stock solutions in triplicate after 8 h storage at room temperature and freshly prepared stock solutions. The long-term stock stability was assessed after storage for 4 months at -80°C. The stocks were considered as stable when the deviation of the mean response between the old and fresh stock solutions was < 5% for 1-hydroxymidazolam and < 20% for the internal standard.

Multiple sample stability experiments determined the stability of low and high samples in E/C buffer. Short-term sample stability was assessed after 6 h storage of low and high samples in E/C buffer at room temperature in triplicate. Long-term stability was established after storage of low and high samples in E/C buffer at -80°C for 2 weeks and 1 month. Furthermore, for the freeze (-80°C) and thaw stability of low and high samples in E/C buffer, the concentrations after three freeze-thaw cycles were compared with the concentrations of freshly prepared QC samples in E/C buffer. The concentrations of the QC samples in E/C buffer should not deviate more than 15% from the initial concentrations.

The stability of reconstituted extracts was determined after storage of processed low and high samples at $2-6^{\circ}\text{C}$ for 24 h. Furthermore, the re-injection reproducibility was assessed by re-running the calibration standards in duplicate and low, mid and high samples in triplicate 24 h after the start of the original run. The reconstituted extracts were considered stable when the concentrations deviated $< 15\%$ of the initial concentrations.

RESULTS

Optimization

Mass spectrometry

For the product ion spectrum, the protonated molecule of 1-hydroxymidazolam at m/z 342 was applied. The most abundant fragment ion (m/z 324) was chosen for selected reaction monitoring (SRM) and fragmentation conditions were optimized. During the method development, the protonated parent mass of m/z 345 was selected for the internal standard 1-hydroxymidazolam- $^{13}\text{C}_3$. However, cross analyte interference occurred when this parent mass was chosen because of the isotope pattern of the analyte (m/z 342, 343, 344 and 345). Therefore, for the internal standard the second most abundant parent mass of m/z 347 and product mass of m/z 329 was selected in order to prevent cross interference with the analyte. **Figure 1** shows the MS/MS product ion scan of both the analyte and internal standard, including the proposed fragmentation.

Chromatography

Dostalek *et al.*¹¹ developed a MS/MS method using a reversed phase column and gradient elution mode with a mobile phase, composed of 10 mM ammonium acetate and 10% methanol (A) and HPLC-grade acetonitrile. In the present study the mobile phase is composed of 10 mM ammonium acetate (A) and methanol (B) and an isocratic elution (A:B, 40:60 v/v). These conditions resulted in small symmetric peaks and an optimal

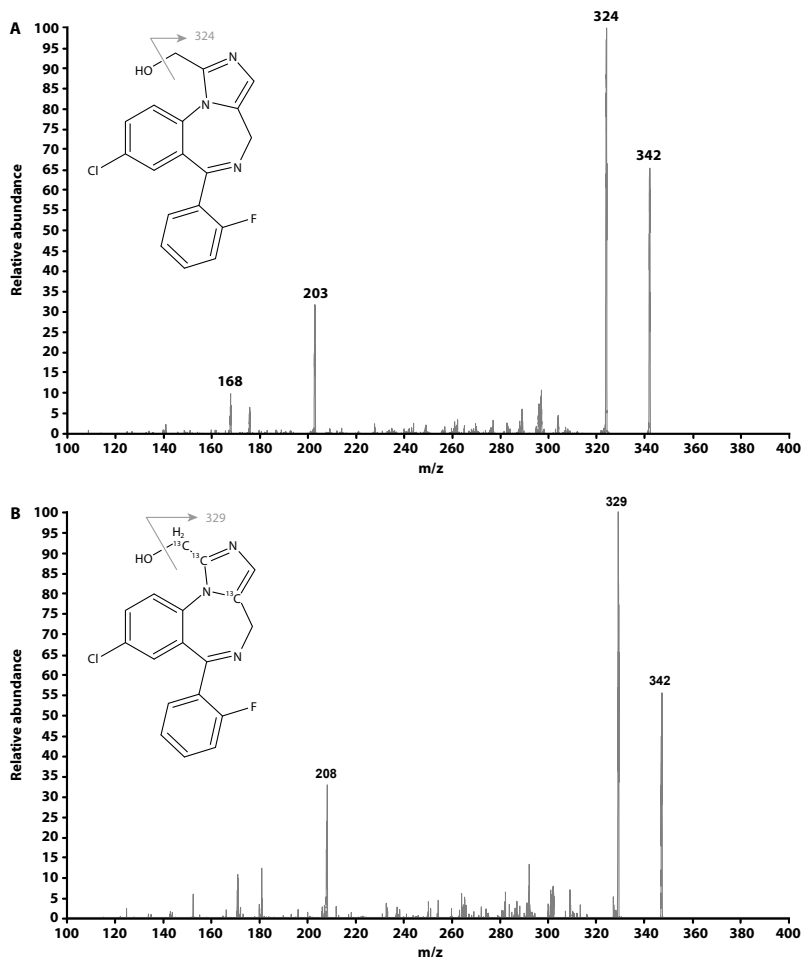


Figure 1. (A) MS/MS product ion scan of 1-hydroxymidazolam (precursor ion m/z 342) and (B) MS/MS product ion scan of 1-hydroxymidazolam- $^{13}\text{C}_3$ (precursor ion m/z 347).

chromatographically separation of 1-hydroxymidazolam and the minor metabolite 4-hydroxymidazolam. Representative chromatograms of a processed double blank sample and an LLQ sample are shown in **Figure 2**.

Since in most cases interference is only observed at the beginning of the chromatographic run¹⁵, it is important to determine whether prolongation of the retention of 1-hydroxymidazolam could reduce the interference by CAM. Therefore, human liver microsomes were incubated with 100 $\mu\text{g}/\text{mL}$ of the known CAM β -carotene, St. John's wort, green tea and milk thistle as described above. It is important to incubate because CAM consist of multiple components that can be metabolized by CYP3A4. After the incubation, the samples were spiked with LLQ samples and compared with LLQ samples without CAM addition. All samples were measured with two different mobile phases:

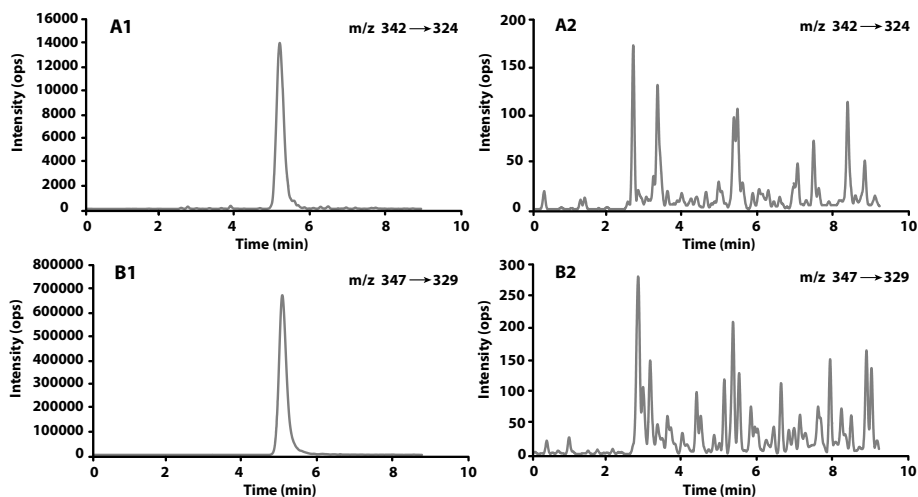


Figure 2. Representative LC-MS/MS chromatograms of 1 nM 1-hydroxymidazolam (A1) and 2.5 μM 1-hydroxy-midazolam- $^{13}\text{C}_3$ (B1) in reconstitution solvent; and of blanks in reconstitution solvent (A2, B2). Retention time, 5.13 min.

A:B, 40:60 v/v, and A:B, 30:70 v/v, resulting in an average retention time of 5.2 min and 2.9 min, respectively. The results in **Table 4** demonstrate that a longer retention time caused less interference by CAM.

Sample pre-treatment

For the preparation of the QC samples, working solutions should be diluted in E/C buffer. For the optimization it is important to determine if this dilution can cause solubility problems. Therefore, triplicate LLQ, low, medium and high samples were prepared and processed within one tube and in multiple tubes. The results in **Table 5** show that it is especially important for the LLQ and low samples to be processed within one tube.

Table 4. Comparison CAM interference for different retention times.

CAM	Mobile phase isocratic A:B, 40:60 v/v			Mobile phase isocratic A:B, 30:70 v/v		
	Mean measured conc. (nM, \pm SD)	Mean % of difference	% of failed QC's	Mean measured conc. (nM, \pm SD)	Mean % of difference	% of failed QC's
No inhibitor	1.16 (\pm 0.04)	15.74	0	1.19 (\pm 0.01)	18.98	0.0
β -carotene	1.17 (\pm 0.02)	17.31	0	1.30 (\pm 0.04)	29.61	100.0
Milk thistle	1.18 (\pm 0.01)	18.12	0	1.21 (\pm 0.03)	21.35	66.7
St. John's wort	1.16 (\pm 0.05)	15.72	0	1.20 (\pm 0.01)	19.49	33.3
Green tea	1.21 (\pm 0.05)	20.93	33.3	1.19 (\pm 0.06)	19.28	66.7

Data are means \pm SD from a representative experiment performed in triplicate.

Abbreviations: RT, retention time; mobile phase A, 10 mM ammonium hydroxide in water; mobile phase B, methanol.

Table 5. QC samples compared in different processing methods.

QC samples	Processing in one tube			Processing in multiple tubes		
	Mean measured conc. (nM, \pm SD)	Mean % of difference	% of failed QC's	Mean measured conc. (nM, \pm SD)	Mean % of difference	% of failed QC's
LLQ	1.07 (\pm 0.04)	7.17	0	0.62 (\pm 0.08)	38.16	100
Low	3.00 (\pm 0.02)	0.09	0	2.36 (\pm 0.14)	21.41	100
Medium	39.83 (\pm 0.36)	0.44	0	38.19 (\pm 0.87)	4.54	0
High	385.55 (\pm 2.61)	3.61	0	382.67 (\pm 7.61)	4.33	0

Data are means \pm SD from a representative experiment performed in triplicate.

Although the underlying explanation is unclear, it is most likely that absorption loss of 1-hydroxymidazolam to the plastic tubes caused the failure of the LLQ and low samples after processing in multiple tubes. In this case, the percentage absorption loss is higher in the LLQ and low samples than in the medium and high samples.

Since the E/C buffer and CAM could decontaminate and disturb the LC-MS/MS apparatus, it was necessary to obtain clean sample extracts for the QC samples. Therefore, LLE was examined for triplicate LLQ samples, using different extraction fluids known from the literature: diethylether, TBME and TBME-dichloromethane (75:25, v/v) (**Table 6**)^{10, 15}. The ratio between these extraction fluids and the spiked E/C buffer samples was 1:4, v/v. The highest overall recovery was obtained for TBME, and therefore TBME was selected.

Table 6. Representative overall recoveries of 1-hydroxymidazolam and 1-hydroxymidazolam-¹³C₃ in different extraction solvents.

	Diethylether	TBME	TBME: dichloromethane
Overall recovery of 1-hydroxymidazolam	75%	84%	36%
Overall recovery of 1-hydroxymidazolam-¹³C₃	79%	92%	41%

Abbreviations: TBME, tert-butyl methyl ether.

In addition, the interference by CAM was determined after incubation of human liver microsomes with CAM, processing the samples with LLE and protein precipitation. After LLE, no interference was observed between the analyte or internal standard and milk thistle, green tea, St. John's wort and β -carotene. Milk thistle and green tea also did not show interference after protein precipitation. However, St. John's wort and β -carotene did significantly interfere with the analyte. After incubation of human liver microsomes with solely St. John's wort and β -carotene and protein precipitation, co-eluting peaks of 32.4 and 84.3% of the analyte peak area were present, respectively (**Figure 3**).

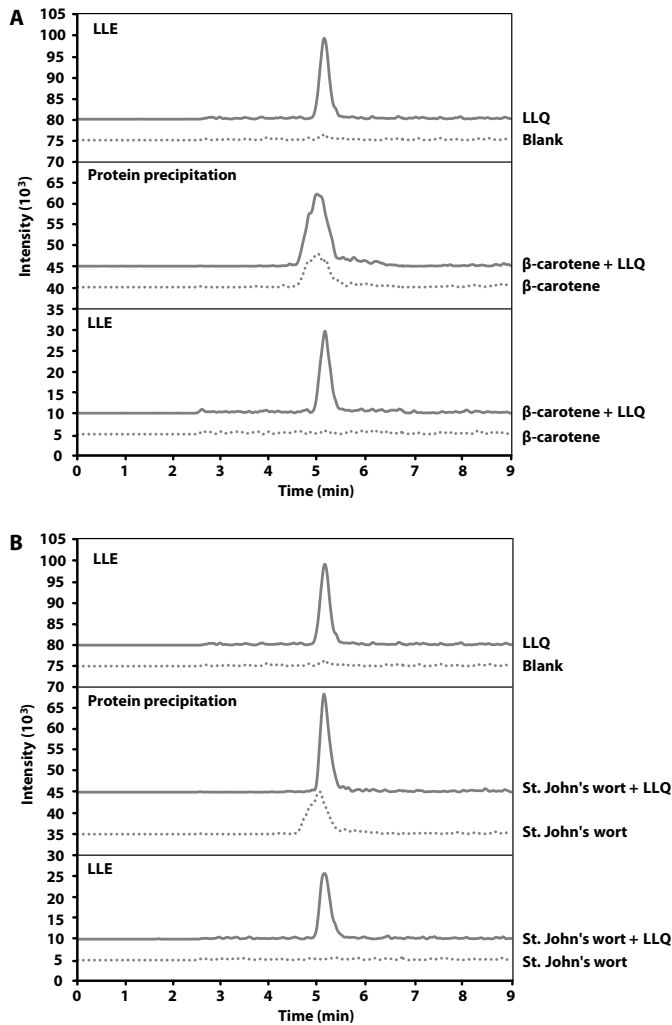


Figure 3. Interference with 1-hydroxymidazolam by β -carotene (A) and St. John's wort (B) after liquid-liquid extraction (LLE) and protein precipitation.

The interference by CAM from the extracted matrices was also assessed by infusing neat solutions of 1-hydroxymidazolam into the MS, using a syringe pump at 25 $\mu\text{l}/\text{min}$ ¹¹. None of the CAM showed ion suppression under continuous infusion of the analyte and internal standard when LLE was used as the processing method. In contrast, when protein precipitation was applied, all CAM caused ion suppression of both the analyte and internal standard (**Figure 4**).

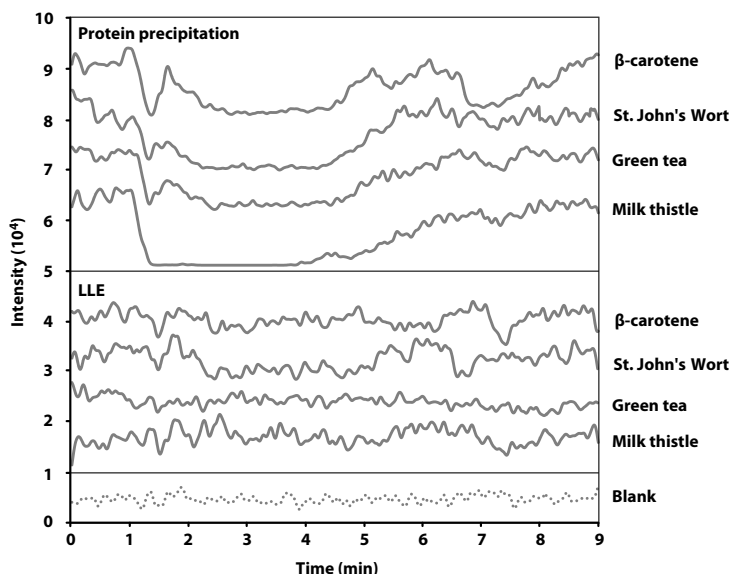


Figure 4. Ion suppression of 1-hydroxymidazolam by complementary and alternative medicines, after liquid-liquid extraction and protein precipitation.

Validation

Linearity

The described assay was linear for a concentration range 1.0-500 nM of 1-hydroxymidazolam in E/C buffer. The lowest total bias and the most constant bias across this range were obtained using the linear regression with $1/\chi^2$ as weighting factor. The average regression parameters of three independent runs were $y = -4.24 \times 10^{-3} (\pm 0.22 \times 10^{-3}) + 0.0204 (\pm 0.0007) x$ with an average correlation coefficient of $0.998 (\pm 0.0010)$. For the QC samples, the deviations from the nominal levels were between 8.92 and 19.6% for LLQ and -8.62 and 13.7% for the other concentration levels. CV values varied between 2.65 and 3.35% for LLQ and 1.45 and 6.38% for the remaining concentration levels.

Accuracy and precision

The assay performance data for 1-hydroxymidazolam in E/C buffer is summarized in **Table 7**. The inter-assay accuracy was < 115% for all concentrations and thus met the required accuracy within 80-120% for LLQ and 85-115% for the other concentration levels. The within-day and between-day precisions did not exceed 3.83% and 4.37%, respectively. Therefore these both parameters met the required precision of 20% for LLQ and 15% for the other QC levels.

Table 7. The assay performance for 1-hydroxymidazolam.

Nominal conc. (nM)	Mean measured conc. (nM, \pm SD)	Inter-assay accuracy (%)	Within-day precision (%CV)	Between-day precision (%CV)
1	1.15 (\pm 0.03)	114.7	2.45	2.73
3	3.09 (\pm 0.14)	103.0	3.83	4.37
40	40.09 (\pm 1.84)	100.2	3.16	4.43
400	380.94 (\pm 11.72)	95.2	2.35	2.97

n = 15 (five replicates for each validation run for three separate runs).

Recovery and ion suppression

An overview of the LLE and overall recoveries for both 1-hydroxymidazolam and the internal standard is given in **Table 8**. Furthermore, minor ion enhancement was demonstrated for both 1-hydroxymidazolam and the internal standard. The mean ion enhancement was 7.4% (range -2.1-17%) for 1-hydroxymidazolam and 2.6% (range -1.3-7.7%) for the internal standard.

Table 8. The recovery of 1-hydroxymidazolam.

Concentration levels	Total recovery (%)		LLE recovery (%)	
	1-OH-MDZ	1-OH-MDZ- ¹³ C ₃	1-OH-MDZ	1-OH-MDZ- ¹³ C ₃
Low	76.0	76.3	-	-
Medium	93.7	88.9	87.2	86.6
High	92.2	86.8	-	-

Abbreviations: LLE, liquid-liquid extraction.

Carry-over

The carry-over in the first processed blank was 2.1 and 0.037% of the peak areas of 1-hydroxy-midazolam and 1-hydroxymidazolam-¹³C₃ in a processed LLQ sample, respectively. These percentages were accepted because the required criterion was 20%.

Specificity and selectivity

In the double blank samples no co-eluting peaks > 20% of the analyte peak area at the LLQ level and > 5% of the internal standard peak area were present. The deviation from the nominal concentration at the LLQ level was < 20% and was approved.

Regarding to selectivity, no cross-interference was observed between the analyte and internal standard. When analyzing the samples containing only the internal standard, the mean interfering peak area at the retention time of 1-hydroxymidazolam was 2.5% of the peak area of 1-hydroxymidazolam at LLQ level. The mean interfering peak area at the retention time of 1-hydroxymidazolam-¹³C₃ was 0.32% of the peak area of this internal standard, when analyzing samples containing only 1-hydroxymidazolam. There

was no cross-interference since this requires co-eluting peak areas < 20% of the peak areas at LLQ levels and < 5% of the peak areas of the internal standard.

The co-administration interference by CAM was determined as described above. No co-eluting peaks > 20% of the analyte peak area and > 5% of the internal standard peak area were present after spiking the blank samples with milk thistle, green tea, St. John's wort and β -carotene.

Stability

The stability data of 1-hydroxymidazolam and 1-hydroxymidazolam- $^{13}\text{C}_3$ are summarized in **Table 9**. These results show that the stocks of both 1-hydroxymidazolam and 1-hydroxymidazolam- $^{13}\text{C}_3$ were stable for at least 10 h at ambient temperature. The long-term stock stability of 1-hydroxymidazolam was at least 6 months and that of 1-hydroxymidazolam- $^{13}\text{C}_3$ 3 months. Regarding short-term stability in E/C buffer, 1-hydroxymidazolam was stable in this matrix for at least 10 h at -80°C . Also long-term stability experiments demonstrated that 1-hydroxymidazolam was stable in E/C buffer for at least 1 month at -80°C . In addition, 1-hydroxymidazolam was stable in E/C buffer for at least 3 freeze (-80°C) and thaw cycles. Finally, the final extract stability of 1-hydroxymidazolam was demonstrated for at least 96 h at $2-8^\circ\text{C}$.

Table 9. The stability data for 1-hydroxymidazolam and 1-hydroxymidazolam- $^{13}\text{C}_3$.

Parameters	Conditions	Matrix	Deviation of mean response	CV(%)	No. of replicates
1-hydroxymidazolam					
Stock stability (short)	Ambient, 10 h	Acetonitrile	3.96%	5.68	3
Stock stability (long)	-80°C , 6 months	Acetonitrile	4.32%	8.29	3
Sample stability (short)	low, ambient, 10 h	E/C buffer	-5.91%	5.68	3
	high, ambient, 10 h	E/C buffer	-4.10%	0.52	3
Sample stability (long)	Low, -80°C , 2 weeks	E/C buffer	4.82%	3.17	3
	high, -80°C , 2 weeks	E/C buffer	0.39%	0.72	3
Sample stability (long)	Low, -80°C , 1 month	E/C buffer	-13.65%	1.63	3
	low, -80°C , 1 month	E/C buffer	-5.76%	1.36	3
Freeze-thaw stability	Low, -80°C , 3 F/T cycles	E/C buffer	-5.53%	1.12	3
	High, -80°C , 3 F/T cycles	E/C buffer	-5.60%	3.50	3
Re-injection reproducibility	LLQ, $2-8^\circ\text{C}$, 48h	Final extract	15.77%	1.99	5
	Low, $2-8^\circ\text{C}$, 48h	Final extract	0.31%	2.84	5
	Medium, $2-8^\circ\text{C}$, 48h	Final extract	-2.53%	1.79	5
	High, $2-8^\circ\text{C}$, 48h	Final extract	-3.26%	1.54	5
Processed sample stability	Low, $2-8^\circ\text{C}$, 96h	Final extract	0.3%	3.72	5
	High, $2-8^\circ\text{C}$, 96h	Final extract	5.56%	2.09	5
1-hydroxymidazolam-$^{13}\text{C}_3$					
Stock stability (short)	Ambient, 10h	Acetonitrile	9.55%	2.37	3
Stock stability (long)	-80°C , 2 months	Acetonitrile	10.12%	8.61	3

Abbreviations: F/T, freeze-thaw.

APPLICATION

To demonstrate the applicability of the validated assay, the inhibiting effects of the positive control ketoconazole and multiple CAM (β -carotene, green tea, milk thistle and St. John's wort) towards CYP3A4 activity was determined.

Human liver microsomes were incubated with 2.5 μ M midazolam with and without 50 μ g/mL of each CAM or 1.0 μ M ketoconazole in cofactor solution for 5 min at 37°C. All samples were processed as described above. To determine the percentage of CYP3A4 activity after incubation with all compounds, the concentrations of 1-hydroxymidazolam were calculated based on the calibration curve and compared with the concentration after incubation without potential inhibitors. Results are shown in **Table 10** and **Figure 5**.

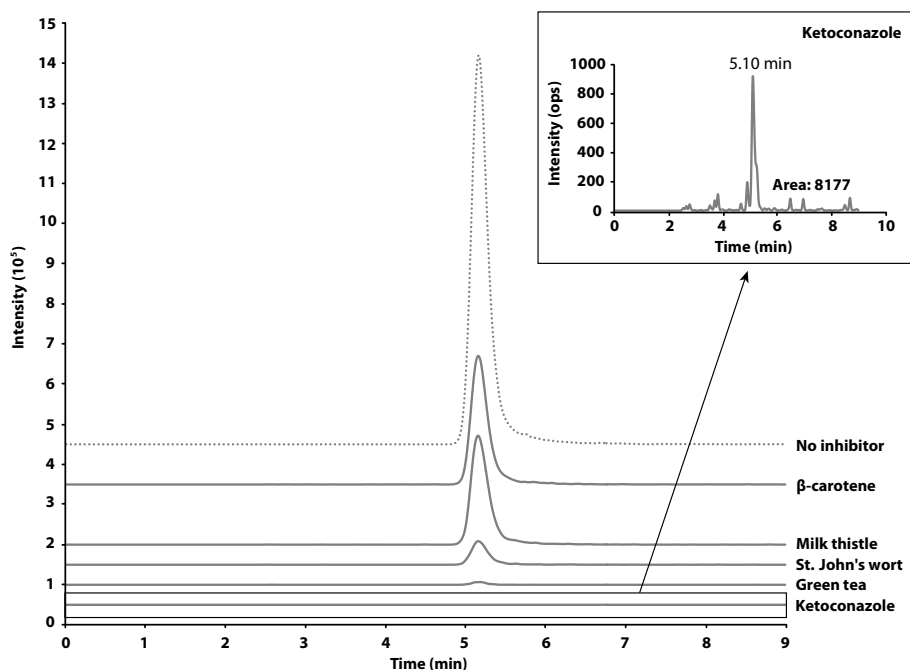


Figure 5. Chromatograms of 1-hydroxymidazolam after incubation of human liver microsomes with ketoconazole and complementary and alternative medicines.

Table 10. Summary of the concentrations of 1-hydroxymidazolam and CYP3A4 activity in human liver microsomes.

Compounds	Mean measured conc. (nM, \pm SD)	CYP3A4 activity (% , \pm SD)	Significance (p-value)
No inhibitor	140.91 (\pm 7.38)	100.00 (\pm 7.58)	0.0018 **
β -carotene	44.44 (\pm 17.03)	31.54 (\pm 5.85)	0.0003 ***
Milk thistle	43.29 (\pm 11.86)	30.72 (\pm 4.29)	0.0008 ***
St. John's wort	11.54 (\pm 15.17)	8.19 (\pm 1.38)	0.0017 **
Green tea	1.45 (\pm 6.32)	1.03 (\pm 0.16)	0.0018 **
Ketoconazole	0.54 (\pm 1.76)	0.39 (\pm 0.03)	0.0018 **

CONCLUSION

In this paper the development, validation and application of a sensitive LC-MS/MS method are described for the *in vitro* quantification of 1-hydroxymidazolam in human liver microsomes. Although multiple LC-MS/MS methods have been published for the quantification of 1-hydroxymidazolam, this is the first validated and optimized quantitative assay to determine CYP3A4 inhibition by CAM in human liver microsomes. It is necessary to optimize the assay because CAM consist of multiple compounds and have a high potential to interfere with the selective measurement of 1-hydroxymidazolam. Consequently, it is possible to erroneously conclude that a CAM inhibits CYP3A4 while this compound solely caused ion suppression. To avoid interference by CAM, the most critical processes are the use of LLE and prolongation of the retention time of 1-hydroxymidazolam. Furthermore, the applicability of this assay for the determination of CYP3A4 inhibition in complex matrix mixtures has been successfully demonstrated in an *in vitro* experiment in which CYP3A4 inhibition by known CAM (β -carotene, green tea, milk thistle and St. John's wort) was determined.

REFERENCES

1. Harmsen S, Meijerman I, Beijnen JH, Schellens JH. Nuclear receptor mediated induction of cytochrome P450 3A4 by anticancer drugs: A key role for the pregnane X receptor. *Cancer Chemother Pharmacol* 2009; 64(1): 35-43.
2. Sparreboom A, Cox MC, Acharya MR, Figg WD. Herbal remedies in the United States: Potential adverse interactions with anticancer agents. *J Clin Oncol* 2004; 22(12): 2489-503.
3. Tascilar M, de Jong FA, Verweij J, Mathijssen RH. Complementary and alternative medicine during cancer treatment: Beyond innocence. *Oncologist* 2006; 11(7): 732-41.
4. Werneke U, Earl J, Seydel C, Horn O, Crichton P, Fannon D. Potential health risks of complementary alternative medicines in cancer patients. *Br J Cancer* 2004; 90(2): 408-13.
5. Pal D, Mitra AK. MDR- and CYP3A4-mediated drug-herbal interactions. *Life Sci* 2006; 78(18): 2131-45.
6. Seden K, Dickinson L, Khoo S, Back D. Grapefruit-drug interactions. *Drugs* 2010; 70(18): 2373-407.
7. Svanstrom C, Hansson GP, Svensson LD, Sennbro CJ. Development and validation of a method using supported liquid extraction for the simultaneous determination of midazolam and 1'-hydroxy-midazolam in human plasma by liquid chromatography with tandem mass spectrometry detection. *J Pharm Biomed Anal* 2012; 58: 71-7.
8. Jabor VA, Coelho EB, Dos Santos NA, Bonato PS, Lanchote VL. A highly sensitive LC-MS-MS assay for analysis of midazolam and its major metabolite in human plasma: Applications to drug metabolism. *J Chromatogr B Analyt Technol Biomed Life Sci* 2005; 822(1-2): 27-32.
9. Li W, Luo S, Smith HT, Tse FL. Simultaneous determination of midazolam and 1'-hydroxymidazolam in human plasma by liquid chromatography with tandem mass spectrometry. *Biomed Chromatogr* 2007; 21(8): 841-51.
10. Xue X, Huang M, Xiao H, Qin X, Huang L, Zhong G, Bi H. Rapid and simultaneous measurement of midazolam, 1'-hydroxymidazolam and digoxin by liquid chromatography/tandem mass spectrometry: Application to an *in vivo* study to simultaneously measure P-glycoprotein and cytochrome P450 3A activity. *J Pharm Biomed Anal* 2011; 55(1): 187-93.
11. Dostalek M, Macwan JS, Chitnis SD, Ionita IA, Akhlaghi F. Development and validation of a rapid and sensitive assay for simultaneous quantification of midazolam, 1'-hydroxymidazolam, and 4-hydroxy-midazolam by liquid chromatography coupled to tandem mass-spectrometry. *J Chromatogr B Analyt Technol Biomed Life Sci* 2010; 878(19): 1629-33.
12. Yao M, Zhu M, Sinz MW, Zhang H, Humphreys WG, Rodrigues AD, Dai R. Development and full validation of six inhibition assays for five major cytochrome P450 enzymes in human liver microsomes using an automated 96-well microplate incubation format and LC-MS/MS analysis. *J Pharm Biomed Anal* 2007; 44(1): 211-23.
13. Youdim KA, Lyons R, Payne L, Jones BC, Saunders K. An automated, high-throughput, 384 well cytochrome P450 cocktail IC50 assay using a rapid resolution LC-MS/MS end-point. *J Pharm Biomed Anal* 2008; 48(1): 92-9.
14. Walsky RL, Obach RS. Validated assays for human cytochrome P450 activities. *Drug Metab Dispos* 2004; 32(6): 647-60.
15. Van Eeckhaut A, Lanckmans K, Sarre S, Smolders I, Michotte Y. Validation of bioanalytical LC-MS/MS assays: Evaluation of matrix effects. *J Chromatogr B Analyt Technol Biomed Life Sci* 2009; 877(23): 2198-207.
16. US Food and Drug Administration. FDA Guidance for Industry: Bioanalytical Method Validation. US Department of Health and Human Services, Food and Drug Administration, Center for Drug Evaluation and Research; Rockville, MD, 2001.



2.3

THE EFFECT OF COMPLEMENTARY AND ALTERNATIVE MEDICINES (CAM) ON CYP2C9 ACTIVITY

K.D. Mooiman
A.K.L. Goey
T.J. Huijbregts
R.F. Maas-Bakker
J.H. Beijnen
J.H.M. Schellens
I. Meijerman

Submitted for publication

ABSTRACT

The use of complementary and alternative medicines (CAM) is popular among cancer patients. However, the concomitant use of anticancer drugs and CAM could result in pharmacokinetic (PK) interactions. One major cause for these interactions is the changed functionality or expression of drug efflux transporters and cytochrome P450 (CYP) enzymes. CYP2C9 is important for the metabolism of numerous drugs and inhibition of this enzyme could result in elevated plasma levels of drugs that are CYP2C9 substrates. Especially for anticancer drugs, which have a narrow therapeutic window, small changes in their plasma levels could easily result in clinically relevant toxicities. In literature, a few *in vitro* studies have been conducted to determine the inhibiting effects of CAM on CYP2C9 activity. Due to differences in test systems, methods of quantification, tested CAM products and interlaboratory differences, it is complicated to compare the inhibitory potencies of CAM.

The aim of the present study is therefore to establish the inhibitory effects of fourteen commonly used CAM on CYP2C9-mediated metabolism of CYP2C9 substrates 7-methoxy-4-trifluoromethyl-coumarine (MFC) and tolbutamide.

The results indicated milk thistle as the most potent CYP2C9 inhibitor, of which silybin (main constituent of milk thistle) was mainly responsible for the inhibition of CYP2C9. Clinical studies with milk thistle are recommended to establish the clinical relevance of the demonstrated CYP2C9 inhibition in the present study.

INTRODUCTION

Cytochrome P450 (CYP) enzymes are major players in the metabolism of drugs. CYP2C9 is one of the most important CYP enzymes as it is the second most abundant enzyme in the liver and it metabolizes 11% of all currently available drugs such as tolbutamide, warfarin and diclofenac^{1,2}. Certain drugs can affect the activity or expression of CYP enzymes, possibly leading to pharmacokinetic (PK) interactions with co-administered drugs. Inhibition of CYP2C9 can result in increased plasma levels of drugs that are substrates for CYP2C9³. Especially for drugs with a narrow therapeutic window, small changes in plasma levels can easily result in clinically relevant toxicity problems.

Anticancer drugs have a narrow therapeutic window and many of these drugs are metabolized by CYP2C9 (e.g. cyclophosphamide, ifosfamide, trabectedin, bortezomib, imatinib, idarubicin and tamoxifen)⁴. Cancer patients are therefore vulnerable for PK interactions. Especially since their treatment frequently consists of anticancer drugs or hormonal agents, combined with supplemental therapies to prevent or treat side effects⁵. In addition, cancer patients often use complementary and alternative medicines (CAM) to reduce side effects of the anticancer drugs, to improve their quality of life, to strengthen the immune system and to retard the cancer progression^{3,6}. The concomitant use of anticancer drugs and CAM could, however, result in serious safety problems due to the increased risk for PK interactions⁷.

The most popular CAM among cancer patients are dietary supplements such as β -carotene and vitamins B₆, B₁₂ and C, and herbal supplements such as valerian, St. John's wort, saw palmetto, milk thistle, ginseng, Ginkgo biloba, garlic and Echinacea^{3,8,9}. When these CAM are combined with anticancer drugs, it is important to determine whether these supplements have the ability to inhibit CYP2C9.

In literature, only a few *in vitro* studies have been conducted to determine the inhibiting potency of frequently used CAM on CYP2C9. Both valerian and Echinacea were categorized as weak CYP2C9 inhibitors, both tested in one *in vitro* study^{10,11}. Grape seed, saw palmetto, β -carotene and garlic were shown to inhibit CYP2C9 in a different degree in various *in vitro* studies¹¹⁻¹⁴. For milk thistle, Ginkgo biloba and grape seed both inhibition and no effect on CYP2C9 activity was described^{2,10-12,15-20}. In contrast, St. John's wort was shown to both inhibit and induce CYP2C9^{10,21,22}. No *in vitro* studies with green tea were reported, hitherto.

Based on the results from the available *in vitro* studies, comparison of the inhibitory potencies of CAM is complicated due to interlaboratory differences, the use of different test systems (e.g. human hepatocytes) and the use of multiple methods of quantification (e.g. fluorescence assay). More importantly, the performed *in vitro* studies used multiple CAM products and the phytochemical content of these products is usually highly variable among different brands. Also the potency of the CAM components can vary due to

differences in storage and processing methods²³. In order to predict which CAM is most likely to cause PK interactions via CYP2C9 in cancer patients, it is crucial to compare the inhibitory potencies of CAM within one test system²⁴.

The aim of the present study is therefore to compare the potencies of β -carotene, Echinacea (*Echinacea purpurea*), garlic (*Allium sativum*), green tea (*Camellia sinensis*), *Ginkgo biloba*, ginseng (*Eleutherococcus senticosus*), grape seed (*Vitis vinifera*), milk thistle (*Silybum marianum*), saw palmetto (*Serenoa serrulata*), St. John's wort (*Hypericum perforatum*), valerian (*Valeriana officinalis*) and vitamins B₆, B₁₂, and C to inhibit CYP2C9 activity. To address this issue, two CYP2C9 substrates 7-methoxy-4-trifluoromethylcoumarine (MFC) and tolbutamide were applied in order to improve the prediction of the clinical effects of CAM on CYP2C9-mediated metabolism of anticancer drugs.

MATERIALS AND METHODS

Reagents and chemicals

Standardized extracts of β -carotene, Echinacea, garlic, *Ginkgo biloba*, ginseng, grape seed, green tea, milk thistle, saw palmetto, St. John's wort, valerian, vitamin B₆, B₁₂ and C from the same suppliers were used as previously described²⁵. The details of these standardized extract are described in **Table 1**. Milk thistle's constituents silybin A+B and taxifolin were obtained from Sigma-Aldrich (Zwijndrecht, The Netherlands) and

Table 1. Details of the standardized CAM extracts.

CAM	Product Information	Contents	
β -carotene	ABCR GmbH&Co KG [Lot # 1030612]	97% β -carotene	
Echinacea <i>Echinacea purpurea</i>	Chromadex [Lot # 00030217-012]	0.94% caftaric acid 0.03% chlorogenic acid 0.04% cynarin	0.05% echinacoside 1.80% cichoric acid
Garlic <i>Allium sativum</i>	Organic Herb Inc. [100-20100122]	Garlic extract (100:1) Alliin scordinin alliin	
<i>Ginkgo biloba</i>	Chromadex [Lot # 00030299-1917]	4.78% quercetin 3.73% kaempferol 2.13% isorhamnetin 12.0% quercetin glycoside 9.65% kaempferol glycoside 5.19% isorhamnetin glycoside	1.61% bilobalide 1.41% ginkgolide A 0.31% ginkgolide J 5.57% ginkgolide B 0.38% ginkgolide C
Ginseng <i>Eleutherococcus senticosus</i>	Chromadex [Lot # 00030302-019]	0.439% eleutheroside E	0.245% eleutheroside B
Grape seed <i>Vitis vinifera</i>	Chromadex [Lot # 00036130-11]	5.08% epigallocatechin 0.93% catechin 6.30% epicatechin	0.02% epigallocatechin gallate 0.03% epicatechin gallate

Table 1. Details of the standardized CAM extracts. (continued)

CAM	Product Information	Contents	
Green tea <i>Camellia sinensis</i>	LTK Laboratories Inc. [G6817]	99.61% tea polyphenols 65.38% EGCG 82.79% catechins	1.17% caffeine 3.98% water 0.18% sulfated ash
Milk Thistle <i>Silybum marianum</i>	Chromadex [Lot # 00030402-101]	29.6% silybin A+B 2.97% taxifolin	14.7% silychristin
Saw Palmetto <i>Serenoa serrulata</i>	Chromadex [Lot # 00030726-841]	0.13% campesterol 0.07% stigmasterol 0.43% β -sisterol 0.21% methyl caproate 0.93% methyl octanoate 2.53% methyl decanoate 28.61% methyl dodecanoate 10.63% methyl myristate	8.55% methyl palmitate 1.81% methyl stearate 30.40% methyl oleate 5.28% methyl linolenate 0.75% methyl linoleate 0.17% methyl arachidate 0.02% methyl EPA 0.11% methyl DHA
St. John's wort <i>Hypericum perforatum</i>	Chromadex [Lot # 00030798-155]	1.87% rutin 0.24% pseudohypericin	0.01% hyperforin 0.06% hypericin
Valerian <i>Valeriana officinalis</i>	Chromadex [Lot # 34899-045]	0.16% valerenic acids	
Vitamin B ₆	Sigma-Aldrich [Lot # 120M13271V]	> 98% pyridoxine	
Vitamin B ₁₂	Sigma-Aldrich [Lot # 030M1567]	> 98% vitamin B ₁₂	
Vitamin C	Chromadex [Lot # 111021-641]	Vitamin C	

Abbreviations: DHA, docosahexaenoic acid; EPA, eicosapentaenoic acid.

isosilybin A+B, silydianin and silychristin from PhytoLab (Vestenbergsgreuth, Germany). In **Table 2** details about these constituents are shown. Human cDNA expressed CYP2C9 + reductase and b5 (CYP2C9+OR+b5+) Supersomes™ and CYP2C9 substrate MFC were obtained from BD-Bioscience (Breda, The Netherlands). Human pooled liver microsomes (HLM) were purchased from BD-Bioscience (Breda, The Netherlands) and hydrochloric acid from Lamers & Pleuger (Den Bosch, The Netherlands). Sulfa-phenazole, β -nicotinamide adenine dinucleotide phosphate (NADPH) tetra sodium salt, β -nicotinamide adenine dinucleotide phosphate sodium salt (NAPD+), glucose-6-phosphate and glucose-6-phosphate dehydrogenase were purchased from Sigma-Aldrich

Table 2. Details of the milk thistle's constituents.

CAM	Product Information	Purity
Silybin A+B	Sigma-Aldrich CAS nr. [22888-70-6]	99.3%
Isosilybin A+B	PhytoLab CAS nr. [72581-71-6]	98.7% (A:B = 1.98:1)
Silychristin	PhytoLab CAS nr. [33889-69-9]	99.8%
Silydianin	PhytoLab CAS nr. [29782-68-1]	99.9%
Taxifolin	Sigma-Aldrich CAS nr. [480-18-2]	87.9%

(Zwijndrecht, The Netherlands). Acetonitrile, LC-MS grade water and methanol of HPLC quality were obtained from Biosolve (Valkenswaard, The Netherlands). Tolbutamide and 4-hydroxytolbutamide originated from Sigma-Aldrich (Zwijndrecht, The Netherlands) and labeled 4-hydroxytolbutamide-D9 from Toronto Research Canada (TRC, North York, Canada). Formic acid, magnesium chloride and tert-butyl methyl ether (TBME) for liquid chromatography were obtained from Merck (Darmstadt, Germany).

CYP2C9-mediated metabolism of MFC in Supersomes™

The fluometric CYP2C9 inhibition assay is based on the method described by Stresser *et al.*²⁶. For the CAM screen, CYP2C9 expressing Supersomes™ were incubated in black 96-well plates with 2 µM sulfaphenazole and 50 µg/mL of each CAM in 1 mg/mL NADPH solution. For the IC₅₀ (concentration required to achieve 50% of the maximum inhibition) curves, the final concentrations ranged from 0-500 µg/mL for most CAM extracts, except for grape seed, milk thistle, St John's wort (0-56 µg/mL); and β-carotene, green tea and Ginkgo biloba (0-167 µg/mL).

For further investigation of milk thistle, its constituents were also evaluated in the fluorescence assay. Milk thistle is a mixture of the following constituents: silybin, isosilybin, silychristin, silydianin and taxifolin³⁴. Each of these constituents was separately tested at one concentration (50 µM) and in a range from 0-900 µM for the IC₅₀ curves.

The ranges of the CAM and milk thistle's constituents were based on the strength of CYP2C9 inhibition and adjusted for quenching. The dilutions of CAM, silybin, isosilybin, silychristin, silydianin, taxifolin and sulfaphenazole were prewarmed for 10 minutes at 37°C and subsequently 200 pmol of CYP2C9+OR+b5 Supersomes™ and 25 µM of non-fluorescent MFC in 100 mM phosphate buffer (pH 7.4) were added. The final concentration of acetonitrile (the solvent for all compounds) was 2% during the incubations. The reaction mixtures were incubated for 60 minutes at 37°C and the reaction was stopped by a solution of 80% acetonitrile and 20% 0.5M Tris base on ice. The formation of highly fluorescent metabolite of MFC, 7-hydroxy-trifluoromethylcoumarin (HFC), was measured at 405/535 nm on a Mithras LB940 microplate reader (Berthold Technologies, Bad Wildbad, Germany).

CYP2C9-mediated metabolism of tolbutamide in human liver microsomes

The effects of CAM on the metabolism of tolbutamide by CYP2C9 were assessed by measuring the levels of the CYP2C9-mediated metabolite 4-hydroxytolbutamide with liquid-chromatography coupled to tandem mass spectrometry (LC-MS/MS) analysis.

Incubations

The incubations were performed in 2.0 mL polypropylene tubes (Sarstedt, Etten-Leur, The Netherlands). For the CAM screen, the stock solutions of all fourteen CAM (12.5 mg/mL in

50% acetonitrile) were diluted in a cofactor solution consisting of 2.6 mM NADP⁺, 7.1 mM glucose-6-phosphate, 6.5 mM magnesium chloride and 0.8 U/mL glucose-6-phosphate dehydrogenase in 50 mM phosphate buffer at pH 7.4 to achieve a final concentration of 100 µg/mL. For the IC₅₀ curves, the concentrations of all tested CAM ranged from 0 to 300 µg/mL. The positive control sulfaphenazole was diluted similarly to achieve a final concentration of 2 µM for the CAM screen and range of 0-10 µM for the IC₅₀ curves. In addition, milk thistle's constituents were evaluated at 100 µM and in a range of 0-300 µM. The solution of 10 mM tolbutamide in 100 mM phosphate buffer was added to the CAM cofactor solution, resulting in a final concentration of 100 µM tolbutamide during the incubation. This final concentration is close to the Michaelis Menten constant K_m as determined in previous experiments (data not shown) and in accordance to Komatsu *et al.* and Yuan *et al.*^{27, 28}. The dilutions of CAM, sulfaphenazole and tolbutamide were prewarmed for 10 minutes at 37°C and by adding a HLM solution in 50 mM phosphate buffer, the reaction was started. The concentration of acetonitrile in the 200 µL reaction volume was 2%. After 30 minutes the reaction was stopped by adding 100 µL ice cold 1M hydrochloric acid. At last, 5 µL of the internal standard 4-hydroxytolbutamide-D9 (10,000 µg/mL) was added.

LC-MS/MS analysis

Sample preparation consisted of liquid-liquid extraction (LLE) with TBME and all samples were vortex-mixed for 30 seconds. After centrifugation for 10 minutes at 13,500 *g* at 4°C, the samples were stored for -80°C for 1 h. Subsequently, the organic fluid was decanted in clean 1.5 mL polypropylene tubes and evaporated under a stream of nitrogen at 40°C. The residue was reconstituted in 200 µL of 0.2% formic acid in water-methanol-acetonitrile (75:12.5:12.5 v/v) and vortex-mixed for 30 seconds. After centrifugation for 10 minutes at 13,500 *g*, the supernatant was transferred in a 250 µL glass inserts placed in autosampler vials for LC-MS/MS analysis.

The samples were injected on a Polaris 3 C18-A column (50 mm × 2 mm ID, particle size 3 µm, Varian, Middelburg, The Netherlands) with a Polaris 3 C18-A pre-column (10 mm × 2 mm ID, particle size 3 µm, Varian). The Shimadzu LC10-AD liquid chromatography equipment comprised of a DGU-14A degasser, a CTO-10Avp column oven (40°C), a Sil-HTc autosampler (4°C) and two LC10-ADµ-pumps (Shimadzu, Kyoto, Japan). The mobile phase consisted of 0.2% formic acid in water (A) and acetonitrile: methanol (50:50 v/v) (B), with a flow rate of 0.5 mL/min. During the first 2.5 min of the run 25% of mobile phase B was applied, followed by increasing % B from 25% to 100% from 2.5 min to 3.5 min. Subsequently, % B was kept constant at 100% for until 4.0 min. At last, a gradient was introduced by rapidly decreasing % B from 100% to 25% within 6 seconds and stabilization at 25% B for 1 min. The total run time was 5 min.

Tolbutamide and 4-hydroxytolbutamide were detected with a Finnigan TSQ Quantum Discovery Max triple quadrupole mass spectrometer (Thermo Fischer Scientific, Waltham,

MA, USA) with electrospray ionization (ESI). To quantify the data reconstituted calibration standards of 4-hydroxytolbutamide were analyzed in a range of 5-1,000 ng/mL.

Statistical Analysis

Data were analyzed by using Student's *t*-test and were considered statistically significant when $p < 0.05$. All statistical determinations were performed with SPSS version 16.0 (SPSS Inc., Chicago, IL, USA).

RESULTS

To determine the effects of fourteen CAM extracts on CYP2C9-mediated metabolism of tolbutamide and MFC, HLM and Supersomes™ were used, respectively. HLM contain multiple enzymes²⁹ and Supersomes™ contain an overexpression of a single CYP enzyme³⁰. HLM are preferred as *in vitro* test system because HLM more closely mimic the clinical situation compared to Supersomes™. However, it is not possible to reliably determine the effect of CAM on the metabolism of MFC in HLM since this test system contains multiple CYP enzymes and the metabolism of MFC is not only primarily catalyzed by CYP2C9³¹. Since the metabolism of tolbutamide into 4-hydroxy-tolbutamide is CYP2C9 specific, the preferred HLM could be used.

CYP2C9-mediated metabolism of MFC in Supersomes™: fluorescence assay

The possible inhibiting effects of fourteen commonly used CAM on CYP2C9 activity were first screened in a fluorescence assay, applying the extensively used CYP2C9 probe MFC³². The results are shown in **Figure 1A**. The most potent inhibitors of CYP2C9-mediated metabolism of MFC are milk thistle and green tea (>89% CYP2C9 inhibition), followed by grape seed, St. John's wort, saw palmetto and Ginkgo biloba (>66% CYP2C9 inhibition).

In order to establish the potency of the inhibiting CAM, the IC_{50} values of the top 6 inhibiting CAM were determined (**Table 3**) and the IC_{50} curves of the top 3 inhibiting CAM are shown in **Figure 2**. The IC_{50} values confirm green tea, milk thistle and grape seed as the most potent CYP2C9 inhibitors: $IC_{50} < 7 \mu\text{g/mL}$.

CYP2C9-mediated metabolism of tolbutamide in HLM: LC-MS/MS

The effect of all fourteen CAM on CYP2C9 activity was further evaluated by measuring the effect on the metabolism of the sensitive CYP2C9 substrate tolbutamide³³. In **Figure 1B** the results are shown. The most potent inhibitors of CYP2C9-mediated metabolism of tolbutamide are milk thistle and grape seed (>96% CYP2C9 inhibition), followed by green tea, Ginkgo biloba, St. John's wort, ginseng and saw palmetto (>32% CYP2C9 inhibition). This order of inhibitory potency is partially comparable to the screen with MFC

as CYP2C9 substrate (**Figure 1A**). The IC_{50} values of the top 6 inhibiting CAM confirmed green tea and milk thistle as the most potent CYP2C9 inhibitors: $IC_{50} < 20 \mu\text{g/mL}$ (**Table 3**). The IC_{50} curves of the top 3 inhibiting CAM are shown in **Figure 3**.

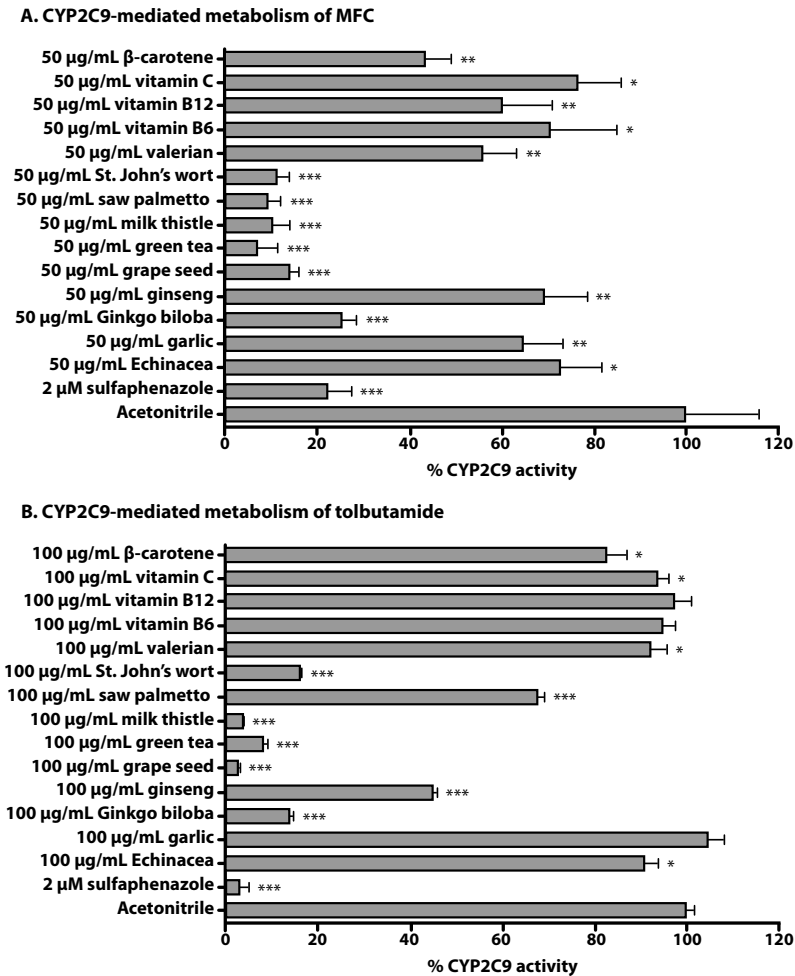


Figure 1. The effects of CAM on CYP2C9-mediated metabolism of MFC (A) and tolbutamide (B). For CYP2C9-mediated metabolism of MFC, CYP2C9+OR+b5 SupersomesTM were incubated with 2% negative control acetonitrile, 2 μM of the positive control sulfaphenazole and 50 $\mu\text{g/mL}$ CAM for 60 minutes. After stopping the reaction, the formation of highly fluorescent HFC was measured (A). For CYP2C9-mediated metabolism of tolbutamide, HLM were incubated with respectively 2% negative control acetonitrile, 2 μM of sulfaphenazole and 100 $\mu\text{g/mL}$ CAM for 30 minutes. After stopping the reaction, the formation of the metabolite 4-hydroxytolbutamide was measured with LC-MS/MS (B). The data are means \pm SD of triplicate incubations from a representative experiment. The % CYP2C9 inhibition compared to 2% acetonitrile are shown (* $p < 0.05$, ** $p < 0.01$ and *** $p < 0.001$).

Table 3. IC₅₀ values of top 6 CAM that inhibit CYP2C9-mediated metabolism of MFC and tolbutamide.

Fluorescence assay with MFC			LC-MS/MS with tolbutamide		
CAM *	IC ₅₀ (µg/mL) [95% C.I.]	R ²	CAM *	IC ₅₀ (µg/mL) [95% C.I.]	R ²
Sulfaphenazole	0.458 [0.344-0.610]	0.996	Sulfaphenazole	0.114 [0.089-0.147]	0.999
Milk thistle	2.81 [1.48-5.32]	0.991	Milk thistle	9.69 [7.24-13.0]	0.997
Green tea	6.55 [2.67-16.1]	0.984	Green tea	19.4 [15.9-23.7]	0.998
Grape seed	6.61 [3.41-12.8]	0.990	Ginkgo biloba	38.2 [32.6-44.8]	0.999
St. John's wort	7.00 [3.06-16.0]	0.986	Grape seed	44.2 [43.6-44.7]	1.000
Ginkgo biloba	8.44 [6.40-11.1]	0.994	St. John's wort	60.4 [51.1-71.5]	0.999
Saw palmetto	21.6 [16.0-29.0]	0.994	Ginseng	117 [82.5-167]	0.994

* Except for the positive control sulfaphenazole.

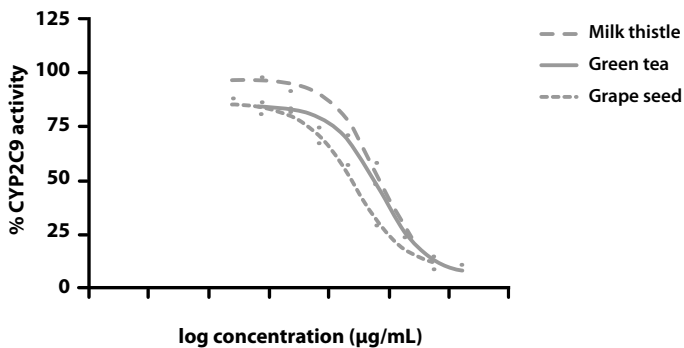


Figure 2. IC₅₀ curves of the top 3 inhibiting CAM, using MFC as CYP2C9 substrate. The data of the IC₅₀ curves are means of duplicate incubations from a representative experiment.

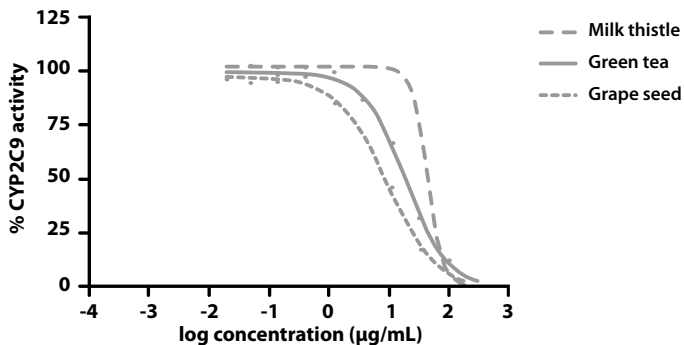


Figure 3. IC₅₀ curves of the top 3 inhibiting CAM, using tolbutamide as CYP2C9 substrate. The data of the IC₅₀ curves are means of duplicate incubations from a representative experiment.

Since milk thistle was shown to be the most potent inhibitor of CYP2C9-mediated metabolism of both MFC and tolbutamide, the constituents of milk thistle were also tested to discover which component is responsible for the inhibition of CYP2C9-mediated metabolism of both MFC and tolbutamide. The results are shown in **Figure 4** and **Table 4**.

As shown in **Figure 4** and **Table 4**, all constituents of milk thistle inhibited CYP2C9-mediated metabolism of both MFC and tolbutamide. Based on the determined IC_{50} values silybin is the most potent inhibitor of CYP2C9, followed by isosilybin.

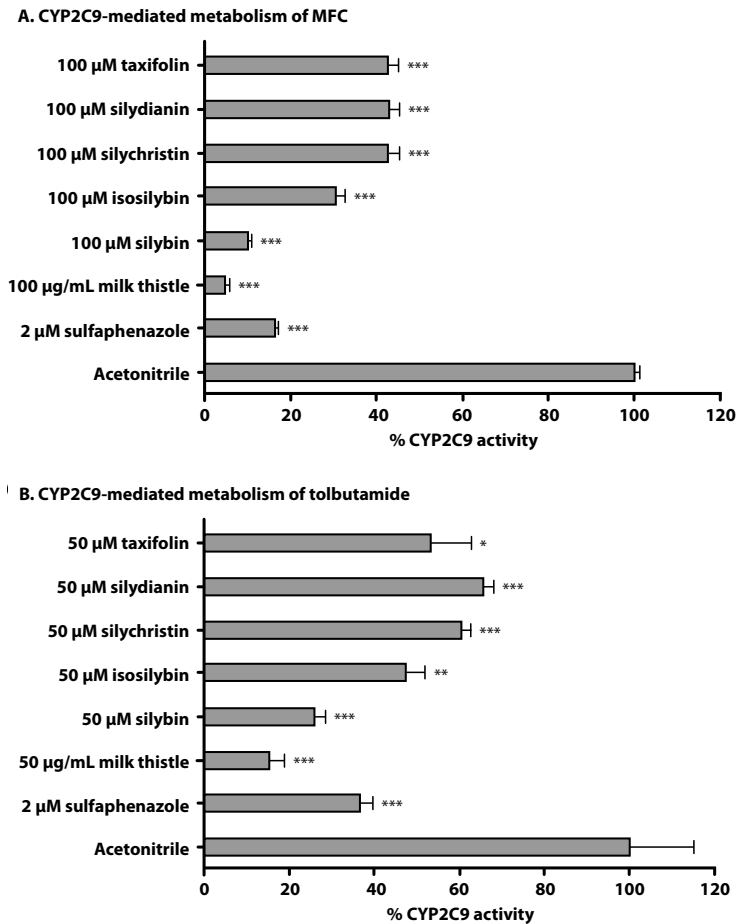


Figure 4. The effects of milk thistle's constituents on CYP2C9-mediated metabolism of MFC (A) and tolbutamide (B). For CYP2C9-mediated metabolism of MFC, CYP2C9+OR+b5 Supersomes™ were incubated with 2% negative control acetonitrile, 2 µM of the positive control sulfaphenazole, 50 µg/mL milk thistle and 50 µM of milk thistle's constituents for 60 minutes. After stopping the reaction, the formation of highly fluorescent HFC was measured (A). For CYP2C9-mediated metabolism of tolbutamide, HLM were incubated with respectively 2% negative control acetonitrile, 2 µM of sulfaphenazole, 100 µg/mL milk thistle and 100 µM of milk thistle's constituents for 30 minutes. After stopping the reaction, the formation of the metabolite 4-hydroxytolbutamide was measured with LC-MS/MS (B). The data are means ± SD of triplicate incubations from a representative experiment. The % CYP2C9 inhibition compared to 2% acetonitrile are shown (* $p < 0.05$, ** $p < 0.01$ and *** $p < 0.001$).

Table 4. IC₅₀ values of milk thistle's constituents.

Fluorescence assay with MFC			LC-MS/MS with tolbutamide		
CAM *	IC ₅₀ (µg/mL) [95% C.I.]	R ²	CAM *	IC ₅₀ (µg/mL) [95% C.I.]	R ²
Sulfaphenazole	0.0368 [0.0301-0.0449]	0.998	Sulfaphenazole	0.0862 [0.0688-0.108]	0.999
Silybin	8.97 [5.60-14.4]	0.989	Silybin	7.67 [6.23-9.43]	0.999
Isosilybin	27.4 [15.5-48.6]	0.984	Isosilybin	40.2 [19.0-85.2]	0.989
Taxifolin	46.7 [41.2-53.0]	0.999	Silydianin	65.0 [40.3-105]	0.995
Silychristin	70.8 [51.8-96.7]	0.996	Silychristin	72.1 [45.6-114]	0.993
Silydianin	92.0 [72.0-118]	0.999	Taxifolin	88.8 [67.1-117]	0.998

* Except for the positive control sulfaphenazole.

DISCUSSION AND CONCLUSION

The present study determined the rank order of CAM inhibiting CYP2C9 activity based on their inhibitory potencies. To address this issue, the inhibitory effects of standardized extracts of fourteen commonly used CAM on CYP2C9-mediated metabolism of MFC and tolbutamide were determined. The clinically applied tolbutamide was used as selective CYP2C9 probe to determine the possible effects of CAM on CYP2C9 activity. In addition, the effect of standardized CAM extracts was evaluated since cancer patients use commercial products of CAM that contain these extracts. The effects of standardized extracts and not extracts of commercial products were evaluated, since the identity and purity of standardized extracts is known.

When comparing the CAM screens using the substrates MFC and tolbutamide, lower concentrations of the CAM were required for the same level of CYP2C9 inhibition in the screen with MFC. Furthermore, the IC₅₀ values were generally higher in the assay with tolbutamide as substrate. Possible explanations for these higher IC₅₀ values are the different protein concentrations of CYP2C9 and incubation times in both assays. Furthermore CYP2C9 inhibition could be substrate dependent, however, for CYP2C9 there is a good correlation between fluorometric substrates and traditional CYP2C9 probes, which is in contrast to CYP3A4³⁵.

Although the IC₅₀ values were generally lower in the fluorescence assay with MFC, the potency of the CAM to inhibit CYP2C9 showed the same rank order for the two most potent inhibitors: milk thistle and green tea. In contrast, the potency of grape seed, St. John's wort and Ginkgo biloba to inhibit CYP2C9-mediated metabolism of MFC and tolbutamide differed. More importantly, in the fluorescence assay saw palmetto was shown to be a top 6 inhibiting CAM, while saw palmetto weakly inhibited the metabolism of tolbutamide. The other way around, ginseng was a top 6 CAM inhibiting the metabolism of tolbutamide, but weakly inhibited CYP2C9-mediated metabolism of MFC. These results underline the importance of using at least two CYP2C9 substrates within one

in vitro study to confirm the effects on CYP2C9 activity and to prevent interlaboratory differences such as differences in protocols, personnel and equipment.

Based on the *in vitro* results, both milk thistle and green tea could cause PK interactions via CYP2C9 *in vivo*. In a clinical study with 42 healthy volunteers, a 4-week supplementation of Polyphenon E (green tea catechin extract) did not significantly affect the average CYP2C9 phenotypic index³⁶. Based on this clinical result, green tea is not likely to cause clinically relevant PK interactions by CYP2C9 inhibition. In contrast, in a clinical phase I dose escalation study with thirteen prostate patients, a 4-week supplementation of 2.5-20 g of Siliphos® (commercial product of milk thistle) resulted in plasma levels of 5-75 µM silybin (the active component of milk thistle)³⁷. The results of the present study revealed IC₅₀ values of 8.97 and 7.67 µM for silybin in the fluorescence assay and LC-MS/MS analysis, respectively. Since the described clinical study revealed plasma levels of 5-75 µM, the IC₅₀ values of silybin could thus be reached in human. Furthermore in a clinical phase II randomized crossover study with healthy volunteers milk thistle inhibited the metabolism of losartan into E-3174 by CYP2C9³⁸. However, clinical studies should be conducted to determine the clinical relevance of inhibition of CYP2C9-mediated metabolism of anticancer drugs by milk thistle.

In conclusion, milk thistle and green tea were confirmed as potent inhibitors of CYP2C9-mediated metabolism of multiple substrates *in vitro* and both CAM could cause clinical PK interactions. Considering the available clinical data, clinical studies are especially recommended for milk thistle to establish the clinical relevance of the demonstrated CYP2C9 inhibition on the metabolism of anticancer drugs.

REFERENCES

1. Anzenbacher P, Anzenbacherova E. Cytochromes P450 and metabolism of xenobiotics. *Cell Mol Life Sci* 2001; 58(5-6): 737-4.
2. He N, Edeki T. The inhibitory effects of herbal components on CYP2C9 and CYP3A4 catalytic activities in human liver microsomes. *Am J Ther* 2004; 11(3): 206-12.
3. Tascilar M, de Jong FA, Verweij J, Mathijssen RH. Complementary and alternative medicine during cancer treatment: Beyond innocence. *Oncologist* 2006; 11(7): 732-41.
4. He SM, Yang AK, Li XT, Du YM, Zhou SF. Effects of herbal products on the metabolism and transport of anticancer agents. *Expert Opin Drug Metab Toxicol* 2010; 6(10): 1195-213.
5. Harmsen S, Meijerman I, Beijnen JH, Schellens JH. Nuclear receptor mediated induction of cytochrome P450 3A4 by anticancer drugs: A key role for the pregnane X receptor. *Cancer Chemother Pharmacol* 2009; 64(1): 35-43.
6. Werneke U, Earl J, Seydel C, Horn O, Crichton P, Fannon D. Potential health risks of complementary alternative medicines in cancer patients. *Br J Cancer* 2004; 90(2): 408-13.
7. Sparreboom A, Cox MC, Acharya MR, Figg WD. Herbal remedies in the United States: Potential adverse interactions with anticancer agents. *J Clin Oncol* 2004; 22(12): 2489-503.
8. Gupta D, Lis CG, Birdsall TC, Grutsch JF. The use of dietary supplements in a community hospital comprehensive cancer center: Implications for conventional cancer care. *Support Care Cancer* 2005; 13(11): 912-9.
9. McCune JS, Hatfield AJ, Blackburn AA, Leith PO, Livingston RB, Ellis GK. Potential of chemotherapy-herb interactions in adult cancer patients. *Support Care Cancer* 2004; 12(6): 454-62.
10. Zou L, Harkey MR, Henderson GL. Effects of herbal components on cDNA-expressed cytochrome P450 enzyme catalytic activity. *Life Sci* 2002; 71(13): 1579-8.
11. Yale SH, Glurich I. Analysis of the inhibitory potential of Ginkgo biloba, Echinacea purpurea, and serenoa repens on the metabolic activity of cytochrome P450 3A4, 2D6, and 2C9. *J Altern Complement Med* 2005; 11(3): 433-9.
12. Etheridge AS, Black SR, Patel PR, So J, Mathews JM. An *in vitro* evaluation of cytochrome P450 inhibition and P-glycoprotein interaction with goldenseal, Ginkgo biloba, grape seed, milk thistle, and ginseng extracts and their constituents. *Planta Med* 2007; 73(8): 731-4.
13. Tam TW, Akhtar H, Arnason JT, Cvijovic K, Boon H, Cameron DW, Drouin CE, Jaeger W, Tsuyuki RT, Vohra S, et al. Inhibition of human cytochrome p450 metabolism by blended herbal products and vitamins. *J Pharm Pharm Sci* 2011; 14(1): 1-16.
14. Foster BC, Foster MS, Vandenhoeck S, Krantis A, Budzinski JW, Arnason JT, Gallicano KD, Choudri S. An *in vitro* evaluation of human cytochrome P450 3A4 and P-glycoprotein inhibition by garlic. *J Pharm Pharm Sci* 2001; 4(2): 176-84.
15. Doehmer J, Weiss G, McGregor GP, Appel K. Assessment of a dry extract from milk thistle (silybum marianum) for interference with human liver cytochrome-P450 activities. *Toxicol in Vitro* 2011; 25(1): 21-7.
16. Sridar C, Goosen TC, Kent UM, Williams JA, Hollenberg PF. Silybin inactivates cytochromes P450 3A4 and 2C9 and inhibits major hepatic glucuronosyltransferases. *Drug Metab Dispos* 2004; 32(6): 587-94.
17. Althagafy HS, Graf TN, Sy-Cordero AA, Gufford BT, Paine MF, Wagoner J, Polyak SJ, Croatt MP, Oberlies NH. Semisynthesis, cytotoxicity, antiviral activity, and drug interaction liability of 7-O-methylated analogues of flavonolignans from milk thistle. *Bioorg Med Chem* 2013; 21(13): 3919-26.

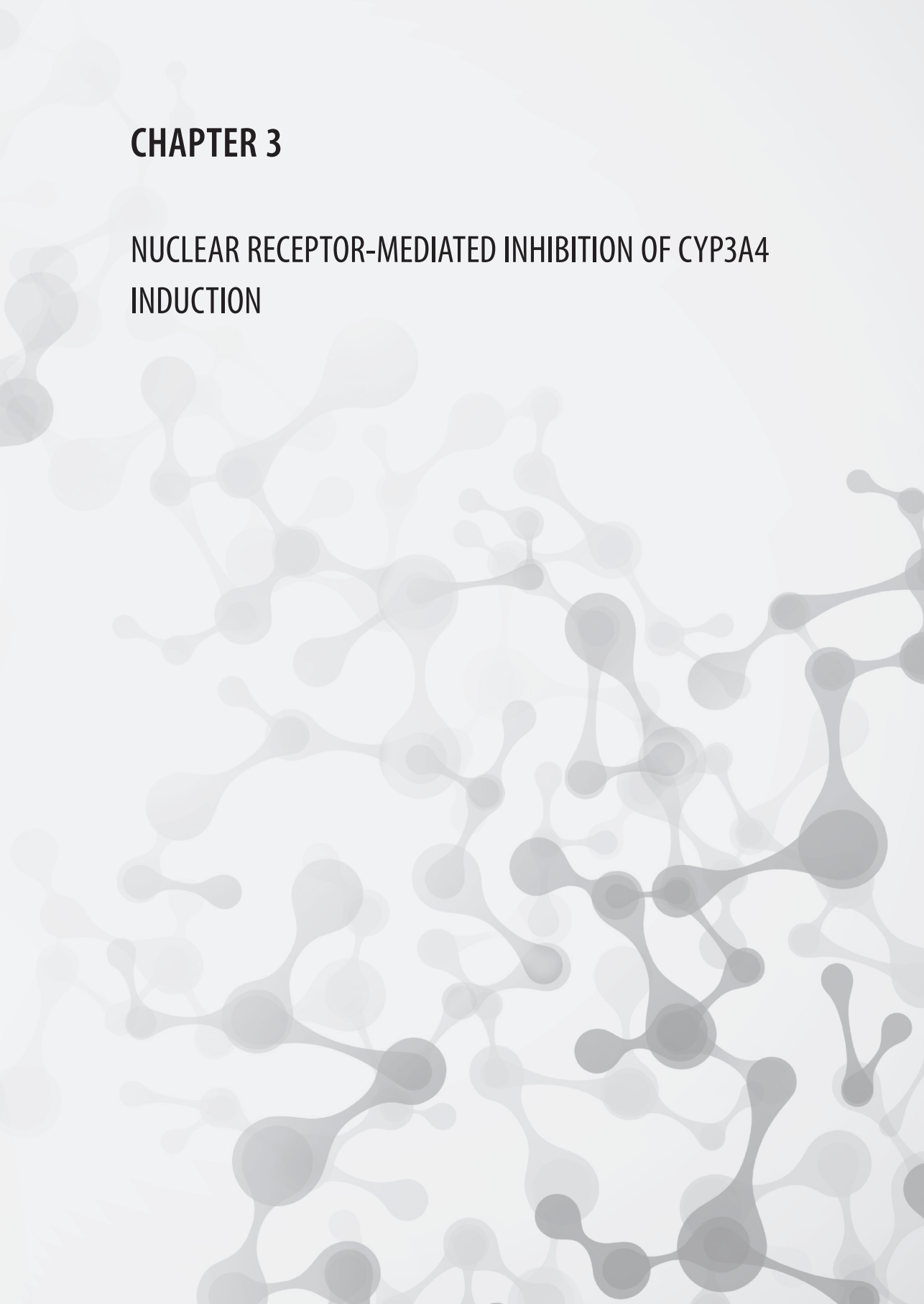
18. Numa AM, Abbott FS, Chang TK. Effect of Ginkgo biloba extract on oxidative metabolism of valproic acid in hepatic microsomes from donors with the CYP2C9*1/*1 genotype. *Can J Physiol Pharmacol* 2007; 85(9): 848-55.
19. von Moltke LL, Weemhoff JL, Bedir E, Khan IA, Harmatz JS, Goldman P, Greenblatt DJ. Inhibition of human cytochromes P450 by components of Ginkgo biloba. *J Pharm Pharmacol* 2004; 56(8): 1039-44.
20. Gaudineau C, Beckerman R, Welbourn S, Auclair K. Inhibition of human P450 enzymes by multiple constituents of the Ginkgo biloba extract. *Biochem Biophys Res Commun* 2004; 318(4): 1072-8.
21. Komoroski BJ, Zhang S, Cai H, Hutzler JM, Frye R, Tracy TS, Strom SC, Lehmann T, Ang CY, Cui YY, et al. Induction and inhibition of cytochromes P450 by the St. John's wort constituent hyperforin in human hepatocyte cultures. *Drug Metab Dispos* 2004; 32(5): 512-8.
22. Obach RS. Inhibition of human cytochrome P450 enzymes by constituents of St. John's wort, an herbal preparation used in the treatment of depression. *J Pharmacol Exp Ther* 2000; 294(1): 88-95.
23. Winslow LC, Kroll DJ. Herbs as medicines. *Arch Intern Med* 1998; 158(20): 2192-9.
24. Goey AKL, Mooiman KD, Beijnen JH, Schellens JH, Meijerman I. Relevance of *in vitro* and clinical data for predicting CYP3A4-mediated herb-drug interactions in cancer patients. *Cancer Treatment Reviews* 2013; 39(7): 773-83.
25. Mooiman KD, Maas-Bakker RF, Moret EE, Beijnen JH, Schellens JH, Meijerman I. Milk thistle's active components silybin and isosilybin: Novel inhibitors of PXR-mediated CYP3A4 induction. *Drug Metab Dispos* 2013; 41(8): 1494-504.
26. Stresser DM, Turner SD, Blanchard AP, Miller VP, Crespi CL. Cytochrome P450 fluorometric substrates: Identification of isoform-selective probes for rat CYP2D2 and human CYP3A4. *Drug Metab Dispos* 2002; 30(7): 845-52.
27. Komatsu K, Ito K, Nakajima Y, Kanamitsu S, Imaoka S, Funae Y, Green CE, Tyson CA, Shimada N, Sugiyama Y. Prediction of *in vivo* drug-drug interactions between tolbutamide and various sulfonamides in humans based on *in vitro* experiments. *Drug Metab Dispos* 2000; 28(4): 475-81.
28. Yuan R, Madani S, Wei XX, Reynolds K, Huang SM. Evaluation of cytochrome P450 probe substrates commonly used by the pharmaceutical industry to study *in vitro* drug interactions. *Drug Metab Dispos* 2002; 30(12): 1311-9.
29. Vogel HG. CYP inhibition studies using human liver microsomes. In: *Drug discovery and evaluation: Safety and pharmacokinetic assays*, Hock FJ, Maas J, Mayer D, editors: 2006.
30. European Medicines Agency. Guideline on the investigation of drug interactions. 2010.
31. Renwick AB, Surry D, Price RJ, Lake BG, Evans DC. Metabolism of 7-benzyloxy-4-trifluoromethylcoumarin by human hepatic cytochrome P450 isoforms. *Xenobiotica* 2000; 30(10): 955-69.
32. Hummel MA, Tracy TS, Hutzler JM, Wahlstrom JL, Zhou Y, Rock DA. Influence of fluorescent probe size and cytochrome b5 on drug-drug interactions in CYP2C9. *J Biomol Screen* 2006; 11(3): 303-9.
33. Miners JO, Birkett DJ. Cytochrome P4502C9: An enzyme of major importance in human drug metabolism. *Br J Clin Pharmacol* 1998; 45(6): 525-38.
34. Kroll DJ, Shaw HS, Oberlies NH. Milk thistle nomenclature: Why it matters in cancer research and pharmacokinetic studies. *Integr Cancer Ther* 2007; 6(2): 110-9.
35. Miller VP, Crespi CL. High-throughput screening for metabolism-based drug drug interactions. In: *Handbook of drug screening*, R. Seethala, P. B. Fernandes, editors: 2005.
36. Chow HH, Hakim IA, Vining DR, Crowell JA, Cordova CA, Chew WM, Xu MJ, Hsu CH, Ranger-Moore J, Alberts DS. Effects of repeated green tea catechin administration on human cytochrome P450 activity. *Cancer Epidemiol Biomarkers Prev* 2006; 15(12): 2473-6.

37. Flaig TW, Gustafson DL, Su LJ, Zirrolli JA, Crighton F, Harrison GS, Pierson AS, Agarwal R, Glode LM. A phase I and pharmacokinetic study of silybin-phytosome in prostate cancer patients. *Invest New Drugs* 2007; 25(2): 139-46.
38. Han Y, Guo D, Chen Y, Chen Y, Tan ZR, Zhou HH. Effect of silymarin on the pharmacokinetics of losartan and its active metabolite E-3174 in healthy Chinese volunteers. *Eur J Clin Pharmacol* 2009; 65(6): 585-91.



CHAPTER 3

NUCLEAR RECEPTOR-MEDIATED INHIBITION OF CYP3A4 INDUCTION





3.1

EVALUATION OF A REPORTER GENE ASSAY AS SUITABLE *IN VITRO* SYSTEM TO SCREEN FOR NOVEL PXR ANTAGONISTS

K.D. Mooiman
R.F. Maas-Bakker
E.E. Moret
J.H. Beijnen
J.H.M. Schellens
I. Meijerman

Submitted for publication

ABSTRACT

The development of multidrug resistance (MDR) and a low bioavailability of anticancer drugs are major drawbacks to a successful treatment of cancer. One of the causes is the up-regulation of drug metabolizing enzymes. Cytochrome P450 (CYP) 3A4 is of considerable interest as it metabolizes the majority of currently prescribed anticancer drugs. Up-regulation of CYP3A4 results in decreased plasma levels, potentially resulting in a reduced efficacy. Since up-regulation of CYP3A4 is predominantly regulated by the pregnane X receptor (PXR), inhibition of PXR might prevent induction and thereby improve the efficacy of anticancer drugs. Therefore, the discovery of potent PXR antagonists is crucial. In literature, a limited number of PXR antagonists is described, which were discovered in different test systems (e.g. human hepatocytes) using multiple methods of quantifications (e.g. reporter gene assay). Consequently, the inhibitory potencies of these PXR antagonists are difficult to compare.

Therefore, the aim of the present study is to compare the PXR antagonists A-792611, trabectedin, ketoconazole, sulforaphane, leflunomide, thymolphtalein and coumestrol within one test system (colon carcinoma derived cell line LS180) in order to rank their inhibitory potencies, using a luciferase reporter gene assay. In addition, quantitative real-time polymerase chain reaction (qRT-PCR), computational docking in PXR and LanthaScreen® time-resolved fluorescence resonance energy transfer (TR-FRET) PXR competitive binding assay were performed to establish whether the reporter gene assay alone is suitable to discover novel PXR antagonists.

Trabectedin, thymolphtalein, A-792611 and ketoconazole were identified as PXR antagonists in rank order of their inhibitory potencies, leflunomide as PXR agonist, and coumestrol and sulforaphane were no PXR ligands. The application of the reporter gene assay is suitable and reliable to discover novel PXR antagonists, which is important to prevent decreased plasma levels of anticancer drugs in humans and to possibly increase the efficacy of oncolytic therapy.

INTRODUCTION

The treatment of cancer is often hindered by a low bioavailability of anticancer drugs and/or the development of multidrug resistance (MDR)¹. One of the causes is the up-regulation of ATP-binding cassette (ABC) drug efflux transporters and drug metabolizing enzymes²⁻⁴. Of these metabolizing enzymes, cytochrome P450 (CYP) 3A4 is of considerable interest as it metabolizes the majority of currently prescribed anticancer drugs⁵. More importantly, CYP3A4 is highly inducible by various drugs such as rifampicin. Furthermore, multiple anticancer drugs were also shown to induce CYP3A4 such as paclitaxel, docetaxel, ifosfamide, flutamide and tamoxifen and co-administered drugs^{2, 6}. Anticancer drugs that induce CYP3A4 can promote their own metabolism (auto-induction)⁷, but also the metabolism of other co-administered anticancer drugs. Consequently, the plasma levels of the affected drugs decrease which potentially results in a reduced therapeutic effect^{8,9}.

Since the induction of CYP3A4 is mainly regulated by activation of the pregnane X receptor (PXR)^{6,10}, inhibition of PXR might prevent induction and thereby prevent decreased efficacy of anticancer drugs and other drugs metabolized by CYP3A4. Therefore, the identification of PXR antagonists is an important target to improve the efficacy of anticancer drugs. Since PXR has a flexible ligand-binding pocket (LBP), it is difficult to predict the interactions between potential antagonists and PXR¹¹. In literature a limited number of PXR antagonists has been described¹². The first described PXR antagonist was trabectedin (ET-743), an antineoplastic agent¹³. In subsequent years other PXR antagonists were discovered such as ketoconazole¹⁴, (S)-1-[(1S,3S,4S)-4-[(S)-2-(3-benzyl-2-oxo-imidazolidin-1-yl)-3,3-dimethyl-butylamino]-3-hydroxy-5-phenyl-1-(4-pyridin-2-yl-benzyl)pentylcarbamoyl]-2,2-dimethyl-propyl-carbamic acid methyl ester (A-792611)¹⁵, sulforaphane¹⁶, leflunomide¹⁷, thymolphthalein¹⁸ and coumestrol¹⁹. These PXR antagonists have been identified in different test systems (e.g. hepatocytes) and methods of quantification (e.g. the reporter gene assay). **Table 1** provides a short overview of the applied test systems, methods of quantification and potency of the known PXR antagonists.

As shown in **Table 1** the described PXR antagonists were discovered in multiple test systems such as HepG2 cells and human hepatocytes, and different methods of quantification such as quantitative real-time polymerase chain reaction (qRT-PCR) and a reporter gene assay were used. Due to these differences and interlaboratory differences, it is difficult to compare the inhibitory potencies of the described PXR antagonists and to predict their rank order of potency. Therefore it is useful to screen all PXR antagonists within one test system and method of quantification.

To address this issue in the present study known PXR antagonists A-792611, trabectedin, ketoconazole, sulforaphane, leflunomide, thymolphthalein and coumestrol

Table 1. Overview of the applied test systems, methods of quantification and potency of the known PXR antagonists.

PXR antagonists	Test system	Method	IC ₅₀ values	References
Trabectedin	CV-1 cells	Reporter gene assay	2 nM	Synold <i>et al.</i> ¹³
Ketoconazole	CV-1 cells HepG2 cells Hepatocytes	Reporter gene assay Real-time RT-PCR, immunoblot analysis Northern blot analysis Scintillation proximity assay	74.4 μM	Huang <i>et al.</i> ¹⁴
A-792611	HepG2 Human hepatocytes	Reporter gene assay Real-time RT-PCR Micro-array	2 μM	Healan-Greenberg <i>et al.</i> ¹⁵
Sulforaphane	HepG2 Hepatocytes/LS180	Reporter gene assay Scintillation proximity assay Real-time RT-PCR GC-MS/MS	12 μM	Zhou <i>et al.</i> ¹⁶
Leflunomide	HepG2	Computational modeling Reporter gene assay	6.8 μM	Ekins <i>et al.</i> ¹⁷
Thymolphthalein	Huh-7 cells	Reporter gene assay	± 10 μM	Dring <i>et al.</i> ¹⁸
Coumestrol	CV-1 cells HEK293T cells Human hepatocytes	Competition binding assay Reporter gene assay LC-MS/MS Subnuclear localization Northern blotting	11.6 μM	Wang <i>et al.</i> ¹⁹

Abbreviations: RT-PCR, real-time polymerase chain reaction; LC-MS/MS, liquid chromatography tandem mass spectrometry; GC-MS/MS, gas chromatography tandem mass spectrometry; RT-PCR, real-time polymerase chain reaction; IC₅₀, half maximal inhibitory concentration.

were tested in the human colon carcinoma cell line LS180, using a luciferase reporter gene assay. This cell-based assay is a suitable alternative to human hepatocytes to study PXR-mediated CYP3A4 induction. Major drawbacks of human hepatocytes are considerable interindividual donor variations, high costs, rapid decrease in CYP expression and poor availability. Therefore, cultured cell lines such as the human hepatocarcinoma cell line HepG2 and the cell line LS180 are frequently used, of which the latter is a more suitable cell line to study PXR-mediated CYP3A4 induction^{6, 20, 21}. Cell-based reporter gene assays are suitable alternatives for hepatocytes because a good correlation has been shown between CYP3A4 induction according to the reporter gene assay and CYP3A4 expression in hepatocytes^{6, 20, 22, 23}. Since the reporter gene assay is generally accepted for PXR agonists²⁴ and PXR is highly expressed in the transfected LS180 cells, this assay is considered to be suitable to discover novel PXR antagonists.

The aim of this study is the comparison of known PXR antagonists (A-792611, trabectedin, ketoconazole, sulforaphane, leflunomide, thymolphthalein and coumestrol) within one test system (LS180 cells) to determine the rank order of their inhibitory potencies. Subsequently, the effect of these compounds was also established with qRT-PCR, computational docking in PXR and LanthaScreen® time-resolved fluorescence reso-

nance energy transfer (TR-FRET) PXR competitive binding assay to determine whether the reporter gene assay alone is suitable to screen for novel PXR antagonists.

MATERIALS AND METHODS

Reagents and chemicals

All cell culture media, supplements and nanofectin transfection reagent were purchased from PAA (Pasching, Austria). Rifampicin, ketoconazole, leflunomide, hyperforin (dicyclohexyl-ammonium) salt and SR-12813 were purchased from Sigma-Aldrich (Zwijndrecht, The Netherlands) and DMSO from Acros Organics (New Jersey, USA). Trabectedin (ET-743) was kindly provided by PharmaMar (Madrid, Spain). Coumestrol was purchased from Enzo Life Sciences BVBA (Zandhoven, Belgium) and thymolphtalein from Merck (Darmstadt, Germany). A-792611 was a kind gift from Abbott Labs (North Chicago, IL, USA) and clotrimazole and sulforaphane were purchased from LTK Laboratories Inc. (St. Paul, USA).

Cell culture

The human colon adenocarcinoma-derived cell line LS180 was obtained from the American Type Culture Collection (Manassas, VA, USA) and maintained in Roswell Park Memorial Institute (RPMI) 1640 medium with 25 mM HEPES and L-glutamine, supplemented with 100 U/mL penicillin, 100 µg/mL streptomycin and 10% (v/v) heat-inactivated fetal bovine serum (RPMI 1640 complete medium) at 37°C under a humidified atmosphere of 5% CO₂.

Plasmids

The pGL3-CYP3A4-XREM (proximal, -362/+53; distal, -7836/-7208) luciferase reporter construct was generously provided by Dr. Richard Kim (University of Western Ontario, London, ON, Canada), the pCDG-hPXR expression vector by Dr. Ron Evans (Salk Institute, La Jolla, CA, USA) and the pRL-TK control plasmid was obtained from Promega (Madison, WI, USA). According to the instructions of the manufacturer, plasmids were checked by enzyme restriction and agarose gel electrophoresis, and purified using Promega's Pureyield Midi-prep (Madison, WI, USA).

CYP3A4 Reporter gene assay

The CYP3A4 Reporter gene assay was performed as described by Mooiman *et al.*²⁵. In short, LS180 cells (5.0 x 10⁴ cells/well) were incubated in 96-well plates (Greiner Bio-One BV) for 24 hours in a 5% CO₂-humidified atmosphere at 37°C. Subsequently, the cells were transfected with a pCDG-hPXR nuclear receptor expression vector, pGL3-CYP3A4-

XREM luciferase reporter construct and pRL-TK *Renilla* luciferase expression control plasmid, using 0.8 μ L/well nanofectin transfection reagent in 150 mM NaCl. After 24 hours, the transfected cells were washed with PBS and incubated with 0.3% DMSO or 10 μ M rifampicin with or without addition of A-792611, ketoconazole, sulforaphane and leflunomide (50 μ M), trabectedin (5 nM), coumestrol (200 μ M), and thymolphthalein (12.5 μ M). These concentrations were not cytotoxic, according to a cell viability assay (data not shown). After 24 hours of exposure, cells were washed with PBS and lysed with 25 μ L/well Passive Lysis Buffer (Promega). Total volumes of 10 μ L of the lysates were measured on a Mithras LB940 microplate reader (Berthold Technologies, Bad Wildbad, Germany). The fold induction was calculated after normalizing the *firefly* luciferase signals to the *Renilla* luciferase signal.

Quantitative real-time PCR

To confirm the results from the CYP3A4 reporter gene assay, qRT-PCR was performed as previously described²⁵. In short, LS180 cells (2.5×10^5 cells/well) were incubated with 0.3% DMSO or 10 μ M rifampicin with or without addition of A-792611, ketoconazole, sulforaphane and leflunomide (50 μ M), trabectedin (5 nM), coumestrol (200 μ M), and thymolphthalein (12.5 μ M). After 24 hours, the cells were washed with PBS and total RNA was isolated with the SV Total RNA Isolations System of Promega. Subsequently, the quantity and integrity of this RNA was checked with a Nanodrop Diode Array Spectrophotometer (Nanodrop 1000, Isogen Life Science, IJsselstein, The Netherlands). For the cDNA synthesis, 1 μ g RNA was reversed transcribed with the RevertAid™ First Strand cDNA Synthesis Kit (Fermentas) using random priming. For 18S (Hs99999901_s1) and human CYP3A4 (Hs00604506_m1) real-time PCR, TaqMan® Gene Expression Assays (Applied Biosystems, Foster City, CA, USA) were used. The mRNA expression levels of CYP3A4 and the housekeeping gene 18S were analyzed with an ABI prism 7000 sequence detection system (Applied Biosystems, Foster City, CA, USA). The relative changes in CYP3A4 gene expression were determined with the cycle threshold (CT) value, delta ct (dct) values and the $2^{-(\text{difference in dct})}$ method²⁶.

Computational molecular docking

In order to verify the interaction between PXR and rifampicin, ketoconazole, A-792611, trabectedin, sulforaphane, leflunomide, thymolphthalein and coumestrol, these compounds were docked in PXR as described earlier²⁵. Autodock 4.2²⁷ was used for the dockings, as part of Yasara 12.4.1²⁸. The structure of the ligand binding domain of hPXR was used (PDB code 1M13¹¹) and first rifampicin was docked after superimposing the hPXR-rifampicin complex 1SKX²⁹ onto 1M13. Based on the structure from Healan-Greenberg *et al.*¹⁵ and structure of the similar HIV-protease inhibitor in PDB file 3GGV³⁰, A-792611 was built. The other compounds ketoconazole, trabectedin, sulforaphane,

leflunomide, thymolphtalein and coumestrol were derived from ChemIDplus Advanced (<http://chem.sis.nlm.nih.gov/chemidplus/>) as Sybyl Mol2 files. Furthermore, Yasara was applied to clean the molecules with regard to atom types and bond types. A total of 250 rigid docking runs, with *ga_pop_size* set at 15000, were performed after initial minimization and stimulated annealing with the Amber03 forcefield³¹ of the ligands and sidechains of hPXR residues within 7Å.

Lanthascreen® TR-FRET Competitive Binding Assay

A LanthaScreen® TR-FRET PXR Competitive Binding Assay was performed according to the manufacturer's (Invitrogen) protocol and as previously described²⁵. In short, the assay was performed in black non-coated, low-volume and round-bottomed 384-well Corning® plates. First, 10 µL/well of the test compounds (diluted in TR-FRET PXR Assay buffer) was dispensed in quadruplicate: ketoconazole and A-792611 (100 µM), trabectedin (5 nM), sulforaphane and leflunomide (50 µM), coumestrol (200 µM) and thymolphtalein (12.5 µM). In addition, known PXR agonists rifampicin, clotrimazole and hyperforin (100 µM), and SR-12813 (1 µM) were evaluated. Second, 5 µL/well of Fluoromone PXR green was added at a final concentration of 40 nM. Finally, 5 µL/well of a mix of dithiothreitol, terbium-labeled anti-GST antibody and hPXR-LBD was added at final concentrations of 50 µM, 10 nM and 5 nM, respectively. After an incubation of 1 hour at room temperature (protected from light), TR-FRET was measured with the PerkinElmer Envision® plate reader. The following setting were applied: delay time of 120 µs, integration time of 600 µs, 340 nm as excitation wavelength, 520 nm and 495 nm as emission wavelengths for fluorescein and terbium, respectively. For the TR-FRET ratios the emission signal at 520 nm was divided by the emission signal at 495 nm.

Statistical Analysis

All statistical analyses were performed with SPSS version 16.0 (SPSS Inc., Chicago, IL, USA) using the two-tailed Student's t-test. Data were considered statistically significant when $p < 0.05$.

RESULTS

Reporter gene assay

In order to determine the rank of potencies of known PXR antagonists (ketoconazole, A-792611, trabectedin, sulforaphane, leflunomide, thymolphtalein and coumestrol¹³⁻¹⁹), all compounds were tested within one test system (LS180 cells) using a reporter gene assay.

After transfecting LS180 cells with plasmids expressing CYP3A4, hPXR and *Renilla* and an 24-hour incubation with the mentioned PXR antagonists in combination with rifam-

picin, the *firefly* and *Renilla* luciferase signals were measured. The results of the screen at one concentration revealed that trabectedin was the strongest PXR antagonist, which is in accordance with the literature³². Trabectedin significantly inhibited PXR-mediated CYP3A4 induction by 96% at 5 nM. Thymolphtalein was shown to significantly and strongly inhibit PXR-mediated CYP3A4 induction by 87% at 12.5 μ M. A-792611 and ketoconazole also caused a strong and significant inhibition of PXR-mediated CYP3A4 induction by 82% and 76% at 50 μ M, respectively (**Figure 1**).

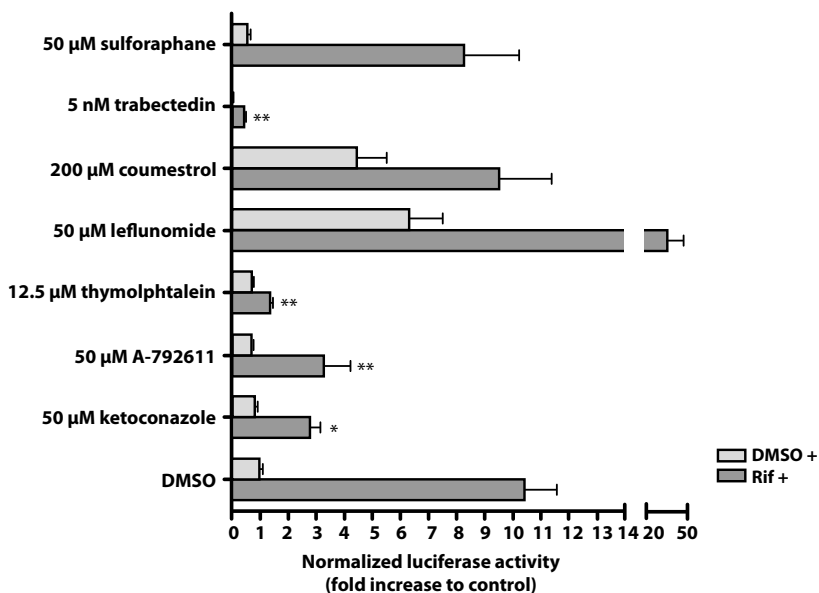


Figure 1. Screen for inhibition of PXR-mediated CYP3A4 induction by rifampicin using a reporter gene assay. After transfecting LS180 cells for 24 hours with the pCDG-hPXR expression vector, pGL3-CYP3A4-XREM reporter construct and pRL-TK control plasmid, these cells were incubated with 0.3% DMSO or the CYP3A4 inducer rifampicin (10 μ M) in combination with the negative control DMSO, ketoconazole, A-792611, trabectedin, sulforaphane, coumestrol, thymolphtalein and leflunomide. After 24 hours of incubation, the luciferase activities were measured. Data are means \pm SD from a representative experiment performed in triplicate. The fold inductions compared to 0.3% DMSO are shown (* $p < 0.05$, ** $p < 0.01$ and *** $p < 0.001$: compared to the fold induction of rifampicin) DMSO +, results after incubation without rifampicin; Rif +, results after incubation with rifampicin.

Instead of inhibiting PXR-mediated CYP3A4 induction, leflunomide significantly enhanced the induction of CYP3A4 by rifampicin by 214% at 50 μ M. In comparison, both sulforaphane and coumestrol did not affect PXR-mediated CYP3A4 induction (**Figure 1**).

Furthermore, the IC_{50} and EC_{50} values of all compounds were determined to predict the difference in their potency to inhibit and activate PXR, respectively (**Table 2**).

Table 2. Potency of different compounds to affect PXR.

PXR antagonists	IC ₅₀ values
Trabectedin	0.614 nM
Thymolphthalein	0.938 μM
A-792611	2.57 μM
Ketoconazole	6.82 μM
PXR agonists	EC ₅₀ values
Leflunomide + rifampicin	1.59 μM
Rifampicin	15.0 μM
Leflunomide	33.3 μM

In addition, the IC₅₀ and EC₅₀ curves are shown in **Figure 2**. In accordance with the results of the screen, trabectedin is the most potent PXR antagonist with an IC₅₀ value of 0.614 nM, followed by thymolphthalein, A-792611 and ketoconazole in order of potency. On the other hand, leflunomide is a PXR agonist with an EC₅₀ value of 33.3 μM. In combination with rifampicin, leflunomide was shown to decrease the EC₅₀ from 33.3 μM to 1.59 μM.

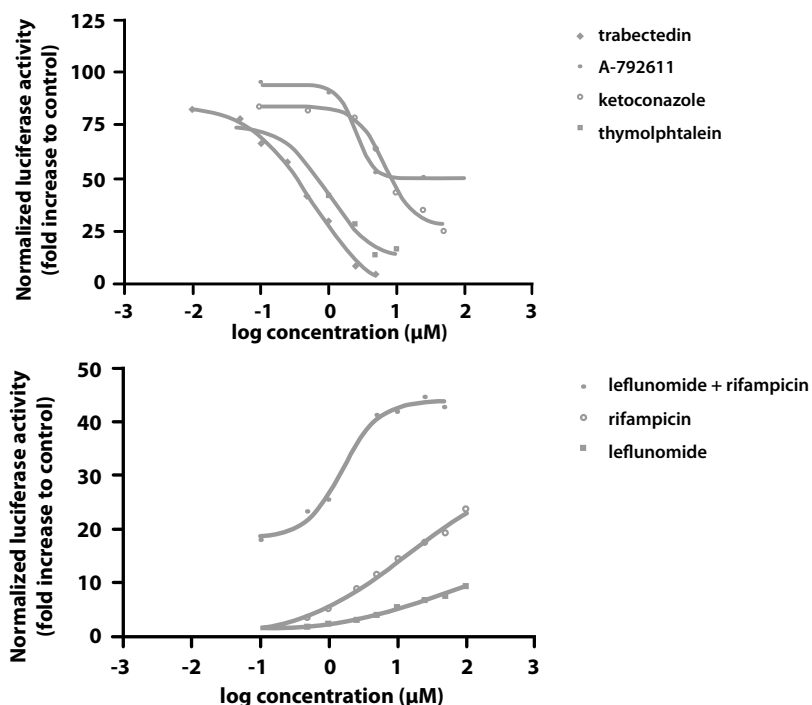


Figure 2. IC₅₀ and EC₅₀ curves of PXR antagonists and agonists. The data of the IC₅₀ and EC₅₀ curves are means of duplicate incubations from a representative experiment. A: IC₅₀ curves of PXR antagonists trabectedin, A-792611, ketoconazole and thymolphthalein. B: EC₅₀ curves of PXR agonists leflunomide, rifampicin and leflunomide together with rifampicin.

Quantitative real-time PCR

The potential of A-792611, ketoconazole, trabectedin and thymolphthalein to inhibit CYP3A4 induction was confirmed in non-transfected LC180 cells, using qRT-PCR (**Figure 3**).

At a concentration of 5 nM, trabectedin significantly inhibited CYP3A4 induction by 51%, which indicates that trabectedin is the strongest PXR antagonist. Also thymolphthalein is a strong PXR antagonist according to the results of the qRT-PCR, which revealed 74% inhibition of CYP3A4 induction at 12.5 μ M. A-792611 significantly inhibited PXR-mediated CYP3A4 induction by 74% at 50 μ M. The same concentration of ketoconazole resulted in 66% inhibition of CYP3A4 induction.

In contrast, 50 μ M of leflunomide resulted in a significant 3-fold induction of CYP3A4. In combination with rifampicin, leflunomide enhanced the CYP3A4 induction from 6-fold to 23-fold. These results are in accordance with results of the reporter gene assay, identifying leflunomide as PXR agonist.

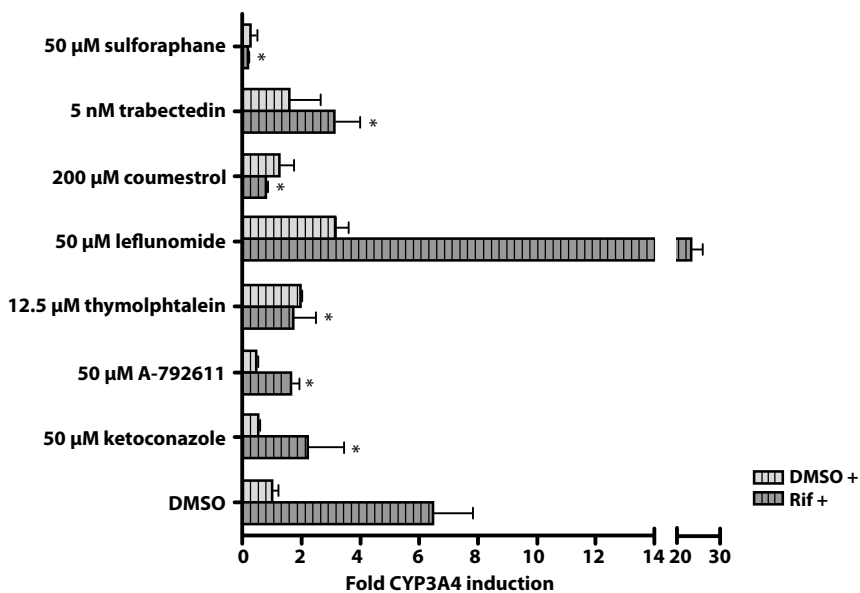


Figure 3. Screen for inhibition of PXR-mediated CYP3A4 induction by rifampicin using quantitative qRT-PCR. LS180 cells were incubated with 0.3% DMSO or the CYP3A4 model inducer rifampicin (10 μ M) in combination with the negative control DMSO, ketoconazole, A-792611, thymolphthalein, leflunomide, coumestrol, trabectedin and sulforaphane. The mRNA expression levels were measured after 24 hours of incubation using singleplexed quantitative qRT-PCR. Data are means \pm SD from a representative experiment performed in triplicate. In the figure the fold inductions compared to 0.3% DMSO are shown (* $p < 0.05$, ** $p < 0.01$ and *** $p < 0.001$: comparison with the fold induction by rifampicin). DMSO +, results after incubation without rifampicin; Rif +, results after incubation with rifampicin in combination with DMSO, milk thistle or positive controls.

Based on the results of the reporter gene assay, both sulforaphane and coumestrol could not be identified as either PXR agonist or antagonist. However, the results of quantitative real-time PXR revealed that both sulforaphane and coumestrol significantly inhibited CYP3A4 induction.

Computational Molecular Docking

All compounds were tested in a computational molecular docking study to establish their affinity for PXR. The results revealed that PXR agonist rifampicin had a high binding affinity of 1.39 pM, which is in accordance to the high degree of CYP3A4 induction from the reporter gene assay (**Table 3**).

The PXR antagonist A-792611 had the highest binding affinity of 26.5 pM, followed by ketoconazole with a binding affinity of 2.60 nM (**Table 3**). This result is also in accordance to the results of the reporter gene assay. Compared to ketoconazole, trabectedin revealed a higher binding affinity of 0.242 nM and thymolphtalein a lower binding affinity of 33.5 nM (**Table 3**). The other compounds leflunomide, coumestrol and sulforaphane showed practically no affinity towards PXR (**Table 3**).

It is difficult to distinguish PXR agonists and antagonists based on the computational molecular docking. However, it is suggested that PXR antagonists bind to the small binding site close to the outer surface of PXR at the AF-2 domain, while PXR agonists bind to the core of the ligand binding domain¹⁵. The binding of steroid receptor co-activator-1 (SRC-1) to AF-2 is necessary to stabilize PXR and this can be interfered by PXR antagonists¹². In this AF-2 domain the amino acid Phe-429 is present and during up-regulation the interaction of SRC-1 with this amino acid stabilizes the active form of PXR³³. The docking revealed that ketoconazole, A-792611 and trabectedin interact with this particular amino acid. However, thymolphtalein did not interact with Phe-429, but showed inhibition of PXR-mediated CYP3A4 induction in the reporter gene assay and with qRT-PCR. Possibly, thymolphtalein inhibits PXR-mediated CYP3A4 induction by competition with PXR agonists such as rifampicin.

Table 3. Binding affinity of different compounds to hPXR.

Compounds	PXR binding affinity
Rifampicin	1.39 pM
Ketoconazole	2.60 nM
A-792611	26.5 pM
Trabectedin	0.242 nM
Sulforaphane	1.92 mM
Coumestrol	1.73 μM
Leflunomide	41.4 μM
Thymolphtalein	33.5 nM

Lanthascreen® TR-FRET Competitive Binding Assay

A Lanthascreen® TR-FRET competitive binding assay was performed in order to confirm the binding affinities of ketoconazole, A-792611, trabectedin, thymolphtalein and leflunomide *in vitro*. In addition, coumestrol and sulforaphane were evaluated to test whether these compounds also have no affinity for PXR *in vitro* (Figure 4).

At a concentration of 5 nM, trabectedin significantly reduced the TR-FRET ratio with 26%, which indicates that trabectedin has the highest binding affinity for PXR. Thymolphtalein, A-792611 and ketoconazole significantly reduced the TR-FRET ratio by 44%, 27% and 24%, in rank order of their affinity to PXR. Sulforaphane and leflunomide significantly decreased this ratio by 22% and 15%, respectively. Coumestrol did not affect the TR-FRET ratio. These results are generally in accordance to the results of the reporter gene assay, except for sulforaphane.

Unfortunately, the known PXR agonist rifampicin could not be measured in the TR-FRET assay because of quenching of the fluorescence. Lau *et al.* and Shukla *et al.* also mentioned this problem in their *in vitro* studies^{34,35}. Therefore the known PXR agonists SR-12813, clotrimazole and hyperforin were evaluated and significantly reduced the TR-FRET ratio by 33%, 56% and 47%, respectively.

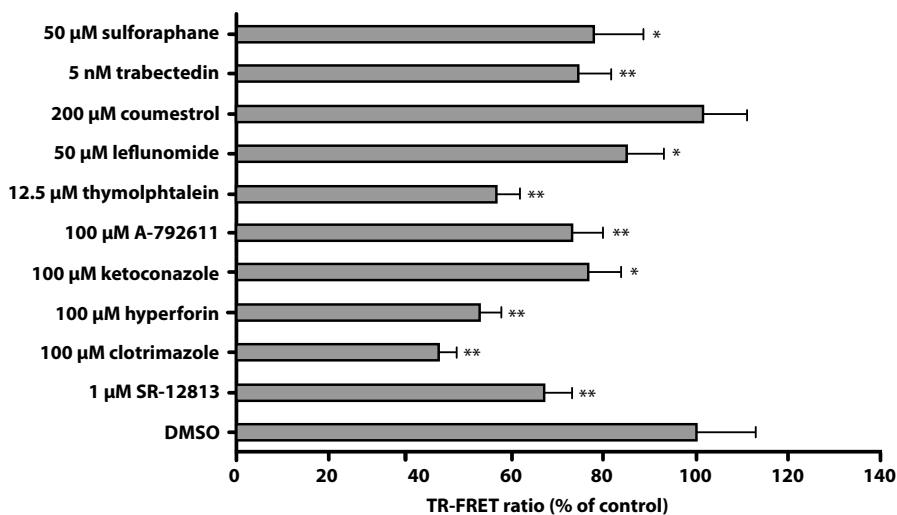


Figure 4. Competitive binding to PXR-LBD in a TR-FRET competitive binding assay. Human PXR-LBD (5 nM) was incubated for 1 hour with Fluormone PXR Green (40 nM) in the presence of DMSO (1% v/v), ketoconazole and A-792611 (100 µM), trabectedin (5 nM), sulforaphane and leflunomide (50 µM), coumestrol (200 µM), thymolphtalein (12.5 µM), rifampicin, clotrimazole and hyperforin (100 µM); and SR-12813 (1 µM). TR-FRET was measured after 1 hour with the PerkinElmer Envision® plate reader. By dividing the response at 520 nm by the response at 495 nm, the TR-FRET ratio was calculated. Data are means ± SD from a representative experiment performed in quadruplicate. In the figure the percentage of the mean values compared to 1% DMSO are shown (* $p < 0.05$, ** $p < 0.01$ and *** $p < 0.001$).

The results of all tested compounds are summarized in **Table 4** per assay for a clear overview.

Table 4. Overview of the results.

Compounds	Reporter gene assay	Quantitative RT-PCR	PXR docking	TR-FRET assay
Ketoconazole	--	-	--/++	--/++
A-792611	---	--	---/+++	--/++
Trabectedin	---	---	--/++	--/++
Sulforaphane	0	--	0	--/++
Coumestrol	0	--	0	0
Leflunomide	+++	++	0	--/++
Thymolphtalein	---	---	-/+	---/+++

Abbreviations: -, weak antagonist; --, moderate antagonist; ---, strong antagonist; 0, no effect; +, weak agonist; ++, moderate agonist; +++, strong agonist; --/++, moderate affinity; ---/+++ , strong affinity.

DISCUSSION AND CONCLUSION

The known PXR antagonists A-792611, trabectedin, ketoconazole, sulforaphane, leflunomide, thymolphtalein and coumestrol have been evaluated and compared in a PXR reporter gene assay to determine the rank order of their inhibitory potencies. Furthermore, qRT-PCR, computational docking in PXR and the Lanthascreen® TR-FRET competitive binding assay were applied to determine whether the reporter gene assay is suitable to screen for novel PXR antagonists.

A-792611, trabectedin and thymolphtalein were shown to strongly inhibit and ketoconazole to moderately inhibit PXR-mediated CYP3A4 induction in the reporter gene assay. According to the Lanthascreen® TR-FRET competitive binding assay and computational docking in PXR, these four compounds had a high affinity for PXR. Although it is difficult to distinguish PXR agonists and antagonists based on the computational molecular docking, it is suggested that PXR antagonists bind to the small binding site close to the outer surface of PXR at the AF-2 domain. A-792611, trabectedin and ketoconazole probably inhibited CYP3A4 induction by interfering with the binding of SRC-1 to the AF-2 domain for stabilization of PXR because the docking data revealed that these compounds interact with the amino acid Phe-429 in the AF-2 domain. However, thymolphtalein did not interact with this amino acid and is assumed to cause CYP3A4 induction by competition with other PXR ligands.

Leflunomide was shown to strongly enhance PXR-mediated CYP3A4 induction in the reporter gene assay and could be identified as PXR agonist. The results of quantitative real-time PXR and the Lanthascreen® TR-FRET competitive binding assay confirmed leflunomide as PXR agonist. However, the computational docking predicted a weak af-

finity of leflunomide for PXR. Maybe the local docking procedure did not detect a better binding site for leflunomide.

Both coumestrol and sulforaphane did not affect PXR-mediated CYP3A4 induction in the reporter gene assay. According to computational docking in PXR, coumestrol and sulforaphane had no affinity for PXR. Also in the Lanthascreen® TR-FRET competitive binding assay, coumestrol did not interact with PXR and sulforaphane weakly. However, in the non-transfected LS180 cells coumestrol and sulforaphane both inhibited CYP3A4 induction. Although CYP3A4 induction is mainly regulated by PXR, also other nuclear receptors regulate the induction of CYP3A4. The effect of sulforaphane and coumestrol could be mediated by constitutive androstane receptor (CAR) and vitamin D receptor (VDR), which are known to regulate CYP3A4 induction too^{6,36}.

Overall, in the present study trabectedin, thymolphtalein, A-792611 and ketoconazole were confirmed as PXR antagonists, in rank order of their inhibitory potencies. Based on the described IC₅₀ values from literature (**Table 1**) trabectedin would also be the strongest and ketoconazole the weakest PXR antagonist. However, A-792611 has been shown to be more potent than thymolphtalein in other *in vitro* studies (**Table 1**)^{13-15, 18}, while thymolphtalein was more potent than A-792611 in the present study. Furthermore, leflunomide was confirmed as PXR agonist in the present study, while leflunomide is a PXR antagonist according to Ekins *et al.*¹⁷. Both coumestrol and sulforaphane did not affect PXR in this study, but in literature coumestrol and sulforaphane are identified as PXR antagonists^{16,19}. These discrepancies underline the importance of testing compounds in one test system to accurately compare the inhibitory potencies of PXR antagonists. The differences in the inhibitory potencies could be explained by differences in affinity for PXR and cell-membrane penetration. For instance, A-792611 had the highest binding affinity towards PXR according to the computational docking, but this compound was not the strongest PXR antagonist in the *in vitro* assays. A possible explanation of these *in vitro* results could be the poor cell-membrane penetration of A-792611 due to a high log D value of 7.3 (at pH 7.4), derived from ChemIDplus Advanced (<http://chem.sis.nlm.nih.gov/chemidplus/>). On the other hand, while trabectedin had a lower binding affinity for PXR compared to A-792611, this compound was probably the strongest PXR antagonist in the *in vitro* assays due to a high cell-membrane penetration (log D value of 3.7 at pH 7.4).

Based on the results of the reporter gene assay alone, similar classifications of PXR antagonists, agonists and no ligands would be made as after confirmation with qRT-PCR, computational docking and the Lanthascreen® competitive binding assay. Therefore, the use of a reporter gene assay alone is suitable to screen for PXR antagonists.

In conclusion, trabectedin, thymolphtalein, A-792611 and ketoconazole were identified as PXR antagonists in rank order of their inhibitory potencies and leflunomide as PXR agonist. In contrast, coumestrol and sulforaphane were no ligands of PXR. Since coumestrol and sulforaphane inhibited CYP3A4 induction in non-transfected LS180 cells, both compounds are probably antagonists of the nuclear receptors CAR and/or VDR. The application of a reporter gene assay is a suitable and reliable assay to discover novel PXR antagonists, which is important to prevent decreased plasma levels of anticancer drugs in humans and to possibly increase the efficacy of oncolytic therapy.

REFERENCES

1. Breedveld P, Beijnen JH, Schellens JH. Use of P-glycoprotein and BCRP inhibitors to improve oral bioavailability and CNS penetration of anticancer drugs. *Trends Pharmacol Sci* 2006; 27(1): 17-24.
2. Harmsen S, Meijerman I, Beijnen JH, Schellens JH. Nuclear receptor mediated induction of cytochrome P450 3A4 by anticancer drugs: A key role for the pregnane X receptor. *Cancer Chemother Pharmacol* 2009; 64(1): 35-43.
3. Chen Y, Tang Y, Robbins GT, Nie D. Camptothecin attenuates cytochrome P450 3A4 induction by blocking the activation of human pregnane X receptor. *J Pharmacol Exp Ther* 2010; 334(3): 999-1008.
4. Dean M, Allikmets R. Complete characterization of the human ABC gene family. *J Bioenerg Biomembr* 2001; 33(6): 475-9.
5. Anzenbacher P, Anzenbacherova E. Cytochromes P450 and metabolism of xenobiotics. *Cell Mol Life Sci* 2001; 58(5-6): 737-47.
6. Harmsen S, Koster AS, Beijnen JH, Schellens JH, Meijerman I. Comparison of two immortalized human cell lines to study nuclear receptor-mediated CYP3A4 induction. *Drug Metab Dispos* 2008; 36(6): 1166-71.
7. Kerbusch T, Huitema AD, Ouwerkerk J, Keizer HJ, Mathot RA, Schellens JH, Beijnen JH. Evaluation of the autoinduction of ifosfamide metabolism by a population pharmacokinetic approach using NONMEM. *Br J Clin Pharmacol* 2000; 49(6): 555-61.
8. Tascilar M, de Jong FA, Verweij J, Mathijssen RH. Complementary and alternative medicine during cancer treatment: Beyond innocence. *Oncologist* 2006; 11(7): 732-41.
9. Sparreboom A, Cox MC, Acharya MR, Figg WD. Herbal remedies in the United States: Potential adverse interactions with anticancer agents. *J Clin Oncol* 2004; 22(12): 2489-503.
10. Pascussi JM, Gerbal-Chaloin S, Drocourt L, Maurel P, Vilarem MJ. The expression of CYP2B6, CYP2C9 and CYP3A4 genes: A tangle of networks of nuclear and steroid receptors. *Biochim Biophys Acta* 2003; 1619(3): 243-53.
11. Watkins RE, Davis-Searles PR, Lambert MH, Redinbo MR. Coactivator binding promotes the specific interaction between ligand and the pregnane X receptor. *J Mol Biol* 2003; 331(4): 815-28.
12. Ekins S, Chang C, Mani S, Krasowski MD, Reschly EJ, Iyer M, Kholodovych V, Ai N, Welsh WJ, Sinz M, et al. Human pregnane X receptor antagonists and agonists define molecular requirements for different binding sites. *Mol Pharmacol* 2007; 72(3): 592-603.
13. Synold TW, Dussault I, Forman BM. The orphan nuclear receptor SXR coordinately regulates drug metabolism and efflux. *Nat Med* 2001; 7(5): 584-90.
14. Huang H, Wang H, Sinz M, Zoeckler M, Staudinger J, Redinbo MR, Teotico DG, Locker J, Kalpana GV, Mani S. Inhibition of drug metabolism by blocking the activation of nuclear receptors by ketoconazole. *Oncogene* 2007; 26(2): 258-68.
15. Healan-Greenberg C, Waring JF, Kempf DJ, Blomme EA, Tirona RG, Kim RB. A human immunodeficiency virus protease inhibitor is a novel functional inhibitor of human pregnane X receptor. *Drug Metab Dispos* 2008; 36(3): 500-7.
16. Zhou C, Poulton EJ, Grun F, Bammler TK, Blumberg B, Thummel KE, Eaton DL. The dietary isothiocyanate sulforaphane is an antagonist of the human steroid and xenobiotic nuclear receptor. *Mol Pharmacol* 2007; 71(1): 220-9.
17. Ekins S, Kholodovych V, Ai N, Sinz M, Gal J, Gera L, Welsh WJ, Bachmann K, Mani S. Computational discovery of novel low micromolar human pregnane X receptor antagonists. *Mol Pharmacol* 2008; 74(3): 662-72.

18. Dring AM, Anderson LE, Qamar S, Stoner MA. Rational quantitative structure-activity relationship (RQSAR) screen for PXR and CAR isoform-specific nuclear receptor ligands. *Chem Biol Interact* 2010; 188(3): 512-25.
19. Wang H, Li H, Moore LB, Johnson MD, Maglich JM, Goodwin B, Ittoop OR, Wisely B, Creech K, Parks DJ, et al. The phytoestrogen coumestrol is a naturally occurring antagonist of the human pregnane X receptor. *Mol Endocrinol* 2008; 22(4): 838-57.
20. Goey AKL, Mooiman KD, Beijnen JH, Schellens JH, Meijerman I. Relevance of *in vitro* and clinical data for predicting CYP3A4-mediated herb-drug interactions in cancer patients. *Cancer Treatment Reviews* 2013; 39(7): 773-83.
21. Gupta A, Mugundu GM, Desai PB, Thummel KE, Unadkat JD. Intestinal human colon adenocarcinoma cell line LS180 is an excellent model to study pregnane X receptor, but not constitutive androstane receptor, mediated CYP3A4 and multidrug resistance transporter 1 induction: Studies with anti-human immunodeficiency virus protease inhibitors. *Drug Metab Dispos* 2008; 36(6): 1172-80.
22. Luo G, Cunningham M, Kim S, Burn T, Lin J, Sinz M, Hamilton G, Rizzo C, Jolley S, Gilbert D, et al. CYP3A4 induction by drugs: Correlation between a pregnane X receptor reporter gene assay and CYP3A4 expression in human hepatocytes. *Drug Metab Dispos* 2002; 30(7): 795-804.
23. Persson KP, Ekehed S, Otter C, Lutz ES, McPheat J, Masimirembwa CM, Andersson TB. Evaluation of human liver slices and reporter gene assays as systems for predicting the cytochrome p450 induction potential of drugs *in vivo* in humans. *Pharm Res* 2006; 23(1): 56-69.
24. Luo G, Cunningham M, Kim S, Burn T, Lin J, Sinz M, Hamilton G, Rizzo C, Jolley S, Gilbert D, et al. CYP3A4 induction by drugs: Correlation between a pregnane X receptor reporter gene assay and CYP3A4 expression in human hepatocytes. *Drug Metab Dispos* 2002; 30(7): 795-804.
25. Mooiman KD, Maas-Bakker RF, Moret EE, Beijnen JH, Schellens JH, Meijerman I. Milk thistle's active components silybin and isosilybin: Novel inhibitors of PXR-mediated CYP3A4 induction. *Drug Metab Dispos* 2013; 41(8): 1494-504.
26. Livak KJ, Schmittgen TD. Analysis of relative gene expression data using real-time quantitative PCR and the $2^{-\Delta\Delta C(T)}$ method. *Methods* 2001; 25(4): 402-8.
27. Morris GM, Goodsell DS, Halliday RS, Huey R, Hart WE, Belew RK, Olson AJ. Automated docking using a Lamarckian genetic algorithm and an empirical binding free energy function. *J Comput Chem*; 19: 1639-62.
28. Krieger E, Darden T, Nabuurs SB, Finkelstein A, Vriend G. Making optimal use of empirical energy functions: Force-field parameterization in crystal space. *Proteins* 2004; 57(4): 678-83.
29. Chrencik JE, Orans J, Moore LB, Xue Y, Peng L, Collins JL, Wisely GB, Lambert MH, Kliewer SA, Redinbo MR. Structural disorder in the complex of human pregnane X receptor and the macrolide antibiotic rifampicin. *Mol Endocrinol* 2005; 19(5): 1125-34.
30. DeGoey DA, Grampovnik DJ, Flentge CA, Flosi WJ, Chen HJ, Yeung CM, Randolph JT, Klein LL, Dekhtyar T, Colletti L, et al. 2-pyridyl P1'-substituted symmetry-based human immunodeficiency virus protease inhibitors (A-792611 and A-790742) with potential for convenient dosing and reduced side effects. *J Med Chem* 2009; 52(8): 2571-86.
31. Duan Y, Wu C, Chowdhury S, Lee MC, Xiong G, Zhang W, Yang R, Cieplak P, Luo R, Lee T, et al. A point-charge force field for molecular mechanics simulations of proteins based on condensed-phase quantum mechanical calculations. *J Comput Chem* 2003; 24(16): 1999-2012.

32. Biswas A, Mani S, Redinbo MR, Krasowski MD, Li H, Ekins S. Elucidating the 'jekyll and hyde' nature of PXR: The case for discovering antagonists or allosteric antagonists. *Pharm Res* 2009; 26(8): 1807-15.
33. Xue Y, Chao E, Zuercher WJ, Willson TM, Collins JL, Redinbo MR. Crystal structure of the PXR-T1317 complex provides a scaffold to examine the potential for receptor antagonism. *Bioorg Med Chem* 2007; 15(5): 2156-66.
34. Lau AJ, Yang G, Yap CW, Chang TK. Selective agonism of human pregnane X receptor by individual ginkgolides. *Drug Metab Dispos* 2012; 40(6): 1113-21.
35. Shukla SJ, Nguyen DT, Macarthur R, Simeonov A, Frazee WJ, Hallis TM, Marks BD, Singh U, Eliason HC, Printen J, et al. Identification of pregnane X receptor ligands using time-resolved fluorescence resonance energy transfer and quantitative high-throughput screening. *Assay Drug Dev Technol* 2009; 7(2): 143-69.
36. Chen T. Nuclear receptor drug discovery. *Curr Opin Chem Biol* 2008; 12(4): 418-26.



3.2

MILK THISTLE'S ACTIVE COMPONENTS SILYBIN AND ISO-SILYBIN: NOVEL INHIBITORS OF PXR-MEDIATED CYP3A4 INDUCTION

K.D. Mooiman
R.F. Maas-Bakker
E.E. Moret
J.H. Beijnen
J.H.M. Schellens
I. Meijerman

Published in Drug Metabolism and Disposition 2013; 41(8): 1494-1504

ABSTRACT

As cancer is often treated with combination therapy, unexpected pharmacological effects can occur because of drug-drug interactions. Several drugs are able to cause up-regulation or down-regulation of drug transporters or cytochrome P450 enzymes, particularly CYP3A4. Induction of CYP3A4 may result in decreased plasma levels and therapeutic efficacy of anticancer drugs. Since the pregnane X receptor (PXR) is one of the major transcriptional regulators of CYP3A4, PXR antagonists can possibly prevent CYP3A4 induction. Currently, a limited number of PXR antagonists is available. Some of these antagonists, such as sulphoraphane and coumestrol, belong to the so-called complementary and alternative medicines (CAM).

Therefore, the aim was to determine the potential of selected CAM (β -carotene, *Echinacea purpurea*, garlic, Ginkgo biloba, ginseng, grape seed, green tea, milk thistle, saw palmetto, St. John's wort, valerian, and vitamins B₆, B₁₂, and C) to inhibit PXR-mediated CYP3A4 induction at the transcriptional level, using a reporter gene assay and real-time polymerase chain reaction assay in LS180 colon adenocarcinoma cells. Furthermore, computational molecular docking and a LanthaScreen® time-resolved fluorescence resonance energy transfer (TR-FRET) PXR competitive binding assay were performed to explore whether the inhibiting CAM components interact with PXR.

The results demonstrated that milk thistle is a strong inhibitor of PXR-mediated CYP3A4 induction. The components of milk thistle responsible for this effect were identified as silybin and isosilybin. Furthermore, computational molecular docking revealed a strong interaction between both silybin and isosilybin and PXR, which was confirmed in the TR-FRET PXR assay. In conclusion, silybin and isosilybin might be suitable candidates to design potent PXR antagonists to prevent drug-drug interactions via CYP3A4 in cancer patients.

INTRODUCTION

Cancer patients are often treated with multiple anticancer drugs or hormonal agents in combination with supplemental therapies to treat or prevent side effects¹. However, this treatment is not always successful and often unwanted pharmacological effects occur in cancer patients, such as unresponsiveness or toxicity. A common cause for these unpredictable effects is up and down regulation of drug transporters or drug-metabolizing enzymes such as cytochrome P450 (CYP)^{1,2}. Of these enzymes, CYP3A4 is quantitatively the most important because it metabolizes more than 50% of all drugs and the majority of the currently prescribed anticancer drugs³.

CYP3A4 is highly inducible by rifampicin and multiple anticancer drugs, such as erlotinib, paclitaxel, docetaxel, ifosfamide, tamoxifen and flutamide¹. These drugs elevate the levels of CYP3A4 and promote their own metabolism by CYP3A4, a process called autoinduction⁴. Furthermore, concomitant use of these drugs can also result in an enhancement of each other's metabolism. As a result, plasma levels decrease, potentially leading to a reduced therapeutic effect. Consequently, the therapeutic outcome of anticancer therapy can become less predictable^{5,6}.

One of the major transcriptional regulators of CYP3A4 is the pregnane X receptor (PXR)^{7,8}. After activation of PXR by ligand binding, PXR forms a heterodimer with retinoid X receptor (RXR) in the nucleus. The heterodimer of PXR with RXR binds and activates response elements present in the regulatory region of target genes⁸. When the transcription of target gene CYP3A4 is activated, the level of CYP3A4 expression increases. Because PXR is the major transcriptional regulator of CYP3A4 induction, the hypothesis is that a PXR antagonist could inhibit CYP3A4 induction and increase the exposure of affected anticancer drugs.

The identification of potent PXR antagonists may therefore be important. However, it is difficult to predict interactions between PXR and potential antagonists, because of its flexible ligand binding pocket⁹. Consequently, there are a limited number of PXR antagonists available. Nevertheless, the list of PXR antagonists is continuously growing. However, the discovery of more potent and selective PXR antagonists is required¹⁰. Some of the existing PXR antagonists, like sulphoraphane and coumestrol¹¹, belong to the so-called complementary and alternative medicines (CAM). Therefore, other CAM may have the potential to inhibit PXR. In addition, it is interesting to screen CAM because these relatively safe supplements are frequently used in combination with chemotherapy by cancer patients⁶.

The aim of the present study is to identify CAM with inhibiting effects toward PXR-mediated CYP3A4 induction. To address this issue, the following CAM were tested *in vitro*: β -carotene, Echinacea (*Echinacea purpurea*), garlic (*Allium sativum*), green tea (*Camellia sinensis*), *Ginkgo biloba*, ginseng (*Eleutherococcus senticosus*), grape seed (*Vitis*

vinifera), milk thistle (*Silybum marianum*), saw palmetto (*Serenoa serrulata*), St. John's wort (*Hypericum perforatum*), valerian (*Valeriana officinalis*) and vitamins B₆, B₁₂ and C. These CAM were selected based on the frequency of use by cancer patients and the potential to interact with anticancer drugs^{5, 6, 12-14}.

MATERIALS AND METHODS

Reagents and chemicals

All cell culture media and supplements were purchased from PAA Laboratories (Pasching, Austria). Standardized extracts of milk thistle, Ginkgo biloba, Echinacea, ginseng, St. John's wort, saw palmetto, grape seed, green tea, valerian and vitamin C were obtained from Chromadex (Irvine, CA). Standardized extracts of β -carotene, garlic, and vitamins B₆ and B₁₂ were purchased from ABCR GmbH & Co KG (Karlsruhe, Germany), Organic Herb Inc. (Changsha City, China), UPS (Rockville, MD) and Sigma-Aldrich (Zwijndrecht, The Netherlands), respectively. **Table 1** provides details of all standardized extracts.

Table 1. Details of the standardized CAM extracts.

CAM	Product Information	Contents	
β -carotene	ABCR GmbH&Co KG [Lot # 1030612]	97% β -carotene	
Echinacea <i>Echinacea purpurea</i>	Chromadex [Lot # 00030217-012]	0.94% caftaric acid 0.03% chlorogenic acid 0.04% cynarin	0.05% echinacoside 1.80% cichoric acid
Garlic <i>Allium sativum</i>	Organic Herb Inc. [100-20100122]	Garlic extract (100:1) Alliin scordinin alliin	
<i>Ginkgo biloba</i>	Chromadex [Lot # 00030299-1917]	4.78% quercetin 3.73% kaempferol 2.13% isorhamnetin 12.0% quercetin glycoside 9.65% kaempferol glycoside 5.19% isorhamnetin glycoside	1.61% bilobalide 1.41% ginkgolide A 0.31% ginkgolide J 5.57% ginkgolide B 0.38% ginkgolide C
Ginseng <i>Eleutherococcus senticosus</i>	Chromadex [Lot # 00030302-019]	0.439% eleutheroside E 0.245% eleutheroside B	
Grape seed <i>Vitis vinifera</i>	Chromadex [Lot # 00036130-11]	5.08% epigallocatechin 0.93% catechin 6.30% epicatechin	0.02% epigallocatechin gallate 0.03% epicatechin gallate
Green tea <i>Camellia sinensis</i>	Chromadex [Lot # 00030331-029]	2.09% epigallocatechin 0.61% catechin 0.94% epicatechin 0.08% theobromine 0.11% theophylline	5.70% epigallocatechin gallate 1.48% epicatechin gallate 11.65% caffeine 0.12% theaflavins
Milk Thistle <i>Silybum marianum</i>	Chromadex [Lot # 00030402-101]	29.6% silybin A+B 2.97% taxifolin	14.7% silychristin

Table 1. Details of the standardized CAM extracts. (continued)

CAM	Product Information	Contents	
Saw Palmetto <i>Serenoa serrulata</i>	Chromadex [Lot # 00030726-841]	0.13% campesterol	8.55% methyl palmitate
		0.07% stigmasterol	1.81% methyl stearate
		0.43% β -sistosterol	30.40% methyl oleate
		0.21% methyl caproate	5.28% methyl linolenate
		0.93% methyl octanoate	0.75% methyl linoleate
		2.53% methyl decanoate	0.17% methyl arachidate
		28.61% methyl dodecanoate 10.63% methyl myristate	0.02% methyl EPA 0.11% methyl DHA
St. John's wort <i>Hypericum perforatum</i>	Chromadex [Lot # 00030798-155]	1.87% rutin	0.01% hyperforin
		0.24% pseudohypericin	0.06% hypericin
Valerian <i>Valeriana officinalis</i>	Chromadex [Lot # 34899-045]	0.16% valerenic acids	
Vitamin B ₆	Sigma-Aldrich [Lot # 120M13271V]	> 98% pyridoxine	
Vitamin B ₁₂	Sigma-Aldrich [Lot # 030M1567]	> 98% vitamin B ₁₂	
Vitamin C	Chromadex [Lot # 111021-641]	Vitamin C	
β -carotene	ABCR GmbH&Co KG [Lot # 1030612]	97% β -carotene	

Abbreviations: DHA, docosahexaenoic acid; EPA, eicosapentaenoic acid.

Siliphos® and Vitotaal® (commercial milk thistle products) were purchased from Thorne Research Inc. (Dover, ID) and Santesa B.V. (Weesp, The Netherlands), respectively. Milk thistle's flavonolignan silybin A+B and flavonoid taxifolin were obtained from Sigma-Aldrich (Zwijndrecht, The Netherlands) and isosilybin A+B, silydianin and silychristin from PhytoLab (Vestenbergsgreuth, Germany). Details about these flavonolignans and flavonoid are shown in **Table 2**. Dimethylsulfoxide (DMSO) was purchased from Acros Organics (Fair Lawn, NJ), rifampicin, hyperforin (dicyclohexylammonium) salt, SR-12813 [tetraethyl 2-(3,5-di-*tert*-butyl-4-hydroxyphenyl)ethenyl-1,1-bisphosphonate], ketoconazole and paclitaxel from Sigma-Aldrich (Zwijndrecht, The Netherlands) and erlotinib from Sequoia Research Products Ltd (Pangbourne, UK). (S)-1-[(1S,3S,4S)-4-[(S)-2-(3-benzyl-2-oxo-imidazolidin-1-yl)-3,3-dimethyl-butylamino]-3-hydroxy-5-phenyl-1-(4-pyridin-2-yl-benzyl)-pentylcarbamoyl]-2,2-dimethyl-propyl-carbamic acid methyl ester (A-792611) was a kind gift from Abbott Laboratories (North Chicago, IL) and clotrimazole was purchased from LTK Laboratories Inc. (St. Paul, MN). Corning (Amsterdam, The Netherlands) kindly provided the 384-well Corning® plates. The following reagents were purchased from Invitrogen (Blijswijk, The Netherlands) for the Lanthascreen® time-resolved fluorescence resonance energy transfer (TR-FRET) PXR competitive binding assay: TR-FRET PXR assay buffer, Fluormone PXR green, dithiothreitol, terbium-labeled anti-glutathione S-transferase antibody, and hPXR-LBD (ligand-binding domain).

Table 2. Details of milk thistle's flavonolignans and flavonoids.

CAM components	Product Information	Purity
Silybin A+B	Sigma-Aldrich CAS nr. [22888-70-6]	99.3%
Isosilybin A+B	PhytoLab CAS nr. [72581-71-6]	98.7% (A:B = 1.98:1)
Silychristin	PhytoLab CAS nr. [33889-69-9]	99.8%
Silydianin	PhytoLab CAS nr. [29782-68-1]	99.9%
Taxifolin	Sigma-Aldrich CAS nr. [480-18-2]	87.9%

Cell Culture

The human colon adenocarcinoma-derived cell line LS180 was purchased from the American Type Culture Collection (Manassas, VA). This cell line was maintained in Roswell Park Memorial Institute (RPMI) 1640 medium with 25 mM HEPES and L-glutamine, supplemented with 10% (v/v) heat-inactivated fetal bovine serum, 100 U/mL penicillin, and 100 µg/mL streptomycin (RPMI 1640 complete medium) at 37°C under a humidified atmosphere of 5% CO₂.

Plasmids

The pCDG-hPXR expression vector was generously provided by Dr. Ron Evans (Salk Institute, La Jolla, CA), the pGL3-CYP3A4-XREM (proximal, -362/+53; distal, -7836/-7208) luciferase reporter construct was provided by Dr. Richard Kim (University of Western Ontario, London, ON, Canada) and the pRL-TK control plasmid was obtained from Promega (Madison, WI). Plasmids were checked by enzyme restriction and agarose gel electrophoresis, and purified using Promega's Pureyield Midi-prep according to the instructions of the manufacturer.

CYP3A4 Reporter Gene Assay

LS180 cells were plated at a density of 5.0×10^4 cells/well in 96-well plates (Greiner Bio-One B.V., Alphen aan den Rijn, The Netherlands) in 200 µL RPMI 1640 complete medium and incubated overnight in a 5% CO₂-humidified atmosphere at 37°C. After 24 hours of incubation, the cells were transfected with 62.5 ng/well nuclear receptor expression vector (pCDG-hPXR), 175 ng/well CYP3A4 luciferase reporter construct (pGL3-CYP3A4-XREM), and 12.5 ng/well *renilla* luciferase expression control plasmid (pRL-TK), using 0.8 µL/well nanofectin transfection reagent from PAA Laboratories in 150 mM NaCl. After 24 hours, the medium was removed and the cells were washed with phosphate-buffered saline (PBS) (37°C). Subsequently, 200 µL/well of fresh medium was added containing 0.3% DMSO or CYP3A4 inducers (10 µM rifampicin, 20 µM erlotinib, or 20 µM paclitaxel¹⁾ with or without addition of known PXR antagonists (10 µM ketoconazole and 10 µM A-792611¹⁵⁾ or 100 µg/mL standardized CAM extracts (β-carotene, Echinacea, garlic, green tea extract, Ginkgo biloba, ginseng, grape seed extract, milk thistle, saw palmetto,

St. John's wort, valerian, or vitamins B₆, B₁₂, and C) for the CAM screen. According to a cell viability assay, these concentrations were not cytotoxic (unpublished data).

For further investigation of milk thistle, standardized milk thistle extract and extracts of the commercial products Siliphos[®] and Vitotal[®] were tested at the concentrations of 50, 75, and 100 µg/mL (see the subsequent section on the preparation of milk thistle extract). Furthermore, milk thistle's flavonolignans silybin (mixture of diastereomers A+B 1:1), isosilybin (mixture of diastereomers A+B 1:1), silychristin, silydianin and flavonoid taxifolin, were evaluated at concentrations of 89, 133, and 200 µM (43, 64, and 96 µg/mL for all components, except for taxifolin, which were 27, 41, and 61 µg/mL). To determine the potency of silybin and isosilybin to inhibit CYP3A4 induction, IC₅₀ curves were prepared at a concentration range from 2 to 250 µM and 2 to 200 µM, respectively. The concentrations of the standardized milk thistle extract, both extracts of commercial products and milk thistle's components, were not cytotoxic according to the performed cell viability assay (unpublished data).

All compounds were dissolved in DMSO and the final solvent concentration did not exceed 0.3%. After 24 hours of exposure, the medium was removed. Subsequently, the cells were washed with PBS and lysed with 25 µL/well Passive Lysis Buffer (Promega) for 15 minutes on a vortex. The cell lysates (10 µL) were transferred to a white half-area 96-well plate (Corning B.V., Schiphol-Rijk, The Netherlands). The reporter activities of *firefly* luciferase and *renilla* luciferase were measured with the Dual-Luciferase[®] Reporter Assay System (Promega) according to the manufacturer's manual, with reagent volumes adjusted to the cell lysate volume. Luminescence was recorded on a Mithras LB 940 microplate reader (Berthold Technologies, Bad Wildbad, Germany). The *firefly* luciferase signals were normalized to the *renilla* luciferase signal. To calculate fold inductions, the ratios of all incubations were compared to normalized signals of the negative control DMSO.

Preparation of Milk Thistle Extracts

The content of the Siliphos[®] and Vitotal[®] capsules was suspended in ethanol (10 mL ethanol per gram capsule content) and refluxed for 1 hour. Subsequently, the residues were centrifuged for 10 minutes at 650 g. After filtration, the fraction containing milk thistle was evaporated and freeze-dried. The yields are calculated by comparing the mass of the extract with the mass of the capsule content (**Table 3**). The extracts of Siliphos[®] and Vitotal[®] were stored at -20°C.

Quantitative Real-Time Polymerase Chain Reaction

LS180 cells were plated at a density of 2.5 x 10⁵ cells/well in 12-well plates (Greiner Bio-One B.V.) in 1 mL of RPMI 1640 complete medium and were incubated for 48 hours in a 5% CO₂-humidified atmosphere at 37°C. After 48 hours, this medium was removed and

fresh medium was added containing 0.3% DMSO or 10 μM rifampicin¹ with or without known PXR antagonists (10 μM ketoconazole and 10 μM A-792611) or 50, 75, and 100 $\mu\text{g}/\text{mL}$ of the standardized milk thistle extract. The quantitative real-time polymerase chain reaction (qRT-PCR) experiment was also performed with 100 μM of milk thistle's components silybin A+B, isosilybin A+B, taxifolin, silychristin and silydianin.

After 24 hours, the cells were washed and total RNA was isolated using the SV Total RNA Isolation System (Promega). The RNA quantity and integrity was determined with a Nanodrop Diode Array Spectrophotometer (Nanodrop 1000; Isogen Life Science, IJsselstein, The Netherlands). To synthesize cDNA, 1 μg RNA was reversed transcribed by using the RevertAid™ First Strand cDNA Synthesis Kit (Fermentas, St Leon-Rot, Germany), using random priming. Assay-on-Demand PCR primers and Taqman probe (Applied Biosystems, Foster City, CA) were used for 18S (Hs99999901_s1) and human CYP3A4 (Hs00604506_m1) RT-PCR. The reactions were singleplexed with 18S. The CYP3A4 and housekeeping gene 18S mRNA expression levels were analyzed using an ABI prism 7000 sequence detection system (Applied Biosystems). The relative quantification defines the changes in CYP3A4 gene expression between the different incubations. First, the cycle threshold (ct) value and the Δ ct values (difference in ct values compared with the control such as DMSO) were determined. Subsequently, the $2^{-(\text{difference in } \Delta \text{ct})}$ method was used to determine the relative changes in CYP3A4 gene expression¹⁶.

Computational Molecular Docking

Dockings were performed with Autodock 4.2 (Scripps Research Institute, La Jolla, CA)¹⁷, as part of Yasara 12.4.1 software¹⁸. The structure of the ligand-binding domain of hPXR of Watkins *et al.* was used (Protein Data Bank ID 1M13⁹). Docking of hyperforin was started from its X-ray position in 1M13. Subsequently, docking of rifampicin was started after superimposing the hPXR-rifampicin complex 1SKX¹⁹ onto 1M13. The PXR antagonist A-792611 was built from the similar HIV-protease inhibitor in Protein Data Bank ID 3GGV²⁰, guided by the structure drawing from Healan-Greenberg *et al.*¹⁵. The other compounds (ketoconazole, paclitaxel, erlotinib, and milk thistle's components) were obtained as Sybyl Mol2 files from ChemIDplus Advanced (<http://chem.sis.nlm.nih.gov/chemidplus/>; National Institutes of Health, Bethesda, MD). The milk thistle's components silybin A+B, isosilybin A+B, silychristin and silydianin were modified to follow the stereochemistry as given by Lee *et al.*²¹, and roughly placed in the hPXR pocket.

Yasara was used for cleaning the molecules with regard to atom types and bond types. After initial minimization and stimulated annealing with the Amber03 forcefield²² of the ligand and the sidechains of the hPXR residues within 7Å, 250 rigid docking runs were performed, with `ga_pop_size` set at 15,000.

Table 3. Yield of the commercial milk thistle products.

Product	Product Information	Ingredients	Yield
Siliphos®	Thorne Research Inc., Dover, USA [Lot # 1337C049]	<i>Silybum marianum</i> extract and phosphatidylcholine complex	45.5%
Vitotaal®	Santesa B.V., Weesp, the Netherlands [Lot # 300269]	80% <i>Silybum marianum</i>	12.2%

LanthaScreen® TR-FRET PXR Competitive Binding Assay

A LanthaScreen® TR-FRET PXR competitive binding assay was conducted according to the manufacturer's (Invitrogen) protocol. In brief, the assay was performed in black noncoated, low-volume and round-bottomed 384-well Corning® plates. The compounds were diluted in TR-FRET PXR assay buffer and 10 µL/well of these dilutions were dispensed in quadruplicate with the following end concentrations: 100 µg/mL milk thistle and 100 µM silybin A+B, isosilybin A+B, silydianin, silychristin and taxifolin. In addition, 100 µM of the positive controls ketoconazole and A-792611 were tested, accompanied by known PXR agonists 100 µM rifampicin, 100 µM clotrimazole, 100 µM hyperforin, and 1 µM SR-12813. Second, 5 µL/well of Fluormone PXR green at a final concentration of 40 nM was added. At last, 5 µL/well of the following mix was added: dithiothreitol, terbium-labeled anti-glutathione *S*-transferase antibody, and hPXR-LBD at final concentrations of 50 µM, 10 nM and 5 nM, respectively. The plate was incubated for 1 hour at room temperature, protected from light. The PerkinElmer Envision® plate reader was used to measure TR-FRET (PerkinElmer, Waltham, MA). **Table 4** gives an overview of the applied settings. For the TR-FRET ratios, the emission signal at 520 nm was divided by the emission signal at 495 nm.

Table 4. Setting of the PerkinElmer Envision® plate reader.

Settings	Value
Excitation wavelength	340 nm
Fluorescein emission wavelength	520 nm
Terbium emission wavelength	495 nm
Delay time	120 µs
Integration time	600 µs

Statistical Analysis

Data were analyzed by using two-sample *t*-test and were considered statistically significant when $P < 0.05$. All statistical determinations were performed with SPSS software (version 16.0; SPSS Inc., Chicago, IL).

RESULTS

CAM screen

The potential inhibition of PXR-mediated CYP3A4 induction by 14 of the most commonly used CAM (β -carotene, Echinacea, garlic, green tea, Ginkgo biloba, ginseng, grape seed, milk thistle, saw palmetto, St. John's wort, valerian, vitamin B₆, B₁₂ and C)^{5, 6, 12-14} was determined in LS180 cells, transfected with plasmids expressing hPXR, CYP3A4, and *renilla*. As shown in **Figure 1**, 100 μ g/mL milk thistle extract is the strongest inhibitor of PXR-mediated CYP3A4 induction by rifampicin, because this CAM significantly inhibited CYP3A4 induction by 83%. Furthermore, extracts of Echinacea and vitamin B₁₂ moderately inhibited this induction by 24 and 18%, respectively. Compared to the 32 and 49% inhibition of CYP3A4 induction by the well-known PXR antagonists ketoconazole and A-792611, the degree of inhibition of CYP3A4 induction is high by milk thistle and is moderate by Echinacea and vitamin B₁₂.

Standardized milk thistle extract

Since 100 μ g/mL standardized milk thistle extract was shown to be a strong inhibitor of PXR-mediated CYP3A4 induction, milk thistle was further investigated by incubating transfected LS180 cells with three concentrations of milk thistle: 50, 75, and 100 μ g/mL. In addition, besides the model inducer rifampicin also the anticancer drugs erlotinib and paclitaxel were used as inducers to determine whether milk thistle can also inhibit CYP3A4 induction caused by anticancer drugs.

CYP3A4 Reporter Gene Assay

A solution of 75 and 100 μ g/mL standardized milk thistle extract significantly inhibited rifampicin-mediated CYP3A4 induction by 38 and 74%, respectively (**Figure 2A**). At a concentration of 75 and 100 μ g/mL, the standardized milk thistle extract also significantly inhibited erlotinib-mediated CYP3A4 induction by 66 and 79%, respectively, and paclitaxel-mediated CYP3A4 induction by 62 and 83% (**Figure 2B and C**). Compared to ketoconazole and A-792611, milk thistle is a strong inhibitor of CYP3A4 induction caused by rifampicin and both anticancer drugs.

CYP3A4 qRT-PCR assay

The potential of milk thistle to inhibit PXR-mediated CYP3A4 induction was also investigated in nontransfected LS180 cells at mRNA expression level, using qRT-PCR analysis.

A solution of 100 μ g/mL standardized milk thistle extract significantly inhibited rifampicin-mediated CYP3A4 induction by 80% (**Figure 3**). These results are in accordance with the inhibition of PXR-mediated CYP3A4 induction by the standardized milk thistle extract, determined using the CYP3A4 reporter gene assay (**Figure 2**).

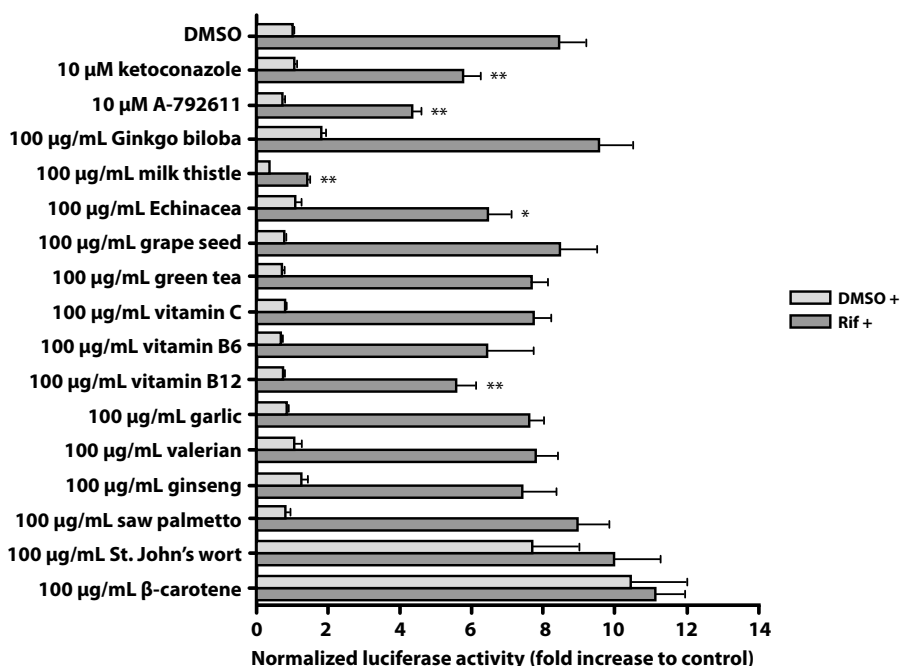


Figure 1. CAM screen for possible inhibition of PXR-mediated CYP3A4 induction by rifampicin using reporter gene. LS180 cells were transfected with the pCDG-hPXR expression vector, pGL3-CYP3A4-XREM reporter construct, and pRL-TK control plasmid. After 24 hours of transfection, the LS180 cells were incubated with 0.3% DMSO or the CYP3A4 model inducer rifampicin (10 µM) in combination with the negative control DMSO, CAM, or the positive controls ketoconazole and A-792611. The luciferase activities were measured after 24 hours of incubation. Data are means \pm SD from a representative experiment performed in triplicate. The fold inductions compared with 0.3% DMSO are shown (comparison with the fold induction by rifampicin: * $p < 0.05$; ** $p < 0.01$). DMSO +, results after incubation without rifampicin; Rif +, results after incubation with rifampicin in combination with DMSO, CAM, or positive controls.

Commercial milk thistle products: Vitotal® and Siliphos®

The standardized milk thistle extract was shown to be a strong inhibitor of rifampicin-, erlotinib-, and paclitaxel-mediated CYP3A4 induction. However, cancer patients do not use this formulation but a variety of commercial milk thistle products. Regarding the differences in the composition between standardized extracts and extracts of commercial milk thistle products, it is important to determine the effect of commercial milk thistle on CYP3A4 induction.

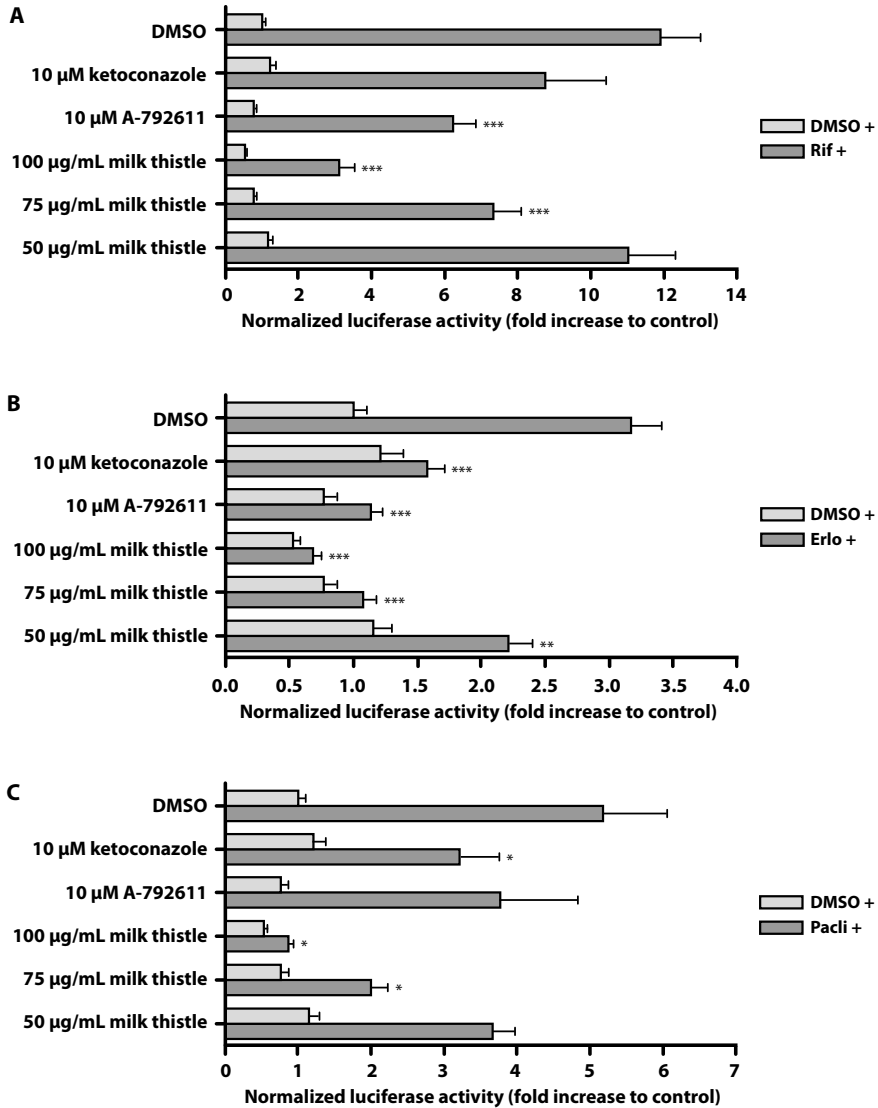


Figure 2. Inhibition of PXR-mediated CYP3A4 induction by the standardized milk thistle extract using reporter gene. Transfected LS180 cells were incubated with 0.3% DMSO or the CYP3A4 inducers rifampicin (10 µM), erlotinib (20 µM), or paclitaxel (20 µM) in combination with the negative control DMSO, the standardized milk thistle extract, or the positive controls ketoconazole and A-792611. The luciferase activities were measured after 24 hours of incubation. Data are means \pm SD from a representative experiment performed in triplicate. The fold inductions compared with 0.3% DMSO are shown (comparison with the fold induction by the inducer: * $p < 0.05$; ** $p < 0.01$; *** $p < 0.001$). CYP3A4 induction by rifampicin (A), erlotinib (B), and paclitaxel (C). DMSO +, results after incubation without CYP3A4 inducer, Rif +, Erlo + or Pacli +, results after incubation with rifampicin, erlotinib or paclitaxel in combination with DMSO, milk thistle or positive controls.

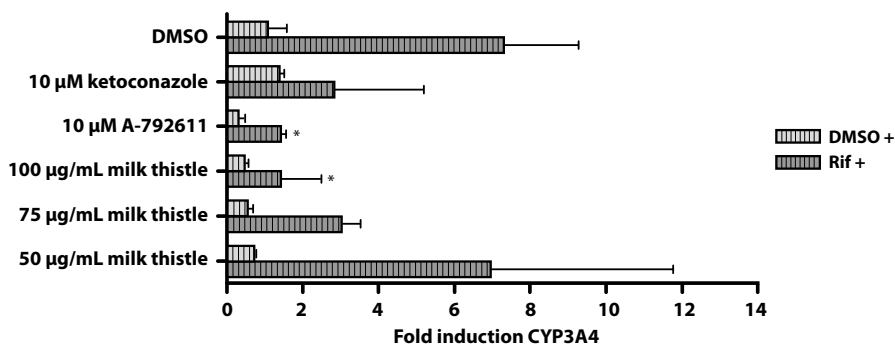


Figure 3. Inhibition of PXR-mediated CYP3A4 induction by the standardized milk thistle extract using qRT-PCR. LS180 cells were incubated with 0.3% DMSO or the CYP3A4 model inducer rifampicin (10 µM) in combination with the negative control DMSO, the standardized milk thistle extract, or the positive controls ketoconazole and A-792611. The mRNA expression levels were measured after 24 hours of incubation using singleplexed qRT-PCR. Data are means \pm SD from a representative experiment performed in triplicate, with exception of the incubation with ketoconazole combined with rifampicin. The fold inductions compared to 0.3% DMSO are shown (comparison with the fold induction by rifampicin: * $p < 0.05$). DMSO +, results after incubation without rifampicin; Rif +, results after incubation with rifampicin in combination with DMSO, milk thistle, or positive controls.

CYP3A4 Reporter Gene Assay

The commercial product Vitotal® also significantly inhibited rifampicin-mediated CYP3A4 induction by 22 and 50% at concentrations of 75 and 100 µg/mL, respectively (**Figure 4A**). These concentrations of Vitotal® also resulted in a significant inhibition of 43 and 59% of CYP3A4 induction by erlotinib (**Figure 4B**). Furthermore, Vitotal® significantly inhibited paclitaxel-mediated CYP3A4 induction by 50 and 75% at concentrations of 75 and 100 µg/mL, respectively (**Figure 4C**).

A solution of 100 µg/mL Siliphos® significantly inhibited rifampicin-, erlotinib- and paclitaxel-mediated CYP3A4 induction by 29%, 50% and 50%, respectively (**Figure 5**). In addition, Siliphos® significantly inhibited erlotinib-mediated CYP3A4 induction by 34% at a concentration of 75 µg/mL.

CYP3A4 RT-qPCR assay

The potential of both commercial milk thistle products to inhibit PXR-mediated CYP3A4 induction was also confirmed in nontransfected LS180 cells, using qRT-PCR analysis.

Both Vitotal® and Siliphos® significantly inhibited rifampicin-mediated CYP3A4 induction by 69 and 61% at a concentration of 100 µg/mL respectively, in accordance with the results of the reporter gene assay (**Figure 6**).

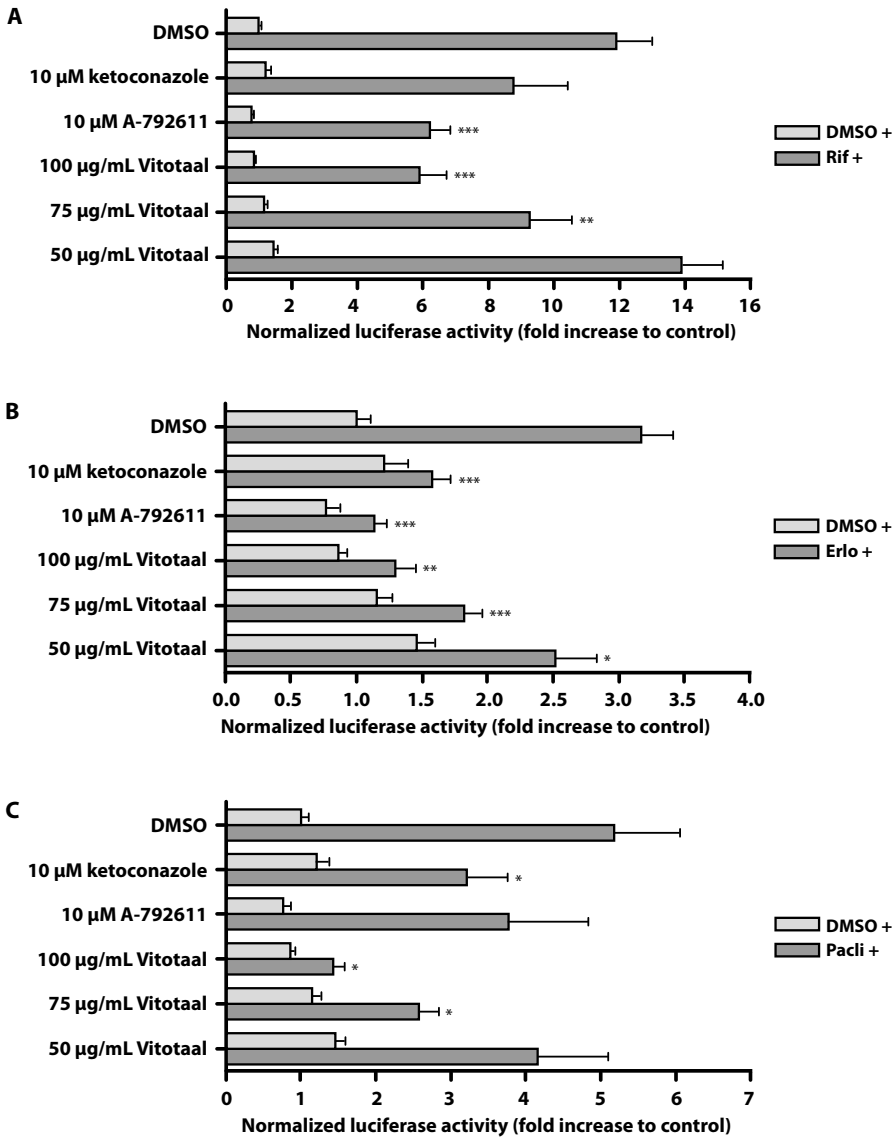


Figure 4. Inhibition of PXR-mediated CYP3A4 induction by Vitotal® using reporter gene. Transfected LS180 cells were incubated with 0.3% DMSO or the CYP3A4 inducers rifampicin (10 μ M), erlotinib (20 μ M), or paclitaxel (20 μ M) in combination with the negative control DMSO, Vitotal®, or the positive controls ketoconazole and A-792611. The luciferase activities were measured after 24 hours of incubation. Data are means \pm SD from a representative experiment performed in triplicate. The fold inductions compared with 0.3% DMSO are shown (comparison with the fold induction by the inducer: * $p < 0.05$, ** $p < 0.01$; *** $p < 0.001$). CYP3A4 induction by rifampicin (A), erlotinib (B), and paclitaxel (C). DMSO +, results after incubation without CYP3A4 inducer; Rif +, Erl + or Pacli +, results after incubation with rifampicin, erlotinib or paclitaxel in combination with DMSO, Vitotal® or positive controls.

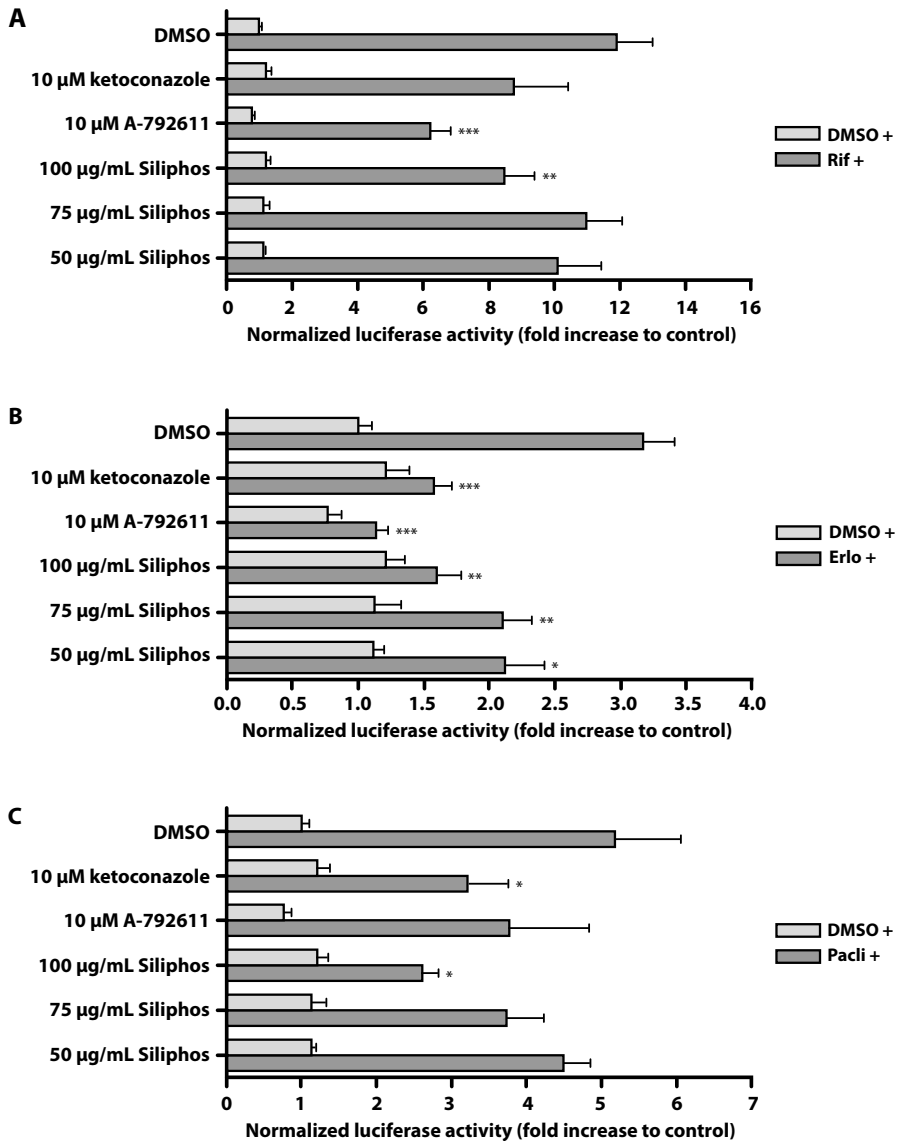


Figure 5. Inhibition of PXR-mediated CYP3A4 induction by Siliphos® using reporter gene.

Transfected LS180 cells were incubated with 0.3% DMSO or the CYP3A4 inducers rifampicin (10 µM), erlotinib (20 µM), or paclitaxel (20 µM) in combination with the negative control DMSO, Siliphos® or the positive controls ketoconazole and A-792611. The luciferase activities were measured after 24 hours of incubation. Data are means ± SD from a representative experiment performed in triplicate. The fold inductions compared with 0.3% DMSO are shown (comparison with the fold induction by the inducer: * $p < 0.05$; ** $p < 0.01$; *** $p < 0.001$). CYP3A4 induction by rifampicin (A), erlotinib (B) and paclitaxel (C). DMSO +, results after incubation without CYP3A4 inducer, Rif +, Erlo + or Pacli +, results after incubation with rifampicin, erlotinib or paclitaxel in combination with DMSO, Siliphos® or positive controls.

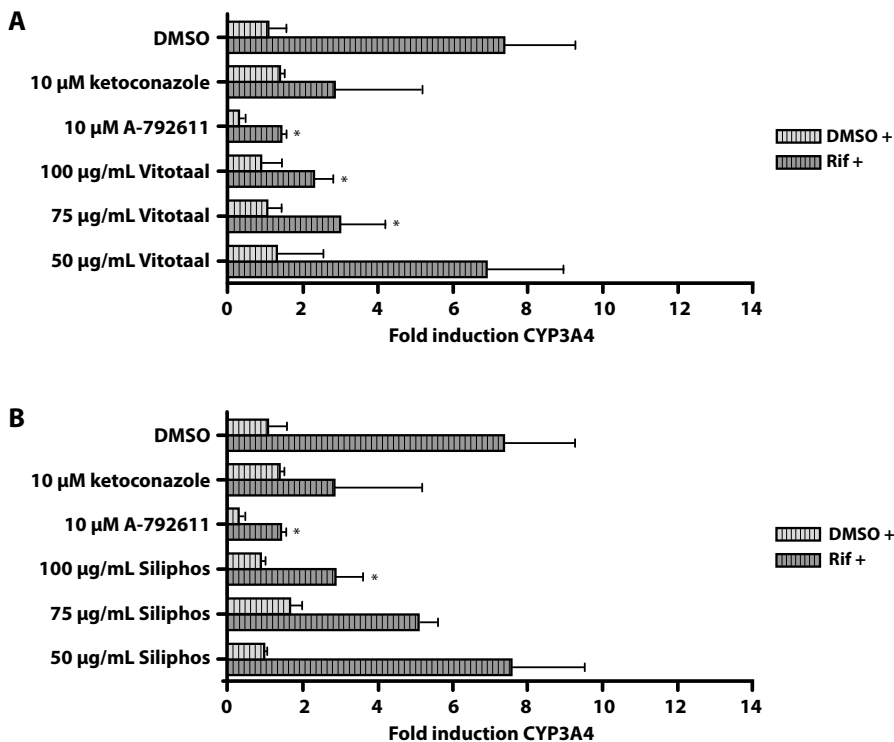


Figure 6. Inhibition of PXR-mediated CYP3A4 induction by Vitotaal® and Siliphos® using qRT-PCR. LS180 cells were incubated with 0.3% DMSO or the CYP3A4 model inducer rifampicin (10 µM) in combination with the negative control DMSO, Vitotaal®, Siliphos®, or the positive controls ketoconazole and A-792611. The mRNA expression levels were measured after 24 hours of incubation using singleplexed qRT-PCR. Data are means \pm SD from a representative experiment performed in triplicate, with exception of the incubation with ketoconazole combined with rifampicin. The fold inductions compared with 0.3% DMSO are shown (comparison with the fold induction by rifampicin: * $p < 0.05$). Inhibition of CYP3A4 induction by Vitotaal® (A) and Siliphos® (B). DMSO +, results after incubation without rifampicin; Rif +, results after incubation with rifampicin in combination with DMSO, Vitotaal®, Siliphos®, or positive controls.

Milk thistle's components

Overall, the inhibition of PXR-mediated CYP3A4 induction by the standardized milk thistle extract, Vitotaal® and Siliphos® is confirmed in two assays: reporter gene and qRT-PCR. However, milk thistle is a mixture of multiple components, including silybin (mixture of diastereomers A+B 1:1), isosilybin (mixture of diastereomers A+B 1:1), taxifolin, silychristin and silydianin. To identify a potent inhibitor of PXR-mediated CYP3A4 induction, it is important to identify which component is responsible for the observed effect. Therefore, all milk thistle's components were investigated in both the reporter gene and qRT-PCR assays.

CYP3A4 Reporter Gene Assay

The results of the reporter gene assay showed that milk thistle's components silybin and isosilybin are responsible for the inhibition of PXR-mediated CYP3A4 induction by milk thistle. Silybin significantly inhibited rifampicin-mediated CYP3A4 induction by 58 and 81% at concentrations of 133 and 200 μM , respectively (**Figure 7A**). Compared to silybin, its isomer isosilybin is a stronger inhibitor of PXR-mediated CYP3A4 induction. A solution of 89, 133 and 200 μM isosilybin significantly inhibited CYP3A4 induction by 64, 82 and 88%, respectively (**Figure 7B**).

Compared to the potent inhibition of rifampicin-mediated CYP3A4 by silybin and isosilybin, the inhibition by 200 μM of taxifolin and silychristin was moderate (**Figure 7C and D**). Silydianin showed no inhibition of rifampicin-mediated CYP3A4 induction (**Figure 7E**).

In addition, IC_{50} curves of silybin and isosilybin reveal the potency of these components to inhibit CYP3A4 induction (**Figure 8**). The IC_{50} value of silybin is 135 μM and isosilybin has an IC_{50} value of 74 μM , which confirms that isosilybin is more potent.

CYP3A4 qRT-PCR assay

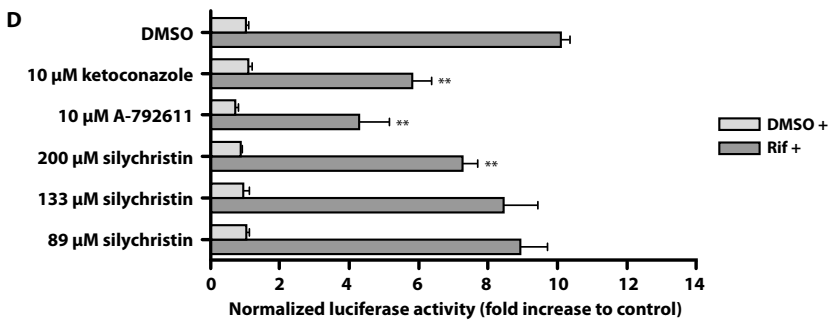
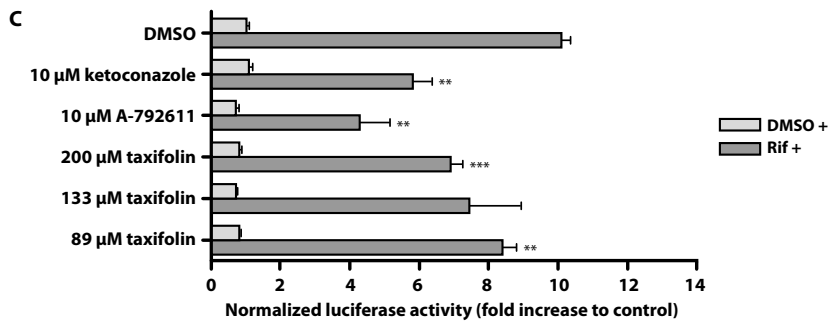
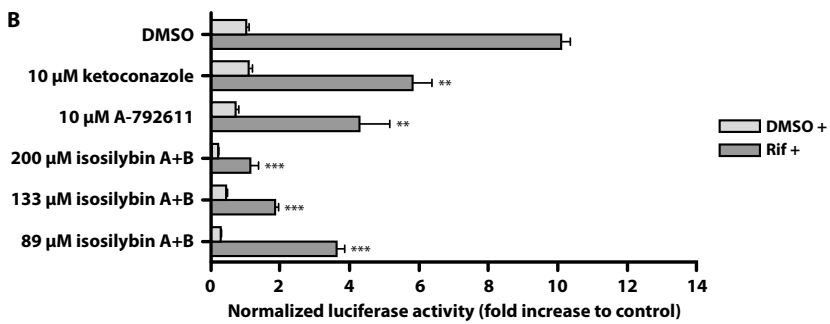
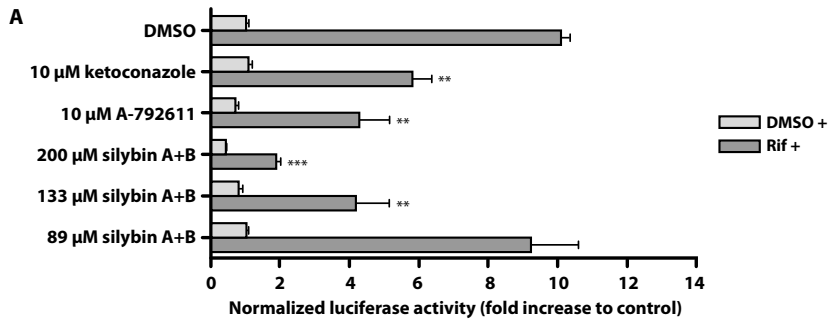
The potential of silybin and isosilybin to inhibit PXR-mediated CYP3A4 induction is also confirmed in nontransfected LS180 cells using qRT-PCR analysis. Silybin and isosilybin significantly inhibited PXR-mediated CYP3A4 induction with 43 and 55% at a concentration of 100 μM , respectively. The other components did not inhibit PXR-mediated CYP3A4 induction (**Figure 9**).

Together, the results confirm that silybin and isosilybin are responsible for the inhibition of PXR-mediated CYP3A4 induction. Besides the use of a reporter gene assay, which is generally accepted to screen for PXR antagonists, the capability of silybin and isosilybin to bind in the PXR pocket was further investigated via computational molecular docking and a TR-FRET PXR competitive binding assay.

Computational molecular docking

For the computational molecular docking, the following compounds were tested: known PXR agonists, known PXR antagonists, and the milk thistle's components. Although PXR is promiscuous, it is able to bind with high to very high affinity to chemically diverse ligands²³.

PXR agonists rifampicin, paclitaxel and erlotinib showed a different degree of binding affinity toward the PXR pocket. Rifampicin had the highest binding affinity (1.39 μM), followed by paclitaxel (20.7 μM) and erlotinib (3.97 μM) (**Table 5**). These results are in accordance with the degree of PXR-mediated CYP3A4 induction from the reporter gene assay. Rifampicin-mediated CYP3A4 induction ranged from 9- to 12-fold, paclitaxel-mediated induction was approximately 5-fold, and erlotinib-mediated induction was approximately 3-fold. For the



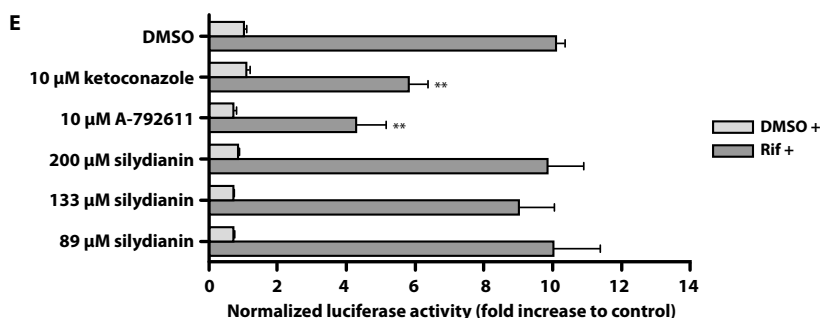


Figure 7. Inhibition of PXR-mediated CYP3A4 induction by milk thistle's components using reporter gene. Transfected LS180 cells were incubated with 0.3% DMSO or the CYP3A4 model inducer rifampicin (10 μM) in combination with the negative control DMSO, milk thistle's components, or the positive controls ketoconazole and A-792611. The luciferase activities were measured after 24 hours of incubation. Data are means ± SD from a representative experiment performed in triplicate. The fold inductions compared with 0.3% DMSO are shown (comparison with the fold induction by rifampicin: ** $p < 0.01$; *** $p < 0.001$). (A) silybin (A+B), (B) isosilybin (A+B), (C) taxifolin, (D) silychristin and (E) silydianin. DMSO +, results after incubation without CYP3A4 inducer, Rif + = results after incubation with rifampicin in combination with DMSO, milk thistle's components, or positive controls.

moderately binding agent erlotinib, more extensive docking (Lamarckian genetic algorithm) was used to check for missed poses. This did not lead to a higher affinity.

Hyperforin (the active component of St. John's wort) is a well-known CAM component that activates PXR, with a predicted binding affinity of 1.03 nM. The reporter gene assay demonstrated the activation of PXR by St. John's wort with an 8-fold CYP3A4 induction (Figure 1).

Known PXR antagonists ketoconazole and A-792611 also differed in their degree of binding affinity toward PXR. Ketoconazole had a lower binding affinity (2.6 nM) than A-792611 (26.45 pM), which is in accordance with the results of the reporter gene assay and qRT-PCR analysis.

The computational molecular docking of milk thistle's components showed that silybin and isosilybin have the highest binding affinity, followed by silydianin, silychristin, and taxifolin, which is partially in accordance with the results of the reporter gene assay. In the reporter gene assay silybin and isosilybin were the strongest antagonists and the other components did not convincingly inhibit CYP3A4 induction. For taxifolin, extensive docking did not improve its moderate PXR affinity.

Based on the computational molecular docking, it is difficult to distinguish PXR agonists and antagonists. However, the pharmacophore of novel PXR antagonists (e.g. A-792611)¹⁵ suggested that PXR antagonists bind the small binding site close to the outer surface of PXR at the AF-2 (activation function 2) domain, whereas PXR agonists bind in the core of the ligand binding domain. Binding of steroid receptor co-activator-1

Table 5. Binding affinity of different compounds to hPXR and the involvement of amino acid residues.

Compounds	PXR binding affinity	Hydrophobic residues	Polar residues	Charged residues
Hyperforin	1.03 nM	Leu209A, Met243A, Phe288A	Ser247A, Gln285A	His407A
Rifampicin	1.39 μ M	Leu209A, Val211A, Trp299A	Ser247A, Gln285A, Cys284A	His407A
Paclitaxel	20.7 μ M	Leu209A, Phe288A, Trp299A, Glu321A, Met323A, His407A, Leu411A	Gln285A	Arg410A
Erlotinib	3.97 μ M	Leu209A, Met323A,	Ser247A, His407A	
Ketoconazole	2.6 nM	Ser247A, Phe281A, Gln285A, Trp299A, Met323A, His407A, Leu411A, Phe429A^a	Gln285A	
A-792611	26.45 μ M	Leu209A, Val211A, Met243A, Phe281A, Trp299A, Tyr306A, Leu308A, Glu321A, His407A, Thr408A, Leu411A, Phe429A^a	Gln285A	
Silybin A	0.42 nM	Phe251A, Phe281A, Phe288A, Trp299A, Phe429A^a		Lys277A, His407A
Silybin B	1.81 nM	Phe281A, His407A, Leu411A, Phe429A^a		Lys277A, His407A
Isosilybin A	1.83 nM	Phe281A, Trp299A, His407A, Phe429A^a	Trp299A, Gln285A, His327A, Thr408A	
Isosilybin B	0.22 nM	Trp299A, Phe281A, Phe429A^a	Ser247A, Gln285A, Thr408A	
Taxifolin	4.59 μ M	Phe281A, Leu411A	Leu240A, Thr408A	
Silychristin	8.68 nM	Met243A, Phe281A, Phe429A^a	Ser247A, Thr408A	
Silydianin	0.65 nM	Met323A	Ser247A, Gln285A, His407A	Arg410A

^a The amino acid Phe429A is located in the AF-2 domain of PXR and it is likely that PXR antagonists bind the small binding site near the outer surface of PXR at the AF-2 domain.

(SRC-1) to AF-2 is necessary to stabilize PXR and this can be interfered with PXR antagonists¹⁰. The amino acid Phe429A is located in the AF-2 domain of PXR and it is likely that interaction of SRC-1 with this amino acid stabilizes the active form of PXR during upregulation²⁴.

According to **Table 5** and **Figure 10**, the known PXR antagonists ketoconazole and A-792611 interact with this particular amino acid. Interestingly, silybin and isosilybin also interact with Phe429A. Based on the similar binding of both milk thistle's components and the known PXR antagonists, it is plausible that silybin and isosilybin are potent PXR antagonists. This was already demonstrated in the reporter gene and qRT-PCR assays, in which CYP3A4 induction was strongly inhibited by silybin and isosilybin. Both silydianin and taxifolin did not interact with Phe429A and together with the results of the reporter gene assay, these components are probably no PXR antagonists. However, silychristin

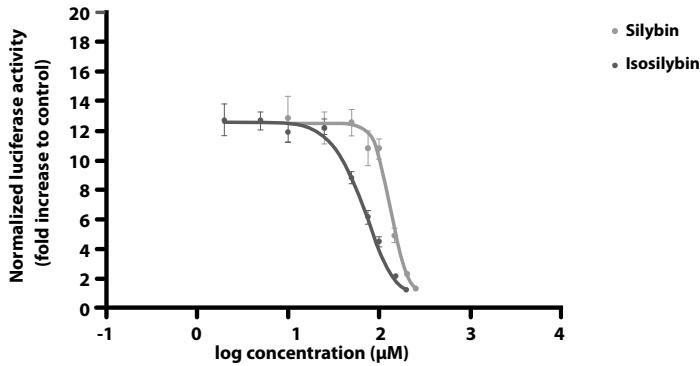


Figure 8. IC₅₀ curves of silybin and isosilybin using reporter gene. Transfected LS180 cells were incubated with CYP3A4 model inducer rifampicin (10 µM) in combination with 2-250 µM silybin and 2-200 µM isosilybin. The luciferase activities were measured after 24 hours of incubation. Data are means ± SD from a representative experiment performed in triplicate. The fold inductions compared with 0.3% DMSO are shown.

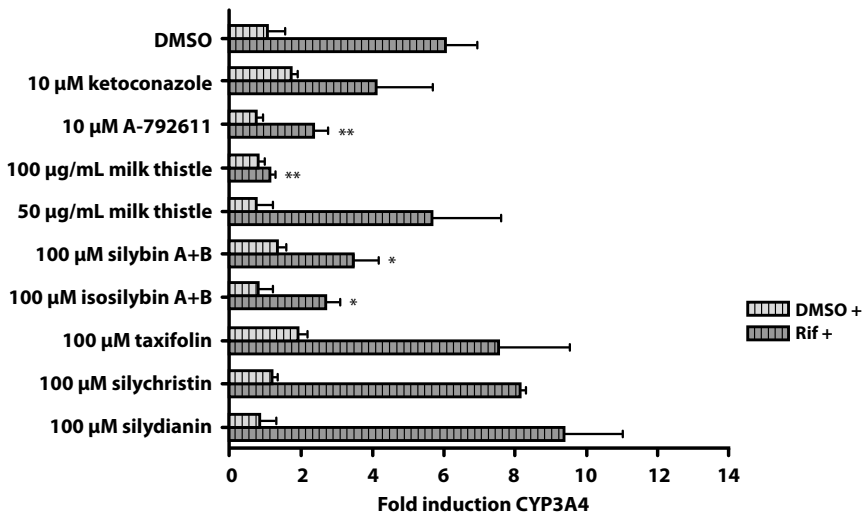


Figure 9. Inhibition of PXR-mediated CYP3A4 induction by milk thistle's components using qRT-PCR. LS180 cells were incubated with 0.3% DMSO or the CYP3A4 model inducer rifampicin (10 µM) in combination with the negative control DMSO, the standardized milk thistle extract, silybin A+B, isosilybin A+B, taxifolin, silychristin, silydianin, or the positive controls ketoconazole and A-792611. The mRNA expression levels were measured after 24 hours of incubation using singleplexed qRT-PCR. Data are means ± SD from a representative experiment performed in triplicate. The fold inductions compared with 0.3% DMSO are shown (comparison with the fold induction by rifampicin: * $p < 0.05$; ** $p < 0.01$). DMSO +, results after incubation without rifampicin; Rif +, results after incubation with rifampicin in combination with DMSO, milk thistle, milk thistle's components, or positive controls.

showed an interaction with Phe429A, but this component has a lower binding affinity toward PXR. Together with the reporter gene results, silychristin is probably a weak PXR antagonist.

Overall, although the binding affinities predicted by docking have a standard deviation of around 1.5 log units, it is possible to conclude that at least six compounds from milk thistle have affinities for hPXR comparable to ketoconazole. Of all milk thistle's components, silybin and isosilybin are probably the most potent PXR antagonists by interfering with the AF-2 domain.

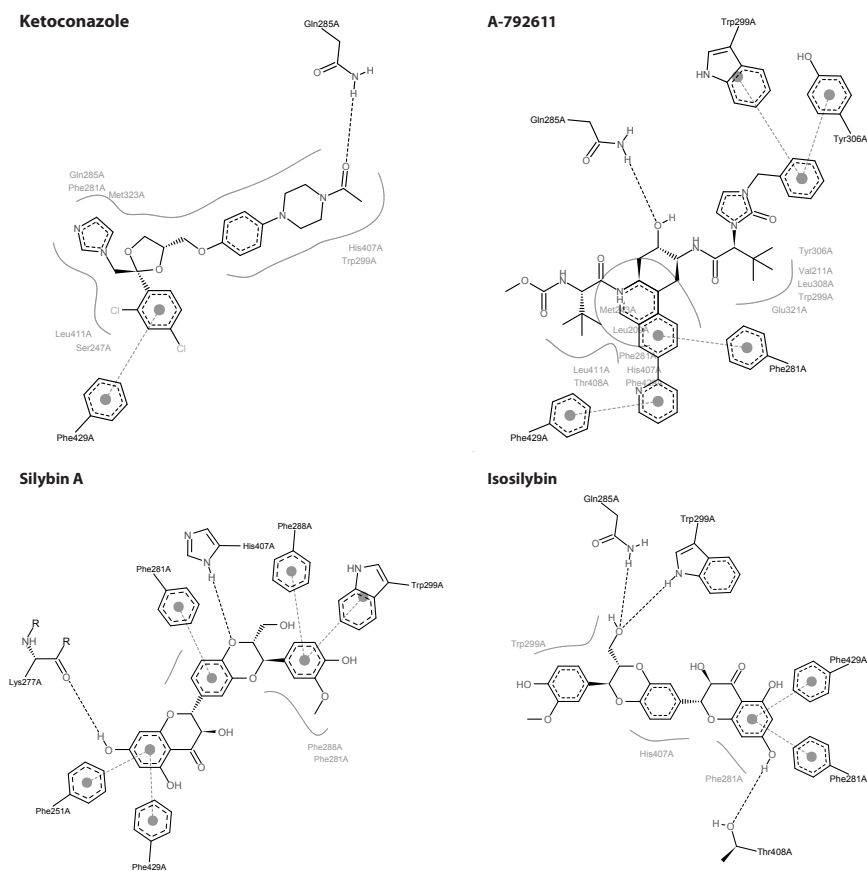


Figure 10. Computational molecular docking of known PXR antagonists (ketoconazole and A-792611) and silybin A and isosilybin to the ligand-binding domain of PXR. The key amino acids that are involved in the hydrophobic and polar interactions with ketoconazole, A-792611, silybin, and isosilybin are shown. The figures are generated with <http://poseview.zbh.uni-hamburg.de/>.

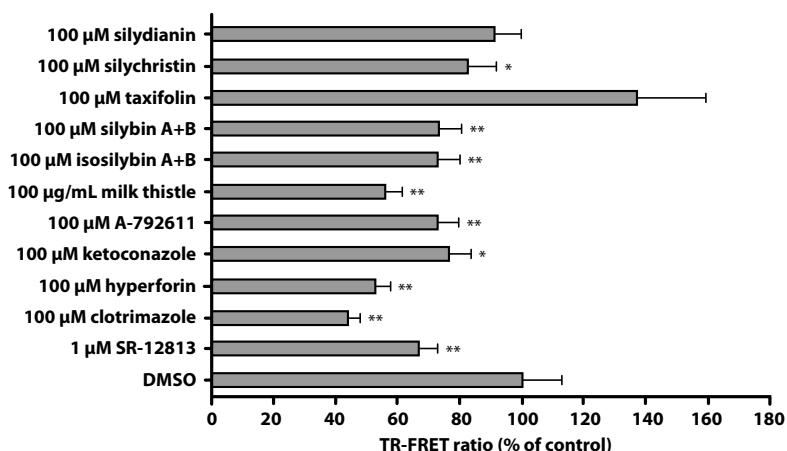


Figure 11. Competitive binding to PXR-LBD in a TR-FRET PXR competitive binding assay. Human PXR-LBD (5 nM) was incubated for 1 hour with Fluormone PXR Green (40 nM) in the presence of DMSO (1% v/v), SR-12813 (1 µM), clotrimazole (100 µM), hyperforin (100 µM), ketoconazole (100 µM), A-792611 (100 µM), milk thistle (100 µg/mL), isosilybin A+B (100 µM), silybin A+B (100 µM), taxifolin (100 µM), silychristin (100 µM), and silydianin (100 µM). After 1 hour, TR-FRET was measuring using the PerkinElmer Envision® plate reader. The TR-FRET ratio was calculated by dividing the response at 520 nm by the response at 495 nm. Data are means \pm SD from a representative experiment performed in quadruplicate. The percentages of the mean values compared with 1% DMSO are shown (* $p < 0.05$; ** $p < 0.01$).

Lanthascreen® TR-FRET PXR competitive binding assay

To confirm binding affinities of silybin and isosilybin toward PXR, the direct interaction with PXR was determined with a TR-FRET PXR competitive binding assay. The results of the TR-FRET PXR competitive binding assay are shown in **Figure 11**. The TR-FRET emission ratio was reduced for 44% by 100 µg/mL milk thistle, compared to 24 and 27% by the positive controls 100 µM ketoconazole and A-792611, respectively. Of all milk thistle's components, both silybin and isosilybin significantly decreased the TR-FRET ratio with 27%. Silychristin and silydianin moderately affected the ratio with 17 and 9%. Taxifolin did not decrease the TR-FRET ratio.

In comparison, the known PXR agonists SR-12813, clotrimazole, and hyperforin decreased the TR-FRET emission ratio by 33, 56 and 47%, respectively. It is important to note that the TR-FRET assay was not applicable for rifampicin, because this compound quenched the fluorescence (unpublished data). This problem was also previously described by Lau *et al.* and Shukla *et al.*^{25,26}.

DISCUSSION AND CONCLUSION

Fourteen of the most commonly used CAM^{5,6,12-14} were screened for their ability to inhibit PXR-mediated CYP3A4 induction by rifampicin, erlotinib and paclitaxel in LS180 cells.

LS180 cells were used in the present study because it was previously demonstrated that these cells are a more suitable cell line to study the induction of CYP3A4 compared to the more frequently used cell line HepG2⁷. Of all tested CAM, Echinacea and vitamin B₁₂ were shown to moderately inhibit PXR-mediated CYP3A4 induction by rifampicin. Milk thistle was shown to strongly inhibit CYP3A4 induction in the reporter gene assay. In addition to the standardized milk thistle extract, the extracts of the commercial products Vitotal® and Siliphos® were investigated. Both the standardized milk thistle extract and the two extracts of the commercial products significantly inhibited PXR-mediated CYP3A4 induction by rifampicin, erlotinib and paclitaxel at the transcriptional level. However, compared with the standardized milk thistle extract, the extracts of Vitotal® and Siliphos® inhibited PXR-mediated CYP3A4 induction to a lesser extent. A plausible explanation for the difference in the degree of inhibition is the unknown compositions and the variability in the content of milk thistle's components: seven primary flavonolignans (silybin A, silybin B, isosilybin A, isosilybin B, silychristin, isosilychristin, silydianin) and a flavonoid taxifolin²⁷. Furthermore, the same weight of the standardized milk thistle extract and the extracts of Vitotal® and Siliphos® do not contain the same number of milk thistle's components because the reprocessing methods differ.

Furthermore, all milk thistle products showed a limited inhibition of CYP3A4 transcription in LS180 cells without the concomitant addition of an inducer. A plausible explanation is the presence of basal activity of PXR in LS180 cells, which can also be inhibited by milk thistle.

Since milk thistle is a mixture of multiple components, it is necessary to identify the component(s) responsible for the inhibition of CYP3A4 induction in the search for new PXR antagonists. Therefore, all components of milk thistle were investigated in the reporter gene assay. Results showed that silybin and isosilybin strongly inhibited rifampicin-mediated CYP3A4 induction.

The inhibition of PXR-mediated CYP3A4 induction by the standardized milk thistle extract, extracts of commercial milk thistle products, and their components was not only determined using a CYP3A4 reporter gene assay, but was also determined in a nontransfected cell system using qRT-PCR. In accordance with the results obtained with the reporter gene assay, the milk thistle extract, both commercial extracts, silybin and isosilybin significantly inhibited the induction of CYP3A4 mRNA expression by rifampicin as well.

The presented results demonstrate that milk thistle is able to prevent CYP3A4 induction and that silybin and isosilybin are responsible for this effect. It is plausible that

the inhibition of CYP3A4 induction occurs via the PXR pathway, because PXR is highly expressed in the transfected LS180 cells during the reporter gene assay and because this assay is generally accepted to screen for PXR agonists²⁸. However, it is not completely certain that milk thistle-mediated inhibition of CYP3A4 induction is only PXR-mediated. When the cells are exposed to milk thistle, CYP3A4 induction could also be inhibited via other pathways. Therefore, additional computational molecular docking of milk thistle's components and a TR-FRET PXR competitive binding assay were performed to confirm that the inhibition of CYP3A4 induction by milk thistle could be PXR-mediated. The results showed that silybin and isosilybin have a high binding affinity toward PXR and both directly interact with PXR. More importantly, in the computational molecular docking, both components showed to interact with the amino acid Phe429A in the AF-2 site similar to the known PXR antagonists ketoconazole and A-792611. Therefore, it is plausible that silybin and isosilybin are PXR antagonists, which is in accordance with the results from the reporter gene assay and qRT-PCR. Silybin and isosilybin can probably also inhibit the PXR-mediated induction of other CYP enzymes and drug transporters (e.g. P-glycoprotein). Further investigation is needed to confirm this.

Based on the structure of the active components silybin and isosilybin, a potent PXR-inhibiting agent can be designed in order to prevent induction of CYP3A4 in cancer patients. Designing a potent (iso)silybin-derived PXR-antagonist may be important because of the low bioavailability of milk thistle. In a clinical study with six cancer patients, a 14-day supplementation of 200 mg milk thistle extract resulted in low plasma levels of silybin ranging between 0.0249 and 0.257 μM ²⁹. The use of a hydrophobic silybin-phosphatidylcholine complex (silipide), however, resulted in higher plasma levels of silybin in healthy volunteers: 0.29 – 0.53 μM ³⁰. When a potent PXR-inhibiting agent is designed with a higher bioavailability, it can possibly reach plasma levels of the determined IC_{50} values of 74 and 135 μM to prevent CYP3A4 induction by anticancer drugs in patients. In cases in which this (iso)silybin-derived agent inhibits CYP3A4 induction in patients, decreased plasma levels of anticancer drugs can be prevented. However, this should be evaluated in the clinic.

In conclusion, milk thistle's components silybin and isosilybin prevent PXR-mediated CYP3A4 induction at the transcriptional level, as demonstrated by reporter gene and qRT-PCR assays. Both silybin and isosilybin have a high binding affinity toward PXR according to computational molecular docking and a TR-FRET PXR competitive binding assay. Thus, silybin and isosilybin might be suitable candidates to design potent PXR antagonists to prevent drug-drug interactions via CYP3A4 in cancer patients or patients that use other drugs metabolized by CYP3A4.

REFERENCES

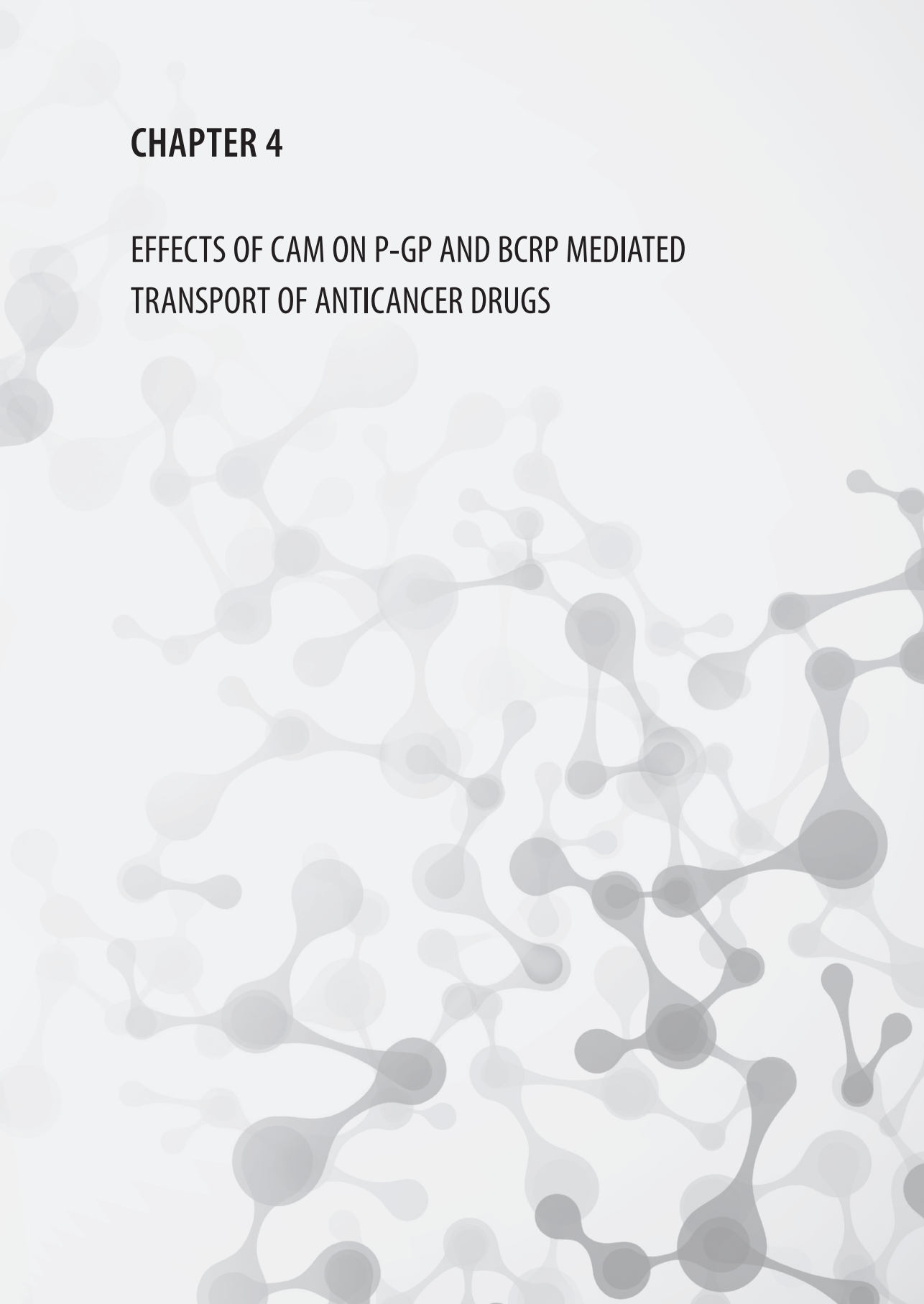
1. Harmsen S, Meijerman I, Beijnen JH, Schellens JH. Nuclear receptor mediated induction of cytochrome P450 3A4 by anticancer drugs: A key role for the pregnane X receptor. *Cancer Chemother Pharmacol* 2009; 64(1): 35-43.
2. Chen Y, Tang Y, Robbins GT, Nie D. Camptothecin attenuates cytochrome P450 3A4 induction by blocking the activation of human pregnane X receptor. *J Pharmacol Exp Ther* 2010; 334(3): 999-1008.
3. Anzenbacher P, Anzenbacherova E. Cytochromes P450 and metabolism of xenobiotics. *Cell Mol Life Sci* 2001; 58(5-6): 737-47.
4. Kerbusch T, Huitema AD, Ouwerkerk J, Keizer HJ, Mathot RA, Schellens JH, Beijnen JH. Evaluation of the autoinduction of ifosfamide metabolism by a population pharmacokinetic approach using NONMEM. *Br J Clin Pharmacol* 2000; 49(6): 555-61.
5. Tascilar M, de Jong FA, Verweij J, Mathijssen RH. Complementary and alternative medicine during cancer treatment: Beyond innocence. *Oncologist* 2006; 11(7): 732-41.
6. Sparreboom A, Cox MC, Acharya MR, Figg WD. Herbal remedies in the United States: Potential adverse interactions with anticancer agents. *J Clin Oncol* 2004; 22(12): 2489-503.
7. Harmsen S, Koster AS, Beijnen JH, Schellens JH, Meijerman I. Comparison of two immortalized human cell lines to study nuclear receptor-mediated CYP3A4 induction. *Drug Metab Dispos* 2008; 36(6): 1166-71.
8. Pascussi JM, Gerbal-Chaloin S, Drocourt L, Maurel P, Vilarem MJ. The expression of CYP2B6, CYP2C9 and CYP3A4 genes: A tangle of networks of nuclear and steroid receptors. *Biochim Biophys Acta* 2003; 1619(3): 243-53.
9. Watkins RE, Davis-Searles PR, Lambert MH, Redinbo MR. Coactivator binding promotes the specific interaction between ligand and the pregnane X receptor. *J Mol Biol* 2003; 331(4): 815-28.
10. Ekins S, Chang C, Mani S, Krasowski MD, Reschly EJ, Iyer M, Kholodovych V, Ai N, Welsh WJ, Sinz M, et al. Human pregnane X receptor antagonists and agonists define molecular requirements for different binding sites. *Mol Pharmacol* 2007; 72(3): 592-603.
11. Biswas A, Mani S, Redinbo MR, Krasowski MD, Li H, Ekins S. Elucidating the 'jekyll and hyde' nature of PXR: The case for discovering antagonists or allosteric antagonists. *Pharm Res* 2009; 26(8): 1807-15.
12. McCune JS, Hatfield AJ, Blackburn AA, Leith PO, Livingston RB, Ellis GK. Potential of chemotherapy-herb interactions in adult cancer patients. *Support Care Cancer* 2004; 12(6): 454-62.
13. Gupta D, Lis CG, Birdsall TC, Grutsch JF. The use of dietary supplements in a community hospital comprehensive cancer center: Implications for conventional cancer care. *Support Care Cancer* 2005; 13(11): 912-9.
14. Werneke U, Earl J, Seydel C, Horn O, Crichton P, Fannon D. Potential health risks of complementary alternative medicines in cancer patients. *Br J Cancer* 2004; 90(2): 408-13.
15. Healan-Greenberg C, Waring JF, Kempf DJ, Blomme EA, Tirona RG, Kim RB. A human immunodeficiency virus protease inhibitor is a novel functional inhibitor of human pregnane X receptor. *Drug Metab Dispos* 2008; 36(3): 500-7.
16. Livak KJ, Schmittgen TD. Analysis of relative gene expression data using real-time quantitative PCR and the $2^{-\Delta\Delta C(T)}$ method. *Methods* 2001; 25(4): 402-8.
17. Morris GM, Goodsell DS, Halliday RS, Huey R, Hart WE, Belew RK, Olson AJ. Automated docking using a Lamarckian genetic algorithm and empirical binding free energy function. *J Comput Chem* 1998; 19: 1639-62.

18. Krieger E, Darden T, Nabuurs SB, Finkelstein A, Vriend G. Making optimal use of empirical energy functions: Force-field parameterization in crystal space. *Proteins* 2004; 57(4): 678-83.
19. Chrencik JE, Orans J, Moore LB, Xue Y, Peng L, Collins JL, Wisely GB, Lambert MH, Kliewer SA, Redinbo MR. Structural disorder in the complex of human pregnane X receptor and the macrolide antibiotic rifampicin. *Mol Endocrinol* 2005; 19(5): 1125-34.
20. Degoey DA, Grampovnik DJ, Flentge CA, Flosi WJ, Chen HJ, Yeung CM, Randolph JT, Klein LL, Dekhtyar T, Colletti L, et al. 2-pyridyl P1'-substituted symmetry-based human immunodeficiency virus protease inhibitors (A-792611 and A-790742) with potential for convenient dosing and reduced side effects. *J Med Chem* 2009; 52(8): 2571-86.
21. Lee JI, Narayan M, Barrett JS. Analysis and comparison of active constituents in commercial standardized silymarin extracts by liquid chromatography-electrospray ionization mass spectrometry. *J Chromatogr B Analyt Technol Biomed Life Sci* 2007; 845(1): 95-103.
22. Duan Y, Wu C, Chowdhury S, Lee MC, Xiong G, Zhang W, Yang R, Cieplak P, Luo R, Lee T, et al. A point-charge force field for molecular mechanics simulations of proteins based on condensed-phase quantum mechanical calculations. *J Comput Chem* 2003; 24(16): 1999-2012.
23. Watkins RE, Wisely GB, Moore LB, Collins JL, Lambert MH, Williams SP, Willson TM, Kliewer SA, Redinbo MR. The human nuclear xenobiotic receptor PXR: Structural determinants of directed promiscuity. *Science* 2001; 292(5525): 2329-33.
24. Xue Y, Chao E, Zuercher WJ, Willson TM, Collins JL, Redinbo MR. Crystal structure of the PXR-T1317 complex provides a scaffold to examine the potential for receptor antagonism. *Bioorg Med Chem* 2007; 15(5): 2156-66.
25. Lau AJ, Yang G, Yap CW, Chang TK. Selective agonism of human pregnane X receptor by individual ginkgolides. *Drug Metab Dispos* 2012; 40: 1113-21.
26. Shukla SJ, Nguyen DT, Macarthur R, Simeonov A, Frazee WJ, Hallis TM, Marks BD, Singh U, Eliason HC, Printen J, et al. Identification of pregnane X receptor ligands using time-resolved fluorescence resonance energy transfer and quantitative high-throughput screening. *Assay Drug Dev Technol* 2009; 7(2): 143-69.
27. Kroll DJ, Shaw HS, Oberlies NH. Milk thistle nomenclature: Why it matters in cancer research and pharmacokinetic studies. *Integr Cancer Ther* 2007; 6(2): 110-9.
28. Luo G, Cunningham M, Kim S, Burn T, Lin J, Sinz M, Hamilton G, Rizzo C, Jolley S, Gilbert D, et al. CYP3A4 induction by drugs: Correlation between a pregnane X receptor reporter gene assay and CYP3A4 expression in human hepatocytes. *Drug Metab Dispos* 2002; 30(7): 795-804.
29. van Erp NP, Baker SD, Zhao M, Rudek MA, Guchelaar HJ, Nortier JW, Sparreboom A, Gelderblom H. Effect of milk thistle (*silybum marianum*) on the pharmacokinetics of irinotecan. *Clin Cancer Res* 2005; 11(21): 7800-6.
30. Gatti G, Perucca E. Plasma concentrations of free and conjugated silybin after oral intake of a silybin-phosphatidylcholine complex (silipide) in healthy volunteers. *Int J Clin Pharmacol Ther* 1994; 32(11): 614-7.



CHAPTER 4

EFFECTS OF CAM ON P-GP AND BCRP MEDIATED TRANSPORT OF ANTICANCER DRUGS





4.1

THE EFFECT OF COMPLEMENTARY AND ALTERNATIVE MEDICINES (CAM) ON P-GP AND BCRP MEDIATED TRANSPORT OF TOPOTECAN AND IMATINIB

K.D. Mooiman
R.F. Maas-Bakker
C. de Waard
M. de Jeu
F.A. Imperiale
E. van Loon
J.H. Beijnen
J.H.M. Schellens
I. Meijerman

Submitted for publication

ABSTRACT

The concomitant use of anticancer drugs and complementary and alternative medicines (CAM) could lead to unpredictable pharmacokinetic (PK) interactions. Most of these interactions are caused by changes in the functionality or expression of cytochrome P450 (CYP) enzymes and drug efflux transporters. Drug efflux transporters P-glycoprotein (P-gp) and Breast Cancer Resistance Protein (BCRP) are responsible for the transport of a broad spectrum of anticancer drugs. Several *in vitro* studies have been conducted to determine the possible inhibiting effects of frequently used CAM on the activity of P-gp and BCRP. However, many of these studies predominantly used model substrates and no oncolytic substrates, and reported contradictory effects.

The aim of the present study was therefore to determine the effects of fourteen extensively used CAM on P-gp and BCRP mediated transport of the widely used anticancer drugs topotecan and imatinib *in vitro* in Madin-Darby canine kidney type II cells (MDCK-II cells) overexpressing P-gp or BCRP, using an accumulation and transwell assay.

The results indicated milk thistle as potent inhibitor of BCRP and P-gp mediated transport of both topotecan and imatinib. P-gp mediated transport of imatinib was also inhibited by β -carotene. Most interestingly, St. John's wort was shown to be a potent inhibitor of P-gp mediated transport of both these anticancer drugs, but St. John's wort only inhibited BCRP mediated transport of imatinib. Clinical studies with milk thistle, β -carotene and St. John's wort are required to establish whether co-administration of these CAM can affect the pharmacokinetics of topotecan or imatinib, resulting in either an increased efficacy or toxicities.

INTRODUCTION

Cancer patients are at considerable risk for pharmacokinetic (PK) and pharmacodynamic (PD) interactions, especially because the treatment of cancer is often a combination therapy of anticancer drugs or hormonal agents with supplemental therapies to prevent or treat side effects¹. In addition, cancer patients often use complementary and alternative medicines (CAM) to reduce side effects of the anticancer drugs, to improve their quality of life, to strengthen the immune system and to retard the cancer progression^{2,3}. Dietary supplements such as β -carotene and vitamins B₆, B₁₂ and C, and herbal supplements such as valerian, St. John's wort, saw palmetto, milk thistle, ginseng, Ginkgo biloba, garlic and Echinacea are popular among cancer patients^{2,4,5}. This concomitant use of anticancer drugs and CAM could lead to unpredictable PK interactions and subsequently serious safety problems due to the narrow therapeutic window of most anticancer drugs^{6,7}.

Most PK interactions are caused by changes in the functionality or expression of cytochrome P450 (CYP) enzymes and drug efflux transporters. An important group of these drug efflux transporters is the ATP-binding cassette (ABC) family, of which P-glycoprotein (P-gp or ABCB1) and Breast Cancer Resistance Protein (BCRP or ABCG2) are expressed in many human tumors, the liver and the gastro-intestinal tract. Both these drug efflux transporters play an important role in the transport of a broad spectrum of clinically relevant drugs such as the anticancer drugs doxorubicin, daunorubicin, topotecan and imatinib^{8,9}. Inhibition of hepatic and intestinal P-gp or BCRP can result in increased plasma levels of these anticancer drugs, which can result in excessive toxicity⁷.

In literature, a number of *in vitro* studies have been conducted to determine the possible inhibiting effects of frequently used CAM on the activity of P-gp and BCRP. However, many of these studies reported contradictory effects. An overview of the reported effects of fourteen CAM on P-gp and BCRP activity is shown in **Table 1A** and **1B**. The contradictory effects reported by different *in vitro* studies may be explained by a number of factors. First, the phytochemical composition of CAM extracts is frequently unknown and highly variable among different brands¹⁰. Second, the type of assay conducted varied from accumulation assays to transwell assays, and in these assays various cell lines were used. Most importantly, different P-gp and BCRP substrates were used in these *in vitro* studies and it has been shown that P-gp inhibition is unique for each combination of inhibitors and substrates¹¹. Whether the inhibition of BCRP is also unique for each combination of inhibitors and substrates is not known hitherto. Additionally, many of the published studies predominantly used model substrates and no oncolytic substrates. However, since the inhibition of P-gp and possibly BCRP can differ for model substrates and oncolytic substrates it is crucial to use oncolytic substrates with respect to the prediction of possible clinical PK interactions between CAM and anticancer drugs.

Table 1A. Overview of the reported effects of CAM on P-gp activity.

CAM	Test systems	Effects	References
β-carotene	L5178 cells – accumulation	No effect on efflux of rhodamine	12
	L5178 cells - accumulation	↓ Efflux rhodamine by monoepoxy-β-carotene	13
	Caco-2 cells - accumulation	↓ Efflux rhodamine, calcein and doxorubicin	14
	CEM/ADR5000 cells - accumulation	↓ Efflux rhodamine, calcein	14
Echinacea	HK-2 cells - accumulation	↓ Efflux calcein	15
	Caco-2 cells - transwell	↓ ↑ Efflux ³ H-digoxin	16
Garlic	Caco-2 cells - transwell	No effect on efflux of ³ H-digoxin	17
	Rat jejunum - transwell	↑ Efflux rhodamine	18
	HepG2 - uptake	↑ Efflux rhodamine	19
	KB-C2 cells - accumulation	No effect on efflux of daunorubicin and rhodamine	20
	K562/A02 cells – accumulation	↓ Efflux adriamycin by diallyl trisulfide	21
	MDCK cells - transwell	↓ Efflux of ³ H-ritonavir by allicin	22
<i>Ginkgo Biloba</i>	Caco-2 cells - transwell	↓ Efflux ³ H-digoxin	16
Ginseng	KB-C2 cells - accumulation	↓ Efflux daunorubicin by Rg1 metabolites, no effect by Rg1	23
	AML-2/D100 cells - accumulation	↓ Efflux daunorubicin by PTG, no effect other components	24
	KBV20C cells - accumulation	↓ Efflux rhodamine and ³ H-vinblastine by Rg3	25
	Caco-2 / MDCK cells - transwell	↓ Efflux of ³ H-ritonavir by kaempferol	22
Grape seed	-	-	-
Green tea	Caco-2 cells - transwell	↓ Efflux ³ H-vinblastine/sucrose by EGCG	26
	Caco-2 cells - transwell	↓ Efflux ³ H-digoxin	17
	CH ^o C5 cells – accumulation/efflux	↓ Efflux rhodamine by EGCG, CG, ECG, GTPs	26
	NIH-3T3-G185 cells - accumulation	↓ Efflux rhodamine and LSD-751 by EGCG, EG, ECG and no effect by epicatechin and catechin	27
	MCF-7Tam cells - accumulation	No effect on efflux of rhodamine by EGCG	28
Milk thistle	Caco-2 / MDCK cells – transwell	No effect on efflux of ³ H-ritonavir by silybin	22
	Caco-2 – accumulation, transwell	↓ Efflux of digoxin and vinblastin by silymarin	29
	MCF-7 and MDA435/LCC6 cells – accumulation	↓ Efflux of daunomycin by silymarin	30
Saw Palmetto	-	-	-

Table 1A. Overview of the reported effects of CAM on P-gp activity. (continued)

CAM	Test systems	Effects	References
St. John's wort	B-CLL cells - accumulation	↓ Efflux rhodamine by hyperforin	31
	Caco-2 cells - transwell	↓ Efflux ³ H-digoxin	16
	Caco-2 cells - transwell	↓ Efflux rhodamine by hypericin	32
	LLC-PK1 cells - transwell	No effect by SJW, hyperforin and hypericin	33
	LS180 cells - accumulation	↓ Efflux rhodamine by SJW, no effect by hypericin	32
	Caco-2 / MDCK cells - transwell	↓ Efflux of ³ H-ritonavir by hypericin	22
Valerian	Caco-2 cells - transwell	↓ Efflux ³ H-digoxin	34
Vitamin B ₆	-	-	-
Vitamin B ₁₂	-	-	-
Vitamin C	-	-	-

Abbreviations: B-CLL, B cell chronic lymphocytic leukemia; Caco-2, human colorectal adenocarcinoma; HK-2, human proximal tubule; LS178, mouse T-cell lymphoma; KB-C2, human multi-resistant carcinoma; MCF-7, human breast adenocarcinoma; CEM/ADR5000, adriamycin resistant leukemia; SJW, St. John's wort.

Table 1B. Overview of the reported effects of CAM on BCRP activity.

CAM	Test systems	Effects	References
β-carotene	-	-	-
Echinacea	-	-	-
Garlic	Caco-2 cells - transwell and rat jejunum	↑ Efflux rosuvastatin	35
Ginkgo biloba	MDCK-II cells - transwell & accumulation	↓ Efflux quercetin by kaempferol	36
Ginseng	BCRP expressing membrane vesicles	↓ Efflux methotrexate	37
Grape seed	-	-	-
Green tea	MCF-7 cells - accumulation	↓ Efflux mitoxantrone	28
Milk thistle	Membrane vesicle uptake	↓ Efflux methotrexate	37
	MCF-7 and NCI-H460 cells - accumulation	↓ Efflux mitoxantrone	38
Saw Palmetto	-	-	-
St. John's wort	B-CLL cells - accumulation	↓ Efflux mitoxantrone by hyperforin	31
Valerian	-	-	-
Vitamin B ₆	-	-	-
Vitamin B ₁₂	-	-	-
Vitamin C	-	-	-

Since much uncertainty still exists as to the precise interactions between CAM and anticancer drugs further research with respect to their concomitant use is warranted.

The aim of the present study is therefore to determine the inhibitory effects of fourteen extensively used CAM on P-gp and BCRP mediated transport of topotecan and imatinib.

To address this issue the following CAM have been tested *in vitro* in Madin-Darby canine kidney type II cells (MDCK-II cells) using both an accumulation and transwell assay: β -carotene, Echinacea (*Echinacea purpurea*), garlic (*Allium sativum*), green tea (*Camellia sinensis*), *Ginkgo biloba*, ginseng (*Eleutherococcus senticosus*), grape seed (*Vitis vinifera*), milk thistle (*Silybum marianum*), saw palmetto (*Serenoa serrulata*), St. John's wort (*Hypericum perforatum*), valerian (*Valeriana officinalis*), vitamin B₆, B₁₂ and C. The selection of these CAM is based on the frequency of use by cancer patients and the potential to interact with anticancer drugs^{2,4,5}. The anticancer drugs topotecan and imatinib are substrates for both P-gp and BCRP and were selected because these drugs are widely applied in the clinic. Furthermore both anticancer drugs have never been used as P-gp and BCRP substrates in previous *in vitro* studies.

MATERIALS AND METHODS

Reagents and chemicals

All cell culture media and supplements were obtained from PAA (Pasching, Austria). Standardized extracts of β -carotene, garlic, vitamin B₆ and B₁₂ were purchased from ABCR GmbH & Co KG (Karlsruhe, Germany), Organic Herb Inc. (Changsha City, China), UPS (Rockville, MD, USA) and Sigma-Aldrich (Zwijndrecht, The Netherlands), respectively. Standardized extracts of milk thistle, *Ginkgo biloba*, Echinacea, ginseng, St. John's wort, saw palmetto, grape seed, green tea, valerian and vitamin C were obtained from Chromadex (Irvine, CA, USA). The details of all standardized extracts are provided in **Table 2**. Triton X-100 and topotecan hydrochloride hydrate (topotecan) were purchased from Sigma-Aldrich (Zwijndrecht, the Netherlands). Imatinib mesylate (imatinib) was purchased from Sequoia Research products Ltd. (Pangbourne, UK) and imatinib-¹³C₂H₃ (internal standard) was obtained from Alsachim (Illkirch Graffenstaden, France). Dimethyl sulfoxide (DMSO) was purchased from Acros Organics (New Jersey, USA). Tert-Butyl methyl ether (TBME) and sodium hydroxide (NaOH) were purchased from Merck (Darmstadt, Germany). Methanol of HPLC quality, acetonitrile of HPLC-S gradient grade and LC-MS grade water were purchased from Biosolve (Valkenswaard, the Netherlands).

Cell culture

Wild type (WT), P-gp and BCRP overexpressed Madin-Darby canine kidney II cells were obtained from Prof. Dr. P. Borst from the Netherlands Cancer Institute (Amsterdam, the Netherlands). These cell lines were maintained in Dulbecco's modified Eagle's medium (DMEM) with 1 g/L glucose with L-glutamine supplemented with 10% (v/v) heat-inactivated fetal bovine serum (FBS-Gold), 50 U/mL penicillin and 50 μ g/mL streptomycin (DMEM complete medium) at 37°C under a humidified atmosphere of 5%

Table 2. Details of the standardized CAM extracts.

CAM	Product Information	Contents	
β -carotene	ABCR GmbH&Co KG [Lot # 1030612]	97% β -carotene	
Echinacea <i>Echinacea purpurea</i>	Chromadex [Lot # 00030217-012]	0.94% caftaric acid 0.03% chlorogenic acid 0.04% cynarin	0.05% echinacoside 1.80% cichoric acid
Garlic <i>Allium sativum</i>	Organic Herb Inc. [100-20100122]	Garlic extract (100:1)	Allicin scordinin alliin
<i>Ginkgo biloba</i>	Chromadex [Lot # 00030299-1917]	4.78% quercetin 3.73% kaempferol 2.13% isorhamnetin 12.0% quercetin glycoside 9.65% kaempferol glycoside 5.19% isorhamnetin glycoside	1.61% bilobalide 1.41% ginkgolide A 0.31% ginkgolide J 5.57% ginkgolide B 0.38% ginkgolide C
Ginseng <i>Eleutherococcus senticosus</i>	Chromadex [Lot # 00030302-019]	0.439% eleutheroside E	0.245% eleutheroside B
Grape seed <i>Vitis vinifera</i>	Chromadex [Lot # 00036130-11]	5.08% epigallocatechin 0.93% catechin 6.30% epicatechin	0.02% epigallocatechin gallate 0.03% epicatechin gallate
Green tea <i>Camellia sinensis</i>	LTK Laboratories Inc. [G6817]	99.61% tea polyphenols 65.38% EGCG 82.79% catechins	1.17% caffeine 3.98% water 0.18% sulfated ash
Milk Thistle <i>Silybum marianum</i>	Chromadex [Lot # 00030402-101]	29.6% silybin A+B 2.97% taxifolin	14.7% silychristin
Saw Palmetto <i>Serenoa serrulata</i>	Chromadex [Lot # 00030726-841]	0.13% campesterol 0.07% stigmasterol 0.43% β -sistosterol 0.21% methyl caproate 0.93% methyl octanoate 2.53% methyl decanoate 28.61% methyl dodecanoate 10.63% methyl myristate	8.55% methyl palmitate 1.81% methyl stearate 30.40% methyl oleate 5.28% methyl linolenate 0.75% methyl linoleate 0.17% methyl arachidate 0.02% methyl EPA 0.11% methyl DHA
St. John's wort <i>Hypericum perforatum</i>	Chromadex [Lot # 00030798-155]	1.87% rutin 0.24% pseudohypericin	0.01% hyperforin 0.06% hypericin
Valerian <i>Valeriana officinalis</i>	Chromadex [Lot # 34899-045]	0.16% valerenic acids	
Vitamin B ₆	Sigma-Aldrich [Lot # 120M13271V]	> 98% pyridoxine	
Vitamin B ₁₂	Sigma-Aldrich [Lot # 030M1567]	> 98% vitamin B ₁₂	
Vitamin C	Chromadex [Lot # 111021-641]	Vitamin C	

Abbreviations: DHA, docosahexaenoic acid; EPA, eicosapentaenoic acid.

CO₂. In addition, G418 was used for selecting P-gp overexpressed MDCK-II cells that are cotransfected with the neomycin resistance gene.

Accumulation assay with topotecan

Incubations

WT, BCRP and P-gp overexpressed MDCK-II cells were plated at a density of 2.5×10^5 cells/well in 12-well plates (Greiner Bio-One BV) in 1 mL of DMEM complete medium and incubated overnight in a 5% CO₂-humidified atmosphere at 37°C. After 24 hours of incubation, this medium was aspirated and replaced by 1 mL of fresh DMEM complete medium. After another 24 hours, the medium was removed and cells were washed with PBS (37°C). Subsequently, 750 µL of fresh medium was added containing 0.1% DMSO, 100 µg/mL CAM, 1 µM KO143 (a selective BCRP inhibitor³⁹) or 10 µM zosuquidar (a selective P-gp inhibitor⁴⁰). After 30 minutes of pre-incubation at 37°C under a humidified atmosphere of 5% CO₂, 750 µL of medium containing 40 µM topotecan was added. After a 1-hour incubation at 37°C under a humidified atmosphere of 5% CO₂, medium was removed and the cells were intensively washed (six times) with ice cold PBS. Furthermore, the cells were lysed with 250 µL of 0.1% Triton X-100 and sonicated for three minutes in an ultrasonic water bath. Subsequently, lysates were transferred in 2.0 mL polypropylene tubes (Sarstedt, Etten-Leur, The Netherlands) and centrifuged for 10 minutes at 13,500 g.

Analysis

Topotecan was measured (at 380/520 nm) on a FLUOstar OPTIMA microplate reader (BMG LABTECH GmbH, Ortenberg, Germany) after transferring 100 µL supernatant in black 96-well plates. Except for β-carotene, none of the CAM quenched the fluorescent signal of topotecan at 100 µg/mL. Therefore, the results of the incubation with β-carotene and topotecan are excluded from the results. The fluorescence results were corrected for the background fluorescence and the intracellular topotecan concentrations expressed as ratio of the DMSO control.

Accumulation assay with imatinib

Incubations

The incubations of WT, BCRP and P-gp overexpressed MDCK-II cells were performed as described for the accumulation study with topotecan with a few exceptions. The required final concentrations of the positive controls KO143 and zosuquidar were 0.1 and 1 µM, respectively. After 30 minutes of pre-incubating the cells with 0.1% DMSO, 100 µg/mL CAM and the positive controls, 750 µL of 0.1 µM or 0.25 µM imatinib was added to BCRP and P-gp overexpressed MDCK-II cells, respectively. The cells were lysed with

500 μL of 0.1% Triton X-100 in order to obtain the required amount of supernatants for the liquid-chromatography coupled to tandem mass spectrometry (LC-MS/MS) analysis.

LC-MS/MS analysis

The concentrations of imatinib were determined with a LC-MS/MS analysis reported for plasma⁴¹, after optimization for incubation samples. A total of 10 μL of the labeled internal standard imatinib- $^{13}\text{C}^2\text{H}_3$ (500 ng/mL) and 200 μL of 100 mM NaOH were added to 200 μL of the supernatant. In order to obtain clean samples, liquid-liquid extraction (LLE) with TBME was performed by adding 1 mL of TBME. The samples were then vortex-mixed for 30 seconds and centrifuged for 10 minutes at 13.500 g . After the samples were placed for one hour at -80°C , the organic layer was decanted in clear 1.5 mL polypropylene tubes and evaporated under a stream of nitrogen at 40°C . The residue was reconstituted in 100 μL of 50% MeOH and vortex-mixed for 30 seconds. After centrifugation of 10 minutes at 13.500 g , the clear supernatant was transferred in 250 μL glass inserts placed in autosampler vials for LC-MS/MS analysis.

Samples were injected on an Acquity UPLC® BEH C18 column (30 mm x 2.1 mm, 1.7 μm , Waters, Milford, USA), protected by the corresponding VanGuard pre-column (5 mm x 2.1 mm, Waters). The column temperature was maintained at 40°C and the samples were stored in autosampler rack at 4°C . The HPLC system comprised of an Accela pump, autosampler and TSQ Quantum Ultra quadrupole mass spectrometer with heated electrospray ionization (HESI, Thermo Fisher Scientific, San Jose, CA, USA).

The mobile phase consisted of 10 mM ammonium hydroxide in water (A) and methanol (B) with a flow rate of 0.5 mL/min and a total run time of 4 minutes. During the first 3 minutes of the run a gradient was introduced by increasing % B from 30% to 80%. Subsequently, the %B was decreased to 30% within 6 seconds and stabilized at 30% for 1 minute. Positive ionization selected reaction monitoring mass transitions were $494.2 > 394.3$ and $498.3 > 394.1$ for imatinib and imatinib- $^{13}\text{C}^2\text{H}_3$, respectively. To quantify the data a calibration curve of imatinib was applied in a range of 2-1000 ng/mL. The intracellular imatinib concentrations were expressed as ratio of the DMSO control.

Transwell assay with imatinib

Imatinib was used as BCRP and P-gp substrate because it could easily be detected by the sensitive LC-MS/MS analysis. For the transwell assay it was, however, not possible to use topotecan as BCRP and P-gp substrate due to the low concentrations of topotecan in the assay, which could not be adequately detected by the fluorescence plate reader.

WT, BCRP and P-gp overexpressed cells were seeded on 24 mm polycarbonate membrane filters (Corning, New York, USA) in 6-well plates at a density of 1.5×10^6 cells/well in 2 mL DMEM complete medium. These cells were grown for 96 hours at 37°C under a humidified atmosphere of 5% CO_2 . The medium was refreshed every day. After 96

hours medium was aspirated and cells were briefly washed with 1 mL PBS (37°C). Subsequently, 2 mL of fresh medium was added containing 0.1% DMSO, 100 µg/mL CAM and 1 µM zosuquidar or KO143 to both the apical and basolateral side. After 1 hour of pre-incubation at 37°C, the medium was replaced on either the apical or basolateral side with 2 mL of similar medium, containing equal concentrations of DMSO or CAM and 0.25 µM imatinib. Cells were incubated at 37°C and aliquots of 50 µL were taken every hour up to 4 hours. In addition, medium with 300 µM lucifer yellow was added to check for the integrity of the cell monolayer. Paracellular flux of Lucifer yellow up to 5% was tolerated as an acceptable limit for cell integrity.

The concentrations of imatinib were analyzed with LC-MS/MS as described above with a few adjustments: 2 µL internal standard, 50 µL NaOH and 250 µL TBME were added to the 50 µL aliquots. After LLE, the residue was reconstituted in 50 µL of 50% MeOH. The percentage of transported imatinib was determined by dividing the concentration in the receiver (either apical or basolateral) compartment by the added concentration in the donor (either apical or basolateral) compartment. In addition, the apparent permeability (P_{app}) and efflux ratios were calculated with the following equations:

$P_{app} \text{ (cm/s)} = \frac{dCr}{dt} \times \frac{Vr}{(A \times C_0)}$	$dCr = \text{change in imatinib conc. in receiver compartment } (\mu\text{M})$
	$dt = \text{time (sec)}$
$\text{Efflux ratio} = \frac{\text{Basolateral to apical } P_{app}}{\text{Apical to basolateral } P_{app}}$	$Vr = \text{volume of the receiver compartment (cm}^3\text{)}$
	$A = \text{membrane growth area (cm}^2\text{)}$
	$C_0 = \text{initial donor concentration } (\mu\text{M})$

Statistical analysis

Statistical analyses of the data were performed by using the two-tailed Student's *t*-test in SPSS version 16.0 (SPSS Inc., Chicago, IL, USA). Data were considered as statistically significant when $p < 0.05$.

RESULTS

The potential of fourteen most commonly used CAM (β -carotene, Echinacea, garlic, green tea, Ginkgo biloba, ginseng, grape seed, milk thistle, saw palmetto, St. John's wort, valerian, vitamin B₆, B₁₂ and C) to inhibit BCRP- and P-gp mediated transport of topotecan and imatinib was determined in BCRP- and P-gp overexpressed MDCK-II cells. In addition, wild-type MDCK-II cells were used to check the influence of other transporters than P-gp and BCRP. None of the CAM affected the accumulation of topotecan and imatinib in wild-type cells (data not shown).

P-gp mediated accumulation of topotecan and imatinib

The accumulation assay conducted with topotecan in P-gp overexpressed cells revealed two CAM that significantly inhibited P-gp (**Figure 1A**). St. John's wort was the most potent P-gp inhibitor resulting in a 3.5-fold accumulation of topotecan, followed by milk thistle that caused a 2.9-fold accumulation.

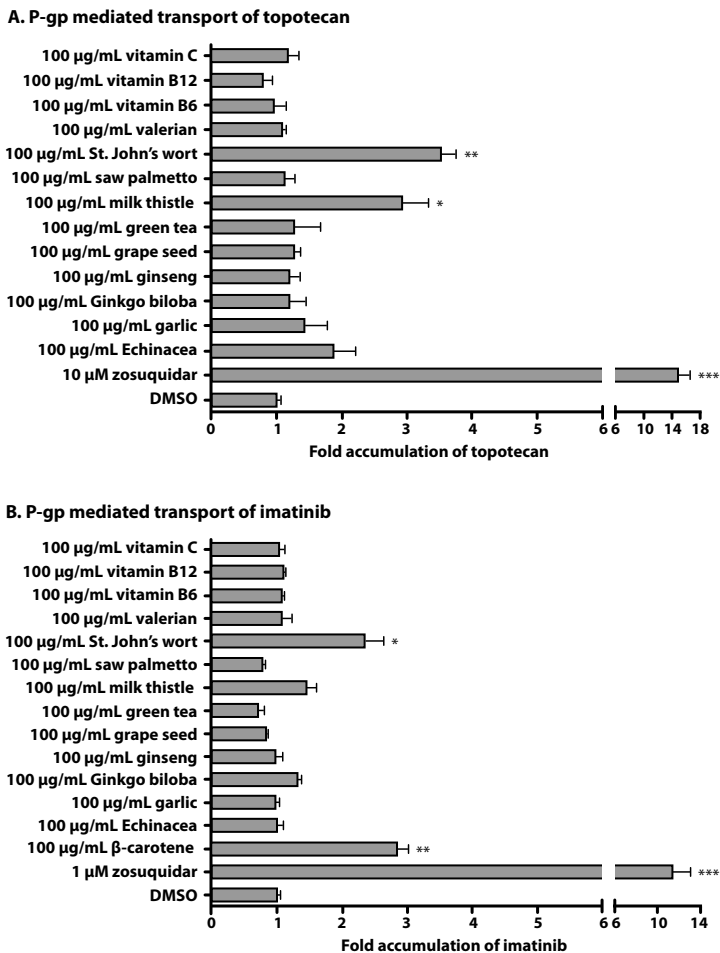


Figure 1. The effects of CAM on P-gp mediated transport of topotecan (A) and imatinib (B). For P-gp mediated transport of topotecan and imatinib, P-gp overexpressed MCDK-II cells were pre-incubated 0.1% DMSO as negative control, P-gp positive control zosuquidar and CAM for 30 minutes and incubated with 40 µM topotecan or 0.25 µM imatinib for one hour. After lysing the cells, the intracellular fluorescence of topotecan was measured and corrected for the background fluorescence and intracellular concentrations of imatinib were measured with LC-MS/MS. The data are means \pm SD of triplicate incubations from a representative experiment. In the figure the fold accumulation of topotecan or imatinib compared to 0.1% DMSO are shown (* $p < 0.05$, ** $p < 0.01$ and *** $p < 0.001$).

The P-gp mediated accumulation of imatinib was also significantly inhibited by St. John's wort which increase the accumulation of imatinib a 2.4-fold (**Figure 1B**). However, β -carotene was the most potent inhibitor of P-gp which significantly increased the accumulation of imatinib a 2.9-fold. Furthermore, milk thistle weakly inhibited P-gp mediated transport of imatinib, but not significantly.

P-gp mediated transport of imatinib

The effects of the CAM inhibiting P-gp in the accumulation assay with imatinib were also tested in a transwell assay and the results are shown in **Table 3** and **Figure 2**. St. John's wort was confirmed as a potent inhibitor of P-gp mediated transport of imatinib. Both the efflux ratio and the percentage of transported imatinib were decreased 79% and 28%, respectively after 4 hours. Also β -carotene inhibited the transport of imatinib 19.9% after 4 hours. According to the transwell assay milk thistle was the most potent inhibitor of P-gp, because it inhibited the transport of imatinib 53% after 4 hours.

Table 3. Summary of P_{app} values ($\times 10^{-6}$ cm/s) and efflux ratios of P-gp inhibiting CAM after 4 hours.

CAM *	P_{app} B \rightarrow A	P_{app} A \rightarrow B	Efflux ratios
DMSO	17.3 \pm 3.32	1.34 \pm 0.63	12.9 \pm 6.52
Zosuquidar	10.2 \pm 0.78	10.7 \pm 0.74	0.95 \pm 0.10
β -carotene	12.9 \pm 2.74	2.35 \pm 0.39	5.47 \pm 1.48
Milk thistle	4.26 \pm 0.22	3.59 \pm 0.89	1.19 \pm 0.30
St. John's wort	10.7 \pm 0.64	3.87 \pm 1.34	2.75 \pm 0.97

* Except for DMSO and zosuquidar. The data are means \pm SD of triplicate incubations from a representative experiment.

BCRP mediated accumulation of topotecan and imatinib

The effect of CAM on the accumulation of topotecan and imatinib was also evaluated in BCRP overexpressed cells (**Figure 3A and 3B**). Milk thistle was shown to significantly increase the accumulation of both topotecan and imatinib a 5.2-fold and 2.6-fold, respectively. In addition, BCRP mediated transport of imatinib was significantly inhibited by St. John's wort resulting in a 2.3-fold accumulation of imatinib.

BCRP mediated transport of imatinib

The effect of the milk thistle and St. John's wort on the BCRP mediated transport of imatinib was also determined in a transwell assay and the results are shown in **Table 4** and **Figure 4**. Both St. John's wort and milk thistle were confirmed as potent BCRP inhibitors. BCRP mediated transport of imatinib was inhibited 30% and 41% by St. John's wort and milk thistle, respectively after 4 hours.

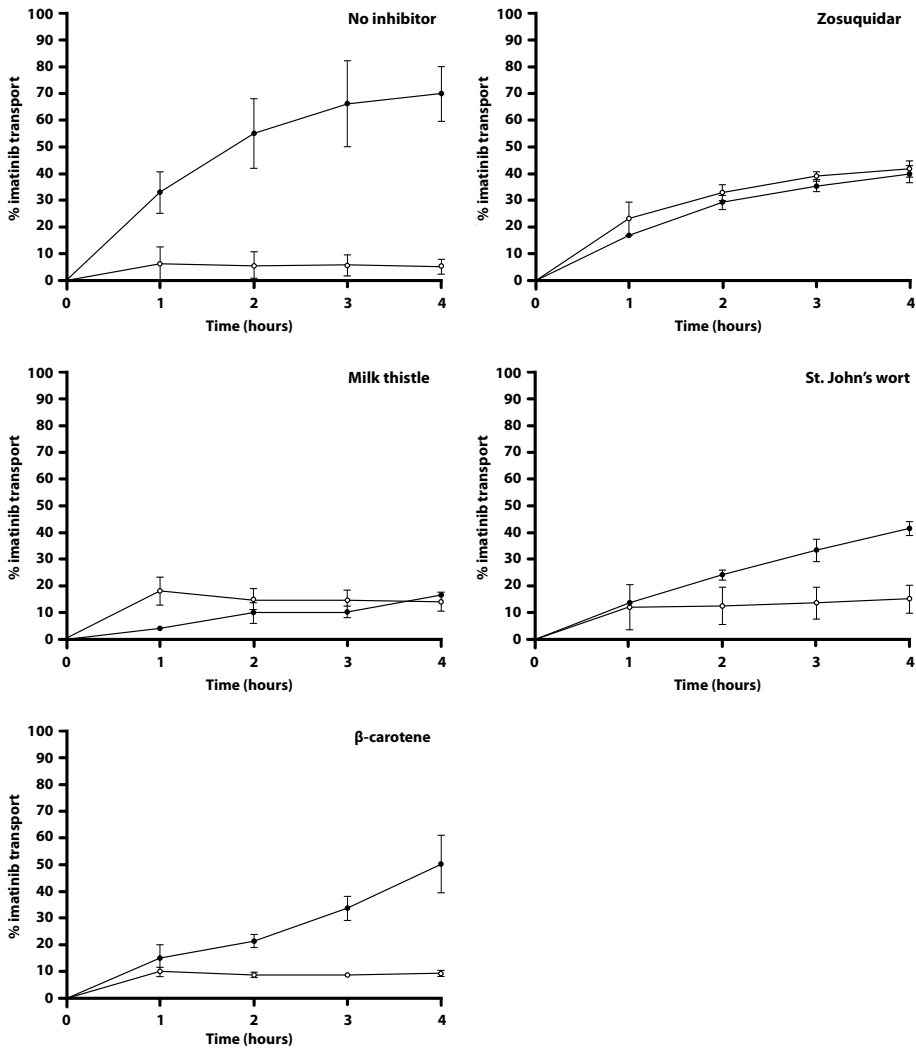


Figure 2. Transport of imatinib in P-gp overexpressed MDCK-II cells in the absence and presence of CAM. P-gp overexpressed MDCK-II cells were pre-incubated with 2 mL of fresh medium was added containing 0.1% DMSO, 100 $\mu\text{g}/\text{mL}$ milk thistle, St. John's wort and β -carotene, and 1 μM zosuquidar to both the apical and basolateral side. After 1 hour, the medium was replaced with 2 mL of similar medium, containing equal concentrations of DMSO or CAM and 0.25 μM imatinib on either the apical or basolateral side. Cells were incubated at 37°C and aliquots of 50 μL were taken every hour up to 4 hours. The data are mean concentrations of imatinib in the apical or basolateral compartment \pm SD of triplicate incubations from a representative experiment. The open symbols represent the translocation from the apical to the basolateral compartment and closed symbols represent the translocation from the basolateral to the apical compartment.

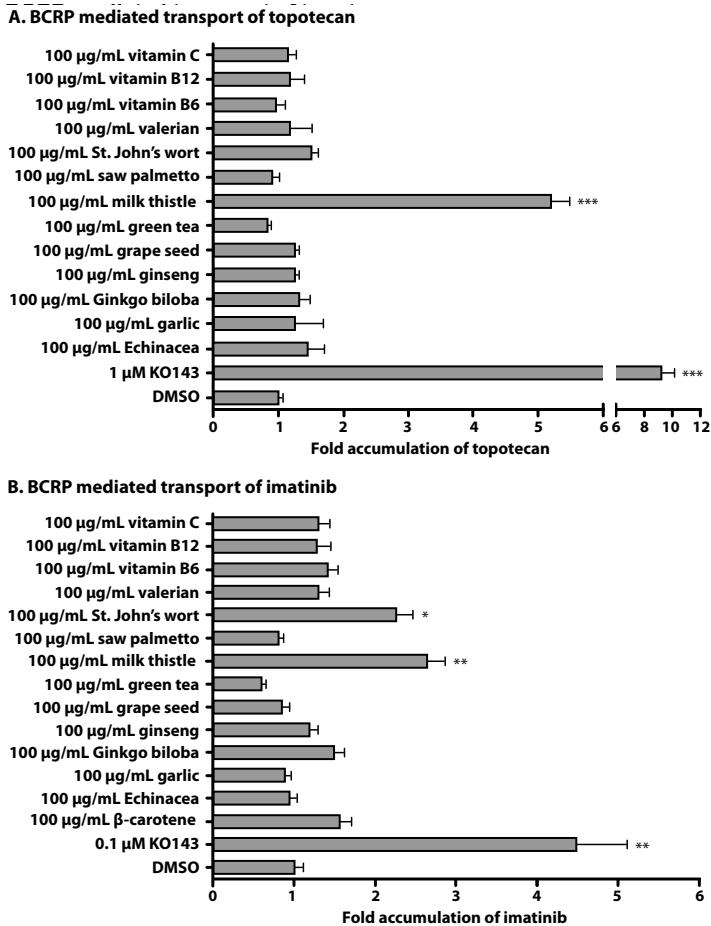


Figure 3. The effects of CAM on BCRP mediated transport of topotecan (A) and imatinib (B). For BCRP mediated transport of topotecan and imatinib, BCRP overexpressed MCDK-II cells were pre-incubated 0.1% DMSO as negative control, BCRP positive control KO143 and CAM for 30 minutes and incubated with 40 µM topotecan or 0.1 µM imatinib for one hour. After lysing the cells, the intracellular fluorescence of topotecan was measured and corrected for the background fluorescence and intracellular concentrations of imatinib were measured with LC-MS/MS. The data are means \pm SD of triplicate incubations from a representative experiment. In the figure the fold accumulation of topotecan or imatinib compared to 0.1% DMSO are shown (* $p < 0.05$, ** $p < 0.01$ and *** $p < 0.001$).

Table 4. Summary of P_{app} values ($\times 10^{-6}$ cm/s) and efflux ratios of BCRP inhibiting CAM after 4 hours.

CAM *	$P_{app} B \rightarrow A$	$P_{app} A \rightarrow B$	Efflux ratios
DMSO	14.1 ± 0.56	4.45 ± 1.65	3.15 ± 1.18
KO143	10.8 ± 0.58	9.69 ± 0.26	1.11 ± 0.07
Milk thistle	2.89 ± 0.21	5.56 ± 0.70	0.52 ± 0.08
St. John's wort	5.76 ± 0.40	5.92 ± 0.31	0.97 ± 0.08

* Except for DMSO and KO143. The data are means \pm SD of triplicate incubations from a representative experiment.

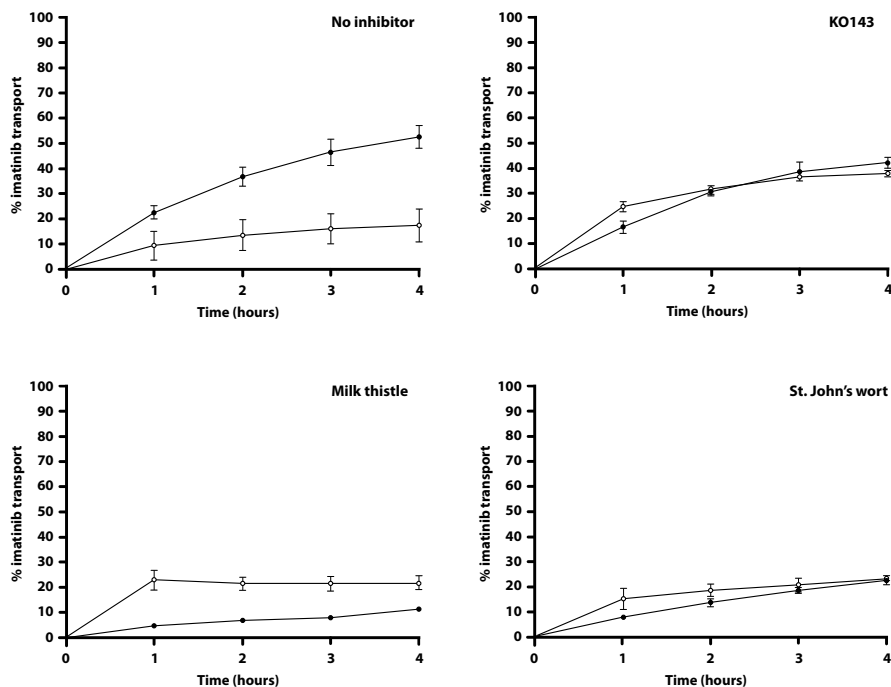


Figure 4. Transport of imatinib in BCRP overexpressed MDCK-II cells in the absence and presence of CAM. BCRP overexpressed MDCK-II cells were pre-incubated with 2 mL of fresh medium was added containing 0.1% DMSO, 100 $\mu\text{g}/\text{mL}$ milk thistle and St. John's wort, and 1 μM KO143 to both the apical and basolateral side. After 1 hour, the medium was replaced with 2 mL of similar medium, containing equal concentrations of DMSO or CAM and 0.25 μM imatinib on either the apical or basolateral side. Cells were incubated at 37°C and aliquots of 50 μL were taken every hour up to 4 hours. The data are mean concentrations of imatinib in the apical or basolateral compartment \pm SD of triplicate incubations from a representative experiment. The open symbols represent the translocation from the apical to the basolateral compartment and closed symbols represent the translocation from the basolateral to the apical compartment.

DISCUSSION AND CONCLUSION

The present study determined the potential of fourteen most commonly used CAM^{2,4,5} to inhibit P-gp and BCRP mediated transport of two anticancer drugs: topotecan and imatinib. The inhibitory effects of CAM on both P-gp and BCRP were assessed in two *in vitro* assays: an accumulation assay in which the accumulated concentration of topotecan and imatinib was determined and a transwell assay in which the transport of imatinib was evaluated. Topotecan and imatinib are substrates for both drug efflux transporters P-gp and BCRP and were selected as they are often applied in the clinic. Furthermore both anticancer drugs have never been used to determine the effects of

CAM on the activity of P-gp and BCRP in previous *in vitro* studies, which makes the present study unique.

To assess the effects of CAM on P-gp and BCRP mediated transport of topotecan and imatinib, P-gp and BCRP overexpressed MDCK-II cells were used. By comparing the results between over-expressed and wild type MDCK-II cells, it is possible to exclude the influence of other drug efflux transporters such as Multidrug Resistance-associated Proteins (MRPs). However, the influence of other drug efflux transporters cannot be completely ruled out as the overexpressed MDCK-II cells do express low levels of endogenous P-gp⁴². The contribution of endogenous P-gp was obvious in the transwell assay with BCRP overexpressed MDCK-II cells, in which the specific BCRP inhibitor KO143 did not strongly inhibit the transport of imatinib. Most likely, endogenous P-gp took over the transport of imatinib. Based on these results, it is recommended to add the P-gp inhibitor zosuquidar in experiments with BCRP overexpressed MDCK-II cells to eliminate the contribution of P-gp. Since P-gp overexpressed MDCK-II cells do not contain endogenous BCRP, P-gp inhibition by zosuquidar resulted in a strong reduction of the transported imatinib.

In the present study, β -carotene significantly inhibited P-gp mediated transport of imatinib in both the accumulation and transwell assay. It was not possible to determine the effect of β -carotene on BCRP- and P-gp mediated transport of topotecan due to quenching of the fluorescent signal. Furthermore, milk thistle was shown to significantly inhibit BCRP and P-gp mediated transport of both topotecan and imatinib. Based on these results, milk thistle appears to inhibit P-gp and BCRP regardless the combination with topotecan or imatinib. However, milk thistle was previously shown not to inhibit P-gp in combination with ritonavir, indicating that the effect of milk thistle on P-gp is dependent on the substrate²². St. John's wort was shown to significantly inhibit P-gp mediated transport of both topotecan and imatinib, but only BCRP mediated transport of imatinib. Furthermore, St. John's wort was previously shown not to inhibit P-gp in combination with other P-gp substrates such as digoxin³³, suggesting that the effect of St. John's wort on both BCRP and P-gp is dependent on the substrate.

By comparing the described effects of milk thistle and St. John's wort on the transport of topotecan and imatinib and their effects on the transport of other substrates, both BCRP and P-gp appear to be dependent on the combination of the inhibitor and substrate. Therefore, it is inevitable to evaluate the *in vitro* inhibitory effects of CAM on P-gp and BCRP in combination with multiple substrates.

In conclusion, milk thistle, St. John's wort and β -carotene were confirmed as potent inhibitors of either P-gp and/or BCRP mediated transport of topotecan or imatinib in an accumulation and transwell assay. Since the inhibition of BCRP and P-gp appears to be dependent on the combination of the inhibitor and substrate, it is crucial to use oncologic substrates *in vitro* to more closely predict possible PK interactions between CAM and the specifically tested anticancer drugs. Based on the results of the present study, milk thistle, β -carotene and St. John's wort are interesting CAM for clinical follow-up to establish the clinical relevance of their inhibitory effects on the excretion of imatinib and/or topotecan.

REFERENCES

1. Harmsen S, Meijerman I, Beijnen JH, Schellens JH. Nuclear receptor mediated induction of cytochrome P450 3A4 by anticancer drugs: A key role for the pregnane X receptor. *Cancer Chemother Pharmacol* 2009; 64(1): 35-43.
2. Tascilar M, de Jong FA, Verweij J, Mathijssen RH. Complementary and alternative medicine during cancer treatment: Beyond innocence. *Oncologist* 2006; 11(7): 732-41.
3. Werneke U, Earl J, Seydel C, Horn O, Crichton P, Fannon D. Potential health risks of complementary alternative medicines in cancer patients. *Br J Cancer* 2004; 90(2): 408-13.
4. Gupta D, Lis CG, Birdsall TC, Grutsch JF. The use of dietary supplements in a community hospital comprehensive cancer center: Implications for conventional cancer care. *Support Care Cancer* 2005; 13(11): 912-9.
5. McCune JS, Hatfield AJ, Blackburn AA, Leith PO, Livingston RB, Ellis GK. Potential of chemotherapy-herb interactions in adult cancer patients. *Support Care Cancer* 2004; 12(6): 454-62.
6. Sparreboom A, Cox MC, Acharya MR, Figg WD. Herbal remedies in the United States: Potential adverse interactions with anticancer agents. *J Clin Oncol* 2004; 22(12): 2489-503.
7. Blower P, de Wit R, Goodin S, Aapro M. Drug-drug interactions in oncology: Why are they important and can they be minimized? *Crit Rev Oncol Hematol* 2005; 55(2): 117-42.
8. Breedveld P, Beijnen JH, Schellens JH. Use of P-glycoprotein and BCRP inhibitors to improve oral bioavailability and CNS penetration of anticancer drugs. *Trends Pharmacol Sci* 2006; 27(1): 17-24.
9. Sharom FJ. ABC multidrug transporters: Structure, function and role in chemoresistance. *Pharmaco-genomics* 2008; 9(1): 105-27.
10. Winslow LC, Kroll DJ. Herbs as medicines. *Arch Intern Med* 1998; 158(20): 2192-9.
11. Wang EJ, Casciano CN, Clement RP, Johnson WW. Active transport of fluorescent P-glycoprotein substrates: Evaluation as markers and interaction with inhibitors. *Biochem Biophys Res Commun* 2001; 289(2): 580-5.
12. Molnar J, Gyemant N, Mucsi I, Molnar A, Szabo M, Kortvelyesi T, Varga A, Molnar P, Toth G. Modulation of multidrug resistance and apoptosis of cancer cells by selected carotenoids. *In Vivo* 2004 Mar-Apr; 18(2): 237-44.
13. Gyemant N, Tanaka M, Molnar P, Deli J, Mandoky L, Molnar J. Reversal of multidrug resistance of cancer cells *in vitro*: Modification of drug resistance by selected carotenoids. *Anticancer Res* 2006 Jan; 26(1A): 367-74.
14. Eid SY, El-Readi MZ, Wink M. Carotenoids reverse multidrug resistance in cancer cells by interfering with ABC-transporters. *Phytomedicine* 2012; 19(11): 977-87.
15. Romiti N, Pellati F, Nieri P, Benvenuti S, Adinolfi B, Chieli E. P-glycoprotein inhibitory activity of lipophilic constituents of *echinacea pallida* roots in a human proximal tubular cell line. *Planta Med* 2008; 74(3): 264-6.
16. Hellum BH, Nilsen OG. *In vitro* inhibition of CYP3A4 metabolism and P-glycoprotein-mediated transport by trade herbal products. *Basic Clin Pharmacol Toxicol* 2008; 102(5): 466-75.
17. Engdal S, Nilsen OG. Inhibition of P-glycoprotein in caco-2 cells: Effects of herbal remedies frequently used by cancer patients. *Xenobiotica* 2008; 38(6): 559-73.
18. Berginc K, Zakelj S, Ursic D, Kristl A. Aged garlic extract stimulates p-glycoprotein and multidrug resistance associated protein 2 mediated effluxes. *Biol Pharm Bull* 2009; 32(4): 694-9.
19. Berginc K, Trontelj J, Kristl A. The influence of aged garlic extract on the uptake of saquinavir and darunavir into HepG2 cells and rat liver slices. *Drug Metab Pharmacokinet* 2010; 25(3): 307-13.

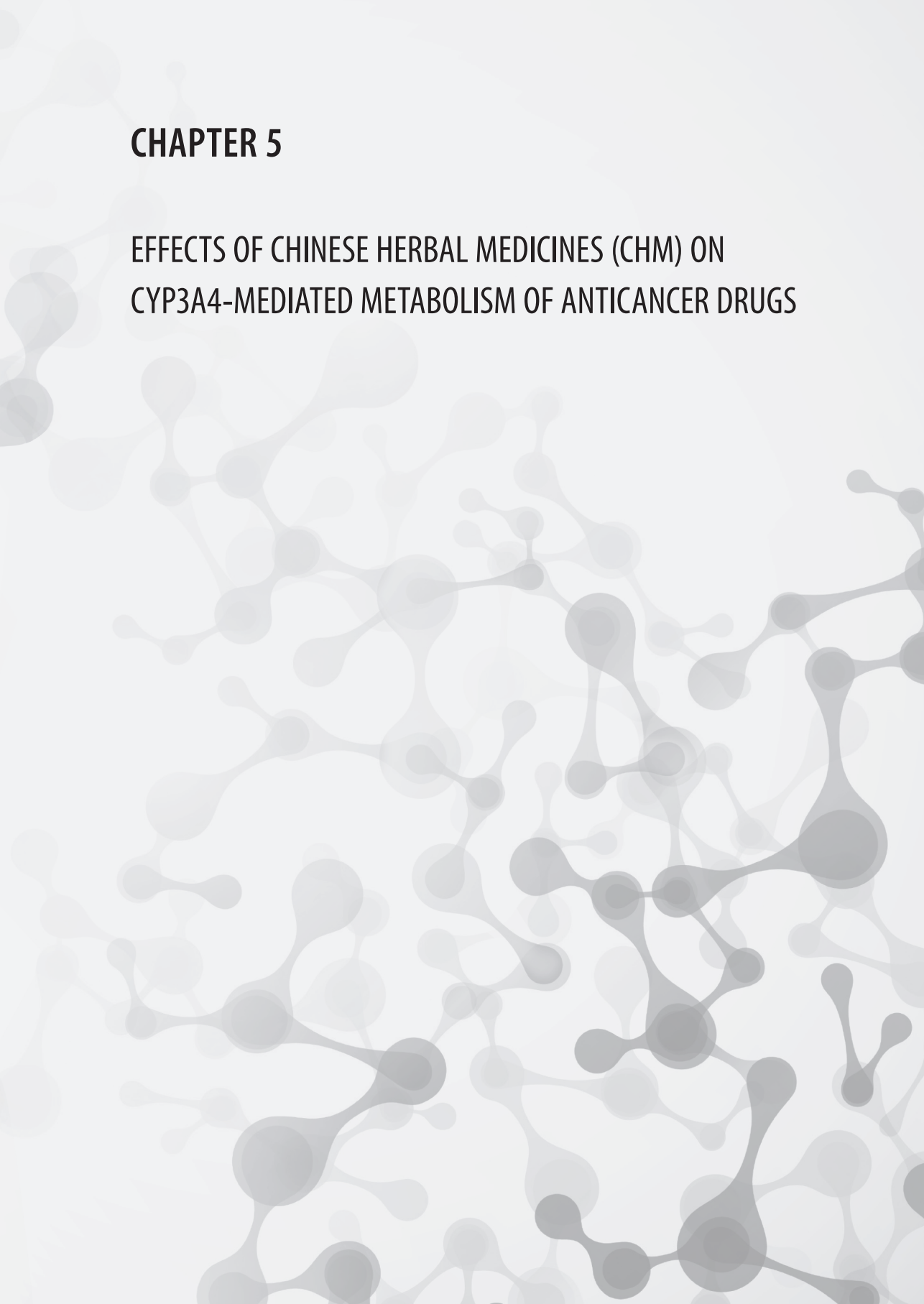
20. Nabekura T, Kamiyama S, Kitagawa S. Effects of dietary chemopreventive phytochemicals on P-glyco-protein function. *Biochem Biophys Res Commun* 2005; 327(3): 866-70.
21. Xia Q, Wang ZY, Li HQ, Diao YT, Li XL, Cui J, Chen XL, Li H. Reversion of P-glycoprotein-mediated multidrug resistance in human leukemic cell line by diallyl trisulfide. *Evid Based Complement Alternat Med* 2012; 2012: 1-11.
22. Patel J, Buddha B, Dey S, Pal D, Mitra AK. *In vitro* interaction of the HIV protease inhibitor ritonavir with herbal constituents: Changes in P-gp and CYP3A4 activity. *Am J Ther* 2004; 11(4): 262-77.
23. Kitagawa S, Takahashi T, Nabekura T, Tachikawa E, Hasegawa H. Inhibitory effects of ginsenosides and their hydrolyzed metabolites on daunorubicin transport in KB-C2 cells. *Biol Pharm Bull* 2007; 30(10): 1979-81.
24. Choi CH, Kang G, Min YD. Reversal of P-glycoprotein-mediated multidrug resistance by proto-panaxatriol ginsenosides from Korean red ginseng. *Planta Med* 2003; 69(3): 235-40.
25. Kim SW, Kwon HY, Chi DW, Shim JH, Park JD, Lee YH, Pyo S, Rhee DK. Reversal of P-glycoprotein-mediated multidrug resistance by ginsenoside rg (3). *Biochem Pharmacol* 2003; 65(1): 75-82.
26. Jodoin J, Demeule M, Beliveau R. Inhibition of the multidrug resistance P-glycoprotein activity by green tea polyphenols. *Biochim Biophys Acta* 2002; 1542(1-3): 149-59.
27. Wang EJ, Barecki-Roach M, Johnson WW. Elevation of P-glycoprotein function by a catechin in green tea. *Biochem Biophys Res Commun* 2002 Sep 20;297(2):412-8.
28. Farabegoli F, Papi A, Bartolini G, Ostan R, Orlandi M. (-)-Epigallocatechin-3-gallate downregulates P-gp and BCRP in a tamoxifen resistant MCF-7 cell line. *Phytomedicine* 2010; 17(5): 356-62.
29. Zhang S, Morris ME. Effect of the flavonoids biochanin A and silymarin on the P-glycoprotein-mediated transport of digoxin and vinblastine in human intestinal caco-2 cells. *Pharm Res* 2003; 20(8): 1184-91.
30. Zhang S, Morris ME. Effects of the flavonoids biochanin A, morin, phloretin, and silymarin on P-glycoprotein-mediated transport. *J Pharmacol Exp Ther* 2003; 304(3): 1258-67.
31. Quiney C, Billard C, Faussat AM, Salanoubat C, Kolb JP. Hyperforin inhibits P-gp and BCRP activities in chronic lymphocytic leukaemia cells and myeloid cells. *Leuk Lymphoma* 2007; 48(8): 1587-99.
32. Perloff MD, von Moltke LL, Stormer E, Shader RI, Greenblatt DJ. Saint John's wort: An *in vitro* analysis of P-glycoprotein induction due to extended exposure. *Br J Pharmacol* 2001; 134(8): 1601-8.
33. Tian R, Koyabu N, Morimoto S, Shoyama Y, Ohtani H, Sawada Y. Functional induction and de-induction of P-glycoprotein by St. John's wort and its ingredients in a human colon adenocarcinoma cell line. *Drug Metab Dispos* 2005; 33(4): 547-54.
34. Hellum BH, Nilsen OG. *In vitro* inhibition of CYP3A4 metabolism and P-glycoprotein-mediated transport by trade herbal products. *Basic Clin Pharmacol Toxicol* 2008; 102(5): 466-75.
35. Berginc K, Kristl A. The mechanisms responsible for garlic - drug interactions and their *in vivo* relevance. *Curr Drug Metab* 2013; 14(1): 90-101.
36. An G, Gallegos J, Morris ME. The bioflavonoid kaempferol is an ABCG2 substrate and inhibits ABCG2-mediated quercetin efflux. *Drug Metab Dispos* 2011; 39(3): 426-32.
37. Tamaki H, Satoh H, Hori S, Ohtani H, Sawada Y. Inhibitory effects of herbal extracts on Breast Cancer Resistance Protein (BCRP) and structure-inhibitory potency relationship of isoflavonoids. *Drug Metab Pharmacokinet* 2010; 25(2): 170-9.
38. Zhang S, Yang X, Morris ME. Flavonoids are inhibitors of Breast Cancer Resistance Protein (ABCG2)-mediated transport. *Mol Pharmacol* 2004; 65(5): 1208-16.

39. Allen JD, van Loevezijn A, Lakhai JM, van der Valk M, van Tellingen O, Reid G, Schellens JH, Koomen GJ, Schinkel AH. Potent and specific inhibition of the Breast Cancer Resistance Protein multidrug transporter *in vitro* and in mouse intestine by a novel analogue of fumitremorgin C. *Mol Cancer Ther* 2002; 1(6): 417-25.
40. Kemper EM, Cleypool C, Boogerd W, Beijnen JH, van Tellingen O. The influence of the P-glycoprotein inhibitor zosuquidar trihydrochloride (LY335979) on the brain penetration of paclitaxel in mice. *Cancer Chemother Pharmacol* 2004; 53(2): 173-8.
41. Lankheet NA, Hillebrand MJ, Rosing H, Schellens JH, Beijnen JH, Huitema AD. Method development and validation for the quantification of dasatinib, erlotinib, gefitinib, imatinib, lapatinib, nilotinib, sorafenib and sunitinib in human plasma by liquid chromatography coupled with tandem mass spectrometry. *Biomed Chromatogr* 2013; 27(4): 466-76.
42. Li J, Wang Y, Hidalgo IJ. Kinetic analysis of human and canine P-glycoprotein-mediated drug transport in MDR1-MDCK cell model: Approaches to reduce false-negative substrate classification. *J Pharm Sci* 2013; 102(9): 3436-46.



CHAPTER 5

EFFECTS OF CHINESE HERBAL MEDICINES (CHM) ON CYP3A4-MEDIATED METABOLISM OF ANTICANCER DRUGS





5.1

EFFECT OF CHINESE HERBS ON CYP3A4 ACTIVITY AND EXPRESSION *IN VITRO*

K.D. Mooiman *

C. Lau *

R.F. Maas-Bakker

J.H. Beijnen

J.H.M. Schellens

I. Meijerman

* These authors contributes equally

Published in the Journal of Ethnopharmacology 2013; 149(2): 543-549

ABSTRACT

Traditional Chinese medicine (TCM) has become more popular among cancer patients in the Western world, who often use Chinese herbs as adjuvant therapy to reduce the adverse effects of conventional chemotherapy. However, pharmacokinetic (PK) interactions between Chinese herbs and anticancer drugs can occur and have dramatic consequences for these patients. Currently, only a few possible PK interactions between Chinese herbs and conventional Western drugs have been documented.

Since the drug-metabolizing enzyme cytochrome P450 3A4 (CYP3A4) contributes to most of the PK interactions with (anticancer) drugs, the effect of four Chinese herbs (*Oldenlandia diffusa*, *Codonopsis tangshen*, *Rehmannia glutinosa* and *Astragalus propinquus*) on the activity and expression of CYP3A4 was investigated *in vitro*.

Ethanol and water-ethanol extracts of the four Chinese herbs were prepared from raw material. CYP3A4 inhibition was assessed by the use of Supersomes™ in a fluorescence assay. Furthermore, CYP3A4 induction was evaluated in a human pregnane X receptor (hPXR)-mediated CYP3A4 reporter gene assay and a quantitative real time PCR assay, both in human colon adenocarcinoma-derived LS180 cells (LS180).

Extracts of *Oldenlandia diffusa*, *Codonopsis tangshen*, *Rehmannia glutinosa* and *Astragalus propinquus* inhibited CYP3A4 in human CYP3A4 Supersomes™ (IC₅₀ values: 17-83 µg/mL). *Oldenlandia diffusa* and *Rehmannia glutinosa* significantly induced PXR-mediated CYP3A4 ($p < 0.001$). *Oldenlandia diffusa* also significantly induced CYP3A4 mRNA levels ($p < 0.001$ at 250 µg/mL).

Concomitant use of *Oldenlandia diffusa* and *Rehmannia glutinosa* could result in induction of CYP3A4 leading to a reduced efficacy of drugs that are CYP3A4 substrates and have a narrow therapeutic window. Because of the possible enhanced toxicity caused by CYP3A4 inhibition, clinical effects of CYP3A4 inhibition by *Astragalus propinquus* and *Codonopsis tangshen* must also be taken into account. In conclusion, herb-drug interactions between Chinese herbs and various CYP3A4 substrates can occur. Further research to investigate the clinical relevance of the interactions caused by *Oldenlandia diffusa*, *Codonopsis tangshen*, *Rehmannia glutinosa* and *Astragalus propinquus* is required.

INTRODUCTION

Chinese herbs are part of traditional Chinese medicine (TCM) and have been used for thousands of years in China¹. Recently, Chinese herbs have become more popular in the Western world². Cancer patients use TCM treatments to improve general health, to strengthen immunity, to reduce side effects of conventional cancer therapies and to increase quality of life²⁻⁴. Moreover, patients appreciate the more personal approach of TCM in contrast to most Western standard therapies^{2,4}. The application of TCM is not only restricted to cancer, but can also be found in other diseases such as rheumatoid arthritis, obesity and HIV/AIDS⁵⁻⁷.

When patients use Chinese herbs and Western drugs together, these herbs can cause unwanted pharmacodynamic (PD) interactions. For example, concomitant use of warfarin and several Chinese herbs such as *Angelica sinensis* (dong quai), *Salvia miltiorrhiza* (dan shen), ginseng (ren shen) and *Ginkgo biloba* (yin xing) has been shown to cause an increased INR (international normalized ratio) and more extensive bleeding as a result of the anticoagulation and antiplatelet properties of these herbs^{8,9}.

In addition, Chinese herbs can also cause pharmacokinetic (PK) interactions via drug metabolizing enzymes¹⁰, such as the phase I metabolizing CYP450 (cytochrome P450) enzyme family. Of this family, CYP3A4 is considered the most important enzyme because it is responsible for the metabolism of most currently available drugs^{11,12}. Inhibition of CYP3A4 can lead to increased plasma levels of drugs that are substrates for CYP3A4 and thus can cause toxicity. In contrast, induction of this enzyme can result in decreased plasma levels of these drugs and consequently reduce their efficacy. Since numerous anticancer, immunosuppressive and antiviral drugs have a small therapeutic window, PK interactions between Chinese herbs and Western drugs can have dramatic consequences. Although Chinese herbs have the potential to generate PK and PD interactions, patients generally consider them to be safe because of their natural origin². Moreover, interactions between TCM and Western drugs are under-reported and little is known about the risks and effects of these interactions^{8,13}.

The Chinese herbs *Oldenlandia diffusa* (bai hua she she cao), *Codonopsis tangshen* (dang shen), *Rehmannia glutinosa* (sheng di huang), and *Astragalus propinquus* (huang qi) are frequently used for various clinical indications in TCM, including cancer^{6,14-19}. Previously, it was reported that *Rehmannia glutinosa* and *Astragalus propinquus* can inhibit CYP3A4 in human microsomes^{20,21}. In the present study, the effect of all four herbs on both CYP3A4 activity and expression was investigated *in vitro*. Based on the results, clinical studies can be designed to determine the clinical relevance of possible interactions. Eventually, new clinical guidelines can be established for the safe use of Chinese herbs.

MATERIALS AND METHODS

Materials

Oldenlandia diffusa, *Codonopsis tangshen*, *Rehmannia glutinosa* and *Astragalus propinquus* (Qixin, An Guo, China) were obtained from the Chinese medicine store “Tong Ji Tang” (Arnhem, The Netherlands). Voucher specimens of these herbs were deposited in the Utrecht Institute for Pharmaceutical Sciences, Department of Pharmaceutical Sciences, Division of Pharmaco-epidemiology and Clinical Pharmacology, Utrecht University. The voucher specimen numbers are listed in **Table 1**. *Ginkgo biloba*, ginseng and St. John’s wort were purchased from Chromadex (Santa Ana, CA, USA) as Extract Reference Materials. These materials are referred as standardized extracts and are conformed to the analytical requirements. Rifampicin, resazurin and ketoconazole were obtained from Sigma Aldrich (St. Louis, MO, USA). cDNA-expressed CYP3A4 + reductase + b5 Supersomes™ and 7-benzyloxy-4-(trifluoromethyl)-coumarin (BFC) were purchased from BD Biosciences (Woburn, MA, USA). The CYP3A4 luciferase reporter construct (pGL3-CYP3A4-XREM) and the nuclear receptor expression vector (pCDG-hPXR) were generously provided by Professor Kim (University of Western Ontario, London, ON, Canada) and Professor Evans (Salk Institute, La Jolla, USA), respectively. Renilla luciferase expression control vector (pRL-TK) was purchased from Promega (Madison, WI, USA). Plasmids were purified with Promega’s Pureyield Midi-prep according to the instructions of the manufacturer. Dual-Luciferase® Reporter (DLR) Assay System was purchased from Promega.

Table 1. General information of selected Chinese herbs.

Latin name	Family	Plant part used	Voucher specimen
<i>Oldenlandia diffusa</i> (Willd.) Roxb. Syn. <i>Hedyotis diffusa</i> (Willd.) Roxb.	Rubiaceae	Herbal	DDW.ARC.6.5.1
<i>Codonopsis tangshen</i> Oliv.	Campanulaceae	Root	DDW.ARC.6.5.2
<i>Rehmannia glutinosa</i> (Gaertn.) DC Syn. <i>Rehmannia glutinosa</i> (Gaertn.) Libosch. ex Fisch & C.A. Mey	Plantaginaceae	Root	DDW.ARC.6.5.3
<i>Astragalus propinquus</i> Schischk. Syn. <i>Astragalus membranaceus</i> (Fisch.) Bge. var. <i>Mongholicus</i> (Bge.) Hsiao	Leguminosae	Root	DDW.ARC.6.5.4

Cell culture

Human colon adenocarcinoma-derived LS180 cells (LS180) were obtained from ATCC (Wesel, Germany). Roswell Park Memorial Institute 1640 (RPMI-1640) medium with 25 mM HEPES and L-glutamine was obtained from PAA Laboratories GmbH (Pasching, Austria) and supplemented with 100 U/mL penicillin, 100 µg/mL streptomycin and 10% fetal

bovine serum. Cells were cultured and maintained in a Hera-cell incubator from Heraeus (Langensfeld, Germany) at 37°C in a humidified atmosphere with 5% CO₂.

Preparation of herbal extracts

To enhance the homogeneity of the samples, herbs were thoroughly grinded by using a laboratory mill (IKA MF 10.1, IKA Laboratory Equipment, Staufen, Germany). To prepare the extraction, 10.0 g of the herbs was suspended in 100 mL absolute ethanol (EtOH) from Merck (Darmstadt, Germany). All extracts were then boiled under reflux for 40 min. After cooling, the extracts were centrifuged at 700 g for 5 min, filtrated and dried under reduced pressure using a rotation evaporator. After determining the exact yield of every extraction based on the recovered mass, the obtained extracts were either reconstituted in EtOH or in water-EtOH with different percentages of EtOH, depending on the solubility of the extract. The yields and composition of the water-EtOH fractions are shown in **Table 2**. The extracts were stored at -30°C until further use.

Table 2. Extraction yields of herbs and composition of water-EtOH fractions.

Herb name	Yield (%)	% EtOH in water-EtOH fraction
<i>Oldenlandia diffusa</i>	3.5	100 *
<i>Codonopsis tangshen</i>	40.5	45
<i>Rehmannia glutinosa</i>	2.5	40
<i>Astragalus propinquus</i>	13.7	65

* *Oldenlandia diffusa* could be completely reconstituted in EtOH only.

CYP3A4 inhibition (fluorometric assay)

The fluorometric CYP3A4 inhibition assay is based on the method as described by Miller *et al.*²². Serial dilutions of herbal extracts and ketoconazole (a CYP3A selective positive control inhibitor²³) were pre-incubated with 1 mg/mL NADPH in 0.05 M potassium phosphate buffer (pH 7.4) containing 4% acetonitrile at 37°C for 15 min. The SupersomesTM (5 nM) were incubated with herbal extracts and 50 µM BFC (substrate for CYP3A) in a total volume of 200 µL at 37°C for 30 min. The conversion of BFC into 7-hydroxy-4-trifluoromethylcoumarin (HFC) was stopped by adding 75 µL of 80% acetonitrile/20% 0.5 M Tris. CYP3A4 activity was measured with a Mithras LB 940 microplate reader (Berthold Technologies, Bad Wildbad, Germany) at excitation/emission wavelengths of 405/535 nm. Results were normalized to maximal activity.

CYP3A4 induction (reporter gene assay)

The human pregnane X receptor (hPXR)-mediated CYP3A4 reporter gene assay was performed as described by Harmsen *et al.*²⁴ with a minor modification. In short, LS180

cells were transfected with the three plasmids pGL3-CYP3A4-XREM (a luciferase reporter construct containing human CYP3A4), pCDG-hPXR (a nuclear receptor expression vector containing human PXR) and pRL-TK (a control *Renilla reniformis* luciferase reporter vector) using 0.8 μL Nanofectin transfection reagents (PAA) per well. After 24 h, cells were washed with PBS and exposed to herbal extract concentrations of 33, 100 or 250 $\mu\text{g}/\text{mL}$ in RPMI-1640 medium for 24 h at $37^\circ\text{C}/5\% \text{CO}_2$. The herbal extract of *Oldenlandia diffusa* was reconstituted in DMSO, the most preferred solvent for the reporter gene assay. Since the other extracts contained water that could not completely evaporate, these fractions were reconstituted in EtOH. Rifampicin (10 μM) was included as a model inducer of CYP3A4²⁵, as well as *Ginkgo biloba*, ginseng and St. John's wort^{26, 27} (all in DMSO). The final organic solvent concentrations (DMSO or EtOH) were 0.3% v/v.

After 24 h incubation, medium was removed and 25 $\mu\text{L}/\text{well}$ of passive lysis buffer from Promega was used to lyse the cells. Volumes of 10 μL of the lysates were measured with Mithras LB 940 microplate reader using the DLR™ Assay System according to the manufacturer's instructions. The fold of induction was calculated after normalizing the ratio Firefly-luciferase to Renilla-luciferase signal.

Cell viability (Alamar Blue assay)

The reporter gene assay was combined with an Alamar Blue assay to test cell viability. After exposing LS180 cells to herbs for 24 h, medium was removed and cells were incubated with 200 $\mu\text{L}/\text{well}$ resazurin in culture medium (50 μM) for 3 h at $37^\circ\text{C}/5\% \text{CO}_2$. Fluorescence was measured with Mithras LB 940 microplate reader at excitation/emission wavelengths of 530/600 nm. To determine the cell viability, the fluorescence after incubations with the herbs was normalized to the fluorescence to the control incubations without herbs. According to the cell viability assay, the applied concentrations of all tested compounds were not cytotoxic (data not shown).

CYP3A4 induction of *Oldenlandia diffusa* (Quantitative real time PCR assay)

Oldenlandia diffusa was also investigated for its ability to induce mRNA levels of CYP3A4 *in vitro*. LS180 cells (2.5×10^5 cells/well) were exposed to extracts of *Oldenlandia diffusa* (33 $\mu\text{g}/\text{mL}$, 100 $\mu\text{g}/\text{mL}$ and 250 $\mu\text{g}/\text{mL}$ in DMSO) in 12-well plates from Greiner Bio-one B.V. (Alphen a/d Rijn, The Netherlands) for 24 h. *Ginkgo biloba* (250 $\mu\text{g}/\text{mL}$), ginseng (250 $\mu\text{g}/\text{mL}$) and rifampicin (10 μM) were included as positive controls. For all exposures, the DMSO concentration was 0.3% v/v. Cells were washed with PBS and the SV Total RNA Isolation System from Promega was used to isolate total RNA. The quality and integrity of RNA was checked with the Nanodrop Diode Array Spectrophotometer from Isogen Life Science (IJsselstein, The Netherlands). Total RNA was reverse transcribed and mRNA expression levels of CYP3A4 and 18S were quantitatively analyzed by RT-PCR as described by Harmsen *et al.*²⁴.

Statistical analysis

IC₅₀ calculations were performed with GraphPad Prism 4.0 (GraphPad Software, San Diego, USA). Statistical analyses were performed with SPSS 16.0 (two tailed Student's t-test, $\alpha=0.05$).

RESULTS

CYP3A4 inhibition

Supersomes™ were incubated with the four Chinese herbs to assess their ability to inhibit CYP3A4. From the tested herbs, *Oldenlandia diffusa* was the most potent inhibitor of CYP3A4 activity (**Figure 1B**). *Codonopsis tangshen*, *Rehmannia glutinosa* and *Astragalus propinquus* also inhibited CYP3A4 activity *in vitro*, but to a lesser extent (**Figure 1C-E**). The IC₅₀ values of the herbal extracts ranged from 17 to 83 µg/mL (**Table 3**). These values were much larger than the IC₅₀ of the positive control inhibitor ketoconazole (0.15 µg/mL).

Table 3. The IC₅₀ values of ketoconazole and the four herbs in human CYP3A4 Supersomes™.

Herb name	IC ₅₀ (µg/mL) [95% CI]	R ² *
Ketoconazole	0.15 [0.12-0.19]	> 0.99
<i>Oldenlandia diffusa</i>	17 [5.6-51]	0.99
<i>Codonopsis tangshen</i>	83 [26-269]	0.96
<i>Rehmannia glutinosa</i>	46 [23-89]	0.98
<i>Astragalus propinquus</i>	61 [36-103]	0.99

* The R² values determine the correlation of non-linear (sigmoidal) regression.

CYP3A4 induction (reporter gene assay)

To investigate whether the four herbs were able to induce CYP3A4 *in vitro*, a reporter gene assay was applied. *Oldenlandia diffusa* and *Rehmannia glutinosa* induced CYP3A4 *in vitro* in dose-dependent manner. *Oldenlandia diffusa* induced CYP3A4 9.5 ± 1.6 times at the highest concentration (**Figure 2A**), which was as strong as the induction by the well-known model inducer rifampicin (upregulation 7.9 ± 1.1 fold). It was also as potent as the CYP3A4 induction caused by St. John's wort and *Ginkgo biloba* (**Figure 3**). *Rehmannia glutinosa* induced CYP3A4 moderately, but nevertheless significantly; the fold of induction was 6.9 ± 1.3 at the highest concentration (**Figure 2B**). The other two herbs hardly induced CYP3A4 (data not shown).

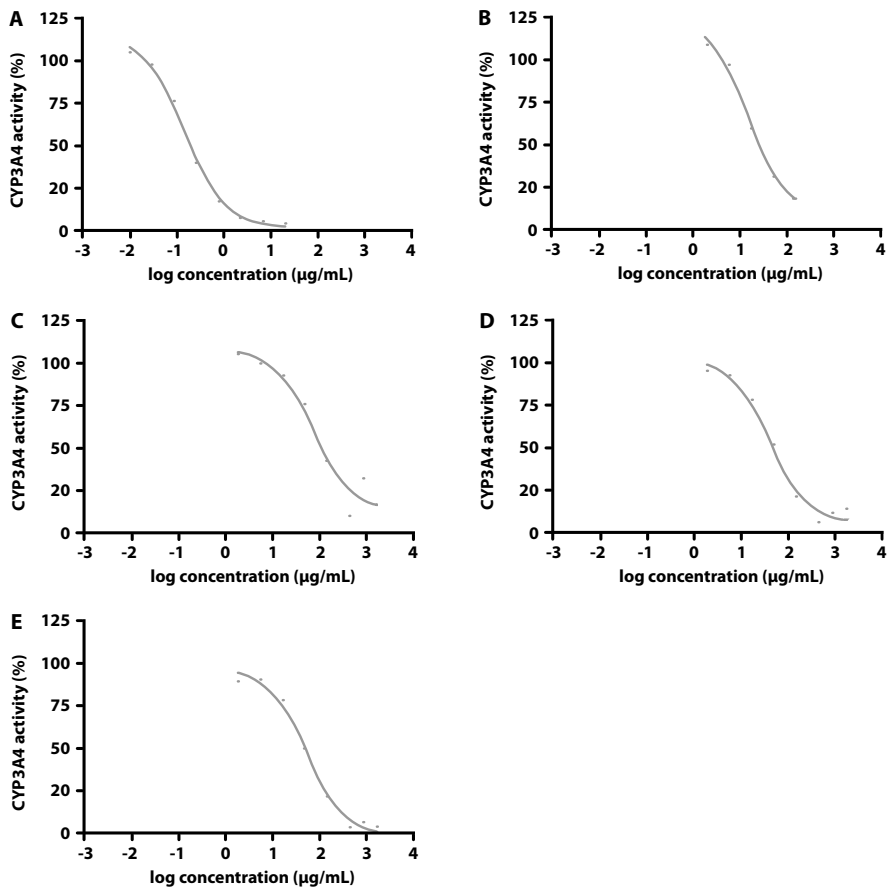


Figure 1. The inhibiting effect of ketoconazole, a positive control inhibitor for CYP3A4 (A), *Oldenlandia diffusa* (B), *Codonopsis tangshen* (C), *Rehmannia glutinosa* (D) and *Astragalus propinquus* (E) on CYP3A4 activity in human CYP3A4 Supersomes™. All experiments were performed twice. Results are shown from one representative experiment. All measurements within the experiments were performed in duplicate. The IC_{50} values of the herbs are shown in **Table 3**.

CYP3A4 induction by *Oldenlandia diffusa* (Quantitative real time PCR assay)

The reporter gene assay indicated *Oldenlandia diffusa* as the most potent CYP3A4-inducer of all tested herbs. Therefore, this herb was also tested for its ability to upregulate mRNA levels of CYP3A4. Indeed, *Oldenlandia diffusa* significantly induced mRNA levels of CYP3A4 after 24 h ($p < 0.001$ at 250 $\mu\text{g/mL}$). The upregulation ranged from 3.5 to 5-fold at concentrations of 33 and 100 $\mu\text{g/mL}$, respectively. At a concentration of 250 $\mu\text{g/mL}$ there was a 16-fold upregulation of the CYP3A4 mRNA levels. *Oldenlandia diffusa* had at least the same potency as rifampicin and ginseng to upregulate CYP3A4 mRNA (**Figure 4**).

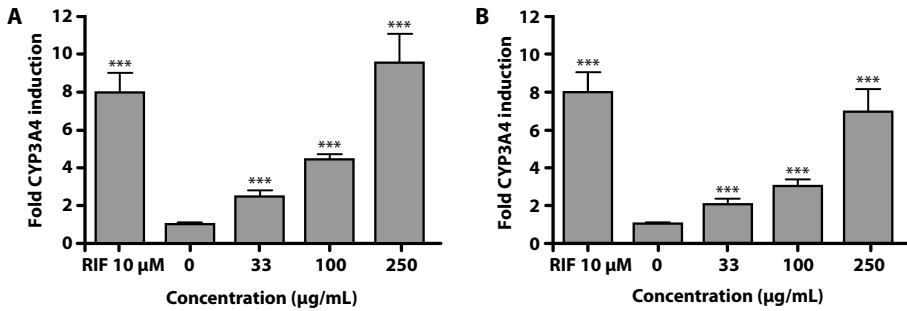


Figure 2. The effect of *Oldenlandia diffusa* (A) and *Rehmannia glutinosa* (B) on CYP3A4 induction in LS180 cells after 24 h. 10 µM rifampicin (RIF) was included as positive control. Values are in mean \pm SD (n=4). * $p < 0.05$; ** $p < 0.01$; *** $p < 0.001$.

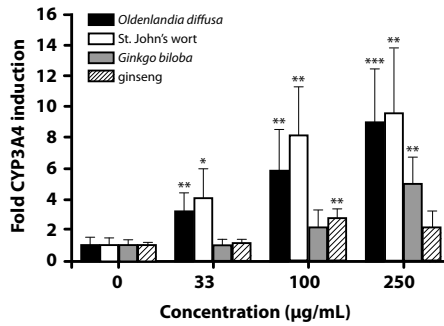


Figure 3. The effect of *Oldenlandia diffusa* on CYP3A4 induction compared to reference CYP3A4 inducers St. John's wort, *Ginkgo biloba* and ginseng. Values are in mean \pm SD (n=4). * $p < 0.05$; ** $p < 0.01$; *** $p < 0.001$.

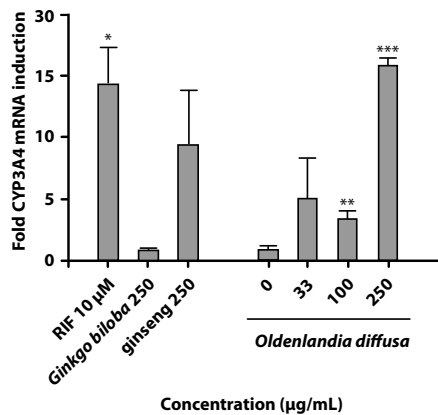


Figure 4. The effect of *Oldenlandia diffusa* on CYP3A4 mRNA levels in LS180 cells after 24 h compared to reference CYP3A4 inducers rifampicin (RIF), *Ginkgo biloba* and ginseng. Values are in mean \pm SD (n=3). * $p < 0.05$; ** $p < 0.01$; *** $p < 0.001$.

DISCUSSION

Although PK interactions between Chinese herbs and Western drugs can occur, little is known about the risks and effects of these interactions. Therefore, four commonly used Chinese herbs were selected to investigate their effect on the activity and expression of CYP3A4, the most relevant drug-metabolizing enzyme. *Oldenlandia diffusa* significantly induced both PXR-mediated CYP3A4 and CYP3A4 mRNA levels. Furthermore, *Rehmannia glutinosa* was shown to significantly induce CYP3A4 in the reporter gene assay, which is in accordance with the results of Yu *et al.*¹⁰. *Oldenlandia diffusa*, *Codonopsis tangshen*, *Rehmannia glutinosa* and *Astragalus propinquus* all slightly inhibited CYP3A4 activity (IC_{50} values: 17-83 $\mu\text{g/mL}$ compared to 0.15 $\mu\text{g/mL}$ for ketoconazole).

The results of the present study indicated that the strength of the CYP3A4 induction caused by *Oldenlandia diffusa* was as strong as observed with rifampicin and St. John's wort, two very potent CYP3A4-inducers and well-known in clinical setting. Concomitant use of rifampicin or St. John's wort and a CYP3A4 substrate was shown to decrease plasma levels of CYP3A4 substrates, such as the anticancer drug imatinib, the immunosuppressant cyclosporine and the antiviral drug indinavir^{28, 29}. Therefore, clinical PK interactions caused by *Oldenlandia diffusa* are highly probable.

The mechanism underlying CYP3A4 induction by *Oldenlandia diffusa* and *Rehmannia glutinosa* is probably PXR-mediated, as suggested by Yu *et al.* for *Rehmannia glutinosa*¹⁰. In our study, *Rehmannia glutinosa* and *Oldenlandia diffusa* were able to both inhibit and induce CYP3A4 in separate systems. Previously, it was shown that hyperforin, the constituent of St. John's wort, was mainly responsible for PXR activation and CYP3A4 induction, but this constituent was also able to inhibit CYP3A4 activity *in vitro* after short-term exposure³⁰. In clinical setting, St. John's wort is well known for its inducing effects during long-term use. As an analogy to St. John's wort, it is likely that *Rehmannia glutinosa* and *Oldenlandia diffusa* are able to inhibit CYP3A4 during short exposure, but primarily induce CYP3A4 activity during prolonged exposure. To determine its overall effect *in vivo*, follow-up experiments in patient populations are required.

The results of our study supported the CYP3A4 inhibition capacities of *Astragalus propinquus* and *Rehmannia glutinosa* in pooled human microsomes reported by previous studies^{20, 21}. While in other studies either *Astragalus propinquus*²¹ or *Rehmannia glutinosa*²⁰ was determined to be a stronger inhibitor than the other herb, in our study the inhibition strengths of both herbs were the same. Pao *et al.* also confirmed the inhibiting effect of *Astragalus propinquus* on CYP3A in rats. However, due to a large interindividual variability in CYP3A4 activity and a low power, the increased C_{max} and AUC were not significantly different²¹.

The mentioned interactions between the tested Chinese herbs and CYP3A4 will only have clinical relevance, if the minimal concentration needed to cause these interactions

is reached *in vivo*. Taken into account that the extraction yields of most herbs were low (3-14%), the overall oral bioavailability of the herbs is estimated to be poor. Furthermore, drugs can have a wide range of volumes of distribution (Vd), depending whether they deeply penetrate into tissues (e.g. imipramine: 21 L/kg in human) or reside in extracellular fluid (e.g. ibuprofen: 0.15 L/kg in human)³¹. Since the applied extraction solvents (EtOH and water-EtOH) are polar, the penetration of the extracted herbal compounds into tissues is assumed to be low. To simulate a small amount of penetration in the tissues, alfentanil was used as a model compound for calculations. The Vd of alfentanil is 53 L³², slightly higher than the total body water volume of 42 L³³ (calculations based on a 30-year-old man with height 175 cm and weight of 70 kg). When using a Vd of 53 L and the extraction yields, a total amount of 11 g *Codonopsis tangshen*, 24 g *Astragalus propinquus*, 26 g *Oldenlandia diffusa*, or 98 g *Rehmannia glutinosa* is needed to inhibit 50% of CYP3A4 effectively. In addition, 50 g of *Oldenlandia diffusa* and 70 g of *Rehmannia glutinosa* is required to establish the CYP3A4 induction caused by 33 µg/mL of these herbal extracts.

Although PK interactions between these herbs and CYP3A4 substrates are only expected when high amounts of herbs are used, they may have clinical relevance at lower doses. Despite the low overall oral availability, the herbal compounds that are responsible for altering CYP3A4 activity can have a high oral availability. If these compounds accumulate in the systemic circulation, lower amounts of herbs can be sufficient for herb-drug interactions. Therefore, further research is required to discover the responsible inhibiting or inducing compounds and their oral bioavailability. Furthermore, these herbs can affect CYP3A4 activity, even when they have a low probability to reach high systemic concentrations. Since CYP3A4 is not only located in the liver but also widely present in the gastrointestinal tract, local interactions between the Chinese herbs and CYP3A4 can occur. As most orally administered drugs are absorbed in the gastrointestinal tract, an altered intestinal CYP3A4 activity could have clinical relevance.

Various batches in Chinese herbs can have different compositions of ingredients, including the compounds that are able to alter CYP3A4 activity. Therefore, various batches can have different effects in herb-drug interactions. As reported for *Rehmannia glutinosa* in the literature³⁴, the processing of raw herbs can lead to differences in herb compositions among the batches. As a follow-up, more different batches of *Oldenlandia diffusa* and *Rehmannia glutinosa* need to be compared for the assessment of CYP3A4 induction activity.

As a limitation of the present study, individual compounds of the four herbs were not isolated and tested on CYP3A4 induction and inhibition. Therefore, it cannot be determined what compounds of the four herbs are responsible for their effect on CYP3A4 activity and whether this correlates with the differences in experimental outcomes. Another limitation is that the extracts were prepared in EtOH or water-EtOH. This may

differ from the traditional use of the herb extracts in water only. Chan *et al.* suggested a method to predict herb-drug interactions. In short, this includes the incorporation of herbal chemical databases to identify ingredients of Chinese herbs. After generating the structures of the compounds, modeling can be applied to predict possible PK interactions³⁵.

Overall, concomitant use of *Codonopsis tangshen* and *Astragalus propinquus* with a CYP3A4 substrate could lead to higher concentrations of CYP3A4 substrates, which could result in an enhanced toxicity. During long-term use, *Oldenlandia diffusa* and *Rehmannia glutinosa* might cause induction of CYP3A4 and reduce the efficacy of therapy. In clinical setting, dose adaptation of drugs that are CYP3A4 substrates might be needed for patients who use these herbs. To assess the clinical relevance of the findings observed in this study, it will be useful to investigate frequently used herbal formulations that contain these herbs, as Chinese herbs are often administered together in herbal formulations. It is possible that the potential interactions in a formulation will have a less serious clinical impact compared to the single herbs. Finally, potential Chinese herb-drug interactions need to be assessed *in vivo*. For example, cancer patients who already use Chinese herbs in addition to their chemotherapy can be appropriate candidates to assess PK interactions between Chinese herbs and conventional anticancer drugs.

CONCLUSION

The four selected Chinese herbs (*Oldenlandia diffusa*, *Codonopsis tangshen*, *Rehmannia glutinosa* and *Astragalus propinquus*) affected CYP3A4 activity *in vitro* and could cause PK interactions with Western drugs that are CYP3A4 substrates. *Oldenlandia diffusa* and *Rehmannia glutinosa* significantly enhanced CYP3A4 activity. In addition, all selected herbs inhibited CYP3A4 activity. Based on these results, it is important to make clinicians aware of the possible risks when patients concomitantly use *Oldenlandia diffusa*, *Codonopsis tangshen*, *Rehmannia glutinosa* or *Astragalus propinquus* with drugs that are CYP3A4 substrates. To determine the clinical relevance of the proposed interactions, follow-up studies are needed.

REFERENCES

1. Leung AY. Traditional toxicity documentation of Chinese Materia Medica: an overview. *Toxicol Pathol* 2006; 34(4): 319-26.
2. Youns M, Hoheisel JD, Efferth T. Toxicogenomics for the prediction of toxicity related to herbs from traditional Chinese medicine. *Planta Med* 2010; 76(17): 2019-25.
3. Wong R, Sagar CM, Sagar SM. Integration of Chinese medicine into supportive cancer care: A modern role for an ancient tradition. *Cancer Treat Rev* 2001; 27(4): 235-46.
4. Xu W, Towers AD, Li P, Collet JP. Traditional Chinese medicine in cancer care: Perspectives and experiences of patients and professionals in China. *Eur J Cancer Care* 2006; 15(4): 397-403.
5. Sui Y, Zhao HL, Wong VC, Brown N, Li XL, Kwan AK, Hui HL, Ziea ET, Chan JC. A systematic review on use of Chinese medicine and acupuncture for treatment of obesity. *Obes Rev* 2012; 13(5): 409-30.
6. Wang J, Zou W. Practices, challenges, and opportunities: HIV/AIDS treatment with traditional Chinese medicine in China. *Front Med* 2011; 5(2): 123-6.
7. Zhang P, Li J, Han Y, Yu XW, Qin L. Traditional Chinese medicine in the treatment of rheumatoid arthritis: A general review. *Rheumatol Int* 2010; 30(6): 713-8.
8. Fugh-Berman A. Herb-drug interactions. *Lancet* 2000; 355(9198): 134-8.
9. Izzo AA. Herb-drug interactions: An overview of the clinical evidence. *Fundam Clin Pharmacol* 2005; 19(1): 1-16.
10. Yu C, Chai X, Yu L, Chen S, Zeng S. Identification of novel pregnane X receptor activators from traditional Chinese medicines. *J Ethnopharmacol* 2011; 136(1): 137-43.
11. Pal D, Mitra AK. MDR- and CYP3A4-mediated drug-herbal interactions. *Life Sci* 2006; 78(18): 2131-45.
12. Scripture CD, Figg WD. Drug interactions in cancer therapy. *Nat Rev Cancer* 2006; 6(7): 546-58.
13. Fasinu PS, Bouic PJ, Rosenkranz B. An overview of the evidence and mechanisms of herb-drug interactions. *Front Pharmacol* 2012; 3: 69.
14. Gupta S, Zhang D, Yi J, Shao J. Anticancer activities of *Oldenlandia diffusa*. *J Herb Pharmacother* 2004; 4(1): 21-33.
15. Hsiao WL, Liu L. The role of traditional Chinese herbal medicines in cancer therapy: from TCM theory to mechanistic insights. *Planta Med* 2010; 76(11): 1118-31.
16. McCulloch M, Broffman M, van der Laan M, Hubbard A, Kushi L, Kramer A, Gao J, Colford JM, Jr. Lung cancer survival with herbal medicine and vitamins in a whole-systems approach: Ten-year follow-up data analyzed with marginal structural models and propensity score methods. *Integr Cancer Ther* 2011; 10(3): 260-79.
17. Qi F, Li A, Inagaki Y, Gao J, Li J, Kokudo N, Li XK, Tang W. Chinese herbal medicines as adjuvant treatment during chemo- or radiotherapy for cancer. *Biosci Trends* 2010; 4(6): 297-307.
18. Tang W, Hemm I, Bertram B. Recent development of antitumor agents from Chinese herbal medicines. part II. high molecular compounds (3). *Planta Med* 2003; 69(3): 193-201.
19. Zhong Y. Alternative and complementary therapies for cancer. In: *Ovarian cancer*, M. Alaoui-Jamali, editor: 2010.
20. Or PM, Lam FF, Kwan YW, Cho CH, Lau CP, Yu H, Lin G, Lau CB, Fung KP, Leung PC, et al. Effects of *Radix astragali* and *Radix rehmanniae*, the components of an anti-diabetic foot ulcer herbal formula, on metabolism of model CYP1A2, CYP2C9, CYP2D6, CYP2E1 and CYP3A4 probe substrates in pooled human liver microsomes and specific CYP isoforms. *Phytomedicine* 2012; 19(6): 535-44.
21. Pao LH, Hu OY, Fan HY, Lin CC, Liu LC, Huang PW. Herb-drug interaction of 50 Chinese herbal medicines on CYP3A4 activity *in vitro* and *in vivo*. *Am J Chin Med* 2012; 40(1): 57-73.

22. Miller VP, Stresser DM, Blanchard AP, Turner S, Crespi CL. Fluorometric high-throughput screening for inhibitors of cytochrome P450. *Ann N Y Acad Sci* 2000; 919: 26-32.
23. Greenblatt DJ, Venkatakrishnan K, Harmatz JS, Parent SJ, von Moltke LL. Sources of variability in ketoconazole inhibition of human cytochrome P450 3A *in vitro*. *Xenobiotica* 2010; 40(10): 713-20.
24. Harmsen S, Koster AS, Beijnen JH, Schellens JH, Meijerman I. Comparison of two immortalized human cell lines to study nuclear receptor-mediated CYP3A4 induction. *Drug Metab Dispos* 2008; 36(6): 1166-71.
25. Antolino-Lobo I, Meulenbelt J, Nijmeijer SM, Maas-Bakker RF, Meijerman I, van den Berg M, van Duursen MB. 3,4-methylenedioxyamphetamine (MDMA) interacts with therapeutic drugs on CYP3A by inhibition of pregnane X receptor (PXR) activation and catalytic enzyme inhibition. *Toxicol Lett* 2011; 203(1): 82-91.
26. Hellum BH, Hu Z, Nilsen OG. The induction of CYP1A2, CYP2D6 and CYP3A4 by six trade herbal products in cultured primary human hepatocytes. *Basic Clin Pharmacol Toxicol* 2007; 100(1): 23-30.
27. Malati CY, Robertson SM, Hunt JD, Chairez C, Alfaro RM, Kovacs JA, Penzak SR. Influence of Panax ginseng on cytochrome P450 (CYP)3A and P-glycoprotein (P-gp) activity in healthy participants. *J Clin Pharmacol* 2012; 52(6): 932-9.
28. Borrelli F, Izzo AA. Herb-drug interactions with St John's wort (*Hypericum perforatum*): An update on clinical observations. *AAPS J* 2009; 11(4): 710-27.
29. Niemi M, Backman JT, Fromm MF, Neuvonen PJ, Kivisto KT. Pharmacokinetic interactions with rifampicin: Clinical relevance. *Clin Pharmacokinet* 2003; 42(9): 819-50.
30. Komoroski BJ, Zhang S, Cai H, Hutzler JM, Frye R, Tracy TS, Strom SC, Lehmann T, Ang CY, Cui YY, et al. Induction and inhibition of cytochromes P450 by the St. John's wort constituent hyperforin in human hepatocyte cultures. *Drug Metab Dispos* 2004; 32(5): 512-8.
31. Berezhkovskiy LM. Prediction of drug terminal half-life and terminal volume of distribution after intravenous dosing based on drug clearance, steady-state volume of distribution, and physiological parameters of the body. *J Pharm Sci* 2013; 102(2): 761-71.
32. Lombardo F, Obach RS, Shalaeva MY, Gao F. Prediction of human volume of distribution values for neutral and basic drugs. 2. extended data set and leave-class-out statistics. *J Med Chem* 2004; 47(5): 1242-50.
33. Watson PE, Watson ID, Batt RD. Total body water volumes for adult males and females estimated from simple anthropometric measurements. *Am J Clin Nutr* 1980; 33(1): 27-39.
34. Zhang RX, Li MX, Jia ZP. *Rehmannia glutinosa*: Review of botany, chemistry and pharmacology. *J Ethnopharmacol* 2008; 117(2): 199-214.
35. Chan E, Tan M, Xin J, Sudarsanam S, Johnson DE. Interactions between traditional Chinese medicines and Western therapeutics. *Curr Opin Drug Discov Devel* 2010; 13(1): 50-65.



5.2

LETTER TO THE EDITOR REGARDING 'A PROSPECTIVE,
CONTROLLED STUDY OF BOTANICAL COMPOUND MIXTURE
LCS101 FOR CHEMOTHERAPY-INDUCED HEMATOLOGICAL
COMPLICATIONS IN BREAST CANCER' BY YAAL-HAHOSHEN
ET AL. (THE ONCOLOGIST 2011; 16; 1197-1202)

K.D. Mooiman *

A.K.L. Goey *

I. Meijerman

J.H. Beijnen

J.H.M. Schellens

* These authors contributes equally

Published in The Oncologist 2012; 17(5): 740-741

Based on the results of a prospective, randomized, placebo-controlled study of Yaal-Hahoshen *et al.*¹, the authors concluded that the botanical mixture LCS101 prevented hematological complications in breast cancer patients undergoing anthracycline- and taxane-based chemotherapy. They also concluded that the addition of LCS101 to conventional chemotherapy regimens “is both safe and feasible in patients with early breast cancer, ...”. However, we believe these conclusions should be interpreted with caution as the present study has a few major limitations.

First, the possible pharmacodynamic (PD) effect of LCS101 on the bone marrow was not evaluated directly in the present study. Yaal-Hahoshen *et al.*¹ primarily determined hematological parameters by counting erythrocytes, leukocytes, neutrophils, lymphocytes, and thrombocytes in the peripheral blood. These parameters only secondarily reflect bone marrow function. It would be more accurate to evaluate the growth of progenitor cells such as colony-forming unit (CFU)-granulocytes, erythroids, macrophages and megakaryocytes; burst-forming units-erythroids; and CFU-granulocyte-macrophages².

Currently, the effect of LCS101 on hematopoietic function has barely been investigated. The authors only reported that “addition of LSC101 to doxorubicin led to significantly better peripheral neutrophil counts, and preserved splenic erythrocyte and leukocyte counts” in a mouse breast cancer model. Unfortunately, these data were not published.

For a few individual LCS101 components, however, a PD effect on bone marrow function could be expected. For example, the production of erythroid progenitor cells has been stimulated by *Ophiopogon japonicus* in mice³, and in patients with chronic aplastic anemia hematopoietic recovery has been promoted by *Astragalus membranaceus*⁴. As Yaal-Hahoshen *et al.*¹ reported, it is still unclear what the implications of these activities are for chemotherapy-induced hematological toxicity. Additionally, it is unknown whether the components may interact synergistically or additively with each other, which complicates predicting the effect of LCS101 on hematopoietic function.

Second, in the present study no pharmacokinetic (PK) analysis of the administered anticancer drugs (such as doxorubicin, paclitaxel and docetaxel) was performed. Therefore, it is not possible to exclude possible PK interactions between LCS101 and these anticancer drugs. Regarding the effects of LCS101 on the PK of anticancer drugs, there is no information available because no PK interaction studies with LCS101 have been performed.

However, based on *in vitro* results with individual LCS101 components, PK interactions between LCS101 and anticancer drugs metabolized by cytochrome P450 (CYP) 3A4 cannot be ruled out. Using a reporter gene assay and real-time polymerase chain reaction, six LCS101 components induced pregnane X receptor (PXR)-regulated CYP3A4 transcription in HepG2 cells: *Astragalus membranaceus*, *Poriae cocos*, *Atractylodes macrocephala*, *Lycium chinense*, *Ophiopogon japonicus* and *Paeonia lactiflora*⁵. Furthermore, accord-

ing to our preliminary results based on a reporter gene assay, the LCS101 compound *Oldenlandia diffusa* is also a potent inducer of PXR-regulated CYP3A4 transcription in LS180 cells (unpublished data). Thus, because CYP3A4 is involved in the metabolism of doxorubicin⁶, docetaxel⁷ and paclitaxel⁸, CYP3A4 induction might lead to lower systemic exposure of these anticancer drugs and consequently to the reported lower incidence of hematological toxicities in cancer patients that received LCS101. Therefore, it is important to evaluate the potential PK interactions between LCS101 and anticancer drugs in clinical PK studies.

Third, the PD effect of LCS101 on the tumor, and thus the efficacy of the administered anticancer drugs, was not evaluated. The statement from Yaal-Hahoshen *et al.*¹ that addition of LCS101 to conventional chemotherapy is safe and feasible implies that the antitumor effect of chemotherapy is not negatively affected by LCS101. However, their study did not evaluate possible PD effects of LCS101 on the tumor. This would have provided valuable information because there currently are no clinical data regarding the effects of LCS101 on the antitumor effect of the administered anticancer drugs. It has only been shown for one individual LCS101 component (*Ligustrum lucidum*) that doxorubicin-induced apoptosis was enhanced in human colorectal carcinoma DLD-1 cells⁹. Determination of PD effects of LCS101 on the tumor could have been assessed by tumor size evaluation using Response Evaluation Criteria in Solid Tumors. In the present study, however, the sample size was too small to exclude a PD effect of LCS101 on the tumor. To assess the PD effect of LCS101 on the tumor during neoadjuvant chemotherapy using a noninferior study design, ~ 1,200 patients would be required based on a significance level of 0.05, probability (power) of 0.80, noninferiority margin of 5%, and overall clinical response rate of 86% for chemotherapy with doxorubicin plus cyclophosphamide¹⁰. This is a substantially larger number of patients than the 18 patients who underwent neoadjuvant chemotherapy in the present study.

In conclusion, Yaal-Hahoshen *et al.*¹ claimed that the addition of LCS101 to conventional chemotherapy is safe and feasible in patients with early breast cancer. However, their study lacks essential information regarding the hematoprotective mechanism of action of LCS101, potential PK interactions with chemotherapy, and the PD effects of LCS101 on the tumor. Therefore, we recommend the execution of PK interaction studies with LCS101 and anticancer drugs. In addition, the PD effects of LCS101 on hematopoietic function and on tumors should also be evaluated clinically. Until these studies have been executed, we advise not to combine LCS101 with anticancer drugs.

REFERENCES

1. Yaal-Hahoshen N, Maimon Y, Siegelmann-Danieli N, Lev-Ari S, Ron IG, Sperber F, et al. A Prospective, Controlled Study of the Botanical Compound Mixture LCS101 for Chemotherapy-Induced Hematological Complications in Breast Cancer. *Oncologist* 2011; 16(9): 1197-202.
2. List AF, Brasfield F, Heaton R, Glinsmann-Gibson B, Crook L, Taetle R, et al. Stimulation of hematopoiesis by amifostine in patients with myelodysplastic syndrome. *Blood* 1997; 90(9): 3364-9.
3. Liu LP, Liu JF, Lu YQ. Effects of Sheng-Mai injection on the PRPP synthetase activity in BFU-es and CFU-es from bone marrows of mice with benzene-induced aplastic anemia. *Life Sci* 2001;69(12): 1373-9.
4. Wang MS, Li J, Di HX, Li ZL, Yang SL, Hou W, et al. Clinical study on effect of Astragalus Injection and its immuno-regulation action in treating chronic aplastic anemia. *Chin J Integr Med* 2007; 13(2): 98-102.
5. Yu C, Chai X, Yu L, Chen S, Zeng S. Identification of novel pregnane X receptor activators from traditional Chinese medicines. *J Ethnopharmacol* 2011; 136(1): 137-43.
6. Pal D, Mitra AK. CYP3A4 and MDR mediated interactions in drug therapy. *Clinical Research and Regulatory Affairs* 2006; 23(3-4): 125-63.
7. Chew SC, Singh O, Chen X, Ramasamy RD, Kulkarni T, Lee EJ, et al. The effects of CYP3A4, CYP3A5, ABCB1, ABCC2, ABCG2 and SLCO1B3 single nucleotide polymorphisms on the pharmacokinetics and pharmacodynamics of docetaxel in nasopharyngeal carcinoma patients. *Cancer Chemother Pharmacol* 2011; 67(6): 1471-8.
8. Marsh S, Somlo G, Li X, Frankel P, King CR, Shannon WD, et al. Pharmacogenetic analysis of paclitaxel transport and metabolism genes in breast cancer. *Pharmacogenomics J* 2007; 7(5): 362-5.
9. Zhang JF, He ML, Qi D, Xie WD, Chen YC, Lin MC, et al. Aqueous extracts of Fructus Ligustri Lucidi enhance the sensitivity of human colorectal carcinoma DLD-1 cells to doxorubicin-induced apoptosis via Tbx3 suppression. *Integr Cancer Ther* 2011; 10(1): 85-91.
10. Bear HD, Anderson S, Brown A, Smith R, Mamounas EP, Fisher B, et al. The effect on tumor response of adding sequential preoperative docetaxel to preoperative doxorubicin and cyclophosphamide: preliminary results from National Surgical Adjuvant Breast and Bowel Project Protocol B-27. *J Clin Oncol* 2003; 21(22): 4165-74.



CHAPTER 6

CONCLUSIONS AND PERSPECTIVES



The use of complementary and alternative medicines (CAM) is popular among cancer patients and is generally considered safe. However, in combination with anticancer drugs pharmacokinetic interactions can occur and may result in undertreatment or increased toxicities. Except for St. John's wort, there is little knowledge of the clinical pharmacokinetic interactions between CAM and anticancer drugs. The aim of this thesis was to determine the *in vitro* potency of fourteen frequently used CAM to affect the metabolism and transport of anticancer drugs. Ultimately, the obtained *in vitro* results are useful as first indication for clinical trials to establish the clinical relevance of CAM-anticancer drug interactions.

In literature several *in vitro* studies have been described about the effects of CAM on CYP enzymes and drug efflux transporters. However, due to various reasons, contradictory effects have been reported and it is therefore difficult to compare the effects of CAM on the metabolism and transport of anticancer drugs. The *in vitro* evaluation of CAM for their ability to inhibit or induce Cytochrome P450 (CYP) enzymes or drug efflux transporters is often performed in separate studies for each CAM. The IC_{50} values, determined in these separate studies, cannot be compared because of differences in the phytochemical content of CAM products, equipment, personnel and protocols. In addition, the majority of the published *in vitro* studies determined the effects of CAM on CYP enzymes and drug efflux transporters by using one substrate. Furthermore, predominantly model substrates were used in previous *in vitro* studies and relevant oncolytic substrates were not or scarcely included. However, especially for CYP3A4 and P-glycoprotein (P-gp; ABCB1) it is recommended to use multiple substrates, including anticancer drugs, since the interaction can significantly differ depending on the substrate. Therefore, in this thesis the effect of the same CAM extracts on the metabolism and transport of both model and oncolytic substrates were determined within one *in vitro* study.

Multiple *in vitro* assays were used in this thesis to address this issue. Fluorescence assays were applied to rapidly screen CAM for their ability to inhibit CYP enzymes and drug efflux transporters since these assays are high throughput, sensitive and cost-effective. However, CAM consist of multiple components and some CAM (mainly β -carotene) resulted in quenching of the fluorescence at high concentrations due to solubility problems. To resolve this disadvantage of the fluorescence assays, LC-MS/MS methods were developed to more adequately determine inhibition of CYP enzymes and drug transporters by CAM. These LC-MS/MS methods are more specific and sensitive, but not high throughput. To avoid interference of CAM in the analytical measurement of the substrates (and their metabolites), the use of liquid-liquid extraction (LLE) and prolongation of the retention time of the substrates were required (**Chapter 2.2**). The effects of CAM on CYP3A4-mediated metabolism of midazolam and docetaxel, CYP2C9-mediated

metabolism of tolbutamide and BCRP/P-gp mediated transport of imatinib were determined with newly developed LC-MS/MS methods. In this way, it was possible to confirm the observed effects of CAM on the metabolism and transport of fluorescent substrates.

Other assays were required to assess inhibition of PXR-mediated CYP3A4 induction by known PXR antagonists and CAM. The luciferase reporter gene assay is a suitable alternative to human hepatocytes since a good correlation has been shown between CYP3A4 induction in a reporter gene assay and CYP3A4 expression in hepatocytes^{1,2}. To establish whether the reporter gene assay is suitable and reliable for the discovery of novel PXR antagonists, quantitative real-time polymerase chain reaction (qRT-PCR) in non-transfected cells, computational PXR docking and a LanthaScreen® time-resolved fluorescence resonance energy transfer (TR-FRET) PXR competitive binding assay were conducted (**Chapter 3.1 and 3.2**). The latter two assays were used to specifically examine the affinity of compounds for PXR. Since computational molecular docking is a structure-based method to rapidly and virtually discover PXR ligands³, the estimated binding affinities of compounds were checked with a robust and sensitive Lanthascreen® TR-FRET PXR competitive binding assay. This binding assay is ideal with respect to CAM because it overcomes interference by autofluorescent or precipitated compounds⁴.

Although the potencies of the same standardized CAM extracts to affect the metabolism and transport of multiple (oncolytic) substrates have been compared in this thesis, several limitations complicate the extrapolation of *in vitro* effects to clinical practice (**Chapter 1.2**). First, the phytochemical content of CAM extracts is highly variable among different brands and within batches of the same brand. Therefore, the composition of standardized CAM extracts and commercial CAM products can differ, and subsequently the clinical effects of these products. Second, the bioavailability of CAM extracts is often poor and variable among multiple commercial CAM products. The phytochemical concentrations that significantly affect CYP enzymes and drug efflux transporters *in vitro* are generally not reached in the systemic circulation due to the poor bioavailability. However, CYP3A4, CYP2C9, BCRP and P-gp are also abundant in the gastrointestinal tract and due to the poor bioavailability the intestinal concentration of CAM is higher compared to the concentration in the systemic circulation. Consequently, the absorption of orally administered anticancer drugs from the gastrointestinal tract could be affected due to the local effect of CAM on intestinal CYP enzymes and drug efflux transporters.

Despite all limitations, *in vitro* studies are useful as first tool to discover and select CAM that possibly affect the activity of metabolizing enzymes and drug efflux transporters. When a CAM does not affect the *in vitro* activity of these major players in the metabolism and excretion of drugs, it is plausible that these CAM will not cause clinical CAM-anticancer drug interactions. Especially since the applied *in vitro* concentrations are higher compared to the concentrations that can be reached in human. Furthermore, *in vitro*

studies are currently one of the best available tools to predict clinical CAM-anticancer drug interactions since there are large interspecies differences between animals with regard to the regulation of CYP enzymes and transporter expression and activity^{6,7}.

In the end, clinical studies are required to assess the clinical relevance of the effects of CAM on CYP enzymes and drug efflux transporters since commercial CAM products vary in their bioavailability, drug-releasing properties and phytochemical content. It is recommended to conduct clinical studies with orally administered anticancer drugs since the effect of CAM on intestinal CYP3A4 and P-gp is expected to be more relevant compared to their effect on hepatic CYP3A4 and P-gp due to the poor bioavailability of most CAM.

Milk thistle is the most interesting CAM for clinical follow-up because it was shown to prevent induction of CYP3A4 (**Chapter 3.2**), to inhibit CYP3A4- and CYP2C9-mediated metabolism of multiple model and oncolytic substrates (**Chapter 2.1 and 2.3**), and to inhibit P-gp and BCRP mediated transport of oncolytic substrates (**Chapter 4**). All these processes possibly result in higher plasma levels of anticancer drugs and ultimately milk thistle could even serve as an adjuvant in the treatment of cancer to improve the efficacy of anticancer drugs. Additionally, milk thistle could also be beneficial for cancer patients because silybin was shown to have hepatoprotective and anticancer activities *in vitro*; and was shown to potentiate the effect of classical anticancer drugs *in vitro* and *in vivo*⁸. Furthermore, the results demonstrated grape seed as potent CYP3A4 inhibitor, green tea as potent CYP3A4 and CYP2C9 inhibitor, St. John's wort as potent P-gp inhibitor, and *Oldenlandia diffusa* and St. John's wort as potent CYP3A4 inducers (**Chapter 5.1**). Therefore, also grape seed, green tea, St. John's wort and *Oldenlandia diffusa* are interesting CAM for clinical follow-up.

In addition to the described *in vitro* potencies of fourteen most commonly used CAM to affect the activity of CYP3A4, CYP2C9, P-gp and BCRP, this thesis contributed to the knowledge about important aspects which are crucial when examining the effects of CAM on the metabolism and transport of anticancer drugs. Multiple CAM extracts from the same supplier should be tested within one *in vitro* study due to differences in phytochemical contents among CAM extracts from various suppliers and interlaboratory differences such as used protocols. In this way it is possible to compare the potencies of CAM to affect CYP enzymes and drug efflux transporters and subsequently to select CAM for clinical follow-up. More importantly, multiple combinations of CAM with model and oncolytic substrates should be tested since the inhibition of CYP enzymes and drug efflux transporters is dependent on the substrate. Especially the use of oncolytic substrates is necessary to more adequately predict the pharmacokinetic interactions between CAM and anticancer drugs. All these aspects were incorporated within the

described *in vitro* study, which makes this study unique compared to the conducted *in vitro* studies from literature.

For future *in vitro* research it is recommended to determine which constituents of the evaluated CAM extracts are responsible for the effects on the metabolism and transport of oncolytic substrates. Especially since the phytochemical contents of CAM extracts is highly variable among different brands and within batches of the same brand. When the responsible constituents and combinations of constituents are known, it is possible to more efficiently predict the *in vitro* and clinical effects of CAM extracts from different brands and batches based on their compositions. Furthermore, the bioavailability of CAM constituents should be determined in future to more adequately predict the clinical effects.

Although research about the safety of combining CAM with conventional drugs is generally considered as important, it was challenging to publish our *in vitro* research in pharmacological journals. Part of the pharmacological journals does not consider publishing research with plant extracts or mixtures of compounds, and only accept research of purified chemicals with known structures.

It is possible to publish in journals that are specialized in publishing work with plant extracts, but the readers of these journals are not the major group of interest. The group of interest that should be aware of new insights about the safety of CAM use are physicians and pharmacists, which predominantly read pharmacological journals. Considering the increased use of CAM among cancer patients, this area of research deserves more attention in these journals in order to inform physicians and pharmacists about the safety and risks of concomitant use of CAM and anticancer drugs. In this way, both physicians and pharmacist are able to adequately inform and advise cancer patients about the safety and risks of using CAM in combination with anticancer drugs.

In conclusion, the results of the *in vitro* research described in this thesis are useful as first indication for clinical trials to establish the clinical relevance of the *in vitro* effects of CAM on metabolism and transport of multiple model and oncolytic substrates. For future *in vitro* studies it is recommended to establish the potencies of CAM to affect the metabolism and transport of multiple oncolytic substrates *in vitro*.

Milk thistle is the most interesting CAM for clinical follow-up because milk thistle was shown to convincingly inhibit CYP3A4, CYP2C9, P-gp and BCRP and to prevent induction of CYP3A4. For clinical studies it is recommended to assess pharmacokinetic interactions between CAM and orally administered anticancer drugs in cancer patients as the effects of CAM on intestinal CYP enzymes and drug efflux transporters is probably more relevant due to the poor bioavailability of CAM.

REFERENCES

1. Harmsen S, Koster AS, Beijnen JH, Schellens JH, Meijerman I. Comparison of two immortalized human cell lines to study nuclear receptor-mediated CYP3A4 induction. *Drug Metab Dispos* 2008; 36(6): 1166-71.
2. Luo G, Cunningham M, Kim S, Burn T, Lin J, Sinz M, Hamilton G, Rizzo C, Jolley S, Gilbert D, et al. CYP3A4 induction by drugs: Correlation between a pregnane X receptor reporter gene assay and CYP3A4 expression in human hepatocytes. *Drug Metab Dispos* 2002; 30(7): 795-804.
3. Ekins S, Kholodovych V, Ai N, Sinz M, Gal J, Gera L, Welsh WJ, Bachmann K, Mani S. Computational discovery of novel low micromolar human pregnane X receptor antagonists. *Mol Pharmacol* 2008; 74(3): 662-72.
4. LanthaScreen® TR-FRET pregnane X reporter competitive binding assay. Invitrogen; 2010. Report nr PV 4839.
5. Healan-Greenberg C, Waring JF, Kempf DJ, Blomme EA, Tirona RG, Kim RB. A human immunodeficiency virus protease inhibitor is a novel functional inhibitor of human pregnane X receptor. *Drug Metab Dispos* 2008; 36(3): 500-7.
6. Martignoni M, Groothuis GM, de Kanter R. Species differences between mouse, rat, dog, monkey and human CYP-mediated drug metabolism, inhibition and induction. *Expert Opin Drug Metab Toxicol* 2006; 2(6): 875-94.
7. Li M, Yuan H, Li N, Song G, Zheng Y, Baratta M, Hua F, Thurston A, Wang J, Lai Y. Identification of interspecies difference in efflux transporters of hepatocytes from dog, rat, monkey and human. *Eur J Pharm Sci* 2008; 35(1-2): 114-26.
8. Dzubak P, Hajduch M, Gazak R, Svobodova A, Psotova J, Walterova D, Sedmera P, Kren V. New derivatives of silybin and 2,3-dehydrosilybin and their cytotoxic and P-glycoprotein modulatory activity. *Bioorg Med Chem* 2006; 14(11): 3793-810.



CHAPTER 7

IN SHORT





SUMMARY

The use of complementary and alternative medicines (CAM), such as herbal and dietary supplements, has become more popular among cancer patients. Cancer patients use these supplements for different reasons such as reducing side effects of chemotherapy, improving their quality of life and slowing the progression of cancer. In general, the use of CAM is considered safe. However, concomitant use of CAM and anticancer drugs could result in serious safety issues since CAM have the potential to cause pharmacokinetic interactions with conventional drugs. Especially for anticancer drugs, pharmacokinetic interactions can easily result in a lower therapeutic efficacy or a higher risk of toxicity due to their small therapeutic windows. Except for St. John's wort, there is little knowledge about clinical pharmacokinetic interactions between CAM and anticancer drugs. Consequently, for the majority of CAM it is unknown whether concomitant use with anticancer drugs is safe. To address this issue it is crucial to expand the knowledge of the effects of CAM on the metabolism and transport of anticancer drugs. Therefore the aim of this thesis was to determine the *in vitro* effects of fourteen frequently used CAM on the metabolism and transport of anticancer drugs. Since almost all pharmacokinetic interactions between CAM and anticancer drugs involve cytochrome P450 (CYP) metabolizing enzymes and drug efflux transporters, the *in vitro* studies focused on the inhibition and induction of these enzymes and transporters by CAM.

In general, *in vitro* studies are conducted prior to the execution of clinical studies to establish the possible pharmacokinetic interactions between CAM and anticancer drugs. Therefore, it is important to establish the extrapolatability of *in vitro* data to the clinic. As described in **Chapter 1.2** a literature research was performed to compare the *in vitro* and clinical effects of St. John's wort, garlic, milk thistle and ginseng on CYP3A4. The published *in vitro* results of both St. John's wort and garlic were extrapolatable to the clinic. However, the inhibition of CYP3A4 by milk thistle and ginseng reported in several *in vitro* studies was not reproducible in previously performed clinical studies. These differences could be caused by several factors, such as the poor bioavailability of CAM and the intra- and interproduct variation in the phytochemical contents of CAM. Although the extrapolatability of *in vitro* data is poor for part of the CAM, *in vitro* data are useful as a first indication for clinical studies to select CAM that possibly result in clinical relevant CAM-anticancer drug interactions.

The *in vitro* studies described in **Chapter 2.1** and **2.3** focused on the inhibition of CYP3A4 and CYP2C9, since these enzymes are the major metabolizers of anticancer drugs. The inhibiting effect of CAM on the metabolism of multiple CYP3A4 and CYP2C9 substrates was evaluated within one *in vitro* study in order to compare the inhibitory potencies. Green tea and milk thistle were shown to convincingly inhibit both CYP3A4 and CYP2C9 activity and grape seed inhibited only CYP3A4.

Besides inhibition of CYP enzymes, the induction of these enzymes can also have serious consequences for cancer patients. Plasma levels of anticancer drugs might decrease,

subsequently resulting in a reduced therapeutic efficacy of anticancer drugs. We focused on the induction of CYP3A4, because this enzyme metabolizes the majority of the anticancer drugs and is highly inducible. More importantly, multiple anticancer drugs such as paclitaxel and erlotinib are also known to induce CYP3A4. The obtained *in vitro* results from this thesis identified St. John's wort and β -carotene as strong CYP3A4 inducers and Ginkgo biloba as moderate CYP3A4 inducer. Since the induction of CYP3A4 is mainly regulated by the Pregnane X Receptor (PXR), PXR antagonists could inhibit CYP3A4 induction and possibly increase the efficacy of anticancer drugs. The results of the *in vitro* study from **Chapter 3.1** demonstrated trabectedin, thymolphthalein, A-792611 and ketoconazole as PXR antagonists in rank order of their inhibitory potencies. Leflunomide was identified as PXR agonist and both coumestrol and sulforaphane were no ligands of PXR. Taken all together, the number of PXR antagonists is limited and the discovery of more potent and selective PXR antagonists is required to prevent CYP3A4 induction and to possibly improve the efficacy of anticancer drugs. Based on the fact that CAM are relatively safe compared to the known PXR antagonists, testing CAM for their ability to inhibit PXR has potential (**Chapter 3.2**). Milk thistle was shown to strongly inhibit PXR-mediated CYP3A4 induction. The components of milk thistle responsible for this effect were identified as silybin and isosilybin. Both components strongly and directly interact with PXR according to computational PXR docking and LanthaScreen[®] time-resolved fluorescence resonance energy transfer (TR-FRET) PXR competitive binding assay. Due to the low bioavailability of milk thistle, it is crucial to design potent PXR antagonists based on the structure of silybin and isosilybin.

In addition to the metabolism of anticancer drugs by CYP enzymes, the transport of these drugs by drug efflux transporters is also involved in the elimination process. Both P-glycoprotein (P-gp; ABCB1) and Breast Cancer Resistance Protein (BCRP; ABCG2) are major players in transporting a broad spectrum of clinically relevant anticancer drugs and became the focus of the *in vitro* study described in **Chapter 4**. Milk thistle, St. John's wort and β -carotene were identified as potent inhibitors of either P-gp and/or BCRP mediated transport of the oncolytic substrates topotecan or imatinib in an accumulation and transwell assay. Since the inhibition of BCRP and P-gp appears to be dependent on the combination of the inhibitor and substrate, it is crucial to use oncolytic substrates *in vitro* to more closely predict possible pharmacokinetic interactions between CAM and the specifically tested anticancer drugs.

In recent years not only Western CAM became popular among cancer patients, but also Chinese herbs. Therefore, in the last *in vitro* study (**Chapter 5.1**) the inhibition and induction of CYP3A4 by four Chinese herbs *Oldenlandia diffusa*, *Codonopsis tangshen*, *Rehmannia glutinosa* and *Astragalus propinquus* was determined. All these herbs were shown to inhibit CYP3A4, of which *Oldenlandia diffusa* was the strongest inhibitor. More convincingly, *Oldenlandia diffusa* and *Rehmannia glutinosa* induced CYP3A4, of which

Oldenlandia diffusa showed induction in a comparable degree as the strong CYP3A4 inducers rifampicin and St. John's Wort. Since Chinese medicine emphasize on treatment of the whole body by including multiple Chinese herbs in an herbal formulation, it is recommended to test frequently used herbal formulations in cancer patients. In a prospective, randomized, placebo-controlled study of Yaal-Hahoshen et al. the effects of the herbal formulation LCS101 (consisting of, inter alia, Oldenlandia diffusa) on conventional chemotherapy was determined. The authors concluded that LCS101 prevented hematological complications in breast cancer patients without measuring the plasma levels of anthacyclines and taxanes. The reported lower incidence of hematological toxicities might be caused by lower plasma levels of the anticancer drugs, which was the most valid comment described in **Chapter 5.2**.

In summary, milk thistle is the most interesting CAM for clinical follow-up as it was shown to prevent induction of CYP3A4 and to inhibit CYP3A4, CYP2C9, P-gp and BCRP. All these processes possibly result in higher plasma levels of anticancer drugs and consequently anticancer drugs could be administered in lower doses. Furthermore, the results demonstrated grape seed as potent CYP3A4 inhibitor, green tea as potent CYP3A4 and CYP2C9 inhibitor, St. John's wort as potent P-gp inhibitor, and Oldenlandia diffusa and St. John's wort as potent CYP3A4 inducers. Therefore, also grape seed, green tea, St. John's wort and Oldenlandia diffusa are interesting CAM for clinical follow-up.

In conclusion, the results of the *in vitro* research described in this thesis are useful as first indication for clinical trials to establish the clinical relevance of the *in vitro* effects of CAM on metabolism and transport of multiple model and oncolytic substrates. For future *in vitro* studies it is recommended to establish the potencies of CAM to affect the metabolism and transport of multiple oncolytic substrates *in vitro*. For clinical studies it is recommended to assess pharmacokinetic interactions between CAM and orally administered anticancer drugs in cancer patients as the effects of CAM on intestinal CYP enzymes and drug efflux transporters is probably more relevant due to the poor bioavailability of CAM.



NEDERLANDSE SAMENVATTING

Het gebruik van complementaire en alternatieve middelen (CAM), zoals voedings- en kruidensupplementen, is de afgelopen jaren steeds populairder geworden onder kankerpatiënten. Zij gebruiken deze middelen onder andere om bijwerkingen van de chemotherapie te verminderen en om de kwaliteit van leven te verbeteren. Over het algemeen wordt het gebruik van CAM als veilig beschouwd en vaak zijn artsen niet op de hoogte van het gebruik van deze middelen. Echter kunnen bij het gelijktijdig gebruik van CAM en oncolytica farmacokinetische interacties optreden. Gezien de smalle therapeutische breedte van oncolytica kunnen kleine veranderingen in de plasmaspiegels van oncolytica ernstige gevolgen hebben voor een kankerpatiënt, waaronder een verminderde effectiviteit van de chemotherapie of een verhoogd risico op bijwerkingen. Voor het merendeel van CAM is onbekend of gelijktijdig gebruik met oncolytica veilig is voor kankerpatiënten. Het is dan ook van groot belang om de kennis over mogelijke klinische farmacokinetische interacties tussen CAM en oncolytica te vergroten. Het doel van het onderzoek beschreven in dit proefschrift was daarom om de *in vitro* effecten van veelgebruikte CAM op het metabolisme en transport van oncolytica te bepalen. Aangezien cytochroom P450 (CYP) enzymen en transporteiwitten betrokken zijn bij vrijwel alle farmacokinetische interacties tussen CAM en oncolytica, vormden de inhibitie en inductie van deze enzymen en transporteiwitten door CAM de focus van dit proefschrift.

Voorafgaand aan klinische studies met kankerpatiënten worden veelal *in vitro* studies uitgevoerd om de effecten van CAM op CYP enzymen en transporteiwitten te bestuderen en om te voorspellen of er mogelijk klinische farmacokinetische interacties kunnen optreden tussen CAM en oncolytica. Hierbij is het belangrijk om de voorspellende waarde van *in vitro* resultaten voor klinische studies te bepalen. In **Hoofdstuk 1.2** zijn daarom de *in vitro* en klinische effecten van Sint-Janskruid, knoflook, mariadistel en ginseng op de activiteit van CYP3A4 vergeleken in een literatuurstudie. Voor Sint-Janskruid en knoflook kwamen de *in vitro* effecten overeen met de klinische effecten, maar dit was niet het geval voor mariadistel en ginseng. De verschillen tussen *in vitro* en klinische effecten kunnen worden verklaard door een aantal factoren, waaronder de matige biologische beschikbaarheid van CAM. Daarnaast is gebleken dat de samenstelling van CAM preparaten van verschillende merken en zelfs tussen preparaten van hetzelfde merk sterk kunnen variëren. Ondanks dat de voorspellende waarde van *in vitro* resultaten niet altijd hoog is, zijn deze resultaten wel bruikbaar als eerste indicatie voor klinische studies om CAM te selecteren die mogelijk leiden tot klinisch relevante farmacokinetische interacties tussen CAM en oncolytica.

De inhibitie van CYP3A4 en CYP2C9 door CAM was de focus van de *in vitro* studies die beschreven staan in **Hoofdstuk 2.1** en **2.3**, omdat deze CYP enzymen de grootste rol spelen in het metabolisme van oncolytica. De inhiberende effecten van CAM op het

metabolisme van verscheidene CYP3A4 en CYP2C9 substraten is vergeleken binnen een *in vitro* studie om te bepalen welke CAM de meest potente CYP remmers zijn. In deze studie is aangetoond dat groene thee en mariadistel potente remmers zijn van zowel CYP3A4 als CYP2C9 en dat druivenpit extract een potente remmer is van CYP3A4.

Naast de inhibitie van CYP enzymen, kan de inductie van deze enzymen ook ernstige gevolgen hebben voor kankerpatiënten. Door CYP inductie kunnen de plasmaspiegels van oncolytica dalen, wat mogelijk resulteert in een verminderde effectiviteit van oncolytica. De inductie van CYP3A4 was de focus van de *in vitro* studies uit **Hoofdstuk 3.1** en **3.2**, omdat dit enzym het merendeel van de oncolytica metaboliseert en zeer induceerbaar is. Daarnaast zijn meerdere oncolytica, zoals paclitaxel en erlotinib, in staat om CYP3A4 te induceren. In de beschreven *in vitro* studies is aangetoond dat Sint-Janskruid en β -caroteen sterke CYP3A4 inducers zijn, gevolgd door Ginkgo biloba. Aangezien de inductie van CYP3A4 voornamelijk wordt gereguleerd via PXR (Pregnane X Receptor), kunnen PXR antagonisten CYP3A4 inductie remmen en mogelijk de effectiviteit van oncolytica verhogen. In **Hoofdstuk 3.1** staat beschreven dat trabectedine, thymolftaleïne, A-792611 en ketoconazol PXR antagonisten zijn, leflunomide is een PXR agonist en zowel coumestrol en sulforafaan zijn geen PXR liganden. Aangezien het aantal PXR antagonisten beperkt is, is de ontdekking van potentere en selectievere PXR antagonisten noodzakelijk om CYP3A4 inductie te voorkomen en om mogelijk de effectiviteit van oncolytica te verhogen. Gebaseerd op het feit van CAM relatief veilig zijn vergeleken met de bekende PXR antagonisten, is onderzocht of CAM PXR kunnen inhiberen. In de *in vitro* studie uit **Hoofdstuk 3.2** is aangetoond dat mariadistel een sterke inhibitor is van PXR gemedieerde CYP3A4 inductie. De componenten van mariadistel, silybine en isosilybine, zijn verantwoordelijk voor de inhibitie van CYP3A4 inductie. Beide componenten vertonen een sterke en directe interactie met PXR volgens computer gesimuleerde PXR docking en de LanthaScreen® time-resolved fluorescence resonance energy transfer (TR-FRET) PXR competitive binding assay. Gezien de lage biologische beschikbaarheid van mariadistel is het cruciaal om aan de hand van de structuur van silybine en isosilybine potente PXR antagonisten te ontwerpen.

Naast het metabolisme van oncolytica via CYP enzymen, is het transport van deze geneesmiddelen via transporteiwitten ook betrokken bij het eliminatieproces. Zowel P-glycoproteïne (P-gp; ABCB1) als Breast Cancer Resistance Protein (BCRP; ABCG2) zijn belangrijke transporteiwitten in het eliminatieproces van vele klinisch relevante oncolytica. In **Hoofdstuk 4** staat beschreven dat mariadistel, Sint-Janskruid en β -caroteen potente remmers zijn van P-gp en/of BCRP gemedieerd transport van de oncolytische substraten topotecan of imatinib in een accumulatie en transwell assay. Aangezien de inhibitie van P-gp en BCRP afhankelijk lijkt te zijn van de combinatie inhibitor en substraat, is het cruciaal om de *in vitro* effecten van CAM op het transport van oncolytische substraten te bepalen om de klinisch farmacokinetische interacties beter te voorspellen.

In de afgelopen jaren zijn niet alleen Westerse CAM populairder geworden onder kankerpatiënten, maar ook Chinese kruiden. In de *in vitro* studie uit **Hoofdstuk 5.1** is de inhibitie en inductie van CYP3A4 door de volgende Chinese kruiden bepaald: Oldenlandia diffusa, Codonopsis tangshen, Rehmannia glutinosa en Astragalus propinquus. Deze vier Chinese kruiden veroorzaakten inhibitie van CYP3A4, waarbij Oldenlandia diffusa de meest potent CYP3A4 remmer was. De inductie van CYP3A4 door Oldenlandia diffusa en Rehmannia glutinosa was meer overtuigend. Oldenlandia diffusa resulteerde zelfs in een vergelijkbare mate van CYP3A4 inductie als de bekende potente CYP3A4 inducers rifampicine en Sint-Janskruid. Aangezien Chinese geneeskunde de nadruk legt op behandeling van het gehele lichaam door het samenvoegen van meerdere Chinese kruiden in een kruidenformule, wordt aanbevolen om deze kruidenformules te onderzoeken in kankerpatiënten. In een prospectieve, gerandomiseerde, placebocontroleerde studie van Yaal-Hahoshen et al. is het effect van de kruidenformule LCS101 (bestaande uit o.a. Oldenlandia diffusa) op de conventionele chemotherapie bepaald. De auteurs concludeerden dat het gebruik van LCS101 hematologische complicaties voorkwam in borstkankerpatiënten, zonder de plasmaspiegels te bepalen van de anthracyclines en taxanen. De lagere incidentie van hematologische toxiciteit kan mogelijk veroorzaakt zijn door lagere plasmaspiegels van deze oncolytica. Naast dit commentaar zijn in **Hoofdstuk 5.2** nog twee andere punten van kritiek beschreven.

Samenvattend, mariadistel is het meest interessant om in klinische studies te onderzoeken, omdat in dit proefschrift is aangetoond dat mariadistel CYP3A4 inductie voorkomt en CYP3A4, CYP2C9, P-gp en BCRP remt. Al deze processen kunnen mogelijk leiden tot hogere plasmaspiegels van oncolytica, waardoor oncolytica in lagere doses kunnen worden toegediend. Daarnaast is aangetoond dat druivenpitextract een potente CYP3A4 inhibitor is, groene thee een potente CYP3A4 en CYP2C9 inhibitor, Sint-Janskruid een potente P-gp inhibitor en CYP3A4 inducer, en Oldenlandia diffusa een potente CYP3A4 inducer. Naast mariadistel, zijn druivenpit extract, groene thee, Sint-Janskruid en Oldenlandia diffusa ook interessant om in klinisch studies te onderzoeken.

Concluderend, de resultaten van het *in vitro* onderzoek beschreven in dit proefschrift zijn bruikbaar als eerste indicatie om de klinische relevantie van de *in vitro* effecten van CAM op het metabolisme en transport van meerdere model- en oncolytische substraten te bepalen. Voor vervolgstudies wordt aanbevolen om de *in vitro* effecten van CAM op het metabolisme en transport van meerdere oncolytische substraten te bepalen. De aanbeveling voor klinische studies is om de farmacokinetische interacties tussen CAM en orale oncolytica te onderzoeken in kankerpatiënten, omdat de effecten van CAM op intestinale CYP enzymen en transporteiwitten waarschijnlijk relevanter is vanwege de lage biologische beschikbaarheid van CAM.



CHAPTER 8

APPENDIX





DANKWOORD

Na ruim 5.700 uren werk, 1.000 liter thee, duizenden epjes en 12.500 injecties in de LC-MS/MS is het dan eindelijk gelukt: mijn proefschrift is af!!! Maar zonder jullie hulp en inzet was het niet mogelijk geweest om dit proefschrift tot stand te brengen. Dank daarvoor! Een aantal mensen wil ik graag in het bijzonder noemen.

Om te beginnen gaat mijn dank uit naar mijn co-promotor Irma Meijerman. Beste Irma, wat was het prettig om jou als dagelijkse begeleider te hebben. Ik waardeer het heel erg dat je altijd tijd had voor een kort overleg en voor het kritisch nakijken van mijn stukken. Ik heb heel erg veel geleerd van jouw commentaar (focus en koppelen van alinea's) en jouw inbreng resulteerde elke keer weer in een zichtbare verbetering van mijn manuscripten. Ook onze gezellige gesprekken over niet-onderzoeksgerelateerde zaken zal ik nooit vergeten. Ontzettend bedankt voor je begeleiding en betrokkenheid de afgelopen jaren!

Tevens gaat mijn dank uit naar mijn promotoren Jan Schellens en Jos Beijnen. Beste Jan, het is alweer ruim 6 jaar geleden dat ik voor het eerst met je in contact kwam voor een project over tromboseprofylaxe bij kankerpatiënten. Op dat moment had ik nooit durven dromen dat ik onder jouw begeleiding kankeronderzoek zou mogen uitvoeren. Je hebt me geïnspireerd op het gebied van kanker en ik ben je dankbaar dat je mij de mogelijkheid hebt gegeven om deel te mogen nemen aan dit interessante KWF-project. Graag wil ik je ook bedanken voor je kritische blik en nuttige aanvullingen op mijn manuscripten. Beste Jos, tijdens mijn promotieonderzoek heb je me met name begeleid op het gebied van LC-MS/MS werk. Op de momenten dat het even niet lekker liep met mijn LC-MS/MS methode wist je me altijd weer te motiveren en ik veel geleerd van de heldere wijze waarop je de mogelijke problemen wist uit te leggen aan mij. Daarnaast heb je me altijd goed aan het denken gezet met jouw kritische vragen en ik waardeer het enorm dat je mijn manuscripten altijd zo snel hebt nagekeken.

Beste Roel, mijn maatje. Wat was het super om met jou samen te werken op het lab! Zonder jou was het nooit gelukt om in 3 jaar zoveel experimenten uit te voeren. Ik ben je ontzettend dankbaar voor je onvoorwaardelijke inzet en hulp bij het uitvoeren van experimenten. Ik zal onze manier van samenwerking tijdens het incuberen en opwerken van LC-MS/MS samples nooit vergeten! Evenals onze gezellige gesprekken! Naast het praktische werk, ben ik je ook dankbaar voor je snelle en nuttige commentaar op mijn manuscripten.

Beste Andrew, mijn AIO buddy. Wat was het geweldig om samen met jou aan het KWF-project te werken, bedankt! Vooral het schrijven van onze review was prettig om samen te doen, wat een 'bevalling' was dat zeg?! Ik vond het heel erg fijn dat ik met allerlei

vragen altijd bij je terecht kon. Ook zal ik zal de gezellige lunches bij het UMCU en onze trip naar Chicago nooit vergeten. Daar stonden we dan allebei met een poster op het grote AACR congres. Braaf gingen we naar allerlei lezingen toe, maar naast het congres hadden we ook tijd voor sightseeing, winkelen bij A&F en een basketbal wedstrijd. Ik hoop dat je in Bethesda je plekje hebt gevonden en ik wens je daar heel veel geluk. Als we weer eens op vakantie gaan naar the States, kom ik je zeker opzoeken.

Beste Hilde, naast Jos was ook jouw hulp bij het opzetten van mijn LS-MS/MS methodes van onschatbare waarde. Drie jaar geleden had ik nooit gedacht dat ik een gevalideerde LC-MS/MS methode voor 1-hydroxymidazolam zou publiceren. Zonder jou was me dit nooit gelukt! Ik ben je ontzettend dankbaar voor je geduld en heldere uitleg bij de problemen die ik heb ondervonden met mijn LC-MS/MS metingen. Dankzij jou heb ik heel veel geleerd op het gebied van LC-MS/MS, bedankt!

Beste Jeroen, bedankt voor de prettige samenwerking tijdens de LC-MS/MS metingen van docetaxel en je kritische feedback op het manuscript over CYP3A4 inhibitie. Mede door jou was het mogelijk om de effecten van CAM op het metabolisme van docetaxel snel te bepalen. Heel veel succes met het afronden van je promotieonderzoek en je opleiding tot ziekenhuisapotheker.

Beste Ed, hartelijk dank voor de kortstondige maar fijne samenwerking. Ik waardeer het enorm dat je voor mij PXR docking hebt uitgevoerd. De resultaten van deze docking waren echt van meerwaarde voor mijn manuscripten over mariadistel en bekende PXR antagonisten.

Naast de collega's waar ik mee heb samengewerkt, ben ik ook de leden van de beoordelingscommissie bestaande uit prof. dr. B. Olivier, prof. dr. G. Folkerts, prof. dr. M. van den Berg, prof. dr. J.N.M. Commandeur en prof. dr. B. van de Water zeer erkentelijk voor het lezen en beoordelen van mijn proefschrift.

Tijdens mijn promotieonderzoek heb ik een aantal fantastische studenten mogen begeleiden en mede door hun inzet was het mogelijk om veel experimenten uit te voeren en genoeg resultaten te vergaren voor het schrijven van artikelen. Beste Esther, bedankt voor het optimaliseren en uitvoeren van de BCRP accumulatie-assay en voor de gezellige gesprekken. Beste Tomy, ik waardeer enorm hoe jij in zo'n korte tijd de CYP2C9 inhibitie assay hebt uitgevoerd en jouw resultaten hebben zeker bijgedragen aan mijn manuscript over de inhiberende effecten van CAM op CYP2C9. Beste Cedric, ik ben je ontzettend dankbaar dat je het initiatief hebt genomen om een extra project over de effecten van Chinese kruiden op CYP3A4 uit te voeren. Wat bent ik trots op onze

mooie publicatie! Beste Cindy en Merit, heel erg bedankt voor jullie enorm inzet bij de transporter experimenten. Zonder jullie was het niet mogelijk geweest om een artikel te schrijven over de inhiberende effecten van CAM op BCRP en P-gp.

De meeste tijd van mijn promotieonderzoek heb ik doorgebracht in het David de Wied-gebouw, waar ik een heleboel leuke collega's heb mogen leren kennen. In het bijzonder wil ik graag Corinne, Marjolein, Rianne, Talitha, Lianne en Joris bedanken voor de gezellige gesprekken en de nodige afleiding tijdens de lunch- en koffiepauzes. Niet alleen in het David de Wied, maar ook daarbuiten heb ik genoten van de leuke momenten dat we lekker de stad in gingen voor een lekker hapje eten en de Pubquiz. Ik wens jullie heel veel succes met het afronden van jullie onderzoek en "we keep in touch"! Wie zeker ook niet mogen ontbreken in mijn dankwoord zijn Ineke, Suzanne en Anja: de drie Musketers van het secretariaat. Hartelijk dank voor jullie behulpzaamheid en gezelligheid, het ga jullie goed!

Lieve familie en vrienden, heel erg bedankt voor jullie interesse in mijn onderzoek en de nodige afleiding tijdens het promoveren. In het bijzonder wil ik mijn lieve vriendinnen Jessica, Monique, Mara, Stéfani, Mariëlle en Hilde bedanken. Ik hoop dat we nog heel lang vriendinnen blijven en samen nog vele mooie momenten mogen beleven. Lieve Jessica, ik ben je ontzettend dankbaar voor al je hulp bij de problemen die ik steeds had met mijn grafieken, het meedenken over de omslag van mijn proefschrift, je goede adviezen en onze gezellige avondjes met heerlijk eten, een wijntje en (niet te vergeten) toastjes met brie. Lieve Monique, ontzettend bedankt dat je mijn paranimf wilt zijn. Ik vond het altijd heerlijk om iedere week samen met jou lekker stoom af te blazen in de sportschool en om onder het genot van een hapje en drankje gezellig bij te kletsen. Lieve Mara, wat was het toch fijn om het lief en leed van onderzoek doen met jou te kunnen delen en jouw optimisme heeft mij echt energie gegeven tijdens mijn promotieonderzoek. Bedankt voor alle gezellige avondjes samen en proost op onze volgende date! Lieve Stéfani, ik ben jou ook heel erg dankbaar voor onze gezellige 'bijklets' avondjes en wat was het fijn om elkaar te helpen met onze weddings. Lieve Mariëlle, ik ben heel erg blij dat we nog steeds vriendinnen zijn ondanks dat we elkaar helaas heel weinig zien. Ik wil je bedanken voor de gezellige momenten die we samen hebben beleefd en ik ben ontzettend trots op je! Lieve Hilde, heel erg bedankt voor de gezellige avonden in Woerden en Amsterdam en ik waardeer je enorme interesse in mijn werk en privéleven.

Lieve Roy, mijn 'kleine' broertje. Echt fantastisch dat je mijn paranimf bent! Ondanks dat we elkaar niet veel zien, ben ik super trots op je en ik ben je dankbaar voor alle gezellige momenten die ik samen met je heb beleefd: heerlijk samen uiteten in Amsterdam, naar

concerten, Halloween vieren, als vanouds thuis lekker chillen en onze mooie reis door Zuid-Afrika. Love you bro!

Lieve pap en mam, bedankt voor jullie onvoorwaardelijk steun, liefde en vertrouwen die jullie mij hebben gegeven. Jullie staan altijd klaar voor me en dat waardeer ik enorm. We zijn altijd welkom om 's avonds lekker mee te eten thuis en ik geniet altijd volop van de gezellige uitstapjes die we maken. Ik had me geen betere ouders kunnen wensen, ik hou van jullie!

Lieve JW, lieve schat, jij bent mijn alles! Dankjewel voor al je liefde, goede zorgen en de heerlijke gerechten die je voor me heb gemaakt. In de extreem drukke periodes op mijn werk, wist je me er altijd doorheen te slepen met je humor. En samen hebben we veel mooie momenten beleefd: de aankoop van ons huis, een fantastische trip naar New York, onze prachtige huwelijksdag op 1-6-12, een heerlijke huwelijksreis naar Curaçao en ga zo maar door. Ik hoop dat we samen nog veel meer mooie momenten mogen beleven. Ik hou van je!!!



LIST OF CO-AUTHORS

Paul C.D. Bank

Division of Pharmacoepidemiology and Clinical Pharmacology, Utrecht Institute for Pharmaceutical Sciences, Faculty of Science, Utrecht University, The Netherlands

Jos H. Beijnen

Department of Pharmacy and Pharmacology, Slotervaart Hospital, Amsterdam, The Netherlands

Division of Pharmacoepidemiology and Clinical Pharmacology, Utrecht Institute for Pharmaceutical Sciences, Faculty of Science, Utrecht University, The Netherlands

Andrew K.L. Goey

Division of Pharmacoepidemiology and Clinical Pharmacology, Utrecht Institute for Pharmaceutical Sciences, Faculty of Science, Utrecht University, The Netherlands

Jeroen J.M.A. Hendriks

Department of Pharmacy and Pharmacology, Slotervaart Hospital, Amsterdam, The Netherlands

Tomy J. Huijbregts

Division of Pharmacoepidemiology and Clinical Pharmacology, Utrecht Institute for Pharmaceutical Sciences, Faculty of Science, Utrecht University, The Netherlands

Fernanda A. Imperiale

Division of Pharmacoepidemiology and Clinical Pharmacology, Utrecht Institute for Pharmaceutical Sciences, Faculty of Science, Utrecht University, The Netherlands

Merit de Jeu

Division of Pharmacoepidemiology and Clinical Pharmacology, Utrecht Institute for Pharmaceutical Sciences, Faculty of Science, Utrecht University, The Netherlands

Cedric Lau

Division of Pharmacoepidemiology and Clinical Pharmacology, Utrecht Institute for Pharmaceutical Sciences, Faculty of Science, Utrecht University, The Netherlands

Esther van Loon

Division of Pharmacoepidemiology and Clinical Pharmacology, Utrecht Institute for Pharmaceutical Sciences, Faculty of Science, Utrecht University, The Netherlands

Roel F. Maas-Bakker

Division of Pharmacoepidemiology and Clinical Pharmacology, Utrecht Institute for Pharmaceutical Sciences, Faculty of Science, Utrecht University, The Netherlands

Irma Meijerman

Division of Pharmacology, Utrecht Institute for Pharmaceutical Sciences, Faculty of Science, Utrecht University, The Netherlands

Ed E. Moret

Division of Medicinal Chemistry and Chemical Biology, Utrecht Institute for Pharmaceutical Sciences, Faculty of Science, Utrecht University, The Netherlands

Hilde Rosing

Department of Pharmacy and Pharmacology, Slotervaart Hospital, Amsterdam, The Netherlands

Jan H.M. Schellens

Department of Clinical Pharmacology, The Netherlands Cancer Institute, Amsterdam, The Netherlands

Division of Pharmacoepidemiology and Clinical Pharmacology, Utrecht Institute for Pharmaceutical Sciences, Faculty of Science, Utrecht University, The Netherlands

Cindy de Waard

Division of Pharmacoepidemiology and Clinical Pharmacology, Utrecht Institute for Pharmaceutical Sciences, Faculty of Science, Utrecht University, The Netherlands



LIST OF PUBLICATIONS

Goey A.K.L., Mooiman K.D., Beijnen J.H., Schellens J.H.M., Meijerman I., Relevance of *in vitro* and clinical data for predicting pharmacokinetic herb-drug interactions in cancer patients. *Cancer Treatment Reviews* 2013; 39(7): 773-783.

Mooiman K.D., Maas-Bakker R.F., Moret E.E., Beijnen J.H., Schellens J.H.M., Meijerman I., Milk thistle's active components silybin and isosilybin: novel inhibitors of PXR-mediated CYP3A4 induction. *Drug Metab Dispos* 2013, 41(8): 1494-1504.

Mooiman K.D., Maas-Bakker R.F., Rosing H., Beijnen J.H., Schellens J.H.M., Meijerman I., Development and validation of a LC-MS/MS method for the *in vitro* analysis of 1-hydroxymidazolam in human liver microsomes: application for determining CYP3A4 inhibition in complex matrix mixtures. *Biomed Chromatogr* 2013; 27(9): 1107-1116.

Lau C., Mooiman K.D., Maas-Bakker R.F., Beijnen J.H., Schellens J.H.M., Meijerman I., Effect of Chinese herbs on CYP3A4 activity and expression *in vitro*. *J Ethnopharmacol* 2013; 149(2): 543-549.

Mooiman K.D., Goey A.K.L., Meijerman I., Beijnen J.H., Schellens J.H.M., Letter to the editor regarding "A prospective, controlled study of the botanical compound mixture LCS101 for chemotherapy-induced hematological complications in breast cancer" by Yaal-Hahoshen et al. (*The Oncologist* 2011; 16: 1197-1202) *The Oncologist* 2012; 17(5): 742-743.

To be continued...

Mooiman K.D., Maas-Bakker R.F., Hendriks J.J.M.A., Bank P.C.D., Rosing H., Beijnen J.H., Schellens J.H.M., Meijerman I., The effect of complementary and alternative medicines (CAM) on CYP3A4-mediated metabolism of three different substrates: 7-benzoyloxy-4-trifluoromethylcoumarin (BFC), midazolam and docetaxel. Submitted for publication.

Mooiman K.D., Maas-Bakker R.F., Moret E.E., Beijnen J.H., Schellens J.H.M., Meijerman I., Evaluation of a reporter gene assay as suitable *in vitro* system to screen for novel PXR antagonists. Submitted for publication.

Mooiman K.D., Goey A.K.L., Huijbregts T.J., Maas-Bakker R.F., Beijnen J.H., Schellens J.H.M., Meijerman I., The effect of complementary and alternative medicines (CAM) on CYP2C9 activity. Submitted for publication.

Mooiman K.D., Maas-Bakker R.F., de Waard C., de Jeu M., Imperiale F.A., van Loon E., Beijnen J.H., Schellens J.H.M., Meijerman I., The effect of complementary and alternative medicines (CAM) on P-gp and BCRP mediated transport of topotecan and imatinib. Submitted for publication.



ABOUT THE AUTHOR

Kim Mooiman was born on May 22 1986 in Woerden, The Netherlands. In 2004, she graduated from secondary school "Minkema College" in Woerden. In September 2004, she started her study Pharmacy at the Utrecht University. After obtaining her Bachelor's degree in Pharmacy in August 2007, she continued with the Master's program Pharmacy at the Utrecht University. She wrote a Master thesis about the role of MAP kinases in the underlying mechanisms of anticancer drug mediated BCRP induction in KG1 α cells. In August 2010, she obtained her Master of Science degree. Subsequently, Kim started with the PhD project described in this thesis at the Department of Pharmacoepidemiology and Clinical Pharmacology at the Utrecht University. Her work was supervised by Prof. J.H.M. Schellens, Prof. J.H. Beijnen and Dr I. Meijerman. As of September 2013, Kim works as a pharmacist of Medication verification at the VU medical center in Amsterdam, The Netherlands.

